Nanocrystalline Silver and Silver-Gold Materials for Inflammation Reduction and Surgical Adhesion
Prevention

by

Colleen Nancy Ward

A thesis submitted in partial fulfillment of the requirements for the degree of

Doctor of Philosophy

Department of Biomedical Engineering
University of Alberta

Abstract

Surgical adhesions are caused by tissue trauma and inflammation and present a high clinical burden. Nanocrystalline silver is known to be a strong anti-inflammatory and antibacterial material. This thesis explores the potential for nanocrystalline silver and silver-gold to be used to treat inflammation in the abdominal cavity after surgery, therefore preventing the formation of adhesions. Nanocrystalline silver and silver-gold films were sputtered onto HDPE substrates. A novel fabrication process using high current and including both oxygen and water as reactive gases was compared to the standard process, and was found to create high-efficacy dressings with higher silver content and stability in solution. The novel process was found to decrease the grain size and percent of ammonia soluble silver compared to the standard process. For nanocrystalline silver-gold films, increasing gold content in the alloy was found to decrease the grain size in the standard process, but not consistently with the novel process. Higher gold content also increased the total mass sputtered onto the HDPE. An animal study is planned to assess the anti-inflammatory properties of nanocrystalline silver-gold film in a pig model of dermatitis. When soaked in water, nanocrystalline silver dissolves into solution, releasing only approximately 3% of the total silver in the film. These solutions are less effective anti-bacterial materials than direct contact with a solid dressing, but have potential to treat inflammation and preventing surgical adhesions. Nanocrystalline silver solutions were combined with hyaluronate (HA) and carboxymethyl cellulose (CMC), biodegradable and biocompatible polymers, to make viscous solutions. The viscosity, degradation, and silver release were studied over a three day period. It was found that increasing the concentration of polymers increased the viscosity, but did not affect the rate of silver release or polymer degradation. pH was also adjusted, but did not have a significant effect within the range studied. An animal study is planned to test the anti-adhesion properties of HA-CMC and nanocrystalline silver viscous solutions in a pig surgical model of adhesions.

Preface

This thesis is original work conducted by Colleen Ward.

Animal studies discussed in this thesis received research ethics approval from the University of Alberta Animal Care and Use Committee (AUP 00003741 "Anti-inflammatory nano-silver and silver-gold", AUP 00004189 "Surgical Adhesions in Pigs") and Medstar Health Research Institute Animal Care and Use Committee (2023-025 "Anti-inflammatory activity of nanocrystalline silver and silver-gold dressings and derived solution in a porcine model of dermatitis", 2023-019 "Treatment of Abdominal Surgical Adhesions in Pigs with Nanocrystalline Silver Gels"). Planned animal studies are in collaboration with Dr. Jeffrey Shupp and Dr. Lauren Moffatt of MedStar Health Research Institute in Washington DC.

Portions of Chapter 4 have been published as:

K. K. A. Hatch, R. E. Burrell, and C. N. Ward, "Effect of a Novel sputtering process on the chemical and biological properties of silver-gold alloys," *Int. Wound J.*, vol. 21, no. 3, p. e14475, 2024, doi: 10.1111/iwj.14475.

Keeley Hatch was responsible for data collection and assisted with writing. I assisted with data collection and was responsible for study conception and manuscript writing.

Portions of Chapter 7 have been published as:

C. N. Ward, P. E. LeBlanc, and R. E. Burrell, "Effects of composition and pH on the degradation of hyaluronate and carboxymethyl cellulose gels and release of nanocrystalline silver," *J. Appl. Biomater.*, vol. 22, 2024, doi:10.1177/22808000241257124

I was responsible for studying planning, data collection, and manuscript preparation. Payton LeBlanc assisted with data collection and writing.

Dedication

To my husband Graham, who supported me through all the emotional ups and downs.

To Dr. Burrell, who believed I would be able to finish this, even when I didn't.

Acknowledgments

Many thanks to Dr. Burrell, for his supervision and support, and for always championing my work.

Thanks to my committee members, Patricia Nadworny, Todd McMullen, and Adam Kinnaird for their time in guiding me and reviewing my thesis.

Thank you to Nancy Zhang and the staff at nanoFAB for their assistance and training with XRD and SEM.

For assistance on XRD, thanks to the EAS X-ray Diffraction Lab at the University of Alberta and Rebecca Funk

Thank you to Shiraz Merali with the University of Alberta Department of Chemical and Materials Engineering and Sherritt Technologies for assistance with chemical analysis

Thank you to my undergraduate student collaborators, Keeley Hatch, Josephine Beaulieu, and Payton LeBlanc. It was a pleasure to work with all of you.

Thank you for animal study assistance from MedStar Health Research Institute at Georgetown University School of Medicine, particularly Lauren Moffatt, Jeffrey Shupp, and Bonnie Carney.

I gratefully acknowledge the financial support of scholarships from Alberta Innovates and NSERC.

Thanks to my coworkers and mentors at Bennu Engineering for their support and encouragement.

Many thanks to my friends and family who cheered me on, especially my parents Tracy and Nancy Moore and parents-in-law Chris and Peggy Ward.

Table of Contents

List of Tables

List of Figures

Abbreviations

AAS	Atomic Absorption Spectroscopy
ANOVA	Analysis of Variance
BCS	Bovine calf serum
CMC	Carboxymethyl cellulose
COX-2	Cyclooxygenase 2
CZOI	Corrected Zone of Inhibition
DNCB	Dinitrochlorobenzene
GST	Gold sodium thiomalate or sodium aurothiomalate
HA	Hyaluronic acid
HCl	Hydrochloric acid
HDPE	High density polyethylene
HPLC	High Performance Liquid Chromatography
ICAM	Intercellular adhesion molecule
ICP-MS	Inductively coupled plasma mass spectrometry
IFN-γ	Interferon-gamma
IL-1β, IL-2, IL-4, IL-6, IL-8, IL-10, IL-12, IL-13	Interleukins
MCP	Monocyte chemoattractant protein
MMP	Matrix metalloproteinase
NaOH	Sodium hydroxide
PAI-1	Plasminogen activator inhibitor-1
PBS	Phosphate Buffered Saline
PEG	Polyethylene glycol
PGE2	Prostaglandin E2
PLA	Poly(lactic acid)
PVA	Polyvinyl alcohol
ROS	Reactive oxygen species
RT-PCR	Real time polymerase chain reaction
SEM	Scanning electron microscope
TGF-β1	Transforming growth factor-Beta
TNF-α	Tumor necrosis factor- alpha

ToF SIMS	Time of flight Secondary Ion Mass Spectrometry
tPA	Tissue plasminogen Activator
VEGF	Vascular endothelial growth factor
XPS	X-ray photoelectron spectroscopy
XRD	X-ray diffraction
αSMA	Alpha smooth muscle actin

Chapter 1 : Introduction

Adhesion Prevalence and Abdominal Cavity Anatomy

Surgical adhesions present a great clinical burden that is the focus of extensive research to understand the process of their formation and to find methods of prevention and treatment. Adhesions are fibrous tissue growths or scars attaching previously unconnected tissue surfaces in the abdominal cavity that can occur after up to 93% of all surgical interventions, depending on the location and procedure [1], [2], [3]. Radiation treatment or inflammatory conditions such as endometriosis, pelvic inflammatory disease, or Crohn's disease can also cause or contribute to adhesions[4], [5]. Surgically-induced adhesions are the most common [2], [6]. In a post-mortem study of 752 autopsies in 1973, 67% of surgical cases had adhesions, compared to 28% of non-surgical subjects[6]. The probability of surgical adhesions is similar across age categories, although factors can increase the incidence of adhesions, such as operation complexity, comorbidities, hypoxia, dehydration, and foreign object involvement [2], [6], [7].

The focus of this thesis is on surgical adhesions occurring in the abdominal cavity. The abdominal wall that forms the cavity is made up of layers of fat and muscle, providing structural integrity and protection, and through which nerve fibers, blood and lymphatic vessels run [8]. The peritoneum is the innermost layer; it is thin, single celled and in closest contact to organs, therefore most relevant to adhesion formation [8], [9]. A layer of extraperitoneal fascia bonds the peritoneum to the deep fascia or outer lining of the gastrointestinal tract [8]. The parietal peritoneum covers the interior wall, diaphragm, and pelvis and receives vascular supply from abdominal wall vessels [3], [10]. The visceral peritoneum covers the abdominal viscera and abdominal organs[3]. There is a greater risk of adhesions in injuries to the visceral peritoneum, compared to the parietal peritoneum [11].

The peritoneum is very metabolically active, with a large surface area for absorption and rapid transfer to vasculature [9]. This rapid absorption is due to stomata and channels between mesothelial cells that drain into the underlying lymphatic system[3]. Convection and diffusion are the main transport mechanisms across the peritoneum [3]. The peritoneum is covered in microvilli to increase the surface area, and this helps to trap proteins in the serosal fluid[3]. The peritoneal cavity maintains homeostatic communication with the pleural space, fallopian tubes, vascular system, and lymphatic system[3]. Peritoneal fluid is an ultra-filtrate of plasma, containing serum proteins, resident inflammatory cells, carbohydrate, and enzymes, and acting as a lubricant[3].

Adhesions involving the omentum, a mobile, blood-vessel rich fatty accessory organ in the abdominal cavity, and the peritoneum are the most common, but adhesions can involve any intra-peritoneal organs and the abdominal wall [11]. As reported in 2010, in 50% of cases, the bowel is involved, and the greater

omentum is involved in 80% of reported cases of adhesions [2]. In a ten year follow-up of 12 584 patients documented in the Scottish National Health Service medical records during 1986, 7.3% of readmissions were directly related to adhesions, with similar levels across all participating sites[12]. This affects even children, as demonstrated by data from Scotland, following up 5 years post-surgery[13]. Excluding appendectomy, which is a large percentage of these pediatric surgeries, there was a 5.3% readmission rate[13]. Small bowel obstruction is one of the most challenging consequences of adhesions, and is a burden to patients, surgeons, and health care systems[14]. Across a study of 110 admissions for adhesive small bowel obstruction over 2 years (1996-1997), all patients admitted under this category had had a previous laparotomy[14]. In a meta-analysis of data from global studies published in 1992-2012, 56% of small bowel obstructions are related to adhesions[15].

Dissection of adhesions requires additional operating time in subsequent surgeries (on average an additional 20 minutes) and increases the chance of complications such as inadvertent enterotomy, abscess formation, bleeding, and organ damage[11], [15]. Adhesions may be symptomatic shortly after the initial procedure, but even if not, there is a lifetime risk of later developing complications[16]. Even less structured, filmy adhesions can cause significant pain when formed between movable organs and the peritoneum [11]. Diagnosing adhesions can be challenging as they are not always visible in conventional imaging modes, don't have any specific lab tests, and a physical examination is not usually conclusive[5]. History is a helpful contributor and differential diagnoses include lactose intolerance, fatty liver, endometriosis and acalculous cholecystitis [5]. Symptom management is available, but no effective pharmacological therapies are available to treat adhesions directly[5].

Adhesion Formation

In abdominal surgeries, the peritoneum is necessarily damaged, leading to an inflammatory response [9], [10]. As this occurs, the immediate vascular response is local vasoconstriction, then vasodilation to bring in cells and molecules[1], [9]. The early inflammatory response is characterized by leukocyte infiltration[17]. In a mouse study, early leukocyte accumulation correlates to the extent, type, and tenacity of adhesions [7]. Inflammatory cells can come from vasculature or peritoneal fluid, drawn by chemoattractants and biochemical changes [9], [18]. After the initial injury, the coagulation cascade is triggered[1], [9]. Cells produce and release a protein-rich exudate, containing high levels of fibrinogen, as well as fibronectin, hyaluronic acid, glycosaminoglycans, and proteoglycans[1], [9], [10], [18]. This exudate can cause organs to stick to one another, beginning the process of adhesion formation[1]. The fibrinogen is converted to fibrin as part of the coagulation cascade[1], [9], [10]. The fibrinolytic system is also activated to destroy the fibrin deposits[10]. A balance between the deposition and lysis of fibrin is

key to normal healing[10]. Fibrin is necessary to form a temporary matrix for healing damaged tissues, but can also be the platform for adhesion formation [9]. If the fibrinolytic system fails, fibrous adhesions will form[10]. The main source of adhesion-forming cells is activated local tissue-resident cells, which proliferate polyclonally[19], [20].

Platelets from megakaryocytes in bone marrow adhere to binding sites exposed by tissue damage, physically contributing to the initial fibrin clot that forms[9]. Platelet deposition and degranulation is the main pathway in the peritoneum for fibrin deposition[9]. Here, the fibrin forms the initial matrix for signalling molecules and inflammatory cells, such as mast cells [1], [18], [21]. This initial cascade phase lasts for approximately 6 hours post-injury[9].

Plasmin, a protease which is the active form of plasminogen, degrades fibrin [10], [18]. Tissue Plasminogen Activator (tPA) is the molecule primarily responsible for plasminogen activation and therefore fibrinolysis [10], [22]. tPA is produced by endothelial cells, mesothelial cells, and macrophages[10]. tPA is present in tissue and introduced by plasma [23]. Plasminogen Activator Inhibitor-1 (PAI-1) is the main inhibitor of tPA, inactivating them by forming 1-1 complexes [1], [18], [23]. The ratio between tPA and PAI-1 is important, because traumatized peritoneal tissue has an increased concentration of PAI-1 and decreased levels of tPA [10], [22]. From 3 to 6 hours after injury, tPA decreases, and PAI-1 increases over 3 to 12 hours[23]. As PAI-1 levels increase, fibrinolytic activity decreases. Fibrinolysis is even more depressed when infection is also present [10]. Additionally, adhesions can turn into abscesses if bacteria are caught in the clots, protected by fibrin against immunological defense [10].

In 12 to 14 hours after injury, mostly neutrophils are recruited [9]. TGF-β1 is secreted by fibroblasts and promotes chemotaxis of monocytes and extracellular matrix (ECM) production by fibroblasts [24]. After 24 hours, the cells present are predominantly macrophages, which have a number of roles: tissue debridement, phagocytosis of pathogens, releasing bioactive proteins, and directing other cells [9]. Macrophages recruit new mesothelial cells to the site of injury[18]. Macrophages secrete various chemokines and signalling molecules, including IL-6, TNF-α, PGE2 and IL-1[18]. In the normal healing process, after 4 days, normal premesenchymal cells are proliferating, but in adhesions, macrophages still dominate [9]. After five days, there are primarily organized fibroblasts in adhesions, which express myofibroblast markers like α-SMA [9]. Resident peritoneal macrophages accumulate and form a barrier to shield fibrin clots; the macrophages are cleared by the fifth day when the mesothelial barrier returns [20].

Normally, within 7 to 10 days there is a complete new sheet of mesothelium and the healing rate is the same regardless of wound size, which is not limited by cell migration[1], [9]. The wound surface is reperitonealized by multiple foci of proliferating mesothelial cells and then these foci merge [9]. The matrix is strengthened and remodeled over 1 week to 1 month as temporary ECM molecules are replaced by more permanent proteins, such as collagens, and water is reabsorbed [9]. Mesothelial cells are key mediators of this process[9], [18]. In adhesions, the protein matrix becomes populated by clusters of inflammatory cells and with time, the composition changes to mostly collagen and fibroblast-like cells[9]. Cellular adhesions are harder to break down than acellular adhesions [9].

Adhesion fibroblasts are different than regular fibroblasts. They have lower apoptotic rates, have decreased tPA/PAI-1 ratio, are slow to replicate, and have higher levels of mRNA for inflammatory markers, matrix metalloproteinases, and matrix molecules [3], [19]. For example, adhesion fibroblasts have an increase in mRNA levels for ColI, fibronectin, MMP-1, TIMP-1, TGF-β1 and 2, COX-2, IL-10[3]. α-SMA is a marker of fibroblast activation [25]. COX-2 is induced by hypoxia, and is involved in adhesions[25]. PGE2 content is increased in the peritoneum where adhesions are present [25]. Adhesions also increase the tissue expression of MMP-9[26].

Adhesion Treatment History

Treatments for adhesions have a five to seven day window for success, which is the timeframe in which the normal healing process progresses and the chance of adhesion formation is low- after this time there is less need for ongoing treatment[9]. The risk of adhesion formation significantly decreases even after 36 hours [27], [28]. Many treatments have been tested over the years to find a product that would be effective in preventing adhesions. Carboxymethyl cellulose treatment, known commercially as Seprafilm® when modified with hyaluronate, is bioabsorbable, and has been shown to reduce adhesions, but does not consistently completely prevent them [27], [28], [29], [30], [31], [32], [33]. This is one of the most well studied treatments. A 2016 study showed a reduction in severity, but not incidence, by Seprafilm® compared to controls, but Seprafilm® had a worse performance compared to other novel treatments[34]. It was found to be effective in a rat model of colon surgery[35]. It does not seem to reduce fibrosis, but does reduce inflammation and overall adhesions[36]. Seprafilm® has also been homogenized into a slurry with similar results to the unmodified film[37]. It can also be modified with glycerol to improve membrane flexibility[38]. It is safe for use in humans, but not overwhelmingly effective[38]. Still, it is one of the best available products and has evidence of some efficacy from human trials[39]. Hyaluronic acid has also been used for its anti-adhesive properties as part of a bilayer electrospun

membrane with poly(ε-caprolactone), improving the stability and mechanical properties over Seprafilm®[40]. Normally, Seprafilm® loses its structure as a film within 24 hours, turning into a gel-like substance [41].

N,O,-carboxymethyl chitosan 1% gel and 2% solution in combination had equal efficacy if applied near, as opposed to on, the defect site in rabbits[42]. It also prevented fibroblast adhesion *in vitro*[42]. Adhesion re-formation was also evaluated for this treatment, demonstrating success in reducing the incidence of adhesion re-formation after surgical lysis[42]. Interceed®, an oxidized regenerated cellulose barrier, caused local inflammation, and blood in the area reduced the efficacy of the treatment[27]. In particular, it was unable to prevent re-formation of surgically lysed adhesions[43]. Zwitterion functionalization of polymer membranes can prevent adhesion of cells and proteins, which prevents adhesions when the material covers the wound site[44], [45].

SurgiWrap® is a polylactic acid (PLA) film that can reduce the incidence rate and severity of adhesions, but does not entirely prevent them in rats[46]. It is biodegradable and its properties can be changed by varying the co-polymer contributions, but it cannot adhere well without suturing[29], [46]. In a 2008 test, this barrier method did not show a significant difference to Seprafilm® in inflammatory scoring or adhesion scores[36]. It did not reduce fibrosis, but did reduce inflammation and adhesions compared to controls[36], [47].

Polyethylene glycol (PEG) has been physically mixed with Poly(lactic-co-glycolic acid) (PLGA) in electrospun nanofibrous membranes[48]. The combination of these polymers gave good mechanical properties and thermal stability, and the nanofibrous morphology prevented cell attachment[48]. A study of this material noted that a superhydrophilic surface was good for cell attachment, but a hydrophobic surface absorbed fibrous proteins[48]. Polyactive™, a bilayered mesh made of PEG and poly(butyleneterephthalate) co-polymer did not stay attached well *in vivo* and was therefore not effective [30]. PEG was also included with PLA in varying ratios to tune degradation time to make films that gelled within several days, while allowing healing and preventing adhesions at 5 and 12 days[32]. PEG hydrogel coating was used in another bilayer mesh with gelatin as an antifouling layer[49].

Solution washes or injections are rarely successful because of the fast absorption rate of the peritoneum. Surprisingly, one study found a reduction in adhesions from a saline or taurolidine wash, but this has not been confirmed by other studies[50]. Ringer's lactate, while a popular choice for washes during surgery, was ineffective at preventing adhesions [27], [30], [37]. A single dose of simvastatin, a fibrinolytic agent, administered intraperitoneally at the time of surgery, was found in one study to reduce adhesion scoring[51]. Fucoidans also inhibit fibrin clot formation and have been administered as a bolus or

continuously through an implanted pump[52]. A subcutaneous pump was also used to administer trametinib, a drug that inhibits the mesothelial-mesenchymal transition that occurs at a cellular level in adhesion tissue[53]. These may be effective in theory, but the implantation of a subcutaneous pump is not ideal clinically[52].

Another previously common treatment is a 4% icodextrin solution, commercially called Adept®, a high molecular weight glucose polymer[54]. It has not been shown to be effective when tested in rabbits or rats [34], [55]. It reportedly lasts for 3-5 day before being absorbed into the lymphatic system, but it has questionable biocompatibility[55]. Still, human trials have proved safe use and indicated reduced the severity of adhesions and the recurrence of adhesive small bowel obstruction [54].

Tamoxifen citrate solution, a synthetic antiestrogen treatment used in breast cancer treatment, was administered by orogastric lavage and showed reduced collagen production and decreased TGF-β1[56]. Orogastric lavage was also used to administer pirfenidone, which is an anti-fibrotic and anti-inflammatory agent easily absorbed in the gastrointestinal tract[57]. This agent can also be administered directly to the peritoneum in a gel, but didn't have a beneficial effect[35]. Gallic acid is also used as a solution treatment to inhibit the inflammatory reaction from surgery[58]. Another daily administered gavage treatment, nintedanib, a lung fibrosis treating drug, showed some reduction in adhesion incidence[59].

Rats treated with the systemic antibiotics cefepime and metronidazole for 5 days showed a delay in adhesion formation and less collagen[60]. Preventing infections is beneficial as they worsen adhesions[10]. COX-2 inhibitors are another pathway for adhesion prevention, as COX-2 is expressed in adhesion fibroblasts, supporting angiogenesis and fibroblast proliferation[61]. Injections to recruit stem cells can reduce severity, but not incidence, of adhesions[62]. Another drug, mesna, with fibrinolytic properties, was applied topically in a single dose, which was enough to show a significant effect with a sufficiently high dose[63]. Berberine injections inhibit TIMP-1, an inhibitor of MMP-3 and MMP-9, which breaks down the adhesion components fibrin and collagen [43].

There is another series of materials that were specifically intended to be hemostatic agents that could also reduce adhesion formation. While these had the potential to cause a foreign-body inflammatory reaction, two of these products, activated starch microspheres and PEG polymers, reduced adhesion scores over seven days[64]. 4DryField® PH is a plant-derived polysaccharide powder that can be mixed *in situ* or premixed with saline solution to form a gel, with a promising ability to reduce adhesions[34], [65]. It is also beneficial for hemostasis[34].

Gels are a promising treatment method. They are easier to apply than solid barriers but aren't absorbed as fast as non-viscous solutions. Their efficacy is related to viscosity, ability to coat the wound area, and ability to stay at the site of application [27]. The gels must have sufficient viscosity and stability to stay in place, not be absorbed too fast, and potentially act as a physical barrier[29]. Viscosity must be high enough, or the treatment will be absorbed too fast[66]. Longer retention is associated with higher viscosity, which is related to the molecule weight of the polymers forming the gel[67]. Volume applied and pH must also be considered.

Many gel treatments have PEG included as an inert and bioabsorbable polymer, as it is easily modified to adjust the properties of the gel[28]. PEG alone, however, was found to be only minimally effective[29]. However, collagen mixed with polyethylene created a neutral solution that gelled on tissue contact, reducing adhesion formation[28].

Hyaluronic acid (HA) is a natural linear polysaccharide[29]. Hyaluronate gels are effective for adhesion prevention at sufficiently large volumes, likely due to hydroflotation of organs to keep surfaces separate, but low concentrations[66]. These gels can also be embedded with other substances like Keratinocyte Growth Factor (KGF) to improve the effect[68]. In one study, the HA gel performed poorly compared to films like Seprafilm® or PLA[29]. In another study, a hyaluronate gel, Hyalobarrier®, seemed to work well until after 5 days, but adhesions formed by evaluation at 12 days[32]. Modified hyaluronic acid hydrogels were crosslinked when co-extruded at the time of application and fully gelled in 3 minutes, which is advantageous for application and handling in a clinical setting[69].

Carboxymethylcellulose (CMC), independent of volume, has been found to reduced adhesions[66]. CMC is a major component of Seprafilm®. Polyvinyl alcohol (PVA) can also be combined with CMC to form a gel that is resorbed within 3-4 weeks for significant reductions in adhesion incidence and area [55]. Oxidized dextran/N-carboxyethyl chitosan is another biocompatible gel treatment, which crosslinks at physiological conditions when mixed and injected, which allows it to be easily applied to wounds[70]. However, it did not fully degrade at 21 days, although authors suggested that degradation could be modified by concentration[70]. A hydrogel of the same composition was degraded within 21 days, and had good bioadhesion, self-healing, and adhesion prevention[71]. Chitogel[TM] is a chitosan gel product, but only had a minimal effect in one study[29]. However, it was also mixed with a drug to reduce reactive oxygen species and proliferation of fibroblasts, that was released over 48 to 72 hours for an improved effect[72].

Gels are more beneficial if used not only as a physical barrier, but also provide another aspect of promoting healing or preventing adhesions. HA and CMC hydrogels were created, then loaded with oxaliplatin, a platinum complex that acts as a chemotherapeutic agent for colorectal cancer[67]. More HA and more crosslinking slowed degradation[67]. Release of oxaliplatin could be controlled, showing 31-34% release of total oxaliplatin over one hour, with a cumulative 56-62% release after 12 hours, which then plateaued after this[67]. Oxaliplatin hydrogels treatment reduced the formation of adhesions[67].

Self-healing polyacrylic acid and gelatin hydrogels crosslinked with Al^{3+} have been created with silver chloride nanoparticles inside that have a promising antibacterial effects and minimal cytotoxic effects[73]. Silver nanoparticles have also been included in poly(vinyl alcohol) and chitosan hydrogels with the intended application as antibacterial wound dressings[74]. Concentration was shown to effect the silver nanoparticle release profile to release gradually over several days [74]. Chitosan-PVA films were used to encapsulate silver-doped titanium dioxide nanoparticles with a release time of over 24 hours and antibacterial effectiveness[75].

Nanocrystalline Silver

Ag^0 is chemically inert and ionic silver is most commonly found as Ag^+, but can also be ionized to Ag^{2+} and Ag^{3+}[76], [77]. Metallic silver is inert in the presence of human tissues, but when it is present in inorganic compounds, it ionizes to release Ag^+[77]. Its uptake at mucosal surfaces is proportional to the concentration of free ions and is active-carrier mediated[77]. Between the Ag^0, Ag^+, and Ag^{2+} states, silver is able to accept or donate an electron, depending on the reaction conditions, which has implications for radial quenching [78].

There have been studies on the mechanisms of the antibacterial properties of silver. Compounds with thiol groups are able to neutralize the activity of Ag^+, indicating that part of the antibacterial mechanism is through binding to thiol groups[79],[80]. *In vitro*, silver ions interacted with the respiratory chain of *E.coli* and inhibited oxygen uptake of substrates [81]. After 24 hours in a silver solution, *E.coli* showed cell death by plasmolysis, loss of membrane, and release of the cytoplasm [82]. Silver's bactericidal activity against *E.coli* was primarily via interactions with cytoplasm, not the cell membrane, where silver denatured ribosomes, impairing synthesis functions that led to cell death [82]. Another study found that ionic silver must be in direct contact with the cells to have an effect [83].

It is also suggested that the mechanism of action of silver ions is related to the generation of reactive oxygen species (ROS), likely by inhibition of respiratory enzymes by silver ions[83] [84]. Lower

oxidation states of silver can act as reducing agents by reducing oxygen to ROS and also disrupting mitochondrial functions, leading to ROS production[85]. Cytotoxic effects are related to concentrations of Ag^+, as well as cell type and cell membrane thickness[86] [85] [87].

A solid nanocrystalline silver material can be created by magnetron sputtering to deposit a layer of nanocrystalline silver on a substrate. Nanocrystalline materials are a class of materials with grain sizes in the nanometer range, typically 20 nm or less [76], [88]. A physical vapor deposition process, magnetron sputtering, yields nanocrystalline silver and silver oxide coated materials due to the combination of inert argon and reactive oxygen in the sputtering chamber[88], [89]. Argon is inert and efficient at sputtering and with low oxygen partial pressures it forms a biphased film of metallic Ag and ionic silver in the form of Ag_2O[89], [90]. At high oxygen concentrations, between 10 and 20 atomic percent, metallic silver is not present and the film consists solely of Ag_2O. Without oxygen present, the result is only metallic silver [90].

Nanocrystalline silver dressings have exceptional antibacterial and anti-inflammatory properties and are used commercially as wound dressings[91], [92], [93], [94]. In chronic ulcers, nanocrystalline silver reduced levels of MMP's, which are part of the inflammatory process in adhesion formation and promoted healing [93]. It is clinically effective for acute and chronic wounds[95]. Nanocrystalline silver dressings are superior to other forms of silver dressings because of its large quantity of silver release over time and the variety of silver species released, although its efficacy of release is best within the first day of use[96], [97]. Nanocrystalline silver is significantly a better antimicrobial than silver nitrate, even for lower concentrations of Ag^+[98]. There are many silver dressings and treatments, but nanocrystalline silver has superior silver release and antibacterial properties compared to other silver compounds including silver sulphate, silver alginate, silver foams, and silver collagen[98].

When moistened and applied directly to skin, nanocrystalline silver releases and deposits various silver species, including higher oxidation state silver clusters[99]. Nanocrystalline silver reduces clinical observations and biomarkers of inflammation, as measured by reduced edema, erythema, MMP levels, and inflammatory cytokines TGF-β, TNF-α, and IL-8 [94]. These effects occur for nanocrystalline silver, but not silver nitrate, where the only silver species is Ag^+ [94]. Not only does nanocrystalline silver have an effect when applied directly to wounds or areas of inflammation, but it also has an indirect effect by inducing apoptosis in inflammatory cells and reducing levels of inflammatory markers distant to the site of application [99].

Smaller grain sizes are associated with a greater percentage of silver oxide, because nanocrystals of silver oxide disrupt the growth of metallic silver crystals, stabilizing the grain sizes at the time of sputtering [100]. This grain size effect was confirmed in a study where heat treatment of nanocrystalline silver caused diffusion of oxygen, then the grains would anneal, increasing the grain size and decreasing the quantity of soluble silver released, leading to decreased antibacterial effects [100].

Silver solutions can be made by soaking nanocrystalline silver films in water[91]. The dissolution profile is rapid at first, then slower until a plateau is reached[91]. The rate and total release depend on the surface area, composition, and film thickness[91]. Further to this, nanocrystalline silver solutions still have anti-inflammatory properties when tested in a pig dermal model of inflammation [102]. They reduced MMP expression and levels of TNF-α and IL-8[102]. The anti-inflammatory properties are not necessarily correlated with the total quantity of silver, because only some silver species are anti-inflammatory[102].

Silver nanoparticles have been more broadly studied than nanocrystalline silver and can contribute to the understanding of the anti-inflammatory effects of silver. One study shows an increased release of pro-inflammatory cytokines such as IL-8, IL-6, ICAM-1 and MCP-1 when treated with silver nanoparticles *in vitro*[103]. Silver nanoparticles were also embedded in polyvinyl alcohol and tetraethoxysilane polymer gel matrix materials, and while they showed antibacterial properties, they also showed strong cell attachment[104]. Silver nanoparticle-polymer combination is also used in a multi-layer polyelectrolyte wound dressings to reduce the bacterial load on contaminated wounds in mice by five log reductions [105].

During *in vitro* tests with keratinocytes and fibroblasts, the inflammatory cytokines TNF-α and VEGF, and inflammatory mediator COX-2 decreased when cells were treated with high concentrations of silver nanoparticles[106]. In porcine retinal endothelial cells, silver nanoparticles inhibit VEGF and IL-1β, particularly at increasing concentrations; both of these increase cell permeability and proliferation [107]. In these same cells, cytotoxicity depended on silver concentration[107]. Silver nanoparticles in solution were used in a limited study for preventing peritoneal adhesions in rats, although the effectiveness may have been limited by the delivery mechanism[108]. An increase in bioavailable silver comes with decreasing nanoparticle size, which increases the total surface area, and is one of the most important factors in determining nanoparticle antibacterial effectiveness[109]. The delivery mechanism is especially important for bacterial toxicity, as the surface charge and coating change how bacteria interact with the particle [109]. Silver nanoparticles were used to decrease adhesion scoring and the presence of

macrophages and neutrophils after 14 days, decreasing IFN-γ production and decreasing TNF-α [110]. Silver nitrate did not reduce adhesions, and even increased adhesion scores compared to controls[110].

Biological Properties of Gold

Gold is the most noble metal and is therefore less reactive than silver, and is resistant to oxidation or ionization [77], [89]. Gold is used most commonly in medical applications as a component of anti-inflammatory rheumatoid arthritis drugs auranofin and gold sodium thiomalate (GST).

It was first reported in 1977 publications that gold salts such as GST inhibited lymphocyte proliferation and cellular functions[111], [112]. When cultured with GST, monocyte functions like adherence and spreading were affected, although not cell viability[113]. Lysosomal enzyme activity was also suppressed in monocytes[113]. Monocytes also have a reduced responsiveness to lymphokines, and without functional monocytes, the lymphocytes are unable to respond to antigens[111], [114]. Markers of monocyte maturation were inhibited by GST, including a loss of peroxidase activity[115]. B-cell functions are suppressed by gold compounds at lower concentrations than would be needed to suppress T-cells by interfering with their activation[116]. Auranofin derivatives decreased lymphocyte proliferation and ROS production by neutrophils[117].

There is a dose and time dependent effect of gold drugs *in vitro*, with greater effects seen with addition earlier in the cell culture period and at higher doses[114], [118]. Another study suggested a bimodal effect, at least for *in vitro* isolated cultures[119]. On isolated neutrophils, a concentration of 1 µM auranofin enhanced oxygen radical formation and encouraged apoptosis, while 5 µM auranofin inhibited oxygen radical formation and necrosis was prevalent[119].

Auranofin had a greater effect than GST at suppressing polymorphonuclear cell lysosomal release, as well as reducing cell aggregation, degranulation, and glucose oxidation[120]. Auranofin alone, compared to other available gold salt compounds, was able to have a significant effect on edema[118]. Auranofin had a greater effect on increasing superoxide production[118]. Auranofin and its derivatives have a dose-dependent suppression of COX-2[117], [121]. Auranofin also has bactericidal activities. It is especially potent against Gram positive organisms, such as *S. aureus*, that lack a conventional redox couple and are therefore more susceptible to the thiol reactivity of auranofin[39]. Auranofin reacts with cysteine groups and sensitizes *S. aureus* to oxidizing agents[122].

When GST was injected intramuscularly in human patients with rheumatoid arthritis, biopsied tissue showed a reduction in inflammatory monocytes and macrophages[123]. By 12 weeks, IL-1α, IL-1β, IL-6, and TNF-α were reduced, and clinical symptoms improved[123]. In later weeks, there was a decrease in macrophages, but not monocytes, suggesting that monocyte differentiation or adhesion to endothelial cells is disrupted[123]. Another study on patient blood recognized that CD14+ monocytes were required for gold to have an effect on IL-10 [124]. In that study, IL-10 and IL-6 increased, and IL-2 and IFN-γ were reduced, with no change in TNF-α[124]. Auranofin also induced IL-6, and inhibited protein expression of fibrinogen, haptoglobin, C3 complement, and VEGF[125]. As a cancer treatment drug, auranofin increased intracellular calcium, which is part of the pathway for apoptosis[126].

Concerns of side effects and cytotoxicity seem to be mostly associated with Au(III), which is a strong oxidizer and causes T cell sensitization[127], [128], [129]. Au^+ is unstable in physiological conditions, and is able to be reduced to Au^0 or oxidized to Au^{3+}[127], [130]. Gold (III) complexes with chloride were found to be very reactive with proteins, binding non-specifically to free cysteine residues on albumin, or remaining in the III oxidation state to bind to DNA[130], [131].[132]

Gold and silver-gold nanoparticles are a more recent application of gold's anti-inflammatory properties. *In vivo* and *in vitro,* gold nanoparticles reduced markers of oxidative stress such as IL-6, IL-8, and TNF-α[133], [134]. Gold nanoparticles had the smallest nanoparticle size compared to silver-gold or silver-only nanoparticles and reduced leukocyte proliferation and migration[132]. Gold nanoparticles also had an effect on oxidative stress markers, such as TNF-α, IL-1β, COX-2, and fibrosis, which is also recognized as an effect of auranofin and GST [135], [136].

Gold may also have promising effects for adhesion prevention because of these anti-inflammatory properties. Gold has been incorporated into nanocrystalline materials by sputtering with silver-gold alloys[137]. When compared to nanocrystalline silver, nanocrystalline silver-gold films have smaller grain sizes, reduced anti-bacterial properties, and may encourage silver release into solution[137].

Animal Models of Adhesions

Animal models are useful for developing and testing medical treatments, although results from animal models may not translate directly to human responses. Variation in results can depend on the species of animal used and the design of the study. As such, it is important to understand the anatomical and physiological differences between humans and the chosen animal model. The best choice of animal model has results that will translate most closely to humans. In adhesion research, the intention is to use an

animal model and adhesion production method that will form adhesions consistently and with similar severity, appearance, or pathophysiology to humans. When comparing possible methods to create adhesions, greater tissue trauma and foreign material involvement increase the consistency and extent of adhesions [138].

Both rats and mice are generally considered to be good animal models for general use anatomy, surgery, and pathology. Particularly, rats are most commonly used in surgical adhesion research, partly because they are small, easy to manipulate, and inexpensive. Rats have similar anatomy in the abdominal cavity as described for humans [139]. They have a single layer of parietal peritoneum lining the abdominal cavity as do humans [139]. Small numbers of resident macrophages, lymphocytes, and neutrophils exist in tissue[139]. There are relatively fewer neutrophils and more lymphocytes in the blood of rats when compared to humans[140]. Rats don't have a cecal appendix or gall bladder, and have a different colon shape to humans[140]. Rats have a more rapid coagulation system compared to humans[141]. They have similar levels of fibrinogen and more platelets and those platelets are less responsive to thrombin, supporting the faster clotting time[141]. They have a lower risk of wound infection and they heal wounds by contraction, unlike humans[141].

Pigs are anatomically and physiologically similar to humans, making them good anatomical and surgical models, with fixed skin and a tight attachment to subcutaneous tissues[140]. In some cases, pigs are used as models for adhesion research, and while they have similar anatomy, size, genetics, and healing processes to humans, they are larger and more challenging to handle and more expensive than rats, which explains their limited use. Pigs are used to study adhesions in models including hernia mesh repair, laparotomy, uterine horn injury, and ileocecal resection[142], [143], [144], [145]. One study used a laparoscopic technique to create an abdominal wall defect on one side, where each pig acted as their own controls because of their size[31]. Another study used nine pigs, with four test materials per pig, following up over 30 days [146]. Pigs and rats have also been directly compared for the tolerance and degradation of polymer scaffolds, finding that degradation occurred faster in pigs, but the procedures could be successfully used for both animal models[147]. No other discussion of model difference is mentioned, except to note that pigs are a superior animal model for their similarity to humans[147].

The most common method of inducing adhesions is some variation of the cecal-sidewall method. In brief, after an open midline incision into the abdominal cavity, the cecum is removed, rubbed or abraded with gauze or a scalpel until bleeding occurs, and the corresponding surface of the abdominal wall peritoneum is most often excised, including a layer of the superficial muscle[27], [28], [34], [46], [57], [70], [138], [148], [149], [150], [151]. This area is fixed, usually 2 cm^2 for rats[27], [28], [149]. Sometimes they are

left to dry for 5-10 minutes in open air [27], [28], [68]. Some studies use abrasion of the peritoneum instead of removing tissue[46], [68], [138], [148], [152]. Additional suturing in the abdominal cavity can also be included to generate a foreign body response, increasing the inflammatory reaction[30], [34], [56], [149], [153]. Meshes are sometimes also included[65], [154]. A powdered chalk, Kaolin, is also used during the simulated surgery for this same reason[72], [155]. Another common method for inducing and studying adhesions is the use of ischemic buttons. Abdominal tissue is stapled or sutured, resulting in an inflammatory response[23], [41], [156], [157]. Ischemic buttons can be ineffective for sufficiently challenging the adhesion treatment, as this method creates inflammation only, and does not include wound healing [41], [138], [156]. Most often groups of between 6 and 35 rats are used for each experimental condition[27], [28], [29], [35], [56], [57], [152]. Most studies assess adhesions after 7 or 10 days, which corresponds to the expected timeline for abdominal trauma healing[27], [28], [154], [156], [157]. Some studies extend beyond this timeline[30], [57], [60], [152], [154].

A number of rating systems exist to assess adhesions. All are semi-quantitative scales, from 0-3 or 0-4 to address various aspects of adhesions such as number, extent, area of coverage, strength, and location. While some studies will develop their own scale to include some or all of these criteria, others will use the scales developed by other researchers. The Lauder score uses one number to take into account the quantity, strength, and distribution [34], [65], [149], [158]. The Hoffmann score includes a rating for the area of formation, strength required to break, and extent, then provides the final sum of these categorical scores [64], [65], [149]. The Zuhlke score includes both the extent of adhesion coverage and their tenacity[33]. The Leach scoring method has scores for percent of wound area involved, vascularity, and traction strength for a total score out of ten [32], [159]. Nair scoring grades adhesions with a scale that accounts for the number and location of adhesions [33], [58], [68], [160]. Fibrosis and inflammation can also be semi-quantitatively scored from histological images of tissue[47], [56], [58], [150]. Adhesions can be quantitatively scored by force required to break[27], [28].

Research Hypothesis

As discussed above, there is a significant clinical burden of surgical adhesions. Polymer-based gel treatments are a promising avenue for preventing adhesions at the time of surgery. In the literature, the most commonly used polymers are hyaluronic acid and carboxymethyl cellulose. The combination of these polymers and nanocrystalline silver will prevent adhesions by protecting tissue surfaces in the abdominal cavity and reducing inflammation. Nanocrystalline silver is a proven antibacterial and anti-inflammatory material. Tuning the sputtering conditions for creation of the film will increase the amount

of silver deposited, and therefore the amount released into solution. The use of a silver-gold alloy in sputtering will change the material properties and may result in better anti-inflammatory and healing properties in a wound dressing.

References

[1] S. Munireddy, S. L. Kavalukas, and A. Barbul, "Intra-abdominal Healing: Gastrointestinal Tract and Adhesions," *Surg. Clin. North Am.*, vol. 90, no. 6, pp. 1227–1236, Dec. 2010, doi: 10.1016/j.suc.2010.08.002.

[2] D. Brüggmann, G. Tchartchian, M. Wallwiener, K. Münstedt, H.-R. Tinneberg, and A. Hackethal, "Intra-abdominal Adhesions," *Dtsch. Ärztebl. Int.*, vol. 107, no. 44, pp. 769–775, Nov. 2010, doi: 10.3238/arztebl.2010.0769.

[3] R. T. Beyene, S. L. Kavalukas, and A. Barbul, "Intra-abdominal adhesions: Anatomy, physiology, pathophysiology, and treatment," *Curr. Probl. Surg.*, vol. 52, no. 7, pp. 271–319, Jul. 2015, doi: 10.1067/j.cpsurg.2015.05.001.

[4] W. H. McBride, K. Mason, H. R. Withers, and C. Davis, "Effect of interleukin 1, inflammation, and surgery on the incidence of adhesion formation and death after abdominal irradiation in mice," *Cancer Res.*, vol. 49, no. 1, pp. 169–173, Jan. 1989.

[5] N. Tabibian, E. Swehli, A. Boyd, A. Umbreen, and J. H. Tabibian, "Abdominal adhesions: A practical review of an often overlooked entity," *Ann. Med. Surg.*, vol. 15, pp. 9–13, Mar. 2017, doi: 10.1016/j.amsu.2017.01.021.

[6] M.-A. Weibel and G. Majno, "Peritoneal adhesions and their relation to abdominal surgery: A postmortem study," *Am. J. Surg.*, vol. 126, no. 3, pp. 345–353, Sep. 1973, doi: 10.1016/S0002-9610(73)80123-0.

[7] R. Corona, J. Verguts, R. Schonman, M. M. Binda, K. Mailova, and P. R. Koninckx, "Postoperative inflammation in the abdominal cavity increases adhesion formation in a laparoscopic mouse model," *Fertil. Steril.*, vol. 95, no. 4, pp. 1224–1228, Mar. 2011, doi: 10.1016/j.fertnstert.2011.01.004.

[8] M. A. Grevious, M. Cohen, S. R. Shah, and P. Rodriguez, "Structural and Functional Anatomy of the Abdominal Wall," *Clin. Plast. Surg.*, vol. 33, no. 2, pp. 169–179, Apr. 2006, doi: 10.1016/j.cps.2005.12.005.

[9] G. M. Boland and R. J. Weigel, "Formation and Prevention of Postoperative Abdominal Adhesions," *J. Surg. Res.*, vol. 132, no. 1, pp. 3–12, May 2006, doi: 10.1016/j.jss.2005.12.002.

[10] M. M. P. J. Reijnen, R. P. Bleichrodt, and H. van Goor, "Pathophysiology of intra-abdominal adhesion and abscess formation, and the effect of hyaluronan," *Br. J. Surg.*, vol. 90, no. 5, pp. 533–541, May 2003, doi: 10.1002/bjs.4141.

[11] H. van Goor, "Consequences and complications of peritoneal adhesions," *Colorectal Dis. Off. J. Assoc. Coloproctology G. B. Irel.*, vol. 9 Suppl 2, pp. 25–34, Oct. 2007, doi: 10.1111/j.1463-1318.2007.01358.x.

[12] M. C. Parker *et al.*, "Postoperative adhesions: Ten-year follow-up of 12,584 patients undergoing lower abdominal surgery," *Dis. Colon Rectum*, vol. 44, no. 6, pp. 822–829, Jun. 2001, doi: 10.1007/BF02234701.

[13] H. W. Grant *et al.*, "Adhesions after abdominal surgery in children," *J. Pediatr. Surg.*, vol. 43, no. 1, pp. 152–157, Jan. 2008, doi: 10.1016/j.jpedsurg.2007.09.038.

[14] D. Menzies, M. Parker, R. Hoare, and A. Knight, "Small bowel obstruction due to postoperative adhesions: treatment patterns and associated costs in 110 hospital admissions.," *Ann. R. Coll. Surg. Engl.*, vol. 83, no. 1, pp. 40–46, Jan. 2001.

[15] R. P. G. ten Broek *et al.*, "Burden of adhesions in abdominal and pelvic surgery: systematic review and met-analysis," *BMJ*, vol. 347, p. f5588, Oct. 2013, doi: 10.1136/bmj.f5588.

[16] H. Ellis and A. Crowe, "Medico-legal consequences of post-operative intra-abdominal adhesions," *Int. J. Surg.*, vol. 7, no. 3, pp. 187–191, Jan. 2009, doi: 10.1016/j.ijsu.2009.04.004.

[17] M. Mollà *et al.*, "Influence of dose-rate on inflammatory damage and adhesion molecule expression after abdominal radiation in the rat," *Int. J. Radiat. Oncol.*, vol. 45, no. 4, pp. 1011–1018, Nov. 1999, doi: 10.1016/S0360-3016(99)00286-2.

[18] A. H. Maciver, M. McCall, and A. M. James Shapiro, "Intra-abdominal adhesions: Cellular mechanisms and strategies for prevention," *Int. J. Surg.*, vol. 9, no. 8, pp. 589–594, Jan. 2011, doi: 10.1016/j.ijsu.2011.08.008.

[19] D. S. Foster *et al.*, "Elucidating the fundamental fibrotic processes driving abdominal adhesion formation," *Nat. Commun.*, vol. 11, no. 1, p. 4061, Aug. 2020, doi: 10.1038/s41467-020-17883-1.

[20] T. Ito *et al.*, "Cell barrier function of resident peritoneal macrophages in post-operative adhesions," *Nat. Commun.*, vol. 12, p. 2232, Apr. 2021, doi: 10.1038/s41467-021-22536-y.

[21] S. M. Liebman, J. C. Langer, J. S. Marshall, and S. M. Collins, "Role of mast cells in peritoneal adhesion formation," *Am. J. Surg.*, vol. 165, no. 1, pp. 127–130, Jan. 1993, doi: 10.1016/S0002-9610(05)80415-5.

[22] M. N. Vipond, S. A. Whawell, H. A. F. Dudley, and J. N. Thompson, "Peritoneal fibrinolytic activity and intra-abdominal adhesions," *The Lancet*, vol. 335, no. 8698, pp. 1120–1122, May 1990, doi: 10.1016/0140-6736(90)91125-T.

[23] A. J. Esposito, S. J. Heydrick, M. R. Cassidy, J. Gallant, A. F. Stucchi, and J. M. Becker, "Substance P is an early mediator of peritoneal fibrinolytic pathway genes and promotes intra-abdominal adhesion formation," *J. Surg. Res.*, vol. 181, no. 1, pp. 25–31, May 2013, doi: 10.1016/j.jss.2012.05.056.

[24] P. A. Lucas, D. J. Warejcka, H. E. Young, and B. Y. Lee, "Formation of Abdominal Adhesions Is Inhibited by Antibodies to Transforming Growth Factor-β1," *J. Surg. Res.*, vol. 65, no. 2, pp. 135–138, Oct. 1996, doi: 10.1006/jsre.1996.0355.

[25] G. Wei *et al.*, "Inhibition of cyclooxygenase-2 prevents intra-abdominal adhesions by decreasing activity of peritoneal fibroblasts," *Drug Des. Devel. Ther.*, vol. 9, pp. 3083–3098, Jun. 2015, doi: 10.2147/DDDT.S80221.

[26] A. I. S. Moretti *et al.*, "Nitric oxide modulates metalloproteinase-2, collagen deposition and adhesion rate after polypropylene mesh implantation in the intra-abdominal wall," *Acta Biomater.*, vol. 8, no. 1, pp. 108–115, Jan. 2012, doi: 10.1016/j.actbio.2011.08.004.

[27] E. S. Harris, R. F. Morgan, and G. T. Rodeheaver, "Analysis of the kinetics of peritoneal adhesion formation in the rat and evaluation of potential antiadhesive agents," *Surgery*, vol. 117, no. 6, pp. 663–669, Jun. 1995, doi: 10.1016/S0039-6060(95)80010-7.

[28] P. B. Arnold, C. W. Green, P. A. Foresman, and G. T. Rodeheaver, "Evaluation of resorbable barriers for preventing surgical adhesions," *Fertil. Steril.*, vol. 73, no. 1, pp. 157–161, Jan. 2000, doi: 10.1016/S0015-0282(99)00464-1.

[29] L.-X. Lin, F. Yuan, H.-H. Zhang, N.-N. Liao, J.-W. Luo, and Y.-L. Sun, "Evaluation of surgical anti-adhesion products to reduce postsurgical intra-abdominal adhesion formation in a rat model," *PLOS ONE*, vol. 12, no. 2, p. e0172088, Feb. 2017, doi: 10.1371/journal.pone.0172088.

[30] B. W. J. Hellebrekers, G. C. M. Trimbos-Kemper, C. A. van Blitterswijk, E. A. Bakkum, and J. B. M. Z. Trimbos, "Effects of five different barrier materials on postsurgical adhesion formation in the rat," *Hum. Reprod.*, vol. 15, no. 6, pp. 1358–1363, Jun. 2000, doi: 10.1093/humrep/15.6.1358.

[31] K. Kramer, N. Senninger, H. Herbst, and W. Probst, "Effective Prevention of Adhesions With Hyaluronate," *Arch. Surg.*, vol. 137, no. 3, pp. 278–282, Mar. 2002, doi: 10.1001/archsurg.137.3.278.

[32] L. Allègre *et al.*, "A new bioabsorbable polymer film to prevent peritoneal adhesions validated in a post-surgical animal model," *PLoS ONE*, vol. 13, no. 11, p. e0202285, Nov. 2018, doi: 10.1371/journal.pone.0202285.

[33] S. van Steensel, H. Liu, E. H. H. Mommers, K. Lenaerts, and N. D. Bouvy, "Comparing Five New Polymer Barriers for the Prevention of Intra-abdominal Adhesions in a Rat Model," *J. Surg. Res.*, vol. 243, pp. 453–459, Nov. 2019, doi: 10.1016/j.jss.2019.05.043.

[34] D. Poehnert *et al.*, "Evaluation of the Effectiveness of Peritoneal Adhesion Prevention Devices in a Rat Model," *Int. J. Med. Sci.*, vol. 13, no. 7, pp. 524–532, Jun. 2016, doi: 10.7150/ijms.15167.

[35] J. A. Bello-Guerrero, C. A. Cruz-Santiago, and J. Luna-Martínez, "Pirfenidone vs Sodium Hyaluronate/carboxymethyl cellulose as Prevention of the Formation of Intra-abdominal Adhesions

After Colonic Surgery. A Randomized Study in an Experimental Model," *Cir. Esp. Engl. Ed.*, vol. 94, no. 1, pp. 31–37, Jan. 2016, doi: 10.1016/j.cireng.2015.06.013.

[36] E. Ersoy, V. Ozturk, A. Yazgan, M. Ozdogan, and H. Gundogdu, "Comparison of the Two Types of Bioresorbable Barriers to Prevent Intra-Abdominal Adhesions in Rats," *J. Gastrointest. Surg.*, vol. 13, no. 2, pp. 282–286, Feb. 2009, doi: 10.1007/s11605-008-0678-5.

[37] K. E. Greenawalt, M. J. Colt, R. L. Corazzini, M. C. Krauth, and L. Holmdahl, "A Membrane Slurry Reduces Postoperative Adhesions in Rat Models of Abdominal Surgery," *J. Surg. Res.*, vol. 168, no. 1, pp. e25–e30, Jun. 2011, doi: 10.1016/j.jss.2010.02.009.

[38] Z. Cohen *et al.*, "Prevention of Postoperative Abdominal Adhesions by a Novel, Glycerol/Sodium Hyaluronate/Carboxymethylcellulose-Based Bioresorbable Membrane: A Prospective, Randomized, Evaluator-Blinded Multicenter Study," *Dis. Colon Rectum*, vol. 48, no. 6, pp. 1130–1139, Jun. 2005, doi: 10.1007/s10350-004-0954-8.

[39] S. Fujii *et al.*, "Reduction of postoperative abdominal adhesion and ileus by a bioresorbable membrane," *Hepatogastroenterology.*, vol. 56, no. 91–92, pp. 725–728, May 2009.

[40] S. Jiang, W. Wang, H. Yan, and C. Fan, "Prevention of Intra-Abdominal Adhesion by Bi-Layer Electrospun Membrane," *Int. J. Mol. Sci.*, vol. 14, no. 6, Art. no. 6, Jun. 2013, doi: 10.3390/ijms140611861.

[41] R. R. M. Vogels *et al.*, "A new poly(1,3-trimethylene carbonate) film provides effective adhesion reduction after major abdominal surgery in a rat model," *Surgery*, vol. 157, no. 6, pp. 1113–1120, Jun. 2015, doi: 10.1016/j.surg.2015.02.004.

[42] J. Zhou, C. Elson, and T. D. G. Lee, "Reduction in postoperative adhesion formation and re-formation after an abdominal operation with the use of N, O - carboxymethyl chitosan," *Surgery*, vol. 135, no. 3, pp. 307–312, Mar. 2004, doi: 10.1016/j.surg.2003.07.005.

[43] X. Liu *et al.*, "Berberine prevents primary peritoneal adhesion and adhesion reformation by directly inhibiting TIMP-1," *Acta Pharm. Sin. B*, vol. 10, no. 5, pp. 812–824, May 2020, doi: 10.1016/j.apsb.2020.02.003.

[44] E. Zhang *et al.*, "Fouling-resistant zwitterionic polymers for complete prevention of postoperative adhesion," *Proc. Natl. Acad. Sci. U. S. A.*, vol. 117, no. 50, pp. 32046–32055, Dec. 2020, doi: 10.1073/pnas.2012491117.

[45] N. Z. Dreger *et al.*, "Zwitterionic amino acid-based Poly(ester urea)s suppress adhesion formation in a rat intra-abdominal cecal abrasion model," *Biomaterials*, vol. 221, p. 119399, Nov. 2019, doi: 10.1016/j.biomaterials.2019.119399.

[46] S. Avital, T. J. Bollinger, J. D. Wilkinson, F. Marchetti, M. D. Hellinger, and L. R. Sands, "Preventing Intra-Abdominal Adhesions With Polylactic Acid Film: An Animal Study," *Dis. Colon Rectum*, vol. 48, no. 1, pp. 153–157, Jan. 2005, doi: 10.1007/s10350-004-0748-z.

[47] E. Ersoy, V. Ozturk, A. Yazgan, M. Ozdogan, and H. Gundogdu, "Effect of Polylactic Acid Film Barrier on Intra-Abdominal Adhesion Formation," *J. Surg. Res.*, vol. 147, no. 1, pp. 148–152, Jun. 2008, doi: 10.1016/j.jss.2007.09.005.

[48] J. Li *et al.*, "Prevention of intra-abdominal adhesion using electrospun PEG/PLGA nanofibrous membranes," *Mater. Sci. Eng. C*, vol. 78, pp. 988–997, Sep. 2017, doi: 10.1016/j.msec.2017.04.017.

[49] A. Kishan *et al.*, "In vivo performance of a bilayer wrap to prevent abdominal adhesions," *Acta Biomater.*, vol. 115, pp. 116–126, Oct. 2020, doi: 10.1016/j.actbio.2020.08.021.

[50] O. R. Tarhan, I. Barut, and M. Sezik, "An evaluation of normal saline and taurolidine on intra-abdominal adhesion formation and peritoneal fibrinolysis," *J. Surg. Res.*, vol. 144, no. 1, pp. 151–157, Jan. 2008, doi: 10.1016/j.jss.2007.09.006.

[51] M. Javaherzadeh, A. Shekarchizadeh, M. Kafaei, A. Mirafshrieh, N. Mosaffa, and B. Sabet, "Effects of Intraperitoneal Administration of Simvastatin in Prevention of Postoperative Intra-abdominal Adhesion Formation in Animal Model of Rat," *Bull. Emerg. Trauma*, vol. 4, no. 3, pp. 156–160, Jul. 2016.

[52] A. J. Charboneau, J. P. Delaney, and G. Beilman, "Fucoidans inhibit the formation of post-operative abdominal adhesions in a rat model," *PLOS ONE*, vol. 13, no. 11, p. e0207797, Nov. 2018, doi: 10.1371/journal.pone.0207797.

[53] E. J. Macarak *et al.*, "Trametinib prevents mesothelial-mesenchymal transition and ameliorates abdominal adhesion formation," *J. Surg. Res.*, vol. 227, pp. 198–210, Jul. 2018, doi: 10.1016/j.jss.2018.02.012.

[54] F. Catena, L. Ansaloni, S. Di Saverio, A. D. Pinna, and On Behalf of the World Society of Emergency Surgery, "P.O.P.A. Study: Prevention of Postoperative Abdominal Adhesions by Icodextrin 4% Solution After Laparotomy for Adhesive Small Bowel Obstruction. A Prospective Randomized Controlled Trial," *J. Gastrointest. Surg.*, vol. 16, no. 2, pp. 382–388, Feb. 2012, doi: 10.1007/s11605-011-1736-y.

[55] R. A. Lang, P. M. Grüntzig, C. Weisgerber, C. Weis, E. K. Odermatt, and M. H. Kirschner, "Polyvinyl alcohol gel prevents abdominal adhesion formation in a rabbit model," *Fertil. Steril.*, vol. 88, no. 4, Supplement, pp. 1180–1186, Oct. 2007, doi: 10.1016/j.fertnstert.2007.01.108.

[56] T. Karaca, A. U. Gözalan, Ö. Yoldaş, B. Ç. Bilgin, and A. Tezer, "Effects of tamoxifen citrate on postoperative intra-abdominal adhesion in a rat model," *Int. J. Surg.*, vol. 11, no. 1, pp. 68–72, Jan. 2013, doi: 10.1016/j.ijsu.2012.11.015.

[57] Z. Bayhan *et al.*, "Antiadhesive and anti-inflammatory effects of pirfenidone in postoperative intra-abdominal adhesion in an experimental rat model," *J. Surg. Res.*, vol. 201, no. 2, pp. 348–355, Apr. 2016, doi: 10.1016/j.jss.2015.11.033.

[58] G. Wei *et al.*, "Gallic Acid Attenuates Postoperative Intra-Abdominal Adhesion by Inhibiting Inflammatory Reaction in a Rat Model," *Med. Sci. Monit. Int. Med. J. Exp. Clin. Res.*, vol. 24, pp. 827–838, Feb. 2018, doi: 10.12659/MSM.908550.

[59] Y. Fu *et al.*, "Nintedanib, a multitarget tyrosine kinase inhibitor, suppresses postoperative peritoneal adhesion formation in a rat model," *Surgery*, vol. 170, no. 3, pp. 806–812, Sep. 2021, doi: 10.1016/j.surg.2021.03.055.

[60] M. Oncel *et al.*, "The Effectiveness of Systemic Antibiotics in Preventing Postoperative, Intraabdominal Adhesions in an Animal Model," *J. Surg. Res.*, vol. 101, no. 1, pp. 52–55, Nov. 2001, doi: 10.1006/jsre.2001.6245.

[61] A. K. Greene *et al.*, "Prevention of Intra-abdominal Adhesions Using the Antiangiogenic COX-2 Inhibitor Celecoxib," *Ann. Surg.*, vol. 242, no. 1, pp. 140–146, Jul. 2005, doi: 10.1097/01.sla.0000167847.53159.c1.

[62] K. Iwasaki *et al.*, "Pharmacological Mobilization and Recruitment of Stem Cells in Rats Stops Abdominal Adhesions After Laparotomy," *Sci. Rep.*, vol. 9, no. 1, p. 7149, May 2019, doi: 10.1038/s41598-019-43734-1.

[63] M. Berkesoglu, Y. Y. Karabulut, D. D. Yildirim, O. M. Turkmenoglu, and M. M. Dirlik, "Topical Application of High-Dose Mesna Prevents Adhesion Formation: An Experimental Animal Study," *J. Surg. Res.*, vol. 251, pp. 152–158, Jul. 2020, doi: 10.1016/j.jss.2020.01.027.

[64] N. Hoffmann *et al.*, "Choice of Hemostatic Agent Influences Adhesion Formation in a Rat Cecal Adhesion Model," *J. Surg. Res.*, vol. 155, pp. 77–81, Nov. 2008, doi: 10.1016/j.jss.2008.08.008.

[65] M. Winny *et al.*, "Adhesion Prevention Efficacy of Composite Meshes Parietex®, Proceed® and 4DryField® PH Covered Polypropylene Meshes in an IPOM Rat Model," *Int. J. Med. Sci.*, vol. 13, no. 12, pp. 936–941, Nov. 2016, doi: 10.7150/ijms.16215.

[66] M. M. P. J. Reijnen, E. M. Skrabut, V. A. Postma, J. W. Burns, and H. van Goor, "Polyanionic Polysaccharides Reduce Intra-abdominal Adhesion and Abscess Formation in a Rat Peritonitis Model," *J. Surg. Res.*, vol. 101, no. 2, pp. 248–253, Dec. 2001, doi: 10.1006/jsre.2001.6288.

[67] J. E. Lee *et al.*, "Oxaliplatin-loaded chemically cross-linked hydrogels for prevention of postoperative abdominal adhesion and colorectal cancer therapy," *Int. J. Pharm.*, vol. 565, pp. 50–58, Jun. 2019, doi: 10.1016/j.ijpharm.2019.04.065.

[68] G. Wei, C. Zhou, G. Wang, L. Fan, K. Wang, and X. Li, "Keratinocyte Growth Factor Combined with a Sodium Hyaluronate Gel Inhibits Postoperative Intra-Abdominal Adhesions," *Int. J. Mol. Sci.*, vol. 17, no. 10, p. 1611, Sep. 2016, doi: 10.3390/ijms17101611.

[69] Y. Yeo *et al.*, "In situ cross-linkable hyaluronic acid hydrogels prevent post-operative abdominal adhesions in a rabbit model," *Biomaterials*, vol. 27, no. 27, pp. 4698–4705, Sep. 2006, doi: 10.1016/j.biomaterials.2006.04.043.

[70] C. A. Falabella, M. M. Melendez, L. Weng, and W. Chen, "Novel Macromolecular Crosslinking Hydrogel to Reduce Intra-Abdominal Adhesions," *J. Surg. Res.*, vol. 159, no. 2, pp. 772–778, Apr. 2010, doi: 10.1016/j.jss.2008.09.035.

[71] H. Li *et al.*, "Antibacterial, hemostasis, adhesive, self-healing polysaccharides-based composite hydrogel wound dressing for the prevention and treatment of postoperative adhesion," *Mater. Sci. Eng. C*, vol. 123, p. 111978, Apr. 2021, doi: 10.1016/j.msec.2021.111978.

[72] R. S. Vediappan *et al.*, "Prevention of adhesions post-abdominal surgery: Assessing the safety and efficacy of Chitogel with Deferiprone in a rat model," *PLOS ONE*, vol. 16, no. 1, p. e0244503, Jan. 2021, doi: 10.1371/journal.pone.0244503.

[73] S. P. Pasaribu, M. Ginting, I. Masmur, J. Kaban, and Hestina, "Silver chloride nanoparticles embedded in self-healing hydrogels with biocompatible and antibacterial properties," *J. Mol. Liq.*, vol. 310, p. 113263, Jul. 2020, doi: 10.1016/j.molliq.2020.113263.

[74] K. Nešović *et al.*, "Chitosan-based hydrogel wound dressings with electrochemically incorporated silver nanoparticles – In vitro study," *Eur. Polym. J.*, vol. 121, p. 109257, Dec. 2019, doi: 10.1016/j.eurpolymj.2019.109257.

[75] P. Shende, B. Oza, and R. S. Gaud, "Silver-doped titanium dioxide nanoparticles encapsulated in chitosan–PVA film for synergistic antimicrobial activity," *Int. J. Polym. Mater. Polym. Biomater.*, vol. 67, no. 18, pp. 1080–1086, Dec. 2018, doi: 10.1080/00914037.2017.1417290.

[76] R. E. Burrell and P. Nadworny, "Nanocrystalline Silver: Novel Structure and Activity," in *The Third International Conference on the Development of Biomedical Engineering in Vietnam*, vol. 27, V. Van Toi and T. Q. D. Khoa, Eds., in IFMBE Proceedings, vol. 27. , Berlin, Heidelberg: Springer Berlin Heidelberg, 2010, pp. 6–9. doi: 10.1007/978-3-642-12020-6_2.

[77] A. B. G. Lansdown, "Silver and Gold," in *Patty's Toxicology*, American Cancer Society, 2012, pp. 75–112. doi: 10.1002/0471435139.tox026.pub2.

[78] CH. Ramamurthy *et al.*, "The extra cellular synthesis of gold and silver nanoparticles and their free radical scavenging and antibacterial properties," *Colloids Surf. B Biointerfaces*, vol. 102, pp. 808–815, Feb. 2013, doi: 10.1016/j.colsurfb.2012.09.025.

[79] S. y. Liau, D. c. Read, W. j. Pugh, J. r. Furr, and A. d. Russell, "Interaction of silver nitrate with readily identifiable groups: relationship to the antibacterialaction of silver ions," *Lett. Appl. Microbiol.*, vol. 25, no. 4, pp. 279–283, 1997, doi: 10.1046/j.1472-765X.1997.00219.x.

[80] G. Mulley, A. T. A. Jenkins, and N. R. Waterfield, "Inactivation of the Antibacterial and Cytotoxic Properties of Silver Ions by Biologically Relevant Compounds," *PLOS ONE*, vol. 9, no. 4, p. e94409, Apr. 2014, doi: 10.1371/journal.pone.0094409.

[81] P. D. Bragg and D. J. Rainnie, "The effect of silver ions on the respiratory chain of *Escherichia coli*," *Can. J. Microbiol.*, vol. 20, no. 6, pp. 883–889, Jun. 1974, doi: 10.1139/m74-135.

[82] M. Yamanaka, K. Hara, and J. Kudo, "Bactericidal Actions of a Silver Ion Solution on Escherichia coli, Studied by Energy-Filtering Transmission Electron Microscopy and Proteomic Analysis," *Appl. Environ. Microbiol.*, vol. 71, no. 11, pp. 7589–7593, Nov. 2005, doi: 10.1128/AEM.71.11.7589-7593.2005.

[83] Y. Matsumura, K. Yoshikata, S. Kunisaki, and T. Tsuchido, "Mode of Bactericidal Action of Silver Zeolite and Its Comparison with That of Silver Nitrate," *Appl. Environ. Microbiol.*, vol. 69, no. 7, pp. 4278–4281, Jul. 2003, doi: 10.1128/AEM.69.7.4278-4281.2003.

[84] C. Beer, R. Foldbjerg, Y. Hayashi, D. S. Sutherland, and H. Autrup, "Toxicity of silver nanoparticles—Nanoparticle or silver ion?," *Toxicol. Lett.*, vol. 208, no. 3, pp. 286–292, Feb. 2012, doi: 10.1016/j.toxlet.2011.11.002.

[85] C. You *et al.*, "The progress of silver nanoparticles in the antibacterial mechanism, clinical application and cytotoxicity," *Mol. Biol. Rep.*, vol. 39, no. 9, pp. 9193–9201, Sep. 2012, doi: 10.1007/s11033-012-1792-8.

[86] K. C. Nguyen, L. Richards, A. Massarsky, T. W. Moon, and A. F. Tayabali, "Toxicological evaluation of representative silver nanoparticles in macrophages and epithelial cells," *Toxicol. In Vitro*, vol. 33, pp. 163–173, Jun. 2016, doi: 10.1016/j.tiv.2016.03.004.

[87] C. E. Albers, W. Hofstetter, K. A. Siebenrock, R. Landmann, and F. M. Klenke, "*In vitro* cytotoxicity of silver nanoparticles on osteoblasts and osteoclasts at antibacterial concentrations," *Nanotoxicology*, vol. 7, no. 1, pp. 30–36, Feb. 2013, doi: 10.3109/17435390.2011.626538.

[88] S. C. Tjong and H. Chen, "Nanocrystalline materials and coatings," *Mater. Sci. Eng. R Rep.*, vol. 45, no. 1, pp. 1–88, Sep. 2004, doi: 10.1016/j.mser.2004.07.001.

[89] J. F. Pierson, D. Wiederkehr, and A. Billard, "Reactive magnetron sputtering of copper, silver, and gold," *Thin Solid Films*, vol. 478, no. 1, pp. 196–205, May 2005, doi: 10.1016/j.tsf.2004.10.043.

[90] S. B. Sant, K. S. Gill, and R. E. Burrell, "The nature of chemical species in novel antimicrobial silver films deposited by magnetron sputtering," *Philos. Mag. A*, Aug. 2009, doi: 10.1080/01418610208240020.

[91] S. B. Sant, K. S. Gill, and R. E. Burrell, "Nanostructure, dissolution and morphology characteristics of microcidal silver films deposited by magnetron sputtering," *Acta Biomater.*, vol. 3, no. 3, pp. 341–350, May 2007, doi: 10.1016/j.actbio.2006.10.008.

[92] J. B. Wright, K. Lam, A. G. Buret, M. E. Olson, and R. E. Burrell, "Early healing events in a porcine model of contaminated wounds: effects of nanocrystalline silver on matrix metalloproteinases, cell apoptosis, and healing," *Wound Repair Regen.*, vol. 10, no. 3, pp. 141–151, 2002, doi: 10.1046/j.1524-475X.2002.10308.x.

[93] R. G. Sibbald, J. Contreras-Ruiz, P. Coutts, M. Fierheller, A. Rothman, and K. Woo, "Bacteriology, Inflammation, and Healing: A Study of Nanocrystalline Silver Dressings in Chronic Venous Leg Ulcers," *Adv. Skin Wound Care*, vol. 20, no. 10, pp. 549–558, Oct. 2007, doi: 10.1097/01.ASW.0000294757.05049.85.

[94] P. L. Nadworny, J. Wang, E. E. Tredget, and R. E. Burrell, "Anti-inflammatory activity of nanocrystalline silver in a porcine contact dermatitis model," *Nanomedicine Nanotechnol. Biol. Med.*, vol. 4, no. 3, pp. 241–251, Sep. 2008, doi: 10.1016/j.nano.2008.04.006.

[95] F. Truchetet, O. Guibon, and S. Meaume, "Clinicians' rationale for using a silver dressing: the French OMAg+E observational study," *J. Wound Care*, vol. 21, no. 12, pp. 620–625, Dec. 2012, doi: 10.12968/jowc.2012.21.12.620.

[96] J. A. Ross *et al.*, "Comparison of the efficacy of silver-based antimicrobial burn dressings in a porcine model of burn wounds," *Burns*, vol. 46, no. 7, pp. 1632–1640, Nov. 2020, doi: 10.1016/j.burns.2020.04.004.

[97] B. Boonkaew, M. Kempf, R. Kimble, P. Supaphol, and L. Cuttle, "Antimicrobial efficacy of a novel silver hydrogel dressing compared to two common silver burn wound dressings: Acticoat™ and PolyMem Silver®," *Burns*, vol. 40, no. 1, pp. 89–96, Feb. 2014, doi: 10.1016/j.burns.2013.05.011.

[98] M. H. Cavanagh, R. E. Burrell, and P. L. Nadworny, "Evaluating antimicrobial efficacy of new commercially available silver dressings," *Int. Wound J.*, vol. 7, no. 5, pp. 394–405, 2010, doi: 10.1111/j.1742-481X.2010.00705.x.

[99] P. L. Nadworny, B. K. Landry, J. Wang, E. E. Tredget, and R. E. Burrell, "Does nanocrystalline silver have a transferable effect?," *Wound Repair Regen.*, vol. 18, no. 2, pp. 254–265, 2010, doi: 10.1111/j.1524-475X.2010.00579.x.

[100] B. K. Landry, P. L. Nadworny, O. E. Omotoso, Y. Maham, J. C. Burrell, and R. E. Burrell, "The kinetics of thermal instability in nanocrystalline silver and the effect of heat treatment on the antibacterial activity of nanocrystalline silver dressings," *Biomaterials*, vol. 30, no. 36, pp. 6929–6939, Dec. 2009, doi: 10.1016/j.biomaterials.2009.09.003.

[101] B. Feng, T. Yokoi, A. Kumamoto, M. Yoshiya, Y. Ikuhara, and N. Shibata, "Atomically ordered solute segregation behaviour in an oxide grain boundary," *Nat. Commun.*, vol. 7, no. 1, p. 11079, Mar. 2016, doi: 10.1038/ncomms11079.

[102] P. L. Nadworny, J. Wang, E. E. Tredget, and R. E. Burrell, "Anti-inflammatory activity of nanocrystalline silver-derived solutions in porcine contact dermatitis," *J. Inflamm.*, vol. 7, no. 1, p. 13, Feb. 2010, doi: 10.1186/1476-9255-7-13.

[103] P. AshaRani, S. Sethu, H. K. Lim, G. Balaji, S. Valiyaveettil, and M. P. Hande, "Differential regulation of intracellular factors mediating cell cycle, DNA repair and inflammation following exposure to silver nanoparticles in human cells," *Genome Integr.*, vol. 3, no. 1, p. 2, Feb. 2012, doi: 10.1186/2041-9414-3-2.

[104] R. Bryaskova, N. Georgieva, T. Andreeva, and R. Tzoneva, "Cell adhesive behavior of PVA-based hybrid materials with silver nanoparticles," *Surf. Coat. Technol.*, vol. 235, pp. 186–191, Nov. 2013, doi: 10.1016/j.surfcoat.2013.07.032.

[105] K. M. Guthrie *et al.*, "Antibacterial Efficacy of Silver-Impregnated Polyelectrolyte Multilayers Immobilized on a Biological Dressing in a Murine Wound Infection Model," *Ann. Surg.*, vol. 256, no. 2, pp. 371–377, Aug. 2012, doi: 10.1097/SLA.0b013e318256ff99.

[106] J. Franková, V. Pivodová, H. Vágnerová, J. Juráňová, and J. Ulrichová, "Effects of Silver Nanoparticles on Primary Cell Cultures of Fibroblasts and Keratinocytes in a Wound-Healing Model," *J. Appl. Biomater. Funct. Mater.*, vol. 14, no. 2, pp. 137–142, Apr. 2016, doi: 10.5301/jabfm.5000268.

[107] S. Sheikpranbabu, K. Kalishwaralal, D. Venkataraman, S. H. Eom, J. Park, and S. Gurunathan, "Silver nanoparticles inhibit VEGF-and IL-1β-induced vascular permeability via Src dependent pathway in porcine retinal endothelial cells," *J. Nanobiotechnology*, vol. 7, no. 1, p. 8, Oct. 2009, doi: 10.1186/1477-3155-7-8.

[108] H. R. Makarchian, A. Kasraianfard, P. Ghaderzadeh, S. M. R. Javadi, and M. Ghorbanpoor, "The effectiveness of heparin, platelet-rich plasma (PRP), and silver nanoparticles on prevention of postoperative peritoneal adhesion formation in rats1," *Acta Cirúrgica Bras.*, vol. 32, pp. 22–27, Jan. 2017, doi: 10.1590/s0102-865020170103.

[109] A. Ivask *et al.*, "Toxicity Mechanisms in Escherichia coli Vary for Silver Nanoparticles and Differ from Ionic Silver," *ACS Nano*, vol. 8, no. 1, pp. 374–386, Jan. 2014, doi: 10.1021/nn4044047.

[110] K. K. Y. Wong *et al.*, "Further Evidence of the Anti-inflammatory Effects of Silver Nanoparticles," *ChemMedChem*, vol. 4, no. 7, pp. 1129–1135, Jul. 2009, doi: 10.1002/cmdc.200900049.

[111] P. E. Lipsky and M. Ziff, "Inhibition of antigen- and mitogen-induced human lymphocyte proliferation by gold compounds.," *J. Clin. Invest.*, vol. 59, no. 3, pp. 455–466, Mar. 1977.

[112] M. Harth, C. R. Stiller, N. R. St C Sinclair, J. Evans, D. McGirr, and R. Zuberi, "Effects of a gold salt on lymphocyte responses.," *Clin. Exp. Immunol.*, vol. 27, no. 2, pp. 357–364, Feb. 1977.

[113] K. Ugai, M. Ziff, and P. E. Lipsky, "Gold-induced changes in the morphology and functional capabilities of human monocytes," *Arthritis Rheum.*, vol. 22, no. 12, pp. 1352–1360, Dec. 1979, doi: 10.1002/art.1780221206.

[114] B. H. Littman and P. Schwartz, "Gold inhibition of the production of the second complement component by lymphokine-stimulated human monocytes," *Arthritis Rheum.*, vol. 25, no. 3, pp. 288–296, Mar. 1982, doi: 10.1002/art.1780250306.

[115] B. H. Littman and R. E. Hall, "Effects of gold sodium thiomalate on functional correlates of human monocyte maturation," *Arthritis Rheum.*, vol. 28, no. 12, pp. 1384–1392, Dec. 1985, doi: 10.1002/art.1780281211.

[116] S. Hirohata, K. Nakanishi, T. Yanagida, M. Kawai, H. Kikuchi, and K. Isshi, "Synergistic Inhibition of Human B Cell Activation by Gold Sodium Thiomalate and Auranofin," *Clin. Immunol.*, vol. 91, no. 2, pp. 226–233, May 1999, doi: 10.1006/clim.1999.4686.

[117] Y. Rasool, "An evaluation of the anti-inflammatory activity and mechanism of action of three novel auranofin derivatives," Dissertation, University of Pretoria, 2009. Accessed: Feb. 23, 2023. [Online]. Available: https://repository.up.ac.za/handle/2263/22792

[118] D. T. Walz, M. J. DiMartino, D. E. Griswold, A. P. Intoccia, and T. L. Flanagan, "Biologic actions and pharmacokinetic studies of auranofin," *Am. J. Med.*, vol. 75, no. 6, Part 1, pp. 90–108, Dec. 1983, doi: 10.1016/0002-9343(83)90481-3.

[119] J. Liu, T. Akahoshi, R. Namai, T. Matsui, and H. Kondo, "Effect of auranofin, an antirheumatic drug, on neutrophil apoptosis," *Inflamm. Res.*, vol. 49, no. 9, pp. 445–451, Sep. 2000, doi: 10.1007/s000110050615.

[120] B. Wolach, J. E. DeBoard, T. D. Coates, R. L. Baehner, and L. A. Boxer, "Correlation of in vitro and in vivo effects of gold compounds on leukocyte function: possible mechanisms of action," *J. Lab. Clin. Med.*, vol. 100, no. 1, pp. 37–44, Jul. 1982.

[121] R. Yamada *et al.*, "Auranofin inhibits interleukin-1β-induced transcript of cyclooxygenase-2 on cultured human synoviocytes," *Eur. J. Pharmacol.*, vol. 385, no. 1, pp. 71–79, Nov. 1999, doi: 10.1016/S0014-2999(99)00707-4.

[122] M. B. Harbut *et al.*, "Auranofin exerts broad-spectrum bactericidal activities by targeting thiol-redox homeostasis," *Proc. Natl. Acad. Sci.*, vol. 112, no. 14, pp. 4453–4458, Apr. 2015, doi: 10.1073/pnas.1504022112.

[123] G. Yanni, M. Nabil, M. R. Farahat, R. N. Poston, and G. S. Panayi, "Intramuscular gold decreases cytokine expression and macrophage numbers in the rheumatoid synovial membrane.," *Ann. Rheum. Dis.*, vol. 53, no. 5, pp. 315–322, May 1994.

[124] J. Lampa, L. Klareskog, and J. Rönnelid, "Effects of gold on cytokine production in vitro; increase of monocyte dependent interleukin 10 production and decrease of interferon-gamma levels.," *J. Rheumatol.*, vol. 29, no. 1, pp. 21–28, Jan. 2002.

[125] N.-H. Kim, M.-Y. Lee, S.-J. Park, J.-S. Choi, M.-K. Oh, and I.-S. Kim, "Auranofin blocks interleukin-6 signalling by inhibiting phosphorylation of JAK1 and STAT3," *Immunology*, vol. 122, no. 4, pp. 607–614, 2007, doi: 10.1111/j.1365-2567.2007.02679.x.

[126] E. Varghese and D. Büsselberg, "Auranofin, an Anti-Rheumatic Gold Compound, Modulates Apoptosis by Elevating the Intracellular Calcium Concentration ([Ca2+]i) in MCF-7 Breast Cancer Cells," *Cancers*, vol. 6, no. 4, Art. no. 4, Dec. 2014, doi: 10.3390/cancers6042243.

[127] C. Goebel, M. Kubicka-Muranyi, T. Tonn, J. Gonzalez, and E. Gleichmann, "Phagocytes render chemicals immunogenic: oxidation of gold(I) to the T cell-sensitizing gold(III) metabolite generated by mononuclear phagocytes," *Arch. Toxicol.*, vol. 69, no. 7, pp. 450–459, Jun. 1995, doi: 10.1007/s002040050198.

[128] S. L. Best and P. J. Sadler, "Gold drugs: Mechanism of action and toxicity," *Gold Bull.*, vol. 29, no. 3, pp. 87–93, Sep. 1996, doi: 10.1007/BF03214741.

[129] L. Messori *et al.*, "Gold(III) complexes as potential antitumor agents: solution chemistry and cytotoxic properties of some selected gold(III) compounds," *J. Med. Chem.*, vol. 43, no. 19, pp. 3541–3548, Sep. 2000, doi: 10.1021/jm990492u.

[130] T. Zou, C. T. Lum, C.-N. Lok, J.-J. Zhang, and C.-M. Che, "Chemical biology of anticancer gold(III) and gold(I) complexes," *Chem. Soc. Rev.*, vol. 44, no. 24, pp. 8786–8801, Nov. 2015, doi: 10.1039/C5CS00132C.

[131] P. Calamai *et al.*, "Biological properties of two gold(III) complexes: AuCl3 (Hpm) and AuCl2 (pm)," *J. Inorg. Biochem.*, vol. 66, no. 2, Art. no. 2, May 1997, doi: 10.1016/S0162-0134(96)00190-0.

[132] R. F. de Araújo *et al.*, "Anti-inflammatory, analgesic and anti-tumor properties of gold nanoparticles," *Pharmacol. Rep.*, vol. 69, no. 1, pp. 119–129, Feb. 2017, doi: 10.1016/j.pharep.2016.09.017.

[133] M. Ø. Pedersen, A. Larsen, D. S. Pedersen, M. Stoltenberg, and M. Penkowa, "Metallic gold reduces TNFα expression, oxidative DNA damage and pro-apoptotic signals after experimental brain injury," *Brain Res.*, vol. 1271, pp. 103–113, May 2009, doi: 10.1016/j.brainres.2009.03.022.

[134] D. Mahl *et al.*, "Silver, gold, and alloyed silver–gold nanoparticles: characterization and comparative cell-biologic action," *J. Nanoparticle Res.*, vol. 14, no. 10, Art. no. 10, Sep. 2012, doi: 10.1007/s11051-012-1153-5.

[135] M. A. Khan and M. J. Khan, "Nano-gold displayed anti-inflammatory property via NF-kB pathways by suppressing COX-2 activity," *Artif. Cells Nanomedicine Biotechnol.*, vol. 46, no. sup1, pp. 1149–1158, Oct. 2018, doi: 10.1080/21691401.2018.1446968.

[136] T. G. de Carvalho *et al.*, "Spherical neutral gold nanoparticles improve anti-inflammatory response, oxidative stress and fibrosis in alcohol-methamphetamine-induced liver injury in rats," *Int. J. Pharm.*, vol. 548, no. 1, Art. no. 1, Sep. 2018, doi: 10.1016/j.ijpharm.2018.06.008.

[137] K. R. Unrau, "Activity of Nanocrystalline Gold and Silver Alloys," ERA. Accessed: May 27, 2022. [Online]. Available: https://era.library.ualberta.ca/items/e0ac4715-3e00-4814-ab41-19700ce1d802

[138] W. B. Gaertner, G. F. Hagerman, I. Felemovicius, M. E. Bonsack, and J. P. Delaney, "Two Experimental Models for Generating Abdominal Adhesions," *J. Surg. Res.*, vol. 146, no. 2, pp. 241–245, May 2008, doi: 10.1016/j.jss.2007.08.012.

[139] B. Zimmerman, "Chapter 8 - Peritoneum, Retroperitoneum, Mesentery, and Abdominal Cavity," in *Boorman's Pathology of the Rat (Second Edition)*, A. W. Suttie, Ed., Boston: Academic Press, 2018, pp. 71–77. doi: 10.1016/B978-0-12-391448-4.00008-3.

[140] L. Lossi, L. D'Angelo, P. De Girolamo, and A. Merighi, "Anatomical features for an adequate choice of experimental animal model in biomedicine: II. Small laboratory rodents, rabbit, and pig," *Ann. Anat. - Anat. Anz.*, vol. 204, pp. 11–28, Mar. 2016, doi: 10.1016/j.aanat.2015.10.002.

[141] B. Weber *et al.*, "Modeling trauma in rats: similarities to humans and potential pitfalls to consider," *J. Transl. Med.*, vol. 17, no. 1, p. 305, Sep. 2019, doi: 10.1186/s12967-019-2052-7.

[142] E. C. Borrazzo, M. F. Belmont, D. Boffa, and D. L. Fowler, "Effect of prosthetic material on adhesion formation after laparoscopic ventral hernia repair in a porcine model," *Hernia*, vol. 8, no. 2, pp. 108–112, May 2004, doi: 10.1007/s10029-003-0181-6.

[143] R. Ferland, D. Mulani, and P. K. Campbell, "Evaluation of a sprayable polyethylene glycol adhesion barrier in a porcine efficacy model," *Hum. Reprod.*, vol. 16, no. 12, pp. 2718–2723, Dec. 2001, doi: 10.1093/humrep/16.12.2718.

[144] C. I. W. Lauder, A. Strickland, and G. J. Maddern, "Use of a Modified Chitosan–Dextran Gel to Prevent Peritoneal Adhesions in a Porcine Hemicolectomy Model," *J. Surg. Res.*, vol. 176, no. 2, pp. 448–454, Aug. 2012, doi: 10.1016/j.jss.2011.10.029.

[145] P. Reissman, Tiong-Ann-Teoh, K. Skinner, J. W. Burns, and S. D. Wexner, "Adhesion Formation After Laparoscopic Anterior Resection in a Porcine Model: A Pilot Study," *Surg. Laparosc. Endosc. Percutan. Tech.*, vol. 6, no. 2, p. 136, Apr. 1996.

[146] J. Jin *et al.*, "Human Peritoneal Membrane Controls Adhesion Formation and Host Tissue Response Following Intra-Abdominal Placement in a Porcine Model," *J. Surg. Res.*, vol. 156, no. 2, pp. 297–304, Oct. 2009, doi: 10.1016/j.jss.2009.04.010.

[147] C. Wang, K. Zhang, H. Wang, S. Xu, and C. C. Han, "Evaluation of biodegradability of poly (DL-lactic-co-glycolic acid) scaffolds for post-surgical adhesion prevention: In vitro, in rats and in pigs," *Polymer*, vol. 61, pp. 174–182, Mar. 2015, doi: 10.1016/j.polymer.2015.02.001.

[148] X. Zhao, J. Yang, Y. Liu, J. Gao, K. Wang, and W. Liu, "An injectable and antifouling self-fused supramolecular hydrogel for preventing postoperative and recurrent adhesions," *Chem. Eng. J.*, vol. 404, p. 127096, Jan. 2021, doi: 10.1016/j.cej.2020.127096.

[149] D. Poehnert, M. Abbas, H.-H. Kreipe, J. Klempnauer, and M. Winny, "High Reproducibility of Adhesion Formation in Rat with Meso-Stitch Approximation of Injured Cecum and Abdominal Wall," *Int. J. Med. Sci.*, vol. 12, no. 1, pp. 1–6, Jan. 2015, doi: 10.7150/ijms.8870.

[150] J. Oh *et al.*, "Recombinant human lubricin for prevention of postoperative intra-abdominal adhesions in a rat model," *J. Surg. Res.*, vol. 208, pp. 20–25, Feb. 2017, doi: 10.1016/j.jss.2016.08.092.

[151] J. A. Bello-Guerrero, C. A. Cruz-Santiago, and J. Luna-Martínez, "Pirfenidone vs Sodium Hyaluronate/carboxymethyl cellulose as Prevention of the Formation of Intra-abdominal Adhesions After Colonic Surgery. A Randomized Study in an Experimental Model," *Cir. Esp. Engl. Ed.*, vol. 94, no. 1, Art. no. 1, Jan. 2016, doi: 10.1016/j.cireng.2015.06.013.

[152] P. S. Hasdemir *et al.*, "Effect of Pirfenidone on Vascular Proliferation, Inflammation and Fibrosis in an Abdominal Adhesion Rat Model," *J. Invest. Surg.*, vol. 30, no. 1, pp. 26–32, Jan. 2017, doi: 10.1080/08941939.2016.1215578.

[153] L. Bresson, E. Leblanc, A. S. Lemaire, T. Okitsu, and F. Chai, "Autologous peritoneal grafts permit rapid reperitonealization and prevent postoperative abdominal adhesions in an experimental rat study," *Surgery*, vol. 162, no. 4, pp. 863–870, Oct. 2017, doi: 10.1016/j.surg.2017.05.005.

[154] M. D. L. P. Biondo-Simões, W. A. Schiel, M. Arantes, T. D. Silveira, R. R. Robes, and F. D. S. Tomasich, "Comparison between polypropylene and polypropylene with poliglecaprone meshes on intraperitoneal adhesion formation," *Rev. Colégio Bras. Cir.*, vol. 43, pp. 416–423, Dec. 2016, doi: 10.1590/0100-69912016006002.

[155] R. S. Vediappan *et al.*, "A Novel Rat Model to Test Intra-Abdominal Anti-adhesive Therapy," *Front. Surg.*, vol. 7, p. 12, Apr. 2020, doi: 10.3389/fsurg.2020.00012.

[156] E. H. Mommers, L. Hong, A. Jongen, and N. D. Bouvy, "Baseline performance of the ischaemic button model for induction of adhesions in laboratory rats," *Lab. Anim.*, vol. 53, no. 1, pp. 63–71, Feb. 2019, doi: 10.1177/0023677218773116.

[157] M. R. Cassidy, A. C. Sherburne, S. J. Heydrick, and A. F. Stucchi, "Combined intraoperative administration of a histone deacetylase inhibitor and a neurokinin-1 receptor antagonist synergistically reduces intra-abdominal adhesion formation in a rat model," *Surgery*, vol. 157, no. 3, pp. 581–589, Mar. 2015, doi: 10.1016/j.surg.2014.09.031.

[158] C. I. W. Lauder, G. Garcea, A. Strickland, and G. J. Maddern, "Use of a Modified Chitosan–Dextran Gel to Prevent Peritoneal Adhesions in a Rat Model," *J. Surg. Res.*, vol. 171, no. 2, pp. 877–882, Dec. 2011, doi: 10.1016/j.jss.2010.06.028.

[159] R. E. Leach, J. W. Burns, E. J. Dawe, M. D. SmithBarbour, and M. P. Diamond, "Reduction of Postsurgical Adhesion Formation in the Rabbit Uterine Horn Model with Use of Hyaluronate/ Carboxymethylcellulose Gel1 1Supported by Genzyme Corporation, Protocol No. 92-0902, Cambridge, Massachusetts.," *Fertil. Steril.*, vol. 69, no. 3, pp. 415–418, Mar. 1998, doi: 10.1016/S0015-0282(97)00573-6.

[160] S. K. Nair, I. K. Bhat, and A. L. Aurora, "Role of Proteolytic Enzyme in the Prevention of Postoperative Intraperitoneal Adhesions," *Arch. Surg.*, vol. 108, no. 6, pp. 849–853, Jun. 1974, doi: 10.1001/archsurg.1974.01350300081019.

Chapter 2 : Methods

Introduction

This chapter describes the techniques used to make and test the experimental materials. Silver and silver-gold sputtered HDPE films were fabricated by physical vapour deposition. The films were analyzed by x-ray diffraction, chemical digests for silver and gold quantity, scanning electron microscope (SEM) imaging, and tests for biological activity. Aqueous solutions were made by soaking the films in water, then analyzed for silver concentration and biological activity. Viscous solutions were made by adding biodegradable polymers to aqueous nanocrystalline silver solutions. The release of silver from dialysis cassettes and degradation of the polymers was measured over three days. Animal studies will be performed in the future, but procedure details will be provided here.

Dressing Fabrication

An in-house sputtering apparatus was used to create the experimental nanocrystalline silver dressings by a physical vapour deposition process. A roll of HDPE mesh was positioned in the chamber underneath a metallic target, which acts as the cathode. The HDPE was on top of a metal plate acting as the anode. Oxygen and argon were allowed into the chamber at a controlled rate for a total flow rate of 400 sccm through a line heated to 130°F. Voltage was applied to the system to create an ionized gas which in contact with the target will eject atoms, some of which react with oxygen in the chamber, and these particles condense on the HDPE mesh, creating a layer approximately 900 nm in thickness [1]. To ensure even distribution across the dressing, the roll of HDPE moved underneath the target at a rate of 1.65 cm/minute. The thickness of the film is dependent on the current and speed of the roller [1]. The process was controlled by current. The working pressure of the machine was 40mTorr, maintained by vacuum pumps. Cooling of the system was provided by city water to cool the target surface. The process was run for up to 3 hours per sample, resulting in up to 10 ft of usable film.

For the experimental "Novel" dressings, the atmosphere was composed of 4.5% oxygen with the balance argon. The current was set at 1.8A. Water was injected at a constant rate of 15 µL/min using a peristaltic pump (Masterflex L/S ®, Cole-Parmer) connected to the argon gas input line. For the "Standard" films, atmosphere was 4.0% oxygen and the current is set at 0.9A. No water was included in these dressings. These standard dressings mimic the properties of commercially available Acticoat™ dressings. Three targets were used during the course of the study. One target was nominally 100% silver (Ag100), one was 65% silver and 35% gold by weight (Ag65), and one was 35% silver and 65% gold by weight (Ag35).

X-ray Diffraction

X-ray diffraction (XRD) analysis of the dressings was performed on a Rigaku Ultima IV diffractometer with a cobalt radiation source at 38kV and 38mA. Samples of the coated HDPE film were placed in the diffractometer and irradiated with x-rays at a set range of angles. Then the intensity of the resultant scattered x-rays leaving the sample was measured. The resulting spectrum's peak intensities at specific angles correspond to a specific material and its crystal structure. A sample with long-range crystalline order has a sharp peak or line at each location, but for crystalline samples with a smaller range of order, the peaks will appear at the same position but are broader, covering a greater span of angles. The data obtained with the cobalt tube was converted automatically to the copper wavelength for data visualization and analysis using a standard formula taking into account the relative wavelengths of the emission sources because copper is the most common radiation source and therefore most recognizable. XRD spectra were plotted using Microsoft Excel. The sample diffraction pattern was obtained between approximately 15 and 90°2θ, to obtain the entire spectrum, using a step size of 0.03 °2θ and a scan speed of 5 °2θ/min.

Grain size was measured using the Scherrer equation, given below[2]:

$$B = \frac{K\lambda}{FWHM * cos\theta}$$

Equation 2-1 Scherrer Equation

B is the grain size in nm, K is the dimensionless shape factor, which is assumed to be 0.9 for our sample, λ is the wavelength of the radiation beam, which is 1.54nm for copper. FWHM is the "full width at half maximum", which is the peak width at the half maximum of the peak, and θ is the peak position. Both FWHM and θ are given in radians. Identification of peak position and measurement of FWHM were performed by hand using Microsoft Excel. The Scherrer equation given here is an accepted approximation for grain size measurement, but depends on various assumptions of atomic scattering and crystal shape that limit its accuracy[3]. There is also a limit in accuracy by the measurement of FWHM by hand. Total sample grain size was calculated as the average of measurable peaks between 30 °2θ and 80 °2θ. Metallic silver is recognized from peak locations at approximately 38, 44, 65, and 77 °2θ. Silver oxide is identified primarily from peaks at 33 and 44 °2θ. Metallic gold is recognized from peak location at approximately 38, 44, 65, and 77 °2θ. However, the exact peak location and shape will shift due to lattice stresses, but strain effects were not directly measured [4].

Chemical Analysis

To determine the total quantity of silver in the dressing, 1 square inch of coated HDPE was dissolved in 20mL of a 50% solution of 65% nitric acid and distilled water for 20 minutes, then diluted in an additional 20mL of distilled water and sent for analysis.

To determine the quantity of ammonia soluble silver, which is an estimate of the quantity of silver oxide or ionic silver in the film, 1 square inch of film was dissolved in 20mL of ammonium hydroxide for 10 minutes, and 10mL of this solution was diluted in 40mL of water and sent for analysis.

To determine the silver release over a period of time, 2 square inches of film were soaked in 7.5mL distilled water, or a quantity at an equivalent ratio, at 37°C for a set period of time, typically 6 hours or overnight. After the time had elapsed, the film was removed and an equal amount of nitric acid was added. This solution was diluted 1:1 in distilled water and sent for analysis.

To determine the total quantity of gold in the dressing, 1 square inch of dressing was dissolved in 20mL of aqua regia for 15 minutes, then diluted in 20 mL of HPLC water and sent for analysis. Aqua regia was prepared in a fume hood with a 1:4 by volume ratio of 65% nitric acid to 35% hydrochloric acid.

The solutions described above were analyzed for quantity of silver using inductively coupled plasma mass spectrometry (ICP-MS) or atomic absorption spectroscopy, given in mg/L. Gold quantity was analyzed by ICP-MS. Samples were corrected for dilution factor and given as mg of silver or gold per square inch of sample or per volume of solution.

Scanning Electron Microscopy

A Hitachi Field Emission Scanning Electron Microscope was used to image the surface of coated samples. Samples were attached to a specimen mount using carbon tape. Images were taken at 50 000x, and 100 000x magnification using an accelerating voltage of 10 kV with a working distance between 4 and 5.5 mm.

Log Reduction

To quantify the antibacterial properties of the materials, log reduction analysis was performed. Two 1 square inch coated HDPE pieces were layered with a 1 square inch piece of cotton gauze. An inoculum of *Pseudomonas aeruginosa* (strain 27317), *Staphylococcus aureus* (strains 983,1926, 25923), *Proteus mirabilis* (strain 29906), *or Proteus vulgaris* (strain 3340) is started the previous day to create a culture in log phase at the time of use. The bacteria were inoculated in 100 mL of growth medium in a flask and placed in a 37°C incubator-shaker, after approximately 16-18 hours culture. These two species were

chosen as representative species of Gram negative and Gram positive bacteria respectively. The growth medium is tryptic soy broth unless otherwise specified. 250 μL of the culture is pipetted on the top surface of the dressing. The dressing was sandwiched in a Petri dish, protected from contacting the dish with layers of flexible plastic. After incubating the inoculated dressings statically for 1 hour at 37°C, the activity of the silver was stopped by placing the dressings in a sodium thiosulfate solution (STS). These solutions were then diluted using peptone water and plated on Mueller-Hinton agar (MHA). Serial dilution was performed by removing 1 mL of a solution, adding it to 9 mL peptone water, mixing, and removing 1 mL of this solution for the next dilution. Samples were diluted to 10^{-6} and the bacterial inoculum is diluted to 10^{-9}. Plates were checked the following day to count bacterial colonies (colony forming units, CFU) and calculate the logarithmic reduction based on the concentration of bacteria in the original culture, as shown in Equation 2.

$$\log reduction = \log_{10} \frac{\frac{CFU}{mL} \, of \, inoculum \, added}{\frac{CFU}{mL} \, after \, incubation}$$

Equation 2-2 Logarithmic Reduction

To test the antibacterial properties of solutions made with nanocrystalline dressings, a similar process was used. First, a silver solution is prepared. Unless otherwise specified, 1.8 mL of the silver solution was combined with 0.2 mL of a log phase inoculum, prepared as described, in a 15 mL conical tube. For "2.5% solutions", 50 μL of inoculum was added to 1.95 mL of silver solutions. After mixing, this solution was incubated for 1 hour at 37°C. The activity of silver was stopped by removing 250 μL of the silver-inoculum solution with sodium thiosulfate (STS) then diluted, plated, and counted as described above.

For viscous solutions, the bacterial inoculum was grown using bovine calf serum (BCS) as growth medium. A 100 mL inoculum is cultured overnight, then the next day, 1 mL was removed and added to a fresh flask of 100 mL of BCS overnight. Viscous solutions were made as described, then 2 mL of gel was added to a 15 mL conical tube with 7.5 mL BCS and 500 μL of inoculum in BCS and mixed by inverting the tube. This mixture was incubated statically for two hours at 37°C. After one hour, each tube was inverted to mix the contents. After 2 hours (one additional hour), each tube was mixed vigorously and a log reduction performed as previously described.

Day-to-Day Corrected Zone of Inhibition (CZOI) Assay

The bacteriostatic longevity of the dressings was assessed using day-to- day transfer corrected zone of inhibition assays. 100 μL of *S. aureus* taken from an overnight culture (16-18 hours to achieve log phase, as above) in tryptic soy broth medium to ensure bacteria were in log phase and spread onto MHA plates.

Silver dressing pieces (two pieces of 1in^2 film sandwiching a layer of gauze) pre- moistened by dipping in distilled water and placed on the center of each plate. The plates were incubated statically for 24 hours at 37°C and then the zones of bacterial inhibition and dressing widths were measured in two perpendicular directions. The CZOI was calculated by subtracting the dressing width from the zone width, and the results for the two directions were averaged. After zone measurement, the dressings were transferred to new MHA plates seeded with bacteria, as described above, and again incubated overnight. CZOI's were determined and this procedure was repeated for seven more days, for a total of nine days.

Measurement of Viscosity

Sodium hyaluronate (NaHA) and sodium carboxymethylcellulose (NaCMC) were purchased from Sigma Aldrich and were used to increase the viscosity of a silver solution. These two components were mixed into silver solutions in combinations from a range of 0.5% to 2.0%. Viscosity was measured using a Brookfield cone and plate rheometer (RVDNX CP, CPA-51) with 0.5 mL samples. HA-CMC solutions are non-Newtonian fluids, so a range of shear rates was used. The range was from 3.84 to 384 s^{-1}, or 1 to 100 rpm, starting at a low shear rate and increasing in order.

Degradation Experiments

After viscous silver solutions were made, 2 mL samples of each solution were loaded into dialysis cassettes (Thermo Scientific, molecular weight cutoff 10 000) in triplicate with an 18 gauge needle and 5 mL syringe. Dialysis cassettes were submerged in 100 mL PBS in 600 mL beakers on an incubator-shaker at 37 °C and 60 rpm. Beakers were covered with Parafilm to prevent evaporation. At predetermined time intervals, a 5 mL sample of the PBS was removed for silver analysis as described. Samples taken were replaced immediately with fresh PBS. The time points for sampling were 1, 2, 4, 8, 24, 48, and 72 hours. After 72 hours, viscous solution was removed from the dialysis cassette using a needle and syringe and the viscosity measured as previously described to estimate the degradation of the polymers during the course of the experiment.

Animal Acquisition and Care

Animal studies were approved by the University of Alberta Animal Care and Use Committee and MedStar Health Research Institute (MHRI) Institutional Animal Care and Use Committee. All animal procedures were conducted at the Burn and Surgical Research Laboratory at Medstar Health Research Institute in Washington DC. Approved protocols surgical procedures can be found in Appendix B. Pigs used in these experiments will be Yorkshire domestic cross swine, with no cross with Red Duroc pigs

because of their scarring profile. They are to be adult pigs between 35-45 kg at the start of the study. All animals used will be healthy and without significant wounds or scars on their backs. A clinical assessment of all pigs will be made before inclusion in the study. The animals will be housed in individual pens with a 12 hour light/dark cycle, where they will be allowed to acclimatize at least five days prior to starting experiments. The pens have grids to allow for animal-animal interaction. The animals received antibiotic-free water and standard hog ration *ad libitum* except for 12 hours prior to surgical procedures. Enrichment devices will be provided. Animals will be monitored twice daily on weekdays and once on weekends during their acclimation period. Animals will be observed for behaviour, appearance, excretions, and feeding.

Sensitization to DNCB for Inflammatory Reaction

For Chapter 5, the dermal study, before any surgical procedures, an inflammatory reaction is created on the pigs' backs using DNCB. Inflammation will be induced using a 10% solution of DNCB in a vehicle of 4:1 acetone:olive oil. There are three pigs per group with eight groups described in Table 2-1. On Day -14, the hair on the left and right sides of the backs of all 24 pigs will be shaved using electric clippers. The DNCB solution will be painted over two areas of approximately 15 cm x 25 cm on the left and right sides of the back for 21 pigs, all except the negative control pigs. The volume used per application per pig was approximately 7 mL. This procedure was repeated on Days -7, -3, and 0. On Day -3, pigs were given fentanyl patches on shaved skin away from the rash, to avoid discomfort to the pigs during the final application and treatment. The remaining 3 pigs, which were used as negative controls, were not given DNCB, but still received fentanyl patches at Day -3.

Table 2-1 Groups for Chapter 5 Animal Study

Group	Code	Description
Negative Control, Sham	NC	No DNCB application, treated with saline-soaked gauze
Positive Control	PC	Treated with saline soaked gauze
Standard Silver Dressing	Ag100S	100% Silver, Standard Sputtering Conditions
Novel Silver Dressing	Ag100N	100% Silver, Novel Sputtering Conditions
Standard Low Gold Dressing	Ag65S	65% Silver, 35% Gold, Standard Sputtering Conditions
Novel Low Gold Dressing	Ag65N	65% Silver, 35% Gold, Novel Sputtering Conditions
Standard High Gold Dressing	Ag35S	35% Silver, 65% Gold, Standard Sputtering Conditions
Novel High Gold Dressing	Ag35N	35% Silver, 65% Gold, Novel Sputtering Conditions

Preparation for Surgery, Anesthesia, and Surgical Monitoring

For all surgical procedures in Chapters 5 and 8, animals are anesthetized and provided with an antibiotic as a precaution against infection. In preparation for surgery, animals will be intubated, given an ear vein IV, and transferred to the surgical suite. Anesthesia is maintained with oxygen and isoflurane inhalation. When a suitable depth of anesthesia is reached, surgical procedures can begin. Vital signs will be monitored every 17 minutes at minimum, as per facility protocol and include percent concentration of isoflurane, heart rate, blood pressure, respiratory rate, O_2 saturation, CO_2 level, and body temperature., and are recorded on the anesthesia monitoring sheet. Pigs are connected to an anesthesia unit, vital signs monitor, ventilator, pulse oximeter, and warming unit. Animal care staff will assess and monitor pigs under anesthesia according the facility procedures. Animals must be in Stage 3 Plane 2 level of anesthesia before surgery, by assessing corneal reflex, jaw reflex, palpebral reflex, or toe pinch methods. Animals are weighed on Day 0. Weight changes from Day 0 to the end of the study are recorded.

After weighing, animals will be restrained and injected with anesthetic induction cocktail. Pigs are to be placed under general anesthetic via ketamine (15-40 mg/kg) and xylazine (3-5 mg/kg) injections and maintained with isoflurane inhalation (2 L/min). Glycopyrrolate (0.004-0.01 mg/kg) or atropine (0.05-0.5 mg/kg) will also be administered at this time. Once the dose has taken effect, the animals are transported to the surgical suite via transport cart and placing on a circulating warm air blanket. Ophthalmic ointment is applied to the animal's eyes. The animal are intubated and ventilated for oxygen and isoflurane inhalation. Lidocaine (20mg/mL) may be used to assist with intubation. A cannula is placed in the ear vein for IV fluid administration.

Adhesion Formation Procedure

Table 2-2 shows the experimental and control groups for the adhesion study in Chapter 8.

Table 2-2 Experimental and Control Groups for Adhesion Animal Study.

Group	Code	Description
Control Group 1	CG1	Sham surgery- laparotomy but no abrasion
Control Group 2	CG2	No treatment controls- abrasion with no treatment
Control Group 3	CG3	Comparison product group – treatment with Seprafilm®
Control Group 4	CG4	Vehicle controls – gel containing no silver
Experimental Group 1	EG1	Gel with silver treatment
Experimental Group 2	EG2	External silver dressing

A midline incision is made into the abdominal cavity, carefully dividing tissue layers. When the peritoneum is reached, the surgeon will bluntly dissect. The surgeon confirms no presence of adhesions, or documents those present. In the right lower quadrant the terminal ileum and cecum will be mobilized. To create adhesions, abrasion until bleeding is performed on the parietal and parenchymal peritoneum using a laparotomy pad or dry sterile gauze pad over a set area of two square inches, except the sham procedure group (CG1). Treatments are applied to both abraded surfaces in CG3, CG4, and EG1. The abdominal cavity is closed in layers with appropriate Vicryl sutures. Animals in EG2 when have the incision area covered by a nanocrystalline silver wound dressing. All other animals will have incision area covered with a standard surgical dressing. Dressings are secured with sutures or staples.

On Day 2 and Day 4 post-surgery, animals will have external dressings changed under anesthesia. Incision sites will also be assessed and photographed. On Day 7, under anesthesia, a blood sample will be collected, then the animals euthanized before re-opening the abdominal cavity to make observations and collect tissues samples of any present adhesions and abdominal wall.

Blood Sampling

Blood samples for serum analysis for Chapters 5 and 8 will be collected into appropriate storage tubes for both. The samples will be kept at room temperature, and then centrifuged for 15 minutes at 1500 rpm. The supernatant is collected (3-4 mL) and stored at -20ºC for analysis.

Dermal Tissue Sampling

For Chapter 5, six samples will be taken per day with a 4 mm full thickness biopsy punch. Biopsies from subsequent days are to be spaced a minimum of 4 cm from the previous days biopsies to limit the effect from past biopsies, but still be well within the bounds of the rash.

Biopsies from each day will be randomly assigned for analysis. Three biopsies will be placed in 4% formalin at room temperature to preserve for staining and imaging. Three biopsies will be snap-frozen in liquid nitrogen and then kept at -80°C until use for protein and gene analysis.

Calcium alginate dressings will be used to reach hemostasis once biopsies are taken. The positive and negative controls will be treated with a sterile dressing saturated with 0.9% sodium chloride in sterile reverse osmosis water. Nanocrystalline silver or silver-gold dressings will be moistened with sterile water and placed over the entire rash and secured. New fentanyl patches will be applied if they had come loose. Surgical drape will be placed over each dressing to provide moisture control, and elastic adhesive dressing will be wrapped around the pigs' rash area to hold the dressings in place. Dressings will be replaced after each set of procedures.

Post-Surgery Recovery

At the end of each procedure, animals will be disconnected from isoflurane and transitioned to ventilation with room air via battery-operated mechanical ventilator. They are returned to their pen and kept on ventilation until breathing on their own. Regular monitoring will continue until animals are conscious and stable. Observation is made for signs of complication such as excessive bleeding, cardiovascular or respiratory depression, hypothermia, hematoma, excessive bruising, or other complications. Food will be offered once animal has fully recovered from anesthesia.

Observation will continue to recognize surgical complications. Analgesia is provided immediately post-surgery on Day 0, with a continuous release fentanyl patch (25mcg/hour) for three days, and additional post-surgical analgesia as needed using buprenorphine (0.3 mg). Pain may be recognized by increased heart rate, rapid breathing, changes in mobility, dilated pupils, and not drinking or eating.

Euthanasia

Animals will be under anesthesia for euthanasia. Once all procedures are completed, Fatal PlusTM (390 mg/ml pentobarbital sodium; 1% propylene glycol; 29% ethyl alcohol, 2% benzyl alcohol) will be administered by intravenous injection, at a concentration of 85-150 mg/kg. If signs of life are still found, additional Fatal PlusTM is injected. KCl is also used as an alternative at a concentration of 0.24- 0.47 mL of a 4.2M KCl solution. Death of the animal is confirmed by measuring heart rate, respiration rate, and O_2 saturation.

If an animal is found moribund, the Study Director will be notified. The veterinarian is consulted to decide if euthanasia is required or if another treatment plan may be developed. If early euthanasia is required, a comprehensive necropsy will be performed if possible.

Statistics

Unpaired two sample t-tests with Welch's correction were used to compare sample groups when data compared two groups. One and two way ANOVA are used when multiple groups and factors are considered. If ANOVA effects are found to be significant, Tukey's post-hoc tests were used to compare individual groups. Comparisons between groups in Chapter 8 will be made using the Kruskal-Wallis test. Dunn's test with the Holm's correction method accounts for the increased rate of false positives from repeated t-tests and will be used for multiple comparisons between groups in Chapter 8. Analysis was performed using Microsoft Excel and R.

References

[1] P. L. Nadworny, "Biological activity of nanostructured silver," ERA. Accessed: Jul. 11, 2022. [Online]. Available: https://era.library.ualberta.ca/items/1d6adcfa-166d-45fb-bddc-37823fbff14d

[2] P. Scherrer, "Bestimmung der inneren Struktur und der Größe von Kolloidteilchen mittels Röntgenstrahlen," in *Kolloidchemie Ein Lehrbuch*, R. Zsigmondy, Ed., in Chemische Technologie in Einzeldarstellungen. , Berlin, Heidelberg: Springer, 1912, pp. 387–409. doi: 10.1007/978-3-662-33915-2_7.

[3] M. a. R. Miranda and J. M. Sasaki, "The limit of application of the Scherrer equation," *Acta Crystallogr. Sect. Found. Adv.*, vol. 74, no. 1, pp. 54–65, Jan. 2018, doi: 10.1107/S2053273317014929.

[4] M. E. Fitzpatrick, A. T. Fry, P. Holdway, F. A. Kandil, J. Shackleton, and L. Suominen, "Determination of residual stresses by X-ray diffraction." Accessed: Mar. 13, 2024. [Online]. Available: https://eprintspublications.npl.co.uk/2391/

Chapter 3 : Fabrication and Analysis of Nanocrystalline Silver Films

Introduction

Nanocrystalline silver is a material with well-documented anti-bacterial and anti-inflammatory properties. It is used in a variety of medical applications, mostly for wound and burn dressings, although its anti-inflammatory properties are attracting greater interest for other medical applications. Nanocrystalline silver dressings are commercially available, under the trade name Acticoat[TM], produced by Smith & Nephew. By using a physical vapour deposition process in an argon-oxygen atmosphere, a nanostructured material with metallic silver and silver oxide is formed [1]. Sputtering in an atmosphere containing oxygen adds silver oxide to the dressing, which is critical for stabilizing the nanostructure and limiting grain growth [2]. The grain sizes are on the scale of 10-30 nm[2]. Energetics and thermodynamics influence the formation and stabilization of structures in nanomaterials; the equilibrium grain size for a material is where the total system energy is best reduced[3], [4]. Nanocrystalline silver has a nanostructure that allows it to release multiple silver species in high quantities and over a period of several days [5], [6].

Previous experiments have studied the anti-inflammatory and antibacterial properties of nanocrystalline silver *in vitro* and *in vivo* [5], [6], [7], [8]. A study using a variety of commercially available silver wound dressings and antibacterial products proved the superiority of nanocrystalline silver over other products on the market[8]. This work also brought evidence that the anti-inflammatory and antibacterial mechanisms of action were due to different silver species [7]. Anti-inflammatory properties are associated with the reduced form of silver, Ag^0, and the antibacterial properties are due to ionic silver, primarily Ag^+[6]. It is even suggested that nanocrystalline silver is able to release higher oxidation state species of silver, which would further support its exceptional antibacterial properties[1]. Atoms in grain boundaries display different material properties than ordered crystals or amorphous materials, and it is more energetically favourable to release Ag^+ and Ag^0 from the grain boundaries than from the bulk[3].

The mechanism of silver's antibacterial effects are suggested to be related to interactions between Ag^+ and proteins on cell membranes with negatively charged thiol groups [9]. Metallic silver is inert in the presence of human tissues, but when in contact with inorganic compounds, it ionizes to Ag^+, which can bind to and damage the cell membrane [9]. Additionally, ionic silver can act as an oxidizing agent, supporting the production of reactive oxygen species (ROS), which impair metabolic processes and cell division[9], [10]. One study also found that nanocrystalline silver reduces MMP levels and increases cell apoptosis, promoting rapid wound healing in contaminated areas[11].

In studies by other research groups, water has been included when sputtering metals such as titanium, aluminum, or zinc, either intentionally or unintentionally, and the properties of the resulting films have been studied. Water is avoided in most applications of physical vapour deposition because it reduces the electrical properties or disrupts crystal growth[12], [13]. For many applications, defects are not desired, but for this present work, increasing the defects and decreasing the grain size is beneficial. Most commonly when sputtering metallic thin films using water, the texture was enhanced, defects increased, and grain size decreased[12], [14], [15]. Adding even a small amount of water can change the composition of the gas in the sputtering chamber due to reactions between water, its dissociation products, and oxygen, which can then impact dressing composition and properties[12], [15]. It has also been suggested that hydroxide or water molecules or radicals may be relevant in migrating and disrupting the film[14]. The hydroxide ion is suggested to have a higher diffusion coefficient through vacancies than the oxide ion because of its small size and low charge[16]. Silver is not a very reactive metal, and although it reacts with oxygen, primarily forming silver oxide in the I oxidation state, it does not react with water in its molecular form[17].

The quantity of silver in the dressing, the species of silver, the grain size, the release into solution, and the overall nanostructure may all be important in creating an effective medical treatment. These will all be studied in the following chapter in the context of changes to sputtering conditions. Because the nanocrystalline films, and the solutions made from their dissolution, are the basis for the treatments to be used in future chapters, it is important to have these dressings and solutions characterized.

Previous work in this laboratory group has established parameters that are ideal for creating nanocrystalline silver materials[18]. The standard conditions mimic conditions under which the original nanocrystalline silver dressings were created- noted as "Standard" films or samples. The Novel conditions which include water in the sputtering chamber are noted as "Novel". One purpose of this chapter is to assess if the Novel conditions are significantly better than the Standard conditions. If the Novel conditions are a significant improvement, they will be used as the basis for the treatments in further studies.

Methods

Detailed methods are described in Chapter 2. Here, a summary of the methods used in this chapter is provided. Deviations from the protocols listed in Chapter 2 will be noted.

Dressing Fabrication

An in-house sputtering apparatus was used to create the experimental nanocrystalline silver films on HDPE by a physical vapour deposition process with a pure silver target, as described in Chapter 2.

For the experimental "Novel" films, the atmosphere was composed of 4.5% oxygen with the balance argon. The current was set at 1.8A. Water was injected at a constant rate of 15 μL/min using a peristaltic pump connected to the argon gas input line. For comparison, another set of films was created using a standard set of conditions, identified as "Standard". For these samples, the atmosphere was 4.0% oxygen and the current was set at 0.9A. No water was included in the sputtering atmosphere. These Standard films mimic the properties of commercially available Acticoat™ dressings. The Novel parameters were chosen as the result of previous research seeking to make more potent dressings more efficiently[18]. The goal of previous work was to find an oxygen concentration which would create films with an ammonia soluble silver content that was between 40% and 50% of the total silver, when sputtered at 1.8A [18]. These experiments resulted in the choice of 4.5% oxygen instead of the standard 4.0%.

For initial tests, three Standard films and three Novel films were sputtered to establish an expected baseline for material properties and confirm the reproducibility of the process. For each sample, the process was run for 30 minutes. Samples were taken from a central portion of the film, 4 inches from either side, and at least 6 inches from the starting position.

In subsequent tests, the process was run for 3 hours per sample, at a speed of 1.65 cm/minute, as described previously, resulting in approximately 10 ft of usable film. To ensure that the properties were uniform throughout, samples for analysis were taken from 6 locations as shown below in Figure 3-1.
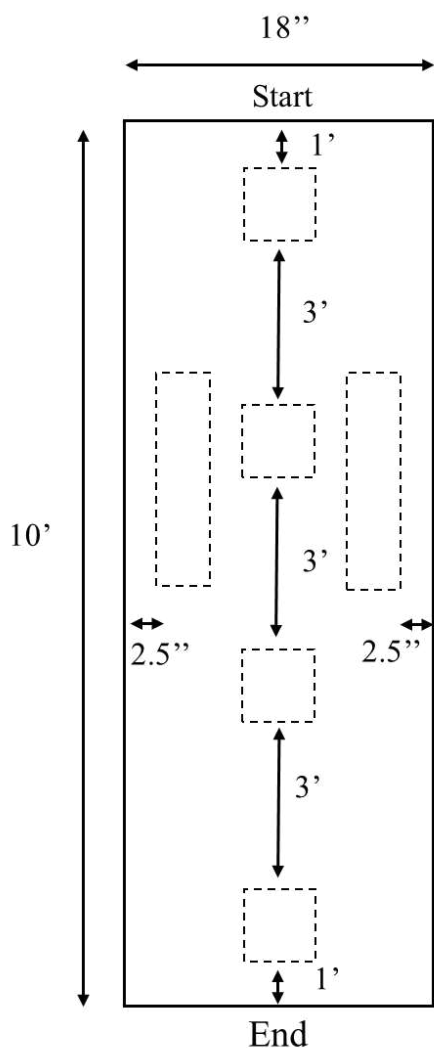
Figure 3-1 Sampling locations for films.

X-ray Diffraction

XRD and grain size measurements were performed as per the procedure given in Chapter 2. Grain sizes were measured from six samples and given as an average. Metallic silver is identified from peak locations at approximately 38, 44, 65, and 77 °2θ. Silver oxide is identified primarily from peaks at approximately 33 and 44 °2θ.

Scanning Electron Microscopy

Images were taken at 50 000x and 100 000x magnification using a Hitachi Field Emission Scanning Electron Microscope magnification with parameters described in Chapter 2.

Chemical Analysis

For chemical analysis, nitric acid and ammonium hydroxide digests were performed as described in Chapter 2 and analyzed by ICP-MS. Samples were corrected for dilution factor and given as mg of silver per square inch of film.

Dissolution

To determine the silver release over a period of time, 2 square inches of film were soaked in 7.5 mL distilled water at 37°C for 2, 6, or 24 hours, then diluted and acidified as previously described. These solutions were analyzed for amount of silver using ICP-MS. Samples were corrected for dilution factor and given as mg of silver per square inch of material and percentage of total silver released.

For a series of 6 hour solutions, after the film was removed from the solution, it was dissolved in ammonium hydroxide as described above to determine the quantity of ammonia soluble silver remaining in the film after dissolution.

Log Reductions

Pseudomonas aeruginosa and *Staphylococcus aureus* were used to perform log reductions, as representative species of Gram negative and Gram positive organisms. After overnight growth, 200 µL of bacterial inoculum was incubated for one hour with solid nanocrystalline silver dressing samples at 37°C. The full procedure is described in Chapter 2.

To test the antibacterial properties of solutions made with nanocrystalline films, 2 square inches were soaked in 7.5 mL distilled water at 37°C for 6 hours. For "10% solutions", 1.8 mL of this silver solution was combined with 0.2 mL of a bacterial inoculum. For "2.5% solutions", 1.95 mL of silver solution was combined with 50 µL of inoculum. Otherwise, the procedure is performed as described in Chapter 2.

Day-to-Day Corrected Zone of Inhibition (CZOI) Assay

The bacteriostatic longevity of the material was assessed using day-to-day transfer corrected zone of inhibition assays for nine days with *S. aureus*. For comparison, two control dressings were made with uncoated HDPE and gauze.

Statistics

Unpaired two sample t-tests with Welch's correction were used to compare sample groups. Quantitative measurements in tables are presented as average ± standard deviation for six samples unless otherwise

indicated. For line charts and bar graphs, each data point is the average of six samples unless otherwise stated and error bars represent the standard deviation. Analysis was performed using Microsoft Excel.

Results

X-ray Diffraction

Figures 3-2 and 3-3 display the XRD spectra for the films with Standard and Novel sputtering conditions. Six samples from each sputtering condition were taken from different locations of the film and were scanned. All spectra were similar within sample groups, so one representative spectrum is shown here. The y-axis scale is arbitrary intensity units. The peaks at approximately 22 and 24°2θ are known to correspond to the HDPE substrate and are not of interest. The peaks of primary interest are the peaks at 33, 38 and 44°2θ. The peak at 33°2θ corresponds to Ag_2O, with silver in the I oxidation state. A peak at 44°2θ degrees corresponds to metallic, neutral silver. The peak at 38°2θ corresponds to both metallic silver and Ag_2O. The peak locations correspond to Ag_2O, but not other forms of silver oxide, so it is understood that the silver oxide present in the sample is Ag_2O. There is an overall stronger intensity for all silver peaks relative to the HDPE background for the Novel films (Figure 3-3). For the Standard spectrum (Figure 3-2), the peak at 44°2θ is barely identifiable, indicating a low signal for metallic silver.
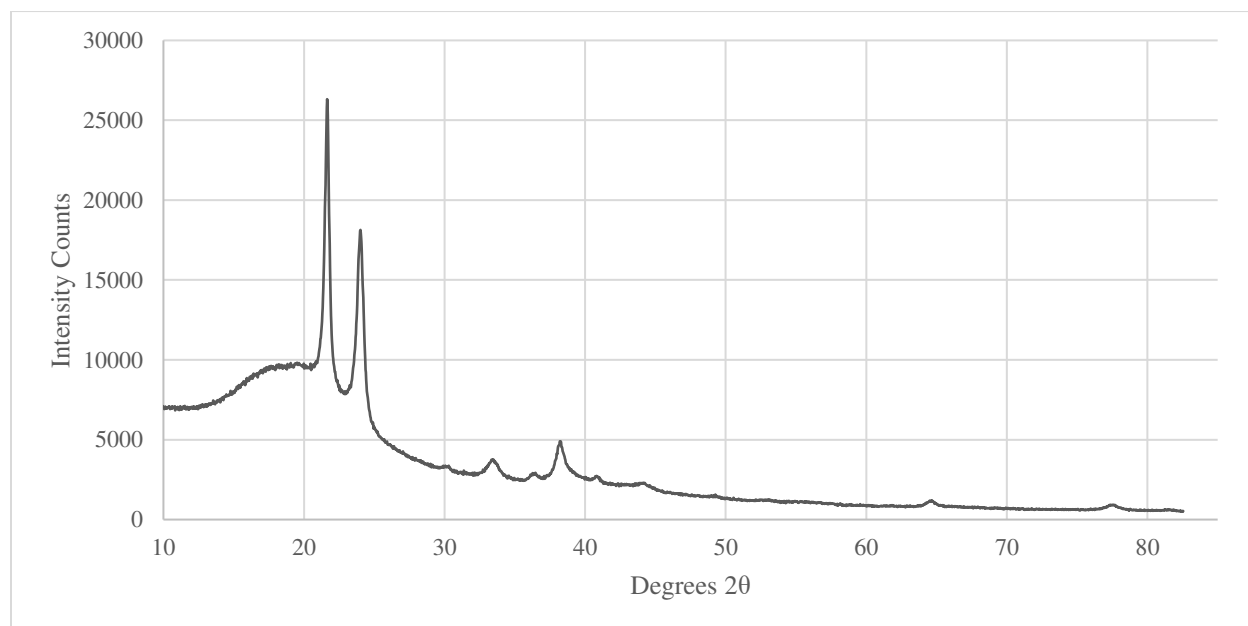
Figure 3-2 Standard film XRD spectrum.
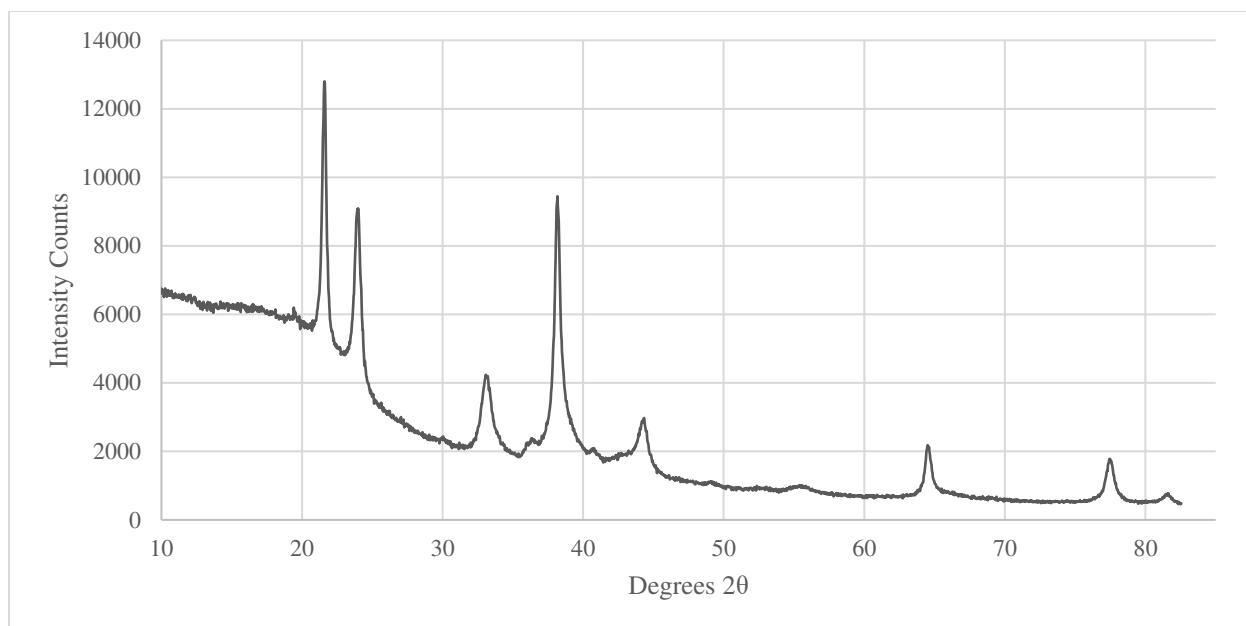
Figure 3-3 Novel film XRD spectrum.

The grain sizes were measured by hand using the Scherrer equation and the results are displayed in Table 3-1. The Standard samples have a smaller average grain size of 10.2 nm compared to 14.2 nm for the Novel samples. There is a significant increase in grain size between the Novel and Standard films.

Table 3-1 Grain size measurements for Standard and Novel films.

	Grain size (nm)	p-value
Standard	10.2 ± 0.8	2.65E-06
Novel	14.2 ± 0.6	

Scanning Electron Microscopy (SEM)

Representative images for the two sample types are shown in Figure 3-4. All images shown were taken using the Hitachi Field Emission SEM. Images A and C are Standard samples and B and D are Novel samples. The Standard sample, sputtered without water, has a smaller feature size. This observation is confirmed by the measurement of grain size performed with x-ray diffraction. The images of Novel films appear to have a greater depth of structure. The Standard samples have a smaller feature size and are more textured.
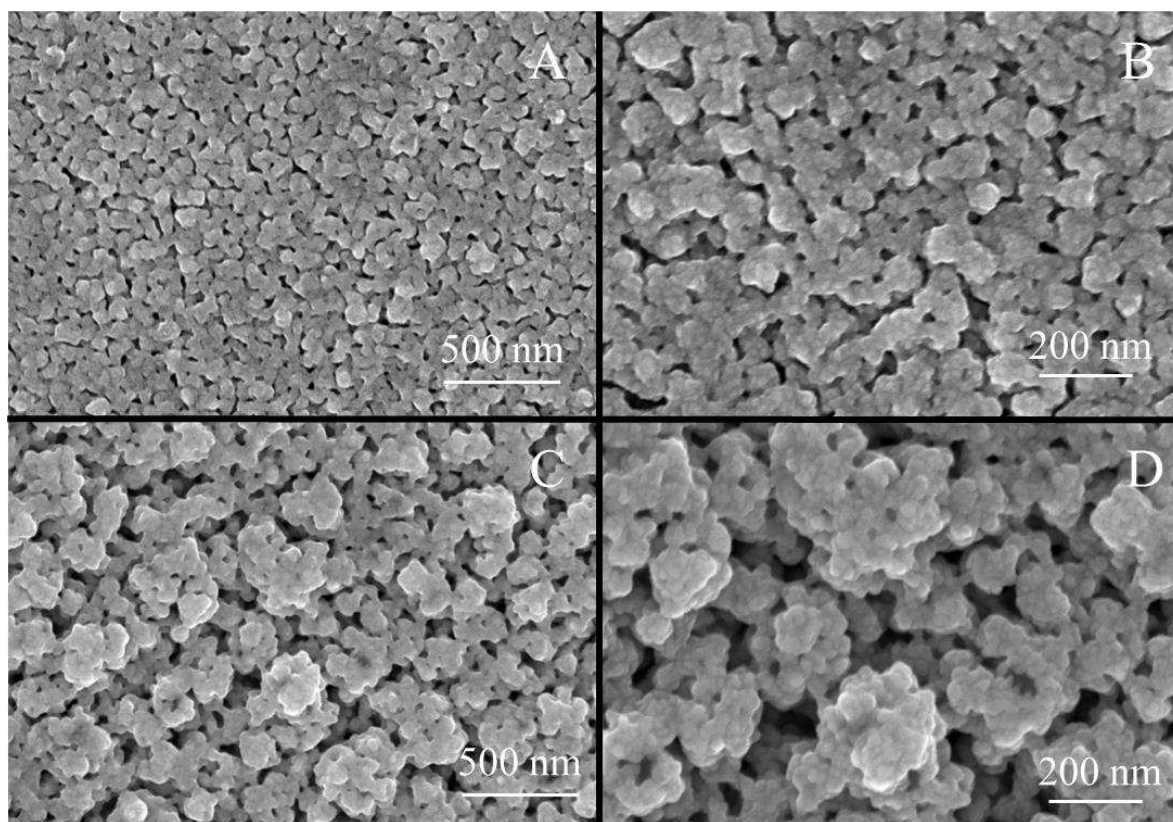
Figure 3-4 Representative SEM images. A) Standard film at 50 000x, B) Novel film at 50 000x, C) Standard film at 100 000x, D) Novel film at 100 000x. Scale bars are shown on images.

Chemical Analysis

The chemical analysis of the Novel and Standard films is displayed in Table 3-2. The Novel conditions created films that have significantly more total silver, which is expected due to the higher current (1.8A versus 0.9A) allowing for a higher rate of silver deposition. The Standard films have a significantly higher percentage of ammonia soluble silver, but the total quantity of ammonia soluble silver is significantly higher in the Novel films. Ammonia soluble silver, while it can encompass a variety of positively charged silver species that can be solubilized, is considered a close correlation to the silver oxide (Ag_2O) in a sample. The Novel films have a higher percentage of oxygen in the sputtering environment (4.5% versus 4.0%), but this does not translate into a higher percentage of silver oxide.

Table 3-2 Total and ammonia soluble silver with percent ammonia soluble for Standard and Novel samples. P-values from t-test comparisons included.

	Total silver (mg/in²)	Ammonia soluble silver (mg/in²)	% Ammonia Soluble
Standard	1.65 ± 0.06	0.95 ± 0.10	57.81 ± 7.04
Novel	4.53 ± 0.27	1.70 ± 0.10	37.73 ± 2.89
p-value	2.23E-07	1.93E-07	1.72E-04

Dissolution

Figure 3-5 displays the trends in silver released from Standard and Novel films in water over 24 hours. There are significant differences ($p<0.05$) between groups at all time points, with increasing statistical strength with increasing time. Table 3-3 shows the p-values for comparisons. However, there are no significant differences between time points for 2 and 6 hours or 6 and 24 hours for either Standard or Novel films.
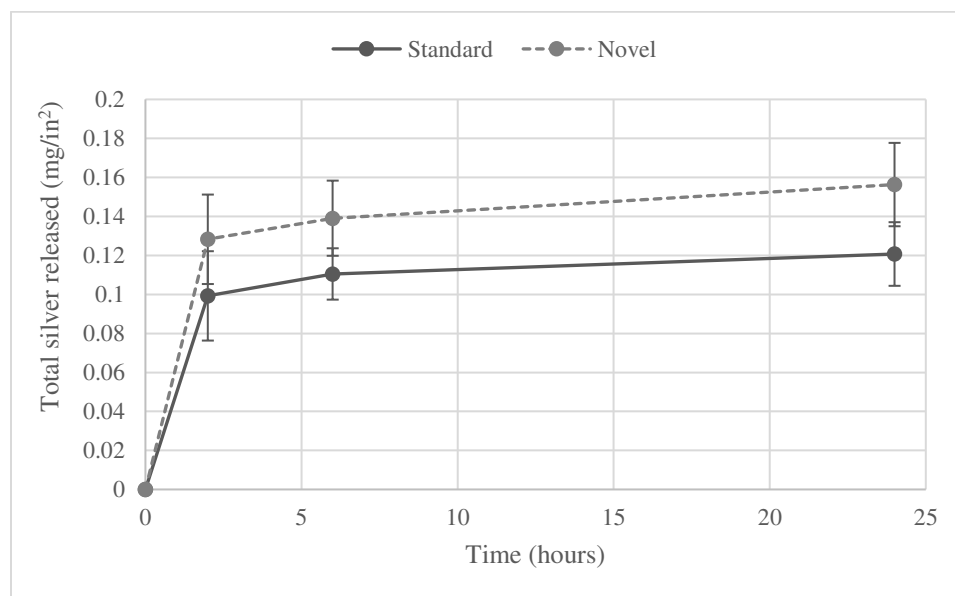
Figure 3-5 Total silver released in water over time for Standard and Novel films.

Table 3-3 p-values for t-tests comparing Standard and Novel silver release at each time point.

	2 hour silver release	6 hour silver release	24 hour silver release
p-value	0.031	0.0087	0.0053

Figure 3-6 displays the trends of silver release into water over 24 hours of Standard and Novel films as a percentage of the total silver previously measured by nitric acid digest (Table 3-2). The percentage of silver released was between 2% and 9% of the total silver measured in the solid film. It can be observed that there is more variation in the Standard samples compared to the Novel samples. While the Novel samples released more total silver, they released a lower percentage of the total silver contained in the film.
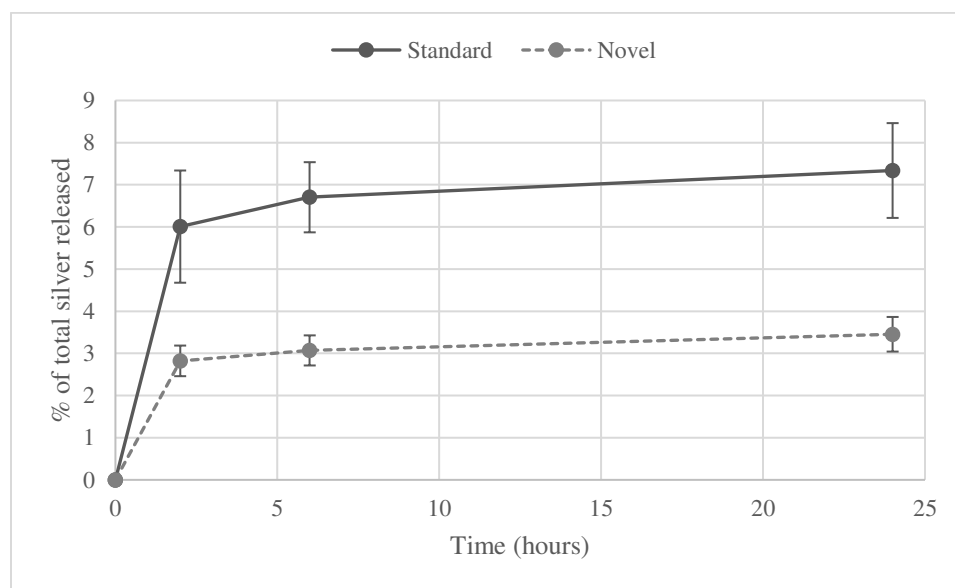
Figure 3-6 Silver released into solution by Standard and Novel films, as a percentage of the total silver measured in the film previously by nitric acid digest.

After 6 hours soaked in water for silver release into solution, the ammonia soluble silver was measured by ammonium hydroxide digest. In this test, there was a large amount of variation in the measurements and no significant differences were found between groups. Unexpectedly, the calculated amount of ammonia soluble silver released per square inch of material was higher than the total amount of silver released into solution when measured directly. The ammonia soluble silver calculation was based on the remaining ammonia soluble silver subtracted from the initial quantity of ammonia soluble silver. Results are shown below in Table 3-4.

Table 3-4 Calculated release of ammonia soluble silver into solution, using total silver released in solution and measured ammonia soluble silver.

	Ammonia soluble silver measured in film after solution (mg/in^2)	Calculated ammonia soluble silver released (mg/in^2)	Theoretical percent ammonia soluble silver released (%)	Measured total silver released (mg/in^2)
Standard	0.74±0.11	0.21±0.15	21±13	0.11±0.01
Novel	1.43±0.21	0.27±0.21	16±13	0.14±0.02
p-value	6.12E-05	0.28	0.24	8.68E-03

Figure 3-7 shows an image of a Novel sample film after 6 hours dissolution in water. Visible in this image are patches in the structure that appear to be degraded. Figure 3-8 also shows a comparison of Novel and Standard samples with and without dissolution. Image 3-8(A) (no dissolution) shows the normal Novel structure. Image 3-8(B) (with dissolution) shows a closer look at a degraded patch that lacks the normal structure. The structure surrounding the patches is comparable to the structure of the undissolved sample. The Standard samples in Figure 3-9 are shown at higher magnification to more clearly show the texture. Image 3-9(A) is the undissolved material and Image 3-9(B) is after dissolution. The microstructure appears to have greater depth and surface area after dissolution, which may indicate more uniform dissolution of the silver on the surface for Standard samples.
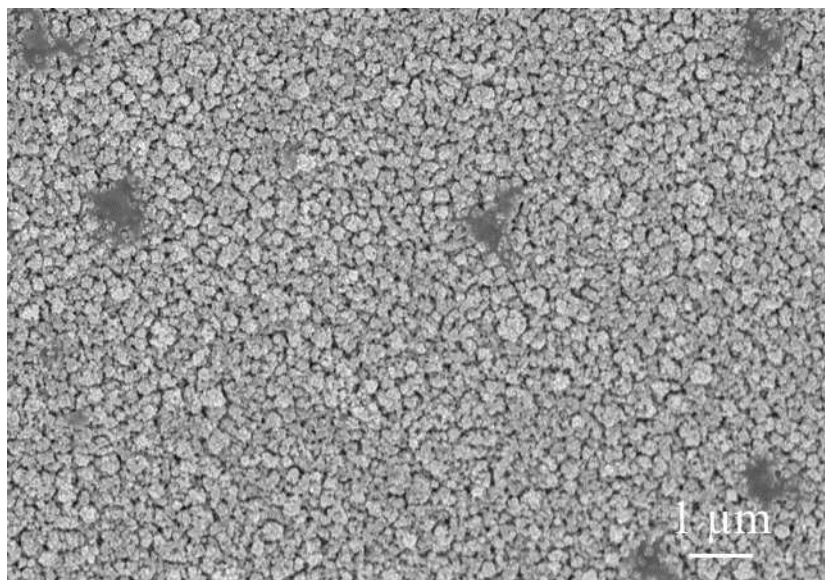
Figure 3-7 Representative SEM image of a Novel film after dissolution at 10 000x magnification.
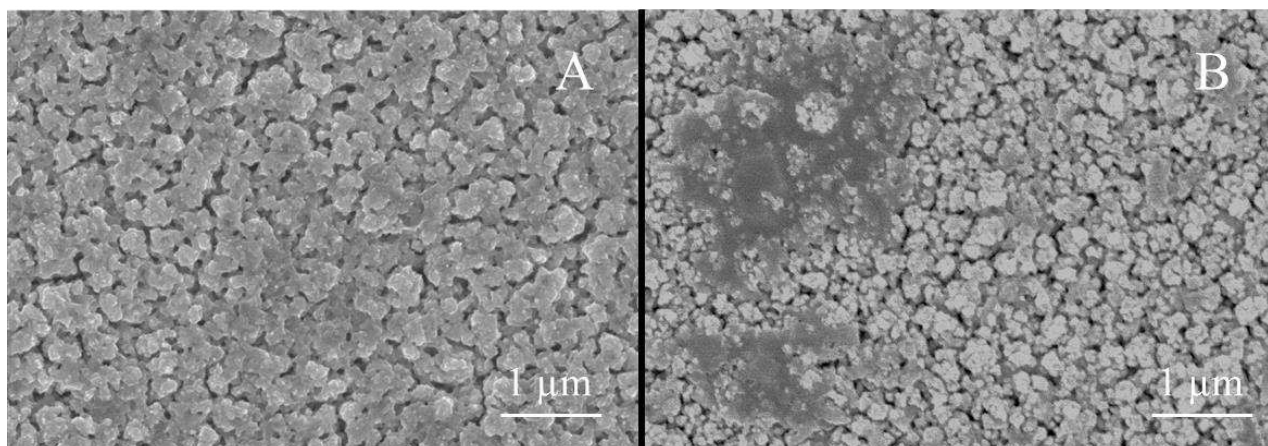
Figure 3-8 Representative SEM images. A) Novel sample without dissolution, B) Novel sample after a 6 hour dissolution. Both images at 20 000x magnification.
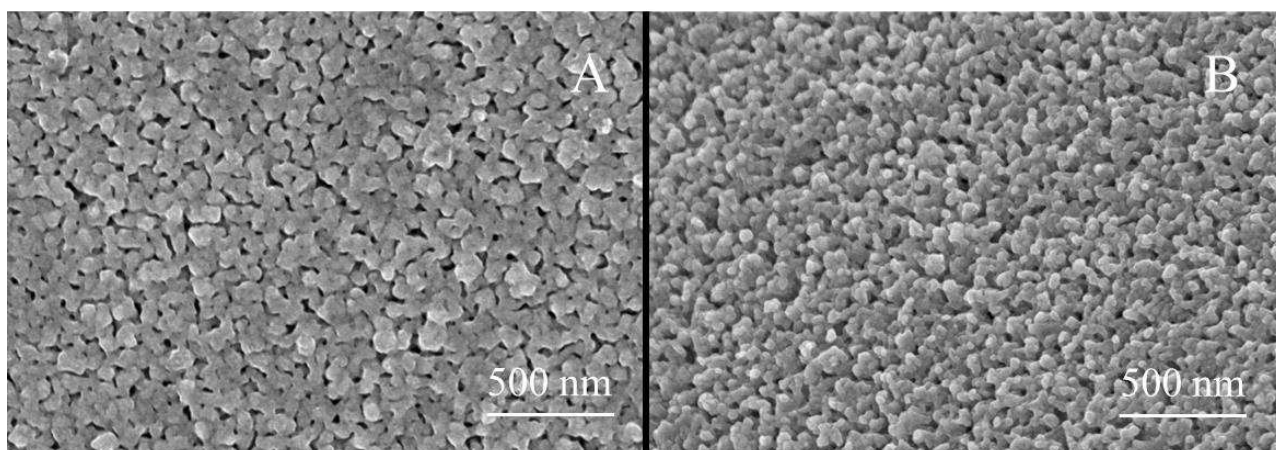
Figure 3-9 Representative SEM images. A) Standard sample without dissolution, B) Standard sample after 6 hour dissolution. Both images at 50 000x magnification.

Log Reduction

As expected, the log reduction for all dressing samples (two pieces of film with absorbent gauze in the middle) resulted in a total kill of all bacterial colonies when challenged with both *P. aeruginosa* and *S. aureus*. The threshold for the designation of bactericidal for a material is a log reduction of at least 3. While no differences could be seen between the two types of dressing, the strong bactericidal capabilities of these dressings were confirmed with log reductions of at least 7 for *P. aeruginosa* and 8 for *S. aureus*.

Log reductions were also performed on silver solutions with two inoculum ratios, 10% and 2.5% of the total solution. The data from 10% solutions, with 200 µL of inoculum and 1.8 mL of silver solution, resulted in relatively small log reductions and are shown in Table 3-5 as average ± standard deviation, with the p-value given for comparison between Standard and Novel dressings. While the log reductions

are low, not reaching the threshold for bactericidal capacity, for *S. aureus*, there is a statistically significant difference between the two dressings.

Table 3-5 Log reductions with 10% inoculum to silver solution ratios, using *S. aureus* and *P. aeruginosa* with Standard and Novel solutions.

	S. aureus	*P. aeruginosa*
Inoculum Size (CFU/mL)	2.33E+07	1.70E+08
Cells in solution (CFU)	4.67E+06	3.40E+07
Standard	0.64±0.20	0.56±0.13
Novel	0.99±0.11	0.53±0.12
p-value	3.89E-03	0.62

For the 2.5% solutions, with 50 µL of inoculum and 1.8 mL of silver solution, averages and p-values could not be given in most cases because many samples had total kills of all colonies and an exact log reduction is not available. Therefore, Table 3-6 displays the log reduction for each individual sample, 6 replicates for each dressing. Even without statistical comparison, it can be identified that the log reductions for Novel samples are larger than those for Standard samples. While the raw number of cells per solution was similar to the 10% solutions for both bacteria, the log reductions were high, well above the threshold of 3. There was some variation, but even in samples with the lowest log reductions, they were still well above 3.

Table 3-6 Log reductions with 2.5% inoculum to silver solution ratios, using *S. aureus* and *P. aeruginosa* with Standard and Novel solutions.

	S. aureus	*P. aeruginosa*
Inoculum size (CFU/mL)	5.17E+08	1.00E+10
Cells in solution (CFU)	2.58E+07	5.00E+08
Standard	4.29	3.33
	3.11	>6
	3.29	>6
	4.04	6.28
	4.29	4.48
	4.19	5.22
Average	3.87±0.53	N/A
Novel	>5	>6
	4.89	>6
	>5	>6
	>5	>6
	4.89	>6
	>5	>6
Average	N/A	N/A

Corrected Zone of Inhibition (CZOI)

The CZOI test measured bacteriostatic properties over a period of 9 days using *S. aureus* using sample dressings made from nanocrystalline silver films and gauze. There was not a significant difference in the maximum value achieved for each sample, which may be due to the high amount of variation in the Novel dressing samples on Day 3, as seen in Figure 3-10. Table 3-7 displays the maximum zone size and ending zone size average for Standard and Novel samples and the p-values for t-test comparison. The Standard and Novel dressings followed similar trends but had significantly different zones at the end of 9 days. All six Novel dressing replicates had measurable zones at the end, but only three out of six of the Standard dressing replicates had measurable zones. Control dressings with uncoated HDPE and gauze had no zones on any day.
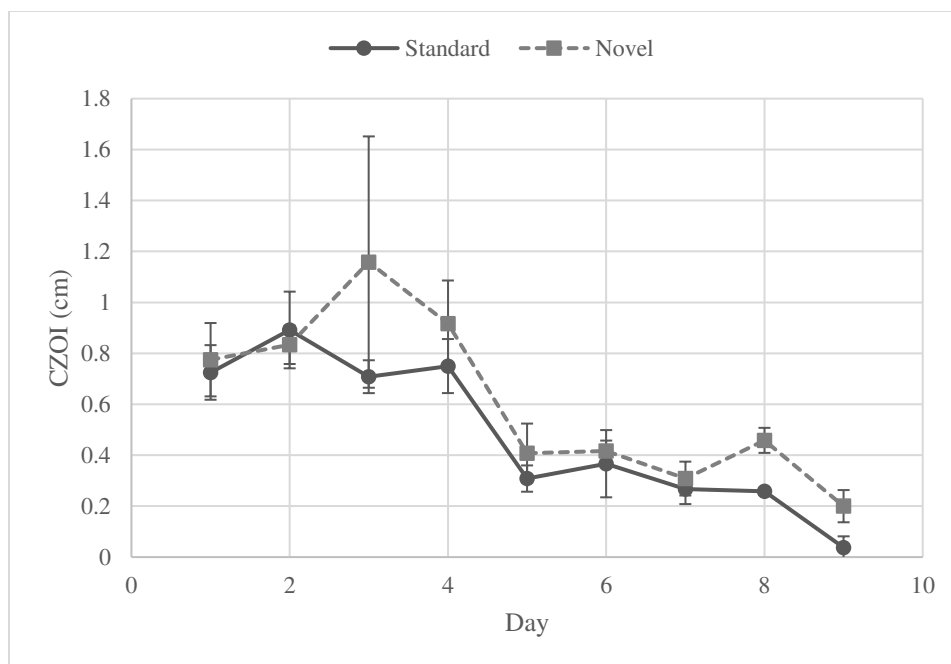
Figure 3-10 Zone lengths for CZOI test over nine days for Standard and Novel samples.

Table 3-7 Maximum and ending values for inhibition zones in CZOI test over 9 days for Standard and Novel samples.

	Maximum (cm)	End (cm)
Standard	0.93 ± 0.08	0.038 ± 0.044
Novel	1.22 ± 0.43	0.20 ± 0.06
p-value	0.081	3.00E-04

The average zone size of the 6 replicates was calculated for each day and presented in Table 3-8, along with p-values indicating if there was a significant difference between the Standard and Novel dressings on that day. There were significant differences on Days 3, 4, 5, 8, and 9, shown by the bolded p-values.

Table 3-8 Average zone length for Standard and Novel film samples on each day of CZOI test, p-values from t-tests between groups on each day are included. Bolded values are those that reach significance.

Day	Standard Zone (Average, cm)	Novel Zone (Average, cm)	p-value
1	0.73	0.78	0.26
2	0.89	0.83	0.21
3	0.71	1.16	**0.03**
4	0.75	0.92	**0.03**
5	0.31	0.41	**0.04**
6	0.37	0.42	0.20
7	0.27	0.31	0.14
8	0.26	0.46	**1.1E-06**
9	0.04	0.20	**2.1E-04**

The quantity of silver remaining in the dressings for three samples per condition was measured by nitric acid digest and converted to mg/in^2. Data is displayed in Table 3-9. There was a significant difference in the amount of silver remaining in the dressing for Novel versus Standard. The Novel dressings released almost twice as much silver during the nine day test than Standard dressings, with still 35.9% of the initial silver remaining. The control dressings of uncoated HDPE showed no silver in the nitric acid digest.

Table 3-9 Silver remaining in film samples after nine days of CZOI test

	Silver remaining (mg/in^2)	Silver released (mg/in^2)	Percent of initial silver remaining (%)
Standard	0.19 ± 0.15	1.42 ± 0.11	11.45 ± 9.33
Novel	1.57 ± 0.20	2.80 ± 0.08	35.9 ± 2.4
p-value	3.50E-4	2.79E-5	0.024

Table 3-10 displays the ending zone size for three Standard and Novel samples along with the silver remaining in the dressing, in mg/in^2, as measured by nitric acid digest. Interestingly, the Standard samples that had no zone by Day 9 had more silver remaining than the Standard sample that still had a zone (0.05cm). Novel samples still had silver remaining, as well as measurable zones, after nine days.

Table 3-10 Ending zone length after nine days of CZOI test, with comparison to quantity of remaining silver in dressing

		Ending zone size (cm)	Silver remaining in dressing (mg/in^2)
Standard	1	0	0.33
	2	0.05	0.027
	3	0	0.20
Novel	1	0.25	1.54
	2	0.25	1.40
	3	0.15	1.80

Discussion

Chemical and Physical Properties

In binary alloy systems, the higher the alloy composition, the smaller the grain size[3]. This applies to the study as the aim for sputtered films is to have between 40 to 50% silver oxide, with the remaining being metallic silver, so that the grain growth of one type is interrupted by the other. Novel nanocrystalline silver materials had a smaller percentage of ammonia soluble silver, but because they have almost three times the quantity of total silver deposition, they have a larger total quantity of ammonia soluble silver. The larger total quantity can be attributed to the higher current (1.8 A versus 0.9 A) used in the sputtering process which allows for increased deposition compared to Standard materials. The addition of water is thought to stabilize the voltage during sputtering, allowing for higher currents to be used to increase total silver deposition. The lower percentage of ammonia soluble silver for Novel samples, even with a larger percentage of oxygen, is also attributable to the current where the higher energy in the sputtering chamber leads to greater diffusion of oxygen.

The total silver released in solution for the Novel samples was higher in total quantity but lower in percentage release of the total silver. This is evidence that the structure of the Novel films is more tightly bound, given that less silver is released. The Standard dressings have a greater percentage of ammonia soluble silver, which contributes to stabilizing the nanostructure, but it is more readily ionized in water. The Standard dressings were seen in the SEM images to have a smaller feature size which would allow for more surface area for silver to be released relative to the total amount.

Unexpectedly, the calculated quantity of ammonia soluble silver released per square inch of material was higher than the total silver released into solution measured directly and converted to mg/in^2, where less ammonia soluble silver was measured than would be expected in the final film. This may be a result of

variability in measurement of ammonia soluble silver, or an inaccurate measurement of the silver initially released in solution, or the dissolution of the film is changing the surface structure.

From the XRD spectra, both metallic silver and silver oxide were identified. Ag_2O was the only recognizable oxide peak from the XRD spectra, which was expected based on previous sources [17]. This confirms that the only stable or detectable oxide species on the surface of the samples is Ag_2O. Metallic silver and silver oxide are both present, but quantitative analysis was only done for grain size, not relative composition. The Standard films have a smaller average grain size. This corresponds to a greater fraction of silver oxide for Standard samples, which stabilizes a smaller grain size.

In alloys, to reduce the elastic strain from the size mismatch, solutes will segregate to the edges and grain boundaries of a material because this reduced the overall Gibb's Free Energy. The energetic cost of increasing the grain boundary area is more than compensated for by the reduction in energy from moving solutes to the grain boundaries, up to a certain grain size[20]. At grain sizes less than 10 nm, the behaviour of the material is more reliant on grain boundary properties than bulk properties [21].

Biological Properties

As expected, the log reductions for both the Standard and Novel dressings showed exceptional antimicrobial properties. However, with total kills for both species of bacteria, there were not quantitative results to compare the differences between the dressings. The solution-based log reductions produced results that were able to be statistically compared. The standard procedure in our laboratory is to use a 10% ratio of 200 μL inoculum in 1.8 mL of silver solution for log reductions. When this resulted in unusually small log reductions, a 2.5% ratio was used. The major difference in log reduction from the 10% and 2.5% inoculum solutions shows that the bactericidal capacity of the same strength of solutions varies significantly based on the ratio, even when the raw number of cells in solution is similar. Even with similar number of cells, a small increase in the relative quantity of silver solution caused a large increase in the antimicrobial properties.

The Corrected Zone of Inhibition test also yielded significant results. At the end of nine days, all Novel dressings had measurable zones, but this was not the case for all Standard dressing samples. This shows that the Novel dressings have better longevity and sustained release of silver. A CZOI test of silver alginate dressings in 2011 using the same organisms for one day resulted in zones between 4.5 mm and 10.8 mm for *S. aureus*, compared to 7.25 mm and 7.75 mm on Day 1 for Standard and Novel dressings respectively [22].

At the end of nine days, the quantity of silver remaining in the dressings was tested for three samples each of Standard and Novel dressings. Novel samples had an average of 1.57 mg/in^2 remaining, which was 35.9% of the silver initially measured, compared to only 0.19 mg/in^2 for 11.45% of initial silver for Standard samples. Novel samples released more silver, and still had a significant amount remaining in the dressing after nine days, leading to a continuing zone of inhibition over nine days. Standard samples had less silver to release and could not maintain a zone of inhibition as long as Novel samples.

Conclusion

The Novel sputtering parameters were used to be a more stable and efficient sputtering process to increase silver deposition while maintaining a composition of approximately 40% ammonia soluble silver. The Novel samples were significantly different from the Standard samples in their chemical, physical, and biological properties. They still had superior bactericidal properties even with a lower fraction of ammonia soluble silver. The Novel films also had larger grain sizes compared to Standard samples which may impact their anti-inflammatory capacity, but this has not noticeably impacted the antibacterial properties. Most notably, the increased release into solution by Novel samples will be beneficial for developing solutions for use in adhesion treatments. Future work may further adapt sputtering parameters with the goal of increasing release into solution. Novel film samples will be used in developing solution-based treatments later in this thesis, particularly for their increased release of silver and greater longevity over Standard films.

References

[1]   F.-R. F. Fan and A. J. Bard, "Chemical, Electrochemical, Gravimetric, and Microscopic Studies on Antimicrobial Silver Films," *J. Phys. Chem. B*, vol. 106, no. 2, pp. 279–287, Jan. 2002, doi: 10.1021/jp012548d.

[2]   R. E. Burrell and P. Nadworny, "Nanocrystalline Silver: Novel Structure and Activity," in *The Third International Conference on the Development of Biomedical Engineering in Vietnam*, V. Van Toi and T. Q. D. Khoa, Eds., in IFMBE Proceedings. Berlin, Heidelberg: Springer, 2010, pp. 6–9. doi: 10.1007/978-3-642-12020-6_2.

[3]   J. R. Trelewicz and C. A. Schuh, "Grain boundary segregation and thermodynamically stable binary nanocrystalline alloys," *Phys. Rev. B*, vol. 79, no. 9, p. 094112, Mar. 2009, doi: 10.1103/PhysRevB.79.094112.

[4]   B. Feng, T. Yokoi, A. Kumamoto, M. Yoshiya, Y. Ikuhara, and N. Shibata, "Atomically ordered solute segregation behaviour in an oxide grain boundary," *Nat. Commun.*, vol. 7, no. 1, p. 11079, Mar. 2016, doi: 10.1038/ncomms11079.

[5]   P. L. Nadworny, J. Wang, E. E. Tredget, and R. E. Burrell, "Anti-inflammatory activity of nanocrystalline silver-derived solutions in porcine contact dermatitis," *J. Inflamm.*, vol. 7, no. 1, p. 13, Feb. 2010, doi: 10.1186/1476-9255-7-13.

[6]   P. L. Nadworny, J. Wang, E. E. Tredget, and R. E. Burrell, "Anti-inflammatory activity of nanocrystalline silver in a porcine contact dermatitis model," *Nanomedicine Nanotechnol. Biol. Med.*, vol. 4, no. 3, pp. 241–251, Sep. 2008, doi: 10.1016/j.nano.2008.04.006.

[7]   P. L. Nadworny, B. K. Landry, J. Wang, E. E. Tredget, and R. E. Burrell, "Does nanocrystalline silver have a transferable effect?," *Wound Repair Regen.*, vol. 18, no. 2, pp. 254–265, 2010, doi: 10.1111/j.1524-475X.2010.00579.x.

[8]   M. H. Cavanagh, R. E. Burrell, and P. L. Nadworny, "Evaluating antimicrobial efficacy of new commercially available silver dressings," *Int. Wound J.*, vol. 7, no. 5, pp. 394–405, 2010, doi: 10.1111/j.1742-481X.2010.00705.x.

[9]   A. B. G. Lansdown, "Silver and Gold," in *Patty's Toxicology*, American Cancer Society, 2012, pp. 75–112. doi: 10.1002/0471435139.tox026.pub2.

[10]   CH. Ramamurthy *et al.*, "The extra cellular synthesis of gold and silver nanoparticles and their free radical scavenging and antibacterial properties," *Colloids Surf. B Biointerfaces*, vol. 102, pp. 808–815, Feb. 2013, doi: 10.1016/j.colsurfb.2012.09.025.

[11]   J. B. Wright, K. Lam, A. G. Buret, M. E. Olson, and R. E. Burrell, "Early healing events in a porcine model of contaminated wounds: effects of nanocrystalline silver on matrix metalloproteinases, cell apoptosis, and healing," *Wound Repair Regen.*, vol. 10, no. 3, pp. 141–151, 2002, doi: 10.1046/j.1524-475X.2002.10308.x.

[12]   T. Nakada, Y. O. Y. Ohkubo, and A. K. A. Kunioka, "Effect of Water Vapor on the Growth of Textured ZnO-Based Films for Solar Cells by DC-Magnetron Sputtering," *Jpn. J. Appl. Phys.*, vol. 30, no. 12R, p. 3344, Dec. 1991, doi: 10.1143/JJAP.30.3344.

[13]   G. Queirolo, M. Dellagiovanna, and G. De Santi, "Effect of the sputtering ambient contamination on the microstructure of Al–Si films: Journal of Vacuum Science & Technology A: Vol 7, No 3," *J. Vac. Sci. Technol. A*, vol. 7, no. 651, 1989, doi: https://doi.org/10.1116/1.575860.

[14]   T. Nakada, Y. Ohkubo, and A. Kunioka, "Textured ZnO:Al films for solar cells by DC-magnetron sputtering in water vapor plasma," in *The Conference Record of the Twenty-Second IEEE Photovoltaic Specialists Conference - 1991*, Oct. 1991, pp. 1389–1392 vol.2. doi: 10.1109/PVSC.1991.169435.

[15]   O. Banakh, P. E. Schmid, R. Sanjinés, and F. Lévy, "Electrical and optical properties of TiOx thin films deposited by reactive magnetron sputtering," *Surf. Coat. Technol.*, vol. 151–152, pp. 272–275, 2002, doi: https://doi.org/10.1016/S0257-8972(01)01605-X.

[16]   Y. Wouters, A. Galerie, and J.-P. Petit, "Thermal oxidation of titanium by water vapour," *Solid State Ion.*, vol. 104, no. 1–2, pp. 89–96, 1997, doi: https://doi.org/10.1016/S0167-2738(97)00400-1.

[17] J. F. Pierson, D. Wiederkehr, and A. Billard, "Reactive magnetron sputtering of copper, silver, and gold," *Thin Solid Films*, vol. 478, no. 1, pp. 196–205, May 2005, doi: 10.1016/j.tsf.2004.10.043.

[18] R. Burrell, "Personal Communication," 2021.

[19] X. Bao *et al.*, "The effect of water on the formation of strongly bound oxygen on silver surfaces," *Catal. Lett.*, vol. 32, no. 1–2, Art. no. 1–2, 1995, doi: 10.1007/BF00806112.

[20] J. Weissmüller, "Alloy thermodynamics in nanostructures," *J. Mater. Res.*, vol. 9, no. 1, pp. 4–7, Jan. 1994, doi: 10.1557/JMR.1994.0004.

[21] J. Musil and J. Vlček, "Magnetron sputtering of alloy-based films and its specifity | SpringerLink," *Czechoslov. J. Phys.*, vol. 48, pp. 1209–1224, 1998.

[22] S. L. Percival, W. Slone, S. Linton, T. Okel, L. Corum, and J. G. Thomas, "The antimicrobial efficacy of a silver alginate dressing against a broad spectrum of clinically relevant wound isolates," *Int. Wound J.*, vol. 9, no. 3, pp. 237–243, 2011, doi: https://doi.org/10.1111/j.1742-481X.2011.00774.x.

Chapter 4 : Fabrication and Analysis of Nanocrystalline Silver-Gold Alloys

Introduction

Silver and gold are both noble metals, and because of their similarity in size, crystal structure, and electronegativity, they form a completely miscible alloy[1]. Previous work has shown that when silver-gold alloys are used as targets in a physical deposition process, the resulting nanocrystalline silver-gold dressings have reduced antibacterial properties when compared to silver, but are expected to have increased anti-inflammatory properties because of gold acting as a grain refiner [2]. Outside of gold and silver, in cases of other alloyed materials, higher alloy combinations are known to lead to more grain boundaries and a more stable nanostructure[3]. For binary nanocrystalline materials, increasing the alloy or solute composition decreases the grain size if the solutes have a similar energy when in the bulk phase as at interfaces [3].

Gold is the most noble metal and is therefore less reactive than silver, and is resistant to oxidation or ionization [1], [4]. Gold can be oxidized in very reactive environments, but oxides of gold are unstable, especially in a humid environment, and therefore typically decompose quickly [5]. A study of gold films treated with oxygen plasma also demonstrated the instability of gold oxide, where a 4 nm gold oxide layer completely dissipated after 4 days at room temperature and this rate was accelerated at higher temperatures[6]. Gold has two valencies and Au(III) is more active than Au(I), so if oxides are to form, they are likely to be in the form of Au_2O_3[1].

Atoms have a greater affinity for electrons when positioned at boundaries, edges, or interfaces rather than in the bulk lattice [7]. Atoms with lower coordination numbers are found on the edges of clusters, and the lower the coordination number, the lower the stabilization and the greater likelihood of being released[8]. In a study of polycrystalline gold, the coordination state of the metal atoms was low at defects and grain boundaries, and the atoms in those positions were especially active[7]. Gold is known to segregate to the edges or shells of silver-gold nanostructured materials or nanoparticles, suggesting that in nanocrystalline silver-gold materials, gold may be in greater concentration at the grain boundaries than in the bulk phase [9].

Gold has low absorption topically and percutaneously because of its inertness, stability, and lack of ionization in body fluids [1]. Because of this, it is thought to have a limited ability to penetrate tissues [1]. Still, the studied antibacterial effects of gold are related to its interactions with the cell membrane,

inhibition of ATPase, disruption of protein synthesis, and radical quenching[10]. In a 1997 study of the mechanism of action of gold complexes, Au(III) acted as an oxidizing agent when in contact with proteins, displaying nonspecific binding to proteins with available sulfur groups, itself reducing to Au(I) [11]. Gold also binds to DNA, changing the conformation [11]. Both gold ions are highly reactive with biological materials, with affinities for ligands on proteins, cells, and organic debris[1].

It was found that the higher gold percentage in the alloy, the smaller the grain size [2]. While the anti-inflammatory effect has yet to be tested in a systemic model, previous work has suggested that a smaller grain size is associated with better anti-inflammatory activity[2]. This is because of the greater percentage of grain boundaries which release atoms and clusters of silver and gold, the molecules associated with improved anti-inflammatory activity.

While there is limited information on nanocrystalline silver-gold materials, there have been studies on gold and silver-gold nanoparticles. In one study, silver-gold nanoparticles had improved antibacterial effects against *E. coli* and *S. aureus* over silver-only, while gold-only had no significant bactericidal or bacteriostatic properties. The mechanisms identified were an increase in ROS production, cell membrane damage, and DNA fragmentation[12]. Silver-gold nanoparticles released more silver than silver-only nanoparticles, so it was suggested that gold aided in the release of silver[12]. In this study, the highest concentration of silver corresponded with maximum antibacterial activity[12]. Gold was found to be less cytotoxic than silver, and at low concentrations, silver-gold nanoparticles were also non-cytotoxic[12]. In another study, functionalized gold spherical nanoparticles were tested in a rat model of liver injury [13]. This treatment reduced biomarkers and observations of inflammation, oxidative stress, and fibrosis [13]. It was also found that the nanoparticles were located intracellularly in the cytoplasm, but not inside the nucleus [13] With higher concentrations of gold nanoparticles, there was a greater biological effect [13].

Adhesions form as part of an inflammatory process. Because of this, silver-gold alloys are studied for their potential as anti-inflammatory materials for use in an animal model of inflammation. In this chapter, the chemical, physical, and antibacterial properties were characterized and compared to nanocrystalline silver to establish their properties in relation to silver before using in an animal model.

Methods

Dressing Fabrication

Silver-gold nanocrystalline coatings were sputtered onto an HDPE mesh substrate using an in-house sputtering system. Two different targets were used: 65% gold and 35% gold by weight, with the balance silver. The standard conditions were a 0.9A current, 4.0% oxygen atmosphere, and no water. The novel

conditions were 1.8A current, 4.5% oxygen, and 15 µL/min water. The total pressure inside the chamber was 400 mTorr for both conditions. Nanocrystalline silver materials were used as comparison in this chapter and are the same materials fabricated for analysis in Chapter 3.

Materials sputtered using standard or novel conditions are noted as "Standard" films or materials and "Novel" films or materials respectively. "Ag100" represents sputtering with the 100% silver target, "Ag65" with the 65% silver and 35% gold target (also referred to as "low gold"), and "Ag35" with the 35% silver and 65% gold target (also referred to as "high gold").

X-ray Diffraction

X-ray diffraction (XRD) analysis of the films was performed on a Rigaku Ultima IV diffractometer with a cobalt radiation source at 38 kV and 38 mA. Scan conditions can be found in Chapter 2. Grain size was measured with the Scherrer equation. Total sample grain size was calculated as the average of measurable peaks between $30\,°2\theta$ and $81°2\theta$.

Chemical Analysis

Nitric acid digest was used to measure the total quantity of silver. Ammonia soluble silver was measured from a digest with ammonium hydroxide. Aqua regia digest was used to measure the total gold. These solutions were analyzed for quantity of silver or gold using inductively coupled plasma mass spectrometry (ICP-MS) or atomic absorption spectroscopy (AAS). Samples were corrected for dilution factor and given as mg of silver or gold per square inch of material.

Silver Release in Solution

To measure silver ion release into solution, two square inches of material were soaked in 7.5 mL distilled water at 37°C for six hours as described previously. The solutions described above were analyzed for quantity of silver using AAS.

Scanning Electron Microscopy

Scanning electron microscopy was used to image film samples as described previously. Images were taken at 20 000x, 50 000x, and 100 000x magnification, using an accelerating voltage of 10 kV and a working distance of 5 to 10 mm.

Log Reduction

To quantify the antibacterial properties, a log reduction was performed as described in Chapter 2. In brief, two 1 square inch pieces of film were layered with one 1 square inch piece of cotton gauze to create dressings, incubated, and the bacteria remaining were plated and counted.

The antibacterial properties of solutions made with nanocrystalline silver and silver-gold films, a standard 6 hour solution was made and 1.8mL was combined with 0.2 mL bacterial inoculum in log phase. The remaining bacteria were diluted, plated, and counted as previously described.

Day-to-Day Corrected Zone of Inhibition (CZOI) Assay

The bacteriostatic longevity was assessed using the corrected zone of inhibition assay, as described in Chapter 2 with *P. aeruginosa* and *S. aureus* for 7 days.

Statistics

Unpaired two sample t-tests with Welch's correction were used to compare sample groups if comparisons between two groups were being performed. For comparisons with multiple factors, ANOVA with Tukey's post-hoc tests were used. The effect of material (Ag100, Ag65, or Ag35) and sputtering condition (Standard or Novel) are the factors considered in ANOVA. The results of Tukey's post-hoc tests can be found in Appendix A. Analysis was performed using Microsoft Excel and R. Unless otherwise stated, quantitative data in tables, and data points in line charts or bar graphs are the average of three samples with a standard deviation error bars.

Results

X-ray Diffraction (XRD)

Figures 4-1, 4-2, 4-3, and 4-4 show the XRD spectra for representative samples of each group. Due to their similarity, metallic silver and gold are both identified by peaks at approximately 38, 44, 65, 78, and 82°2θ. Silver oxide (Ag_2O) is primarily identified by peaks at approximately 33 and 38°2θ. The first two peaks in each spectrum, at approximately 22 and 24°2θ, correspond to the HDPE substrate. Intensity counts on the y-axis are an arbitrary unit.

Figure 4-1 displays spectra for Ag65 and Ag35 Standard samples. The Ag65 (low gold) samples under Standard conditions are observed to have small peak intensities, with the only identifiable peak at approximately 38°2θ. This peak position corresponds to locations for silver, silver oxide, and gold. The peak position and shape are similar for the Standard Ag35 sample, although there is a greater intensity and spread of that peak than for Ag65. There is no recognizable peak at 33°2θ for either sample, likely indicating a low presence of silver oxide.

For Figure 4-2, which displays XRD spectra for Ag65 and Ag35 Novel films, there are stronger peak intensities, and more peaks could be clearly recognized at higher measurement angles than for Standard samples in Figure 4-1. The peaks at 64 and 78°2θ correspond to the presence of elemental silver and gold. The strongest peak was observed at 38°2θ, as expected. The peaks for Novel samples are still relatively broad, although not as broad as those for the Standard samples. Peak broadness indicates a smaller grain size. The Ag65 sample had a discernable peak at 33°2θ compared to Ag35, but Ag35 had a stronger peak at 44°2θ, which may point to more silver oxide in the Ag65. Unlike the Standard sample, the Novel Ag35 did not show a discernable peak at 33°2θ, but all other peak positions (38, 44, 65, 78, and 82°2θ) had clearly identifiable peaks.

Figures 4-3 and 4-4 include spectra from the silver films from the previous chapter. The silver (Ag100) samples sputtered with Standard conditions had smaller and broader peaks compared to the corresponding Novel sample. For both the Novel and Standard samples, the silver oxide peak at 33°2θ is distinctly present in the Ag100 spectra, but becomes smaller for Ag65, and completely disappears for Ag35. This trend is most noticeable for the Novel sample. For the Standard sample, the shared peak at 38°2θ increases in broadness with increasing gold percent.
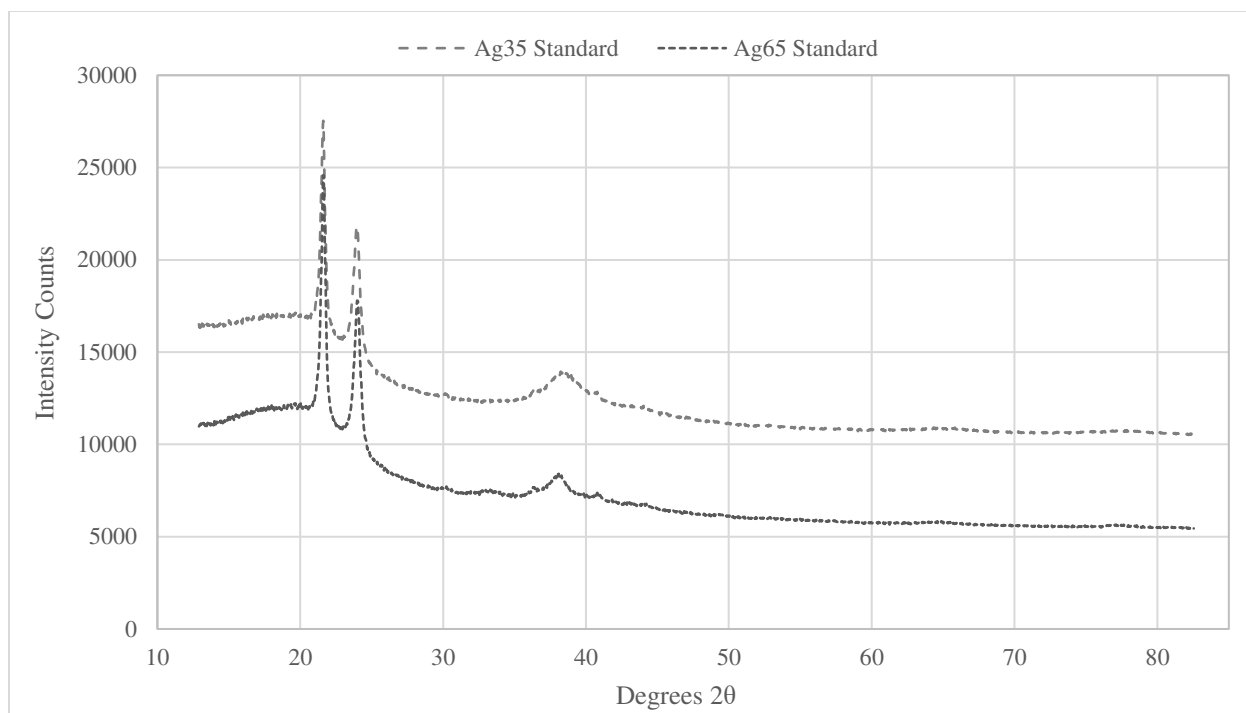
Figure 4-1 Representative XRD spectra of dressings of Standard silver-gold films.
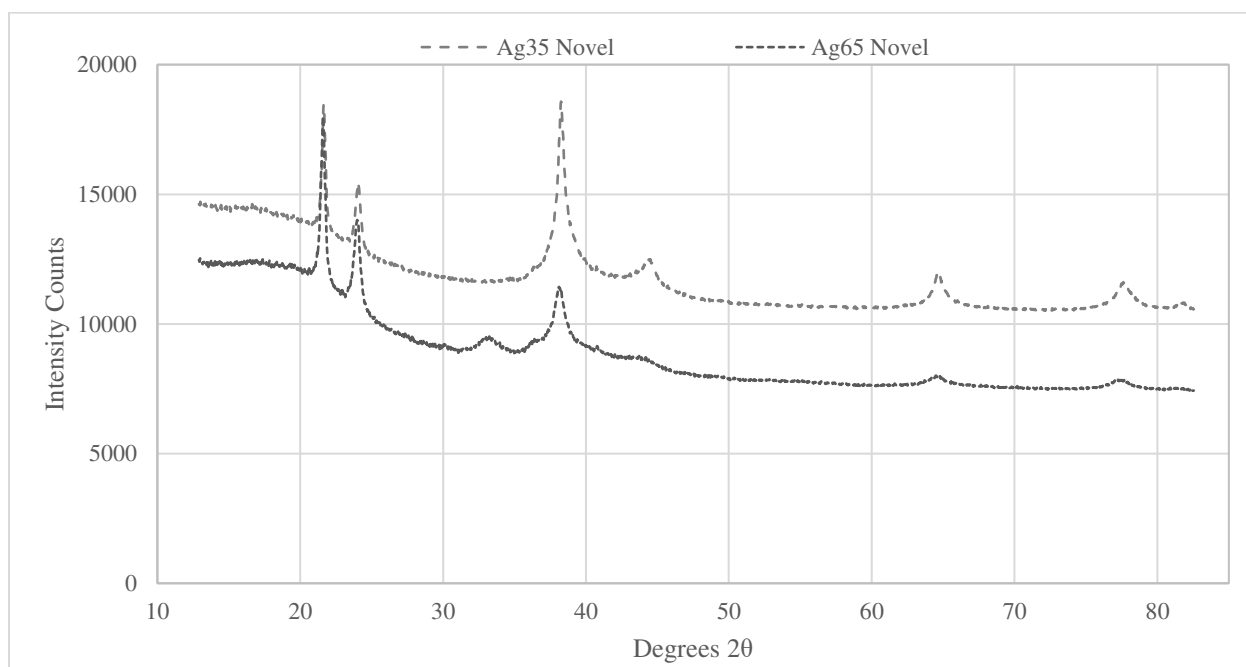
Figure 4-2 Representative XRD spectra of dressings of Novel silver-gold films.
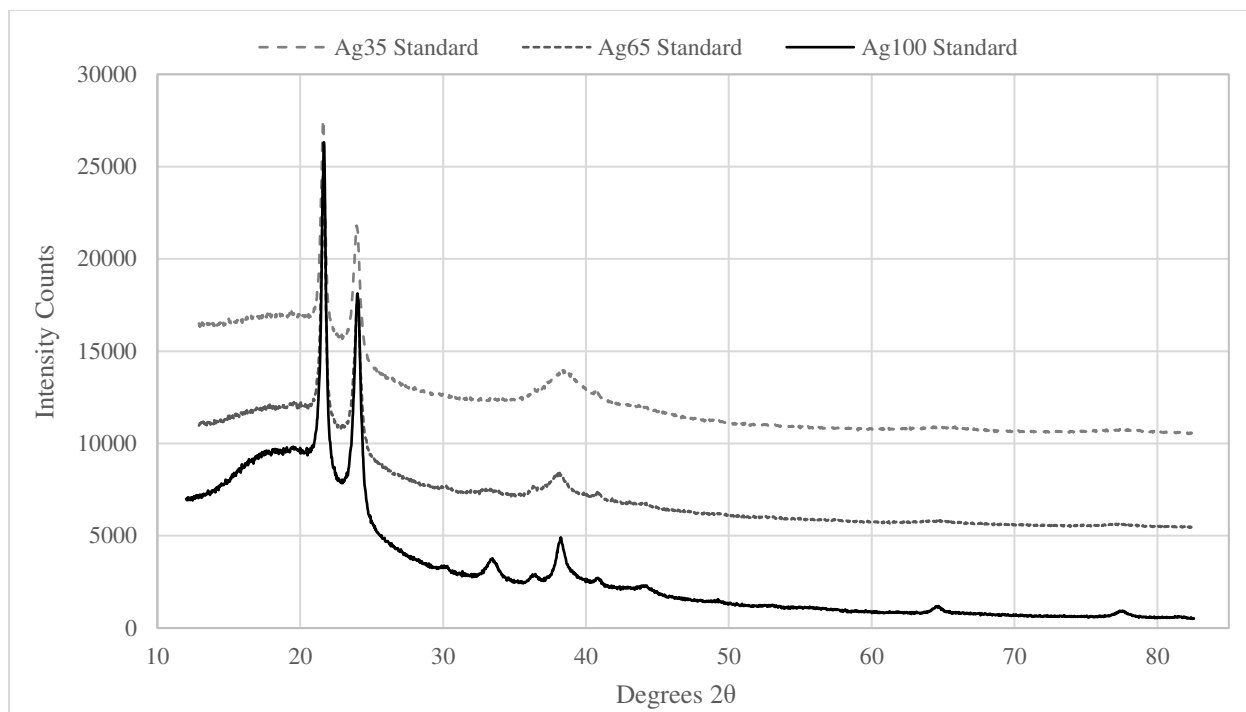
Figure 4-3 Representative XRD spectra of Standard films.
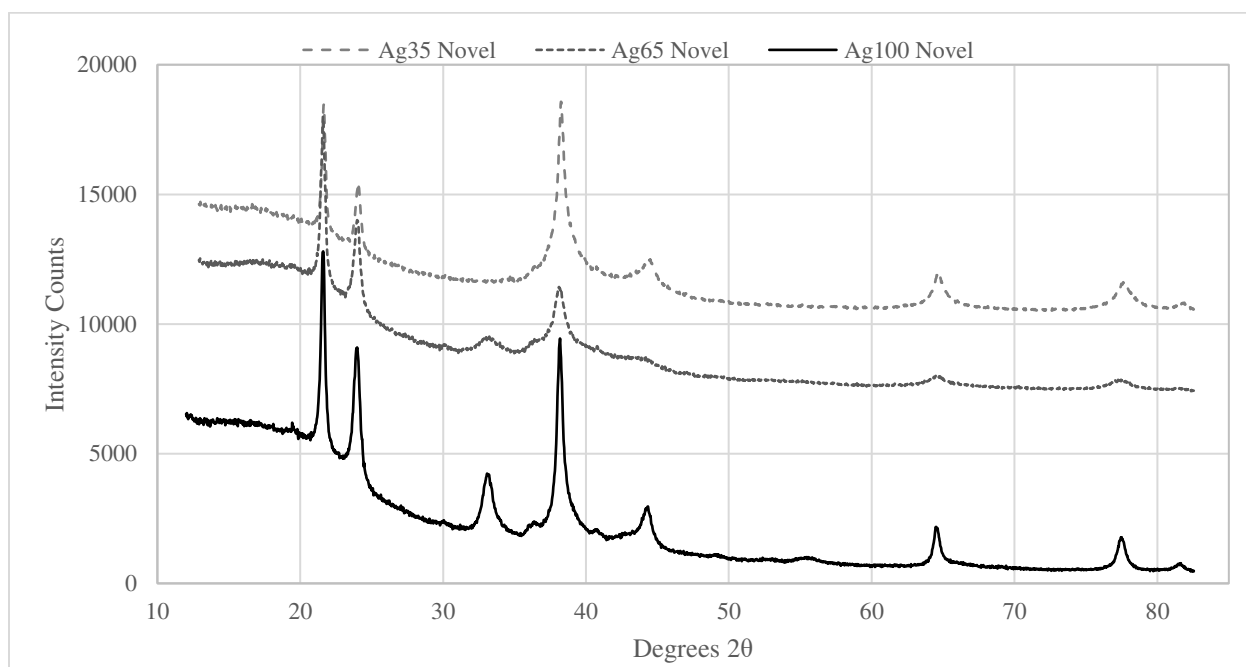
Figure 4-4 Representative XRD spectra of Novel films.

Figure 4-5 shows the grain sizes for the samples discussed above. Grain sizes were measured by hand from the spectra using the Scherrer equation by four trained students independently. Then, the average of the three measurements which most closely agreed was taken and presented here, along with the standard deviation of those three measurements. As was seen previously with silver, the Novel conditions resulted in larger grain sizes than Standard condition. This effect was most pronounced for the Ag35 samples, but the difference between Novel and Standard grain sizes for the Ag65 samples was not significant. There was a trend of decreasing grain size with decreasing silver content for the Standard samples. This same trend was expected for the Novel samples, but the Ag65 sample had a smaller grain size than the Novel Ag35 sample. Table 4-1 shows the results of the ANOVA tests. There was a very significant effect of material, sputtering condition, and the interaction of these two factors. In post-hoc tests, comparisons between all groups were significant, except for between Ag100 Standard and Ag35 Novel.
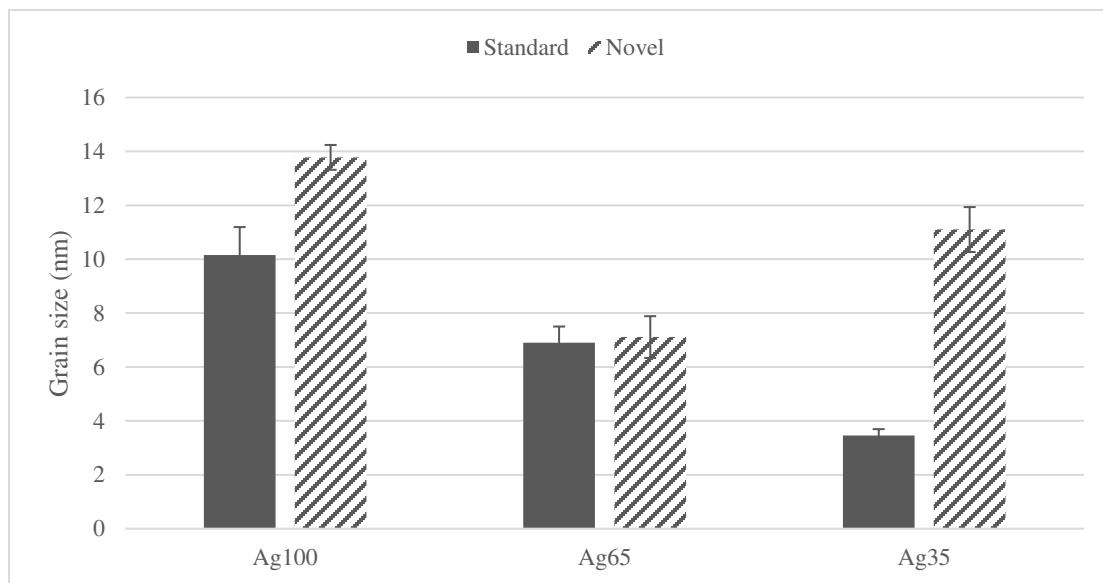
Figure 4-5 Grain sizes of Standard and Novel films of three alloy compositions.

Table 4-1 ANOVA p-values for grain size comparisons by sputtering alloy (material) or sputtering condition.

Effect	p-value
Material	4.85E-08
Condition	7.95E-08
Interaction	4.06E-06

Chemical Analysis

Figure 4-6 shows the total silver deposition in mg/in^2 for all samples, as measured by nitric acid digest. All data in this section is presented as an average of three replicate samples with standard deviations shown as error bars or provided after the average. As expected, silver deposition is lower for the Standard samples as they had a lower current used during sputtering. Novel Ag65 even has significantly more silver than Standard Ag100. All post-hoc comparisons were significant except for the comparison between Standard Ag65 and Novel Ag35. As expected, there is a decreasing trend of total silver for films sputtered with a lower silver alloy. For the Standard Ag35 sample, there is more than 35% of the total silver deposition measured in the Standard Ag100 sample and for Novel Ag35 there is less than 35% of the silver in Ag100 Novel. For the Ag65 samples, there is greater than 65% of the silver in the Ag100 samples for both Standard and Novel conditions.
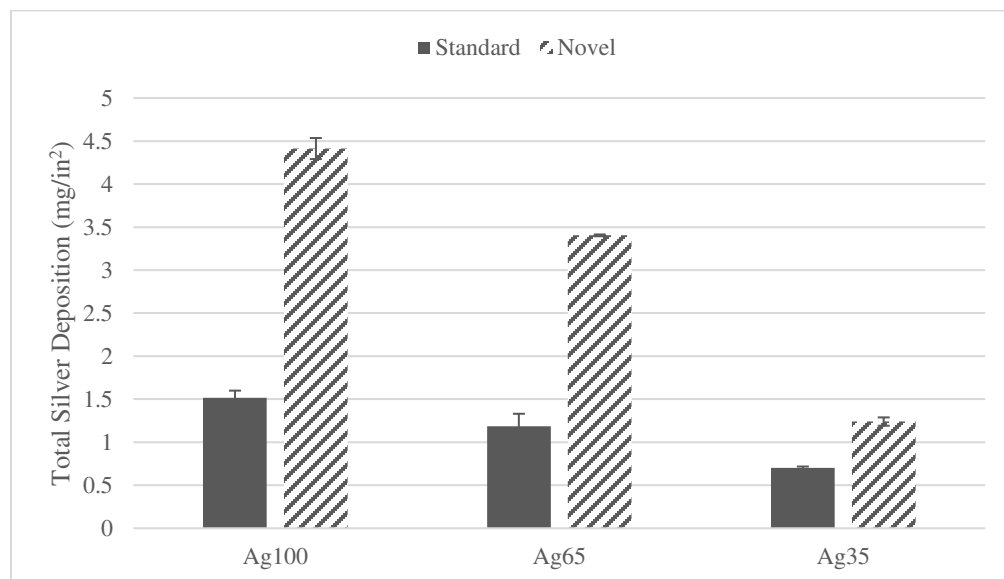
Figure 4-6 Total silver measured in sample films by nitric digest, grouped by alloy composition and sputtering condition.

Table 4-2 shows the material, condition, and interaction effect p-values given by ANOVA. All effects were significant ($p \ll 0.05$). In the post-hoc tests, all comparisons were significant ($p < 0.05$), except for between Ag65 Standard and Ag35 Novel.

Table 4-2 ANOVA p-values for total silver comparisons by sputtering alloy (material) or sputtering condition.

Effect	p-value
Material	1.62E-13
Condition	7.85E-15
Interaction	7.06E-11

Figure 4-7 shows the total quantity of ammonia soluble silver measured in the film, given in mg/in^2. Figure 4-8 shows the ammonia soluble silver as a percentage of total silver. As expected from Chapter 3, the Novel samples tend to have a lower percentage of ammonia soluble silver but a higher total quantity because of the greater silver deposition. For Ag35 samples, there was no significant difference in total ammonia soluble silver between Standard and Novel samples. There was no consistent trend found for percentage gold in the target versus ammonia soluble percentage.
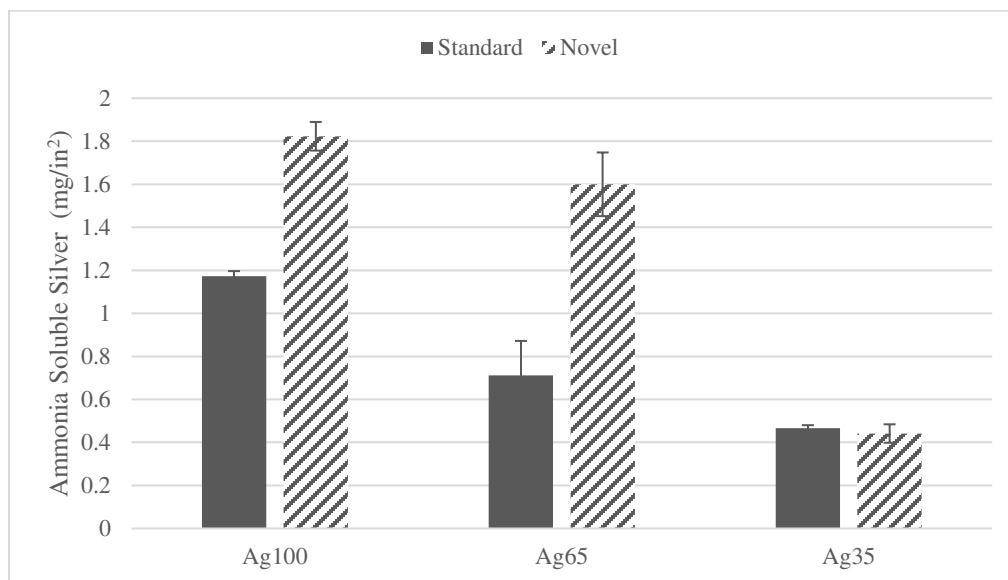
Figure 4-7 Ammonia soluble silver content in mg/in^2, grouped by alloy composition and sputtering condition.
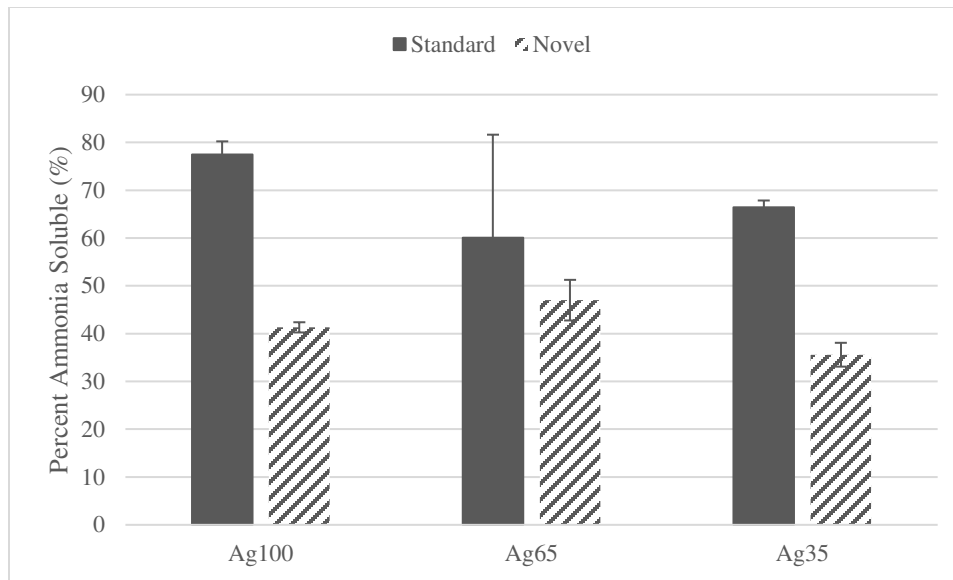
Figure 4-8 Ammonia soluble silver as a percentage of total silver, samples grouped by alloy composition and sputtering condition.

Table 4-3 shows the p-values of the ANOVA test, with a significance level of $p < 0.05$. In the ANOVA test for percent ammonia soluble silver, only the sputtering condition effect was significant. The total quantity of ammonia soluble silver is influenced by the total amount of silver deposition, which is in turn affected by the sputtering conditions and target silver content. So, in the ANOVA test for the ammonia soluble silver quantities, the material, condition, and interaction effects were all significant. In post hoc tests, the ammonia soluble quantity comparisons were almost all significant except for Novel Ag65- Novel Ag100, Standard Ag65-Standard Ag35, and Standard Ag35-Novel Ag35. The absence of significant values for these shows that for the first two comparisons, the increased amount of silver did not result in an increase in the quantity of ammonia soluble silver. For the third comparison listed, the different sputtering conditions would be expected to increase the amount of ammonia soluble silver, but this was not seen for Ag35 samples. The percent ammonia soluble silver data comparisons were mostly not significant. Substantial variation in the Ag65 Standard samples may contribute to the insignificance of most comparisons to this group. Notable significant comparisons were between Standard and Novel Ag100, and Standard and Novel Ag35. It is also worth noting that there were no significant differences in ammonia soluble silver percentage within Standard samples or within Novel samples comparisons as the material did not have a significant effect.

Table 4-3 ANOVA p-values for the effect of sputtering alloy (material) and sputtering condition on ammonia soluble silver amount and composition.

Effect	p-value for Ammonia Soluble Silver, mg/in^2	p-value for Ammonia Soluble Silver, %
Material	4.26E-06	0.31
Condition	3.39E-04	3.72E-05
Interaction	4.18E-03	0.15

Figure 4-9 shows the total gold measured in the films by aqua regia dissolution. As expected, there is more total gold deposition with higher current and more gold initially in the target. Ag35 Novel was the sample with the most deposition of gold, and Ag65 Standard had the lowest quantity of gold.
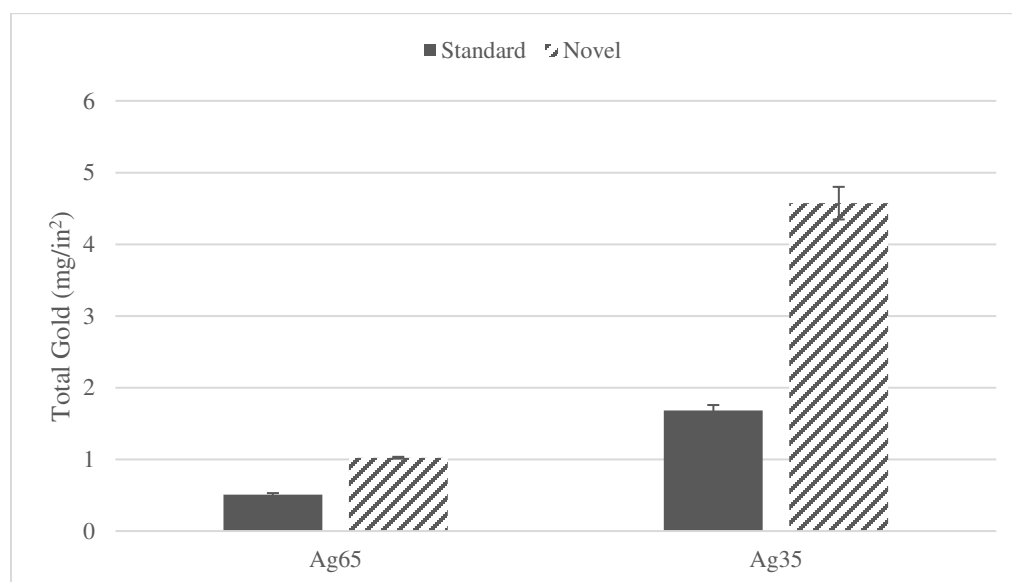
Figure 4-9 Measurements of total gold in nanocrystalline silver-gold sample films, displayed in mg/in^2 and grouped by alloy composition and sputtering condition.

The percentage of gold measured in the films is shown in Figure 4-10. This is calculated from the total gold and silver measured. For the 65% gold target (Ag35), the samples had an average percentage gold of 70.5% (Standard) and 78.7% (Novel), more than would be expected from the nominal target composition. For the 35% gold target (Ag65), the samples had an average percentage gold of 29.9% (Standard) and 23.1% (Novel), which was less than would be predicted. The difference between alloy composition and film composition is greater for the Novel samples, suggesting that this effect is magnified by higher current, oxygen, or water.
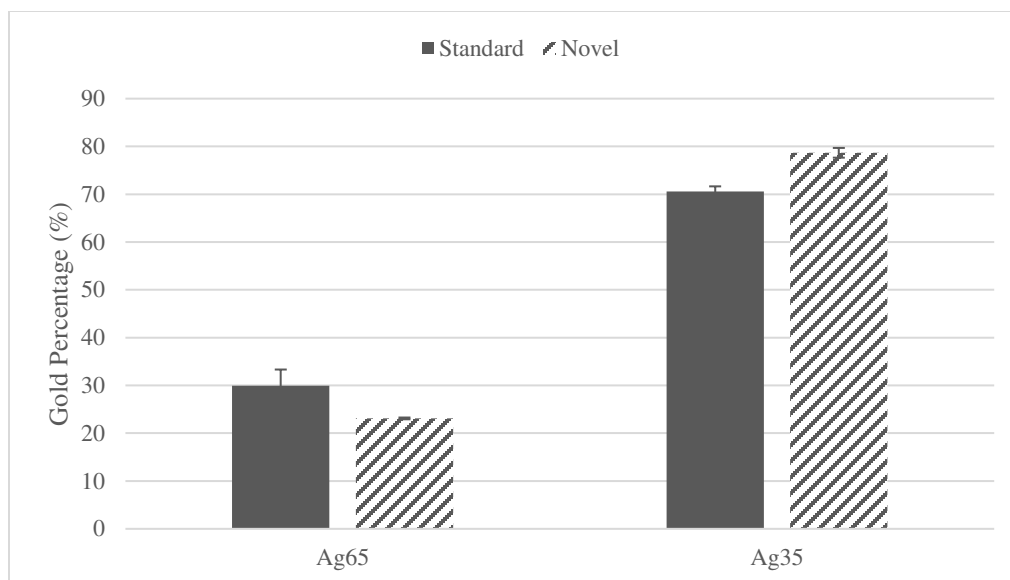
Figure 4-10 Gold composition in films, as a percentage of combined total silver and gold for nanocrystalline silver-gold samples, grouped by alloy composition and sputtering condition.

Table 4-4 shows the significance of effects calculated by ANOVA. The material and sputtering condition both had a significant effect on the quantity of gold, as well as an interaction effect. While the trend was recognized that there appeared to be greater deviation from nominal alloy composition for Novel samples, the condition effect in the ANOVA test was not found to be significant. Still, the post-hoc tests showed all comparisons to be significant, including the difference between Novel Ag35 and Standard Ag35, and Novel Ag65 and Standard Ag65.

Table 4-4 ANOVA p-values for the effect of sputtering alloy (material) and sputtering condition on total and percent gold in samples.

Effect	p-value for total gold, mg/in^2	p-value for gold as a percentage of total
Material	2.62E-15	6.73E-11
Condition	1.55E-11	0.62
Interaction	1.71E-11	1.05E-04

Figure 4-11 shows the total deposition, calculated by adding the total silver and gold measured by nitric acid and aqua regia digests, given in mg/in^2. The deposition is highest for the Novel sputtering conditions, which is expected because of the higher current. Interestingly, the deposition was significantly higher for the Ag35 samples compared to Ag65 or Ag100 for either sputtering condition. This may indicate that the

inclusion of more gold allows for a more substantial sputtering yield. Differences were not significant between Ag100 and Ag65 for either the Standard or Novel groups.
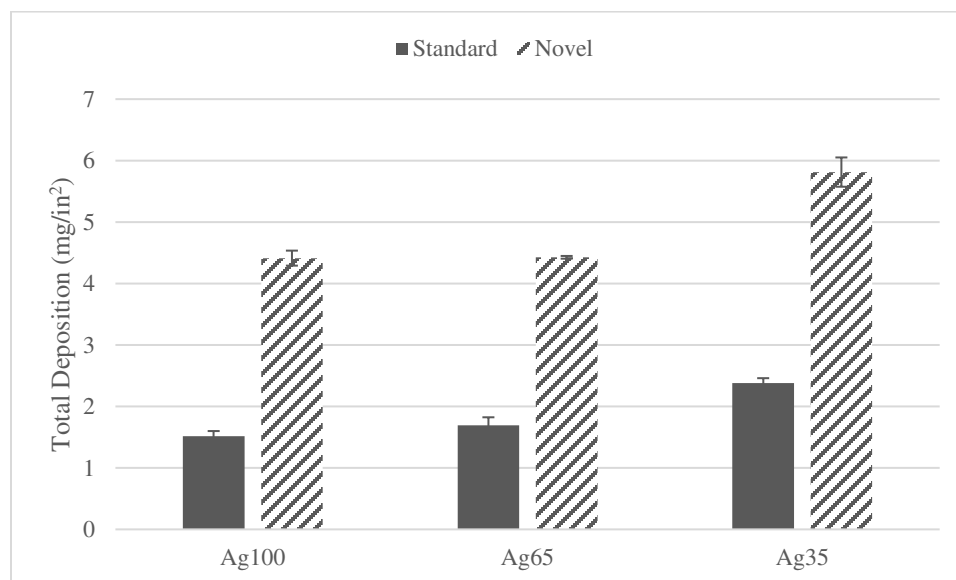
Figure 4-11 Total deposition of silver and gold for all samples, grouped by alloy composition and sputtering condition.

Table 4-5 shows the ANOVA results of total deposition, demonstrating a significant effect of material, sputtering condition, and their interaction. Ag35 samples may heavily contribute to the significance of material in this case.

Table 4-5 ANOVA p-values for the effect of sputtering alloy material and condition on the combined deposition of silver and gold.

Effect	p-value
Material	5.19E-09
Condition	3.47E-15
Interaction	1.56E-03

The Ag65 Standard sample regularly had high standard deviations across the different measurements of chemical analysis. This may be technique error, but it is possible that the dressing properties are inconsistent, which could point to an unstable sputtering process.

Solution Release

Figure 4-12 shows the measured silver release after 6 hours dissolution in water calculated as mg released per inch of material. Figure 4-13 shows the silver release as a percentage of the average total silver measured previously in the film. Silver release into solution after 6 hours was between 3 and 10 mg/L, or

0.14 to 0.04 mg/in^2. This is between 1 and 5 percent of the total silver measured in the films by nitric acid digest. As expected, the greatest raw silver release came from the Ag100 samples. For Ag35 and Ag65 groups, there was only one significant comparison – between Ag65 Novel and Ag35 Standard. Despite the Novel Ag65 having more initial silver (1.60 mg/in^2) than the Ag100 Standard (1.17 mg/in^2), it released less silver in solution. Tests in Chapter 3 showed that the Standard samples released a greater percentage of their silver, likely due to their relatively larger ammonia soluble silver content. This observation is also found here, where within material type, the Standard samples released a greater percentage of silver than their Novel counterparts. Ag65 Novel samples had the lowest percent release of all samples within the groups of Standard and Novel samples. Ag35 released more than 35% of the silver released by the Ag100 samples, but Ag65 samples did release approximately 65% of the silver of the Ag100 samples. While measurements of the gold release were also attempted, they were below detection limit of the equipment used.
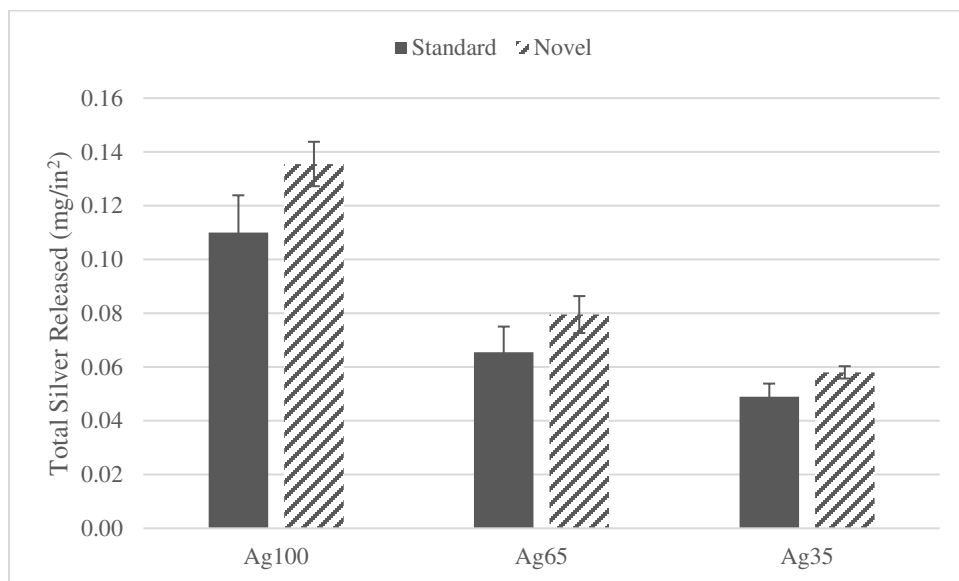
Figure 4-12 Silver release into solution after 6 hours, given as mg/in^2. Samples grouped by alloy composition and sputtering condition.
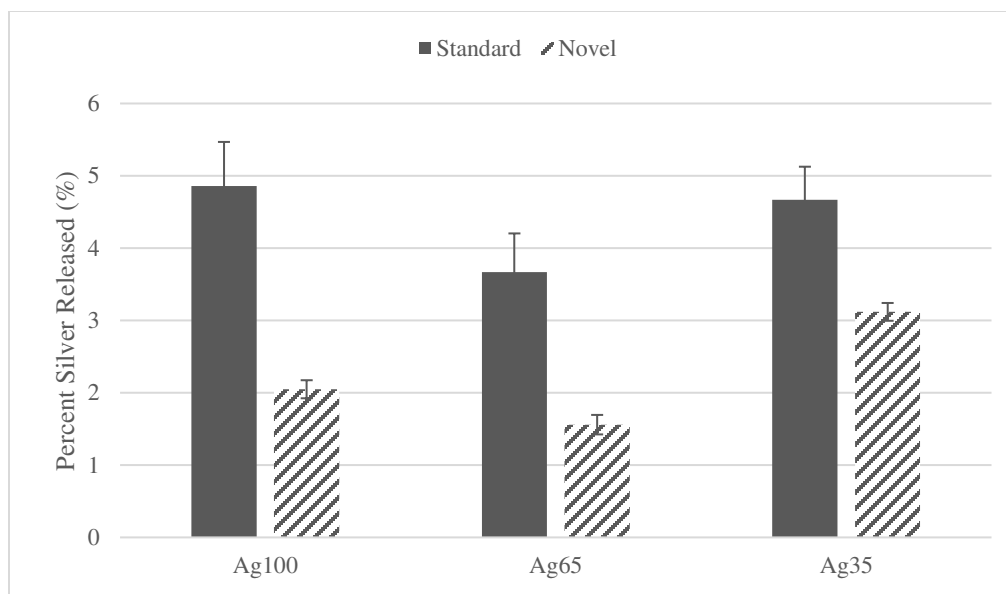
Figure 4-13 Silver release into solution after 6 hours, given as percent of initial silver measured. Samples grouped by alloy composition and sputtering condition.

ANOVA was performed for the total and percent silver released and the p-values for effects are shown in Table 4-6. For the total silver release, there is a significant effect of the material and condition, but not an interaction effect. In the post-hoc tests, most comparisons between Ag35 and Ag65 groups were not significant. All effects are significant for the percentage release, although the interaction effect just reaches the threshold for significance. In the post-hoc tests for percentage silver release, the comparison between Ag100 and Ag35 did not have a significant difference for either Novel or Standard conditions. It is notable that Ag35 samples are releasing a similar percentage of their silver as the Ag100 samples. Novel Ag100 did not show a significant difference to either Novel Ag35 or Novel Ag65, although Novel Ag35 and Novel Ag65 were significantly different compared to each other.

Table 4-6 ANOVA p-values for the effect of sputtering alloy material and condition on the release of silver into solution.

Effect	p-value for total silver released, mg/in^2	p-value for percentage of total silver released
Material	2.13E-08	3.57E-04
Condition	1.56E-03	6.50E-08
Interaction	0.26	0.050

Scanning Electron Microscopy (SEM)

Figures 4-14 and 4-15 show representative SEM images of the materials at 50 000x and 100 000x magnification. Qualitative observations can be made. Novel samples (B, D, F) for each material type have a more textured and greater depth of microstructure compared to their Standard counterparts. There is more total deposition for Novel samples, which corresponds to greater depth. Standard Ag65 and Ag35 (images C and E) have the smoothest appearance. Ag65 Standard (C) and Ag65 Novel (D) samples appear to have the greatest difference in appearance, compared to the differences in Standard and Novel samples for Ag100 and Ag35. Ag100 Novel (B) and Standard (A) have similar structure, with a smaller feature size for the Standard sample. For Ag65, the Standard (C) sample appears to have a smoother structure than the Novel sample (D), but the texture of both is similar. Ag35 Novel (E) and Standard (F) samples look similar.
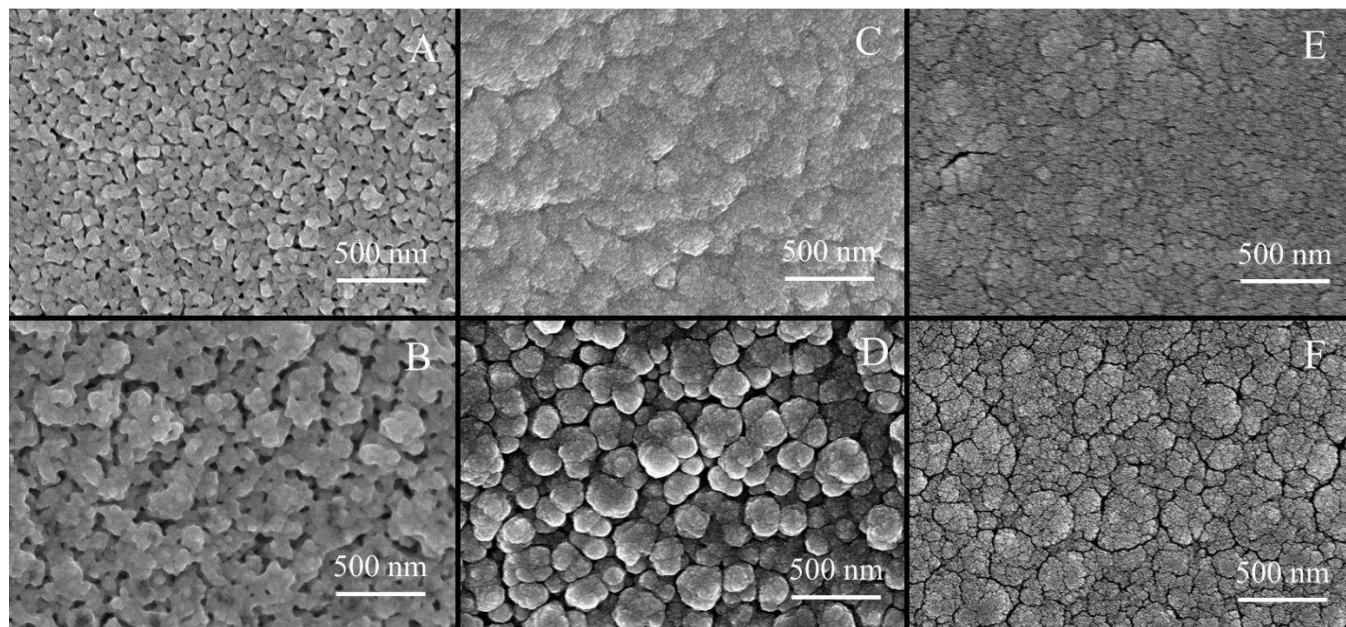
Figure 4-14 50 000x magnification of dressing samples. A) Ag100 Standard, B) Ag100 Novel, C) Ag65 Standard, D) Ag65 Novel, E) Ag35 Standard, F) Ag35 Novel.
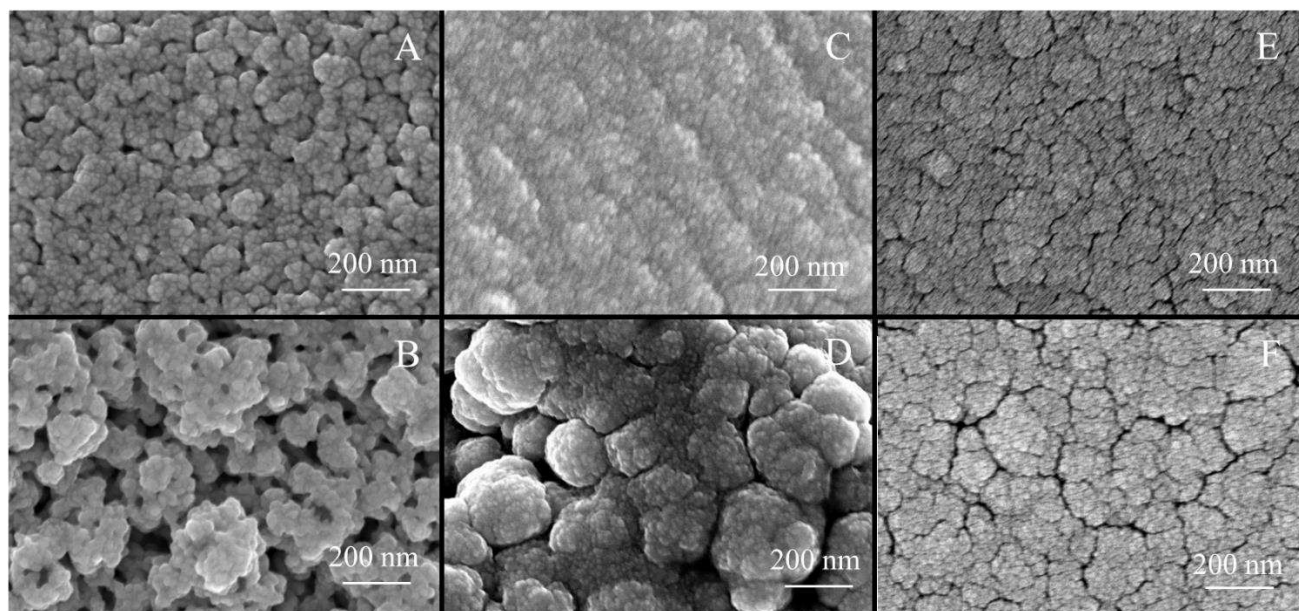
Figure 4-15 100 000x magnification of dressing samples. A) Ag100 Standard, B) Ag100 Novel, C) Ag65 Standard, D) Ag65 Novel, E) Ag35 Standard, F) Ag35 Novel.

Log Reductions

Log reductions for *P. aeruginosa* (Gram positive) and *S. aureus* (Gram negative) were done with 1 hour of direct contact with a dressing sample of two layers of coated HDPE film and one layer of gauze. This resulted in a log reduction of at least 6 for all samples. Data is not shown because all samples had a result of total kill. Two organisms, *Proteus vulgaris* and *Proteus mirabilis* were then used for log reductions because *Proteus* organisms are known to have a low sensitivity to silver. *P. mirabilis* did not appear to be at all affected by silver. Plates were uncountable because it is a swarming organism, and therefore covered the entire plate instead of forming countable colonies. Still, the presence of colonies after contact with the dressings appears to confirm its lack of sensitivity to silver or gold. *P. vulgaris* log reductions results are shown in Table 4-7, and while it had smaller log reductions than *P. aeruginosa* or *S. aureus* (no total kills), all the dressings were bactericidal. Bactericidal is defined as a log reduction greater than 3.

Table 4-7 Log reductions with *P. vulgaris.*

	Standard	**Novel**
Ag100	5.24 ± 0.21	5.02 ± 0.40
Ag65	4.66 ± 0.14	4.86 ± 0.21
Ag35	5.23 ± 0.13	4.40 ± 1.17

Then, log reductions with solutions made from 6 hours of film dissolution in water were performed with either *P. aeruginosa* or *S. aureus* and the resulting log reductions are shown in Tables 4-8 and 4-9. For this test, 200 µL of inoculum (10^8 to 10^9 CFU/mL) was combined with 1.8 mL of silver solution for 1 hour. The resulting log reductions were well below the bactericidal threshold, but the inoculum strength was intentionally high in order to determine if there were any differences in activity. ANOVA p-value results for all log reductions are shown in Table 4-10. Based on the results of ANOVA, there did not appear to be an effect of the material or condition on the log reduction for any bacteria.

Table 4-8 Log reductions with *S. aureus* and nanocrystalline silver and silver-gold solutions.

	Standard	Novel
Ag100	0.73±0.12	0.60±0.04
Ag65	0.15±0.69	0.83±0.06
Ag35	0.89±0.13	0.63±0.03

Table 4-9 Log reductions with *P. aeruginosa* and nanocrystalline silver and silver-gold solutions.

	Standard	Novel
Ag100	0.43±0.11	0.52±0.13
Ag65	0.57±0.15	0.59±0.15
Ag35	0.49±0.12	0.62±0.16

Table 4-10 ANOVA p-values for the effect of sputtering alloy material and condition on log reductions with *S. aureus, P. aeruginosa*, and *P. vulgaris*.

Effect	p-value, *S. aureus*	p-value, *P. aeruginosa*	p-value, *P. vulgaris*
Material	0.22	0.49	0.42
Condition	0.11	0.62	0.26
Interaction	0.014	0.81	0.26

Corrected Zone of Inhibition (CZOI)

The CZOI was intended to test the bacteriostatic properties of the dressings over seven days to measure the longevity of their release of antibacterial species. Three replicates were used for each group. There was a lot of variation, so while many findings are not significant, some conclusions can be drawn. Figures 4-16 to 4-18 display the results for the test with *P. aeruginosa*. Ag100 Novel was used as a comparison to the silver-gold samples. See Chapter 3 for extended tests with Ag100 Standard and Novel samples. Ag100 maintained a consistent zone throughout the test, with little fluctuation in zone size. Ag35 samples

maintained a zone which was comparable to Ag100 or Ag65 initially, but by Day 5, all Ag35 samples had no measurable zone (Figure 4-18). Ag65 samples had decreasing zones over time, but they did not decrease as quickly as Ag35 samples. Only Ag65 Novel, of all the silver-gold samples, maintained a measurable zone at the end of seven days.
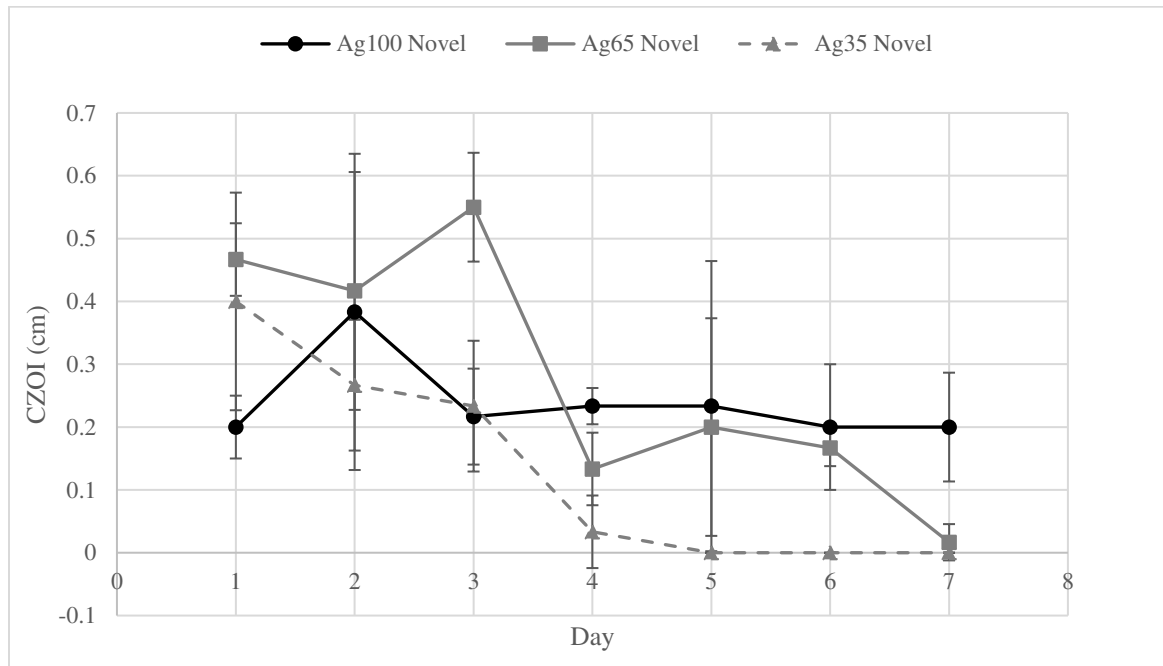
Figure 4-16 Measured zones in CZOI test over seven days for Novel samples with *P. aeruginosa*.
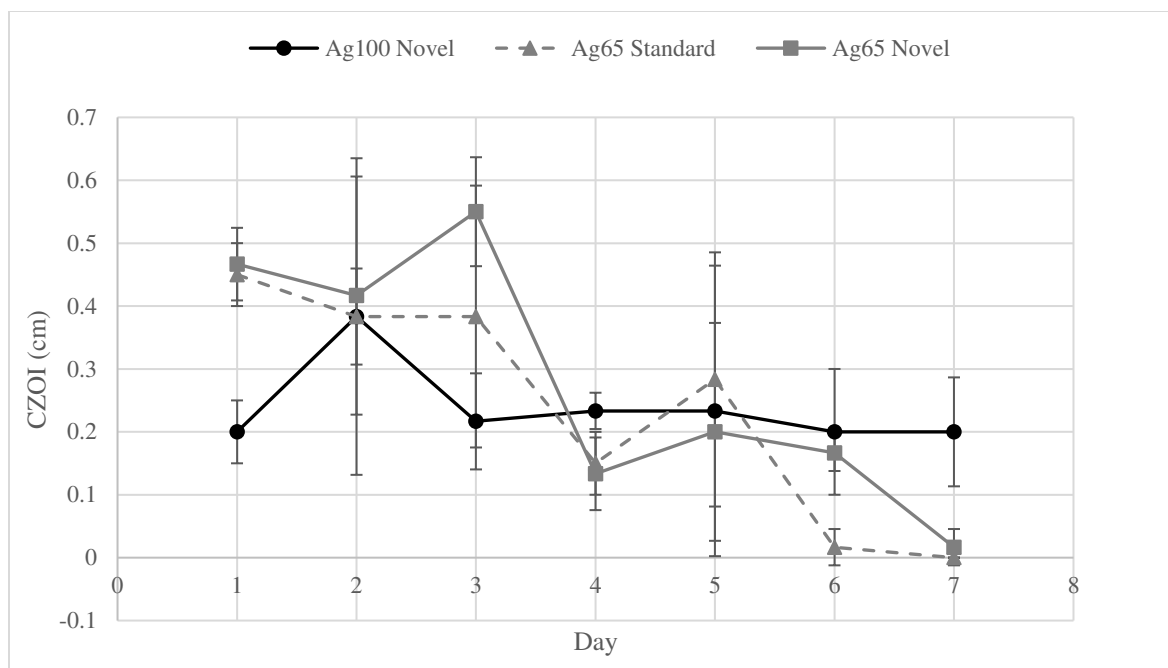
Figure 4-17 Measured zones in CZOI test over seven days for 65% silver samples, with Ag100 Novel for comparison with *P. aeruginosa*.
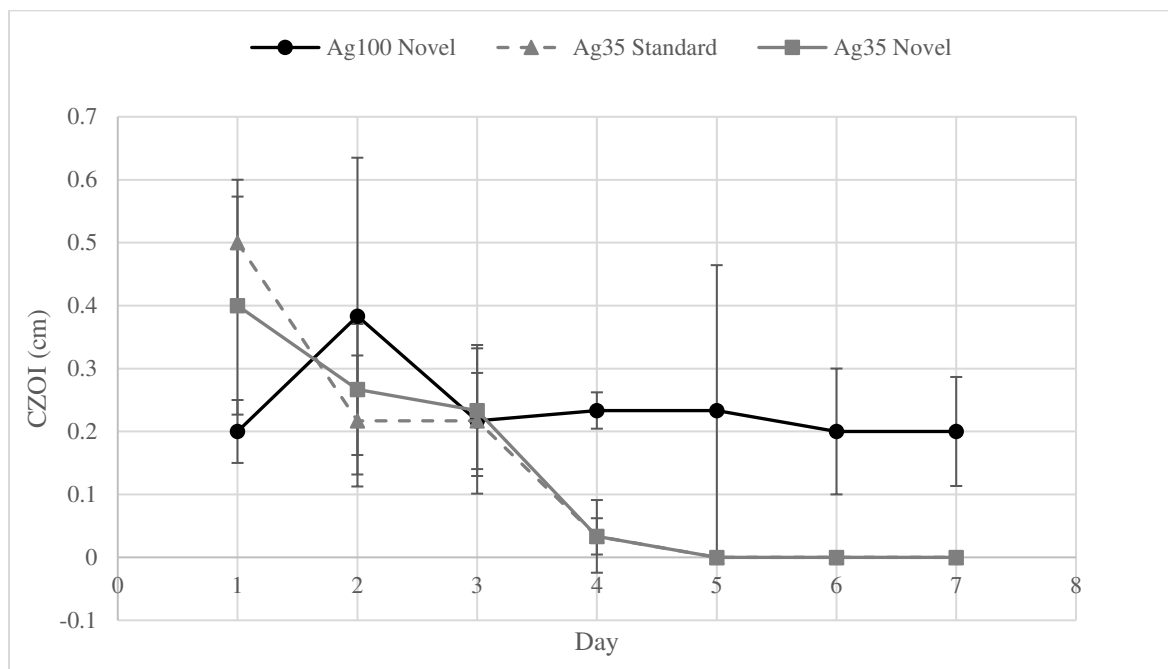
Figure 4-18 Measured zones in CZOI test over seven days for 35% silver samples, with Ag100 Novel for comparison with *P. aeruginosa*.

Table 4-11 compares the starting and ending zones for all samples tested, given with the average and standard deviation of three replicates in cm. Only Ag100 samples had the same average starting and ending zones.

Table 4-11 CZOI zones measured at Day 1 and Day 7 for all samples in study, with *P. aeruginosa*.

	Day 1 Zone (cm)	Day 7 Zone (cm)
Ag100 Novel	0.20±0.05	0.20±0.09
Ag65 Standard	0.45± 0.25	0
Ag65 Novel	0.47±0.08	0.02±0.03
Ag35 Standard	0.50±0.23	0
Ag35 Novel	0.40±0.17	0

Table 4-12 shows the ANOVA results. ANOVA was performed using only the Ag65 and Ag35 samples. Days 3, 4, 5, and 6 had at least one statistically significant effect, most commonly the material effect, so these days were considered in post-hoc tests. This suggests that material made more of a difference in the bacteriostatic abilities that the sputtering condition. This is expected, given that silver, particularly Ag^+, is considered to be the primary antibacterial species. In the post-hoc tests, there were no significant comparisons except on Day 6, when Ag65 Novel had a significant difference compared to other silver-gold groups. Table 4-13 shows the results of t-tests to Ag100, to determine which samples showed a comparable performance. Because of variation within sample groups, there were not many significant differences or discernable patterns.

Table 4-12 ANOVA p-values for the effect of sputtering alloy material and condition for nanocrystalline silver-gold samples on CZOI zone size with *P. aeruginosa*, at each day.

Effect	Day 1 p-value	Day 2 p-value	Day 3 p-value	Day 4 p-value	Day 5 p-value	Day 6 p-value	Day 7 p-value
Material	0.90	0.061	0.016	5.60E-3	0.037	5.34E-05	0.35
Condition	0.52	0.58	0.28	0.78	0.27	2.17E-4	0.35
Interaction	0.37	0.91	0.37	0.78	0.27	2.17E-4	0.35

Table 4-13 T-test p-values for comparison of nanocrystalline silver-gold sample zones to Ag100 zones on the same day in a seven day CZOI test with *P. aeruginosa*.

Group	Day 1 p-value	Day 2 p-value	Day 3 p-value	Day 4 p-value	Day 5 p-value	Day 6 p-value	Day 7 p-value
Ag65 Standard	3.6E-03	1.0	0.26	0.067	0.79	0.038	0.016
Ag65 Novel	3.8E-03	0.86	7.5E-03	0.055	0.47	0.61	0.025
Ag35 Standard	9.7E-03	0.35	1.0	1.1E-03	0.16	0.026	0.016
Ag35 Novel	0.13	0.50	0.83	5.8E-03	0.16	0.026	0.016

Figures 4-19 to 4-21 display the CZOI zones for samples when challenged with *S. aureus*. As seen for *P. aeruginosa*, there is a large amount of variation in zone size within sample groups. Ag65 Standard maintained a larger zone for a longer period than with *P. aeruginosa*. Overall, zones were larger for *S. aureus* than *P. aeruginosa*, because of the release of cyanide by *P. aeruginosa*, which neutralizes the effect of silver[14]. As with *P. aeruginosa*, both Ag35 samples saw a large drop off in bacteriostatic properties after 4 days. Ag65 Standard had a steady decrease over the 7 days, unlike Ag65 Novel, which maintained a zone that was not significantly different from Ag100 for the entire duration.
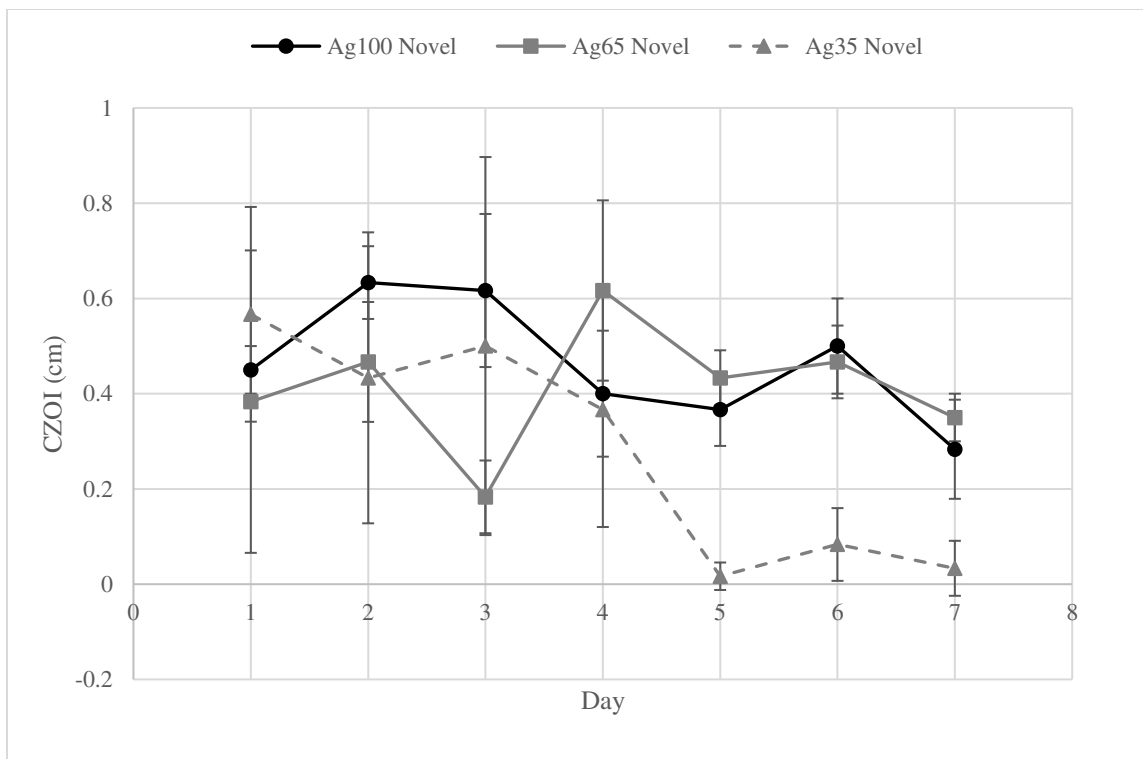
Figure 4-19 Measured zones in CZOI test over seven days for Novel samples with *S. aureus*.
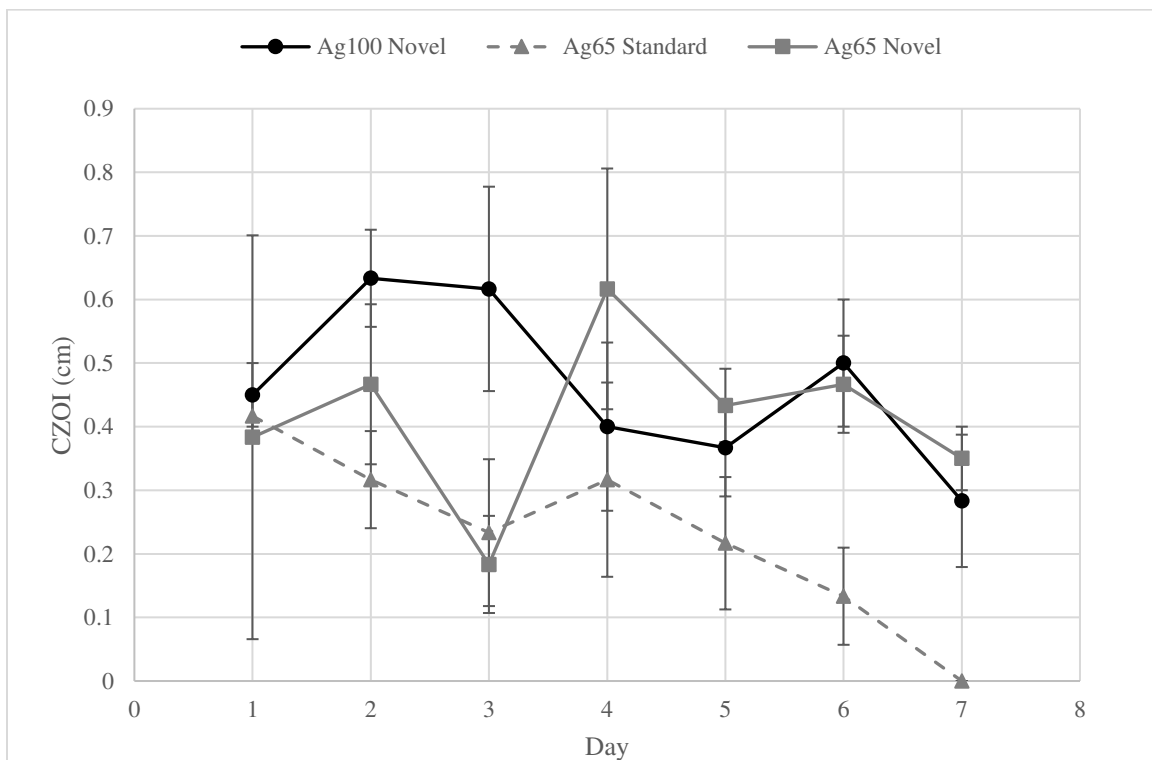
Figure 4-20 Measured zones in CZOI test over seven days for 65% silver samples, with Ag100 Novel for comparison with *S. aureus*.
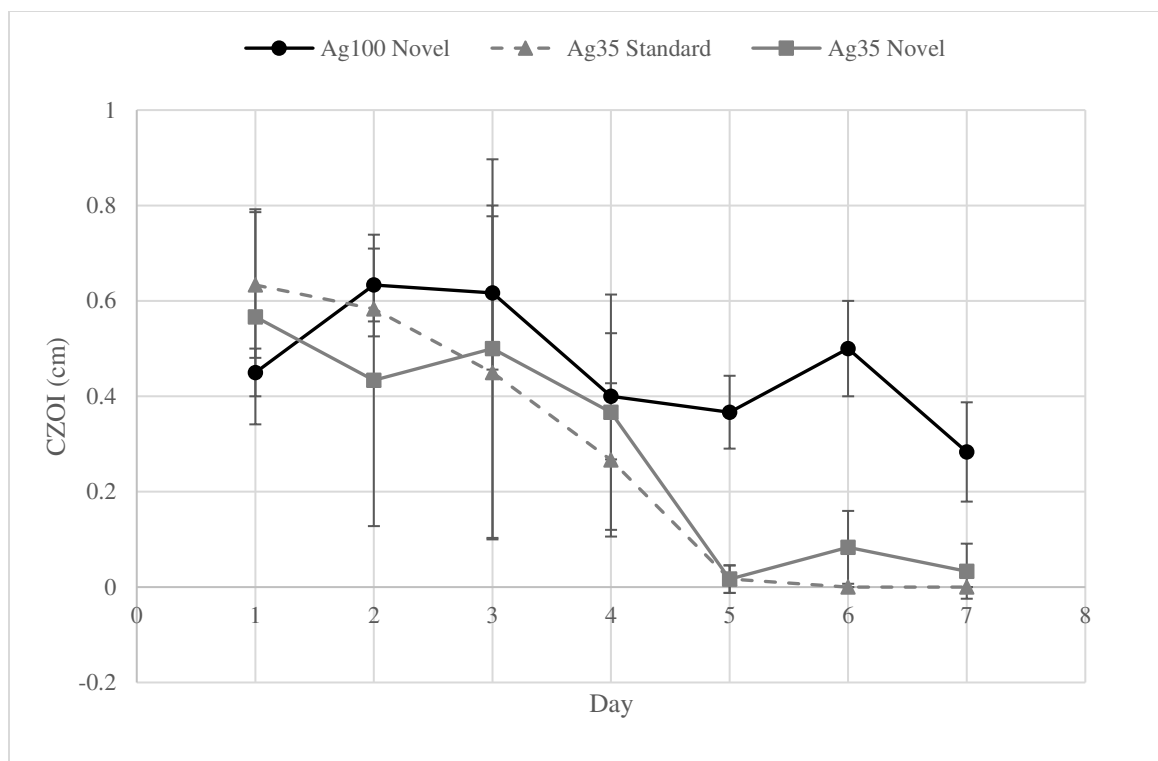
Figure 4-21 Measured zones in CZOI test over seven days for 35% silver samples, with Ag100 Novel for comparison with *S. aureus*.

Table 4-14 compares the starting and ending zones for each sample group, given with the average and standard deviation of three replicates in cm. Ag65 Novel showed the least change in starting and ending values, but both Ag100 Novel and Ag66 Novel maintained a significant zone size after 7 days.

Table 4-14 CZOI zones measured at Day 1 and Day 7 for all samples in study, with *S. aureus*.

	Zone Day 1 (cm)	**Zone Day 7 (cm)**
Ag100 Novel	0.45±0.05	0.28±0.10
Ag65 Standard	0.42±0.03	0
Ag65 Novel	0.38±0.32	0.35±0.05
Ag35 Standard	0.63±0.15	0
Ag35 Novel	0.57±0.23	0.03±0.06

ANOVA results for CZOI with *S. aureus* are shown below in Table 4-15. Only Days 5, 6, and 7 had significant effects. This demonstrates that the effect of the different dressing types was only seen in later days, when some samples no longer had a measurable zone. In the post-hoc tests, all comparisons with Ag65 Novel are significant on Days 5-7, suggesting that this sample had a greater impact relative to other samples with *S. aureus* than with *P. aeruginosa*.

Table 4-15 ANOVA p-values for the effect of sputtering alloy material and condition for nanocrystalline silver-gold samples on CZOI zone size with *S. aureus*, at each day.

Effect	Day 1 p-value	Day 2 p-value	Day 3 p-value	Day 4 p-value	Day 5 p-value	Day 6 p-value	Day 7 p-value
Material	0.14	0.27	0.13	0.21	2.8E-05	1.3E-04	9.4E-05
Condition	0.69	1.0	1.0	0.11	0.018	1.4E-03	2.4E-05
Interaction	0.89	0.17	0.76	0.39	0.018	7.6E-03	9.4E-05

Table 4-16 shows the results of t-test comparisons to Ag100 Novel, the control dressing for this test. Most of the significant differences are seen in later days. By Days 6 and 7, all samples but Ag65 Novel had a significantly different zone compared to Ag100 Novel.

Table 4-16 T-test p-values for comparison of nanocrystalline silver-gold sample zones to Ag100 zones on the same day in a seven day CZOI test with *S. aureus*.

Group	Day 1 p-value	Day 2 p-value	Day 3 p-value	Day 4 p-value	Day 5 p-value	Day 6 p-value	Day 7 p-value
Ag65 Standard	0.37	7.1E-03	0.028	0.51	0.11	7.2E-03	9.2E-03
Ag65 Novel	0.74	0.12	0.014	0.18	0.29	0.67	0.37
Ag35 Standard	0.12	0.42	0.50	0.33	1.8E-03	9.8E-04	9.2E-03
Ag35 Novel	0.43	0.33	0.66	0.85	1.8E-03	4.1E-03	0.022

Discussion

For the XRD spectra, the peak locations and shapes are as expected, but the greatest area of interest in the XRD results is the comparative grain size for Ag65 and Ag35 Novel, which was the opposite direction expected. Previous work by Kevin Unrau, which used Standard conditions, showed a consistent trend of decreasing grain size with increasing gold concentration in the target alloy. With Ag100, more grain boundaries indicate more silver oxide incorporated, which is understood to be stabilizing component in those films. However, with more gold included in the alloy, the silver oxide peak decreases and then disappears. This indicates that silver oxide is likely not the driver of grain refining for silver-gold alloy films, and instead gold grains fulfill this function. However, the similar grain size and therefore concentration of grain boundaries in Ag65 Standard and Novel may be connected to the similar percentages of ammonia soluble silver.

A source of interest in the results is the total deposition quantity and composition of the dressings in comparison to each other. Studies suggest that in the sputtering of a silver-gold alloy, silver will sputter preferentially, leaving an enrichment of gold on the surface of the target with more silver deposited on the substrate [15]. This appears to be the case for the Ag65 samples, where greater than 65% of the total

deposition (by mass) on the HDPE is silver. However, for the Ag35 samples, from a nominally 35% silver and 65% gold target, there is more than 65% gold, which is the opposite of the expected trend for preferential sputtering. The deviations from nominal target composition are more pronounced with the Novel conditions, but this difference was not found to be significant. It is not yet certain why gold sputtered preferentially in the case of the Ag35 and not Ag65, but it may be related to gold being the dominant component of the matrix of the Ag35 target. There may also be a factor of reorganization of the surface of the target. Studies also suggest enhanced diffusion in the surface layers of a sputtered material, where the concentration changes from nominal with the distance from the target surface[16]. The preferential sputtering of gold was also recognized in previous work by Unrau [2].

Another notable result is the high total deposition for Ag35. Part of this can be explained by Ag35 samples having greater than 35% gold in the film, which is a heavier element than silver. However, in a 1980 study of binary alloy sputtering, silver-gold sputtering targets showed an enrichment of gold on the target, with a 1.8 weight ratio in favour of gold on the target [15]. Because of this, it follows that the increase of silver in the alloy would increase the total sputtering yield [15]. However, despite the expected mass difference, Ag100 and Ag65 had comparable total mass deposition, with no significant differences. Another study showed that there is a lower sputtering or deposition rate for alloys than pure materials, proposed to be due to more collisions with gas species on route from the target, which further highlights the unexpected lack of deposition difference [17]. However, given that the distance between the anode and cathode in this study was 0.55 cm, as opposed to 10 cm in the present work, there is less distance for the lower density silver to be deflected on route compared to the higher density gold[17]. It is possible that the increased distance combined with a relatively high working pressure, which increases the number of collisions, would deflect more silver than gold.

In solution, Ag65 and Ag35 samples released similar total quantities of silver, so the silver in Ag65 is more tightly bound, or the structure or composition of Ag35 encourages release. Ag35 samples released more than 35 percent of the silver released by Ag100 samples, so this suggests that the large amount of gold may be contributing to increased silver release, rather than increasing the stability of the structure. Ag100 samples released more total silver in raw quantity (mg) than Ag65 or Ag35, but the comparison for percentage of total silver released was not significant for all comparisons.

The SEM images reveal qualities of the structure that are not captured by other measurements of physical or chemical properties. The biggest difference in appearance between Novel and Standard samples was seen for Ag65. This is surprising because of a similarity in both the percentage ammonia soluble silver and grain size for Standard and Novel Ag65. The greater total deposition of Ag35 is not clear from these

images. Larger clusters and a greater depth of microstructure is seen for Novel samples, but this observed increase in surface area did not correspond to a greater percentage of the total silver released.

The log reductions for both Gram negative and positive organisms, including the silver resistant *P. vulgaris*, were comparable across all the dressing samples. In Unrau's work, with 4% or greater oxygen in the sputtering environment, all the silver and silver-gold nanocrystalline materials had similar log reductions of at least 4. It appears that even in the high gold dressings (Ag35), there are sufficient antibacterial species for a total kill after one hour of direct contact in a log reduction. Despite the large amount of variation, the CZOI showed some differences in longevity between samples by the end of the test, in that Ag65 and Ag100 Novel had zones that were significantly higher than the other samples. Only Ag65 Novel had a sufficiently large zone to be comparable to Ag100 for seven days for *S. aureus*, and six days for *P. aeruginosa*. For CZOI, the trends did not support the claim that greater total silver had an effect, but because Ag100 and Ag65 Novel have a greater quantity of ammonia soluble silver, this likely explains their superior performance. However, these findings do suggest that the silver-gold dressings, despite being considered to have reduced antibacterial properties, are sufficiently bacteriostatic in a short range of 2 to 3 days. Wound dressings are often changed within this time frame, so this supports their suitability in this application.

Foundational work by Kevin Unrau on nanocrystalline silver-gold dressings can serve as a comparison here. Unrau found that there was a trend of less ammonia soluble silver release with increasing gold content, which was not proportional to the quantity of gold increase in the alloy[2]. This was also seen in the results here, where Ag65 had greater than 65% of the ammonia soluble silver of Ag100, and Ag35 had less than 35%. For Unrau, all dressings were bactericidal against *S. aureus* and *P. aeruginosa*, although there was an increasing trend with increasing gold, unlike the present results[2]. For CZOI, the differences in zone sizes were more apparent with more time, although no sample reached a zone of 0 within the 7 day time frame [2]. Most zone sizes for *P. aeruginosa* were between 5 and 15 mm, which is larger than is seen in this study[2]. Unrau identifies that silver mobility is a greater contributor to larger zones, more than the efficacy of silver alone[2]. In x-ray photoelectron spectroscopy (XPS) studies of film composition, target contamination seemed to correlate with contaminants (carbon and magnesium) found in the dressing itself[2]. Unrau also suggests that pure silver captured oxygen better than the alloy mixture[2]. Very little oxygen was found in Ag-O arrangement for samples with more gold, but oxygen was still detected, but just in a different form[2]. Au_2O_3 was consistently and stably produced and could be seen by XPS data[2].

Nanoparticles can serve as a comparison to the material used here. In a 2011 study, gold nanoparticles showed properties of bacterial inhibition against Gram positive and Gram negative species, but had

comparatively high cytotoxic effects when compared to silver nanoparticles [18]. In a 2020 study, silver-gold nanoparticles had better antibacterial properties than pure silver, although gold-only nanoparticles had negligible antibacterial properties[12].

When silver or silver-gold clusters were embedded in a carbon matrix, it was thought that the addition of gold, as a less reactive metal, would increase the release of silver ions, but the opposite effect was seen [19]. Adding gold to make an alloy made the release of silver worse [19]. In the development of a bimetallic silver-gold catalyst, it was shown that alloying with silver gave gold a greater tendency to lose electrons and the inverse was also true [20]. This increase in release of electrons may be beneficial in biological activity, as they participate in redox reactions more readily[20]. This paper determined that the best catalytic activity was found for particles of a Au:Ag molar ratio of 3:1, corresponding to an 85% mass ratio of gold[20].

Conclusion

Silver-gold nanocrystalline dressings were created with an in-house sputtering process from alloys with a nominal composition of 65% silver/35% gold or 35% silver/65% gold by weight. Despite a range of physical and chemical properties, biological testing showed that the anti-bacterial properties were comparable to silver-only dressings in short term tests. 65% silver dressings made with Novel sputtering conditions had better anti-bacterial capabilities over a longer period of time compared to 35% silver. It is expected that for future animal tests, Ag100 and Ag65 Novel films will have the most significant impact.

References

ADDIN ZOTERO_BIBL {"uncited":[],"omitted":[],"custom":[]} CSL_BIBLIOGRAPHY [1]   A. B. G. Lansdown, "Silver and Gold," in *Patty's Toxicology*, American Cancer Society, 2012, pp. 75–112. doi: 10.1002/0471435139.tox026.pub2.

[2]   K. R. Unrau, "Activity of Nanocrystalline Gold and Silver Alloys," ERA. Accessed: May 27, 2022. [Online]. Available: https://era.library.ualberta.ca/items/e0ac4715-3e00-4814-ab41-19700ce1d802

[3]   J. R. Trelewicz and C. A. Schuh, "Grain boundary segregation and thermodynamically stable binary nanocrystalline alloys," *Phys. Rev. B*, vol. 79, no. 9, p. 094112, Mar. 2009, doi: 10.1103/PhysRevB.79.094112.

[4]   J. F. Pierson, D. Wiederkehr, and A. Billard, "Reactive magnetron sputtering of copper, silver, and gold," *Thin Solid Films*, vol. 478, no. 1, pp. 196–205, May 2005, doi: 10.1016/j.tsf.2004.10.043.

[5]   M. Higo, Y. Matsubara, Y. Kobayashi, M. Mitsushio, T. Yoshidome, and S. Nakatake, "Formation and decomposition of gold oxides prepared by an oxygen-dc glow discharge from gold films and studied by X-ray photoelectron spectroscopy," *Thin Solid Films*, vol. 699, p. 137870, Apr. 2020, doi: 10.1016/j.tsf.2020.137870.

[6]   H. Tsai, E. Hu, K. Perng, M. Chen, J.-C. Wu, and Y.-S. Chang, "Instability of gold oxide Au2O3," *Surface Science*, vol. 537, no. 1, pp. L447–L450, Jul. 2003, doi: 10.1016/S0039-6028(03)00640-X.

[7]   L. D. Burke and P. F. Nugent, "The electrochemistry of gold: II the electrocatalytic behaviour of the metal in aqueous media," *Gold Bull*, vol. 31, no. 2, pp. 39–50, Jun. 1998, doi: 10.1007/BF03214760.

[8]   E. Roduner, "Size matters: why nanomaterials are different," *Chem. Soc. Rev.*, vol. 35, no. 7, pp. 583–592, Jun. 2006, doi: 10.1039/B502142C.

[9]   G. Guisbiers *et al.*, "Electrum, the Gold–Silver Alloy, from the Bulk Scale to the Nanoscale: Synthesis, Properties, and Segregation Rules," *ACS Nano*, vol. 10, no. 1, pp. 188–198, Jan. 2016, doi: 10.1021/acsnano.5b05755.

[10]   G. V. Vimbela, S. M. Ngo, C. Fraze, L. Yang, and D. A. Stout, "Antibacterial properties and toxicity from metallic nanomaterials," *Int J Nanomedicine*, vol. 12, pp. 3941–3965, May 2017, doi: 10.2147/IJN.S134526.

[11]   P. Calamai *et al.*, "Biological properties of two gold(III) complexes: AuCl3 (Hpm) and AuCl2 (pm)," *Journal of Inorganic Biochemistry*, vol. 66, no. 2, pp. 103–109, May 1997, doi: 10.1016/S0162-0134(96)00190-0.

[12]   S. Panicker, I. M. Ahmady, C. Han, M. Chehimi, and A. A. Mohamed, "On demand release of ionic silver from gold-silver alloy nanoparticles: fundamental antibacterial mechanisms study," *Materials Today Chemistry*, vol. 16, p. 100237, Jun. 2020, doi: 10.1016/j.mtchem.2019.100237.

[13]   T. G. de Carvalho *et al.*, "Spherical neutral gold nanoparticles improve anti-inflammatory response, oxidative stress and fibrosis in alcohol-methamphetamine-induced liver injury in rats," *International Journal of Pharmaceutics*, vol. 548, no. 1, pp. 1–14, Sep. 2018, doi: 10.1016/j.ijpharm.2018.06.008.

[14]   S. Létoffé *et al.*, "Pseudomonas aeruginosa Production of Hydrogen Cyanide Leads to Airborne Control of Staphylococcus aureus Growth in Biofilm and In Vivo Lung Environments," *mBio*, vol. 13, no. 5, pp. e02154-22, doi: 10.1128/mbio.02154-22.

[15]   G. Betz, "Alloy sputtering," *Surface Science*, vol. 92, no. 1, pp. 283–309, Feb. 1980, doi: 10.1016/0039-6028(80)90258-7.

[16]   P. S. Ho, "Effects of enhanced diffusion on preferred sputtering of homogeneous alloy surfaces," *Surface Science*, vol. 72, no. 2, pp. 253–263, Mar. 1978, doi: 10.1016/0039-6028(78)90294-7.

[17]   S. Habib, A. Rizk, and I. Mousa, "Physical parameters affecting deposition rates of binary alloys in a magnetron sputtering system," *Vacuum*, vol. 49, no. 2, pp. 153–160, Feb. 1998, doi: 10.1016/S0042-207X(97)00158-9.

[18] E. Marsich *et al.*, "Biological response of hydrogels embedding gold nanoparticles," *Colloids and Surfaces B: Biointerfaces*, vol. 83, no. 2, pp. 331–339, Apr. 2011, doi: 10.1016/j.colsurfb.2010.12.002.

[19] I. Carvalho *et al.*, "Antibacterial Effects of Bimetallic Clusters Incorporated in Amorphous Carbon for Stent Application," *ACS Appl. Mater. Interfaces*, vol. 12, no. 22, pp. 24555–24563, Jun. 2020, doi: 10.1021/acsami.0c02821.

[20] A.-Q. Wang, J.-H. Liu, S. D. Lin, T.-S. Lin, and C.-Y. Mou, "A novel efficient Au–Ag alloy catalyst system: preparation, activity, and characterization," *Journal of Catalysis*, vol. 233, no. 1, pp. 186–197, Jul. 2005, doi: 10.1016/j.jcat.2005.04.028.

Chapter 5 : Anti-Inflammatory Properties of Nanocrystalline Silver and Silver-Gold Dressings in an Animal Model

Introduction

Silver-gold alloys were used as targets in a physical vapour deposition process to make nanocrystalline films with grain sizes between 3-12 nm, as discussed in Chapter 4. Tests were performed to characterize the physical, chemical, and antibacterial properties of these materials. However, because inflammation is a systemic process, the anti-inflammatory properties cannot be adequately studied without a systemic model. Pigs are an ideal model for studying inflammation because of their physiological and anatomical similarities to humans, specifically with regards to their skin structure and wound healing process[1]. The ratio of dermis to epidermis is similar in pigs and humans, but more importantly, pigs heal by re-epithelialization, not by contracture as do rodents [1].

The pig model described in this chapter has been used previously by Patricia Nadworny for studying the anti-inflammatory properties of nanocrystalline silver films and solutions [2]. A DNCB-induced contact dermatitis was found to produce a consistent and reproducible inflammatory response ideal for testing the anti-inflammatory benefits of wound dressings without infection [2]. In Nadworny's work, ionic silver treatments from silver nitrate resulted in indiscriminate apoptosis by direct contact with cells, but the Ag^0 component of nanocrystalline silver dressings targeted the apoptosis of inflammatory cells in the dermis only [2]. The application of DNCB resulted in infiltration of leukocytes and red blood cells and an upregulation of inflammatory biomarkers, but nanocrystalline silver decreased the concentration of these cells and biomarkers [2]. Nanocrystalline silver treatment showed the beginning of a new epidermis by 48 hours, and nearly complete healing by 72 hours[2]. Silver nitrate increased the pro and active forms of MMP-2 and MMP-9 with time, which was not seen for nanocrystalline silver[2]. Staining for TGF-β, TNF-α, and IL-8 was most widespread in silver nitrate-treated animals at the end of the experiment, but nanocrystalline silver-treated animals were comparable with negative controls at this same time[2]. When studying tissue samples from this experiment, silver species were not detected in the mid dermis or below[2]. Pigs treated with either silver nitrate or nanocrystalline silver showed deposition of silver primarily in the epidermis and some in the upper portions of the dermis[2]. Nanocrystalline silver showed the presence of multiple silver species in the epidermis, including silver oxide and multi-atom silver clusters, and limited penetration to the dermis[2]. Yet, despite limited penetration of silver compounds, there was significantly improved wound healing and inflammatory response even when the dressing was

placed on the opposite (unwounded) side of the animal, which was seen starting 24 hours after placement [3]. While the results are not as dramatic or immediate as direct contact with nanocrystalline silver, it was still an improvement over saline-only treatment [3].

This work established that nanocrystalline silver had unique properties compared to silver nitrate that allowed it to be a superior anti-inflammatory material. Silver nitrate is only comprised of Ag^+, while nanocrystalline silver includes Ag^+, Ag^0, clusters of higher oxidation state silver, and potentially other silver compounds[4]. The incorporation of gold to the nanocrystalline silver dressings adds a species that has been demonstrated to have an anti-inflammatory effect, highlighted by its use in the rheumatoid arthritis drugs gold sodium thiomalate (GST or sodium aurothiomalate) and auranofin.

GST inhibited lymphocyte proliferation and function in *in vitro* cultures[5], [6]. Monocyte functions like adherence, spreading, and maturation are affected by GST [7], [8]. When cultured with GST, monocytes had enlarged cytoplasmic vacuoles where gold precipitates could be seen[7]. GST also limited monocyte responsiveness to lymphokines, inhibiting the antigen response of lymphocytes as a result[9]. Human B cell activation and cellular functions are also suppressed by gold compounds *in vitro* [10]. In a study of GST using patient blood samples cultured *in vitro*, it was found that CD14 monocytes were required for GST to stimulate the production of IL-10, an anti-inflammatory cytokine [11]. GST also stimulated the production of IL-6 and decreased IL-2 and IFN-γ, but was not found to cause a change in TNF-α expression[11].

The introduction of auranofin was significant for the field of arthritis treatment. Auranofin is a hydrophobic gold compound with no ionic charge[12]. Auranofin was found to have improved effects compared to GST on suppression of polymorphonuclear cell lysosomal release, reduction of cell aggregation and degranulation, and inhibition of glucose oxidation[13]. In another study, auranofin was the only gold compound to show a significant effect on edema in a rat model of arthritis, and it had a more potent effect on superoxide production[14]. Auranofin increased levels of IL-6, but inhibited the transcription factor STAT3, which reduced fibrinogen, haptoglobin, and other protein production when studied *in vitro* [15].

In a 1994 study, GST was injected intramuscularly in human patients with rheumatoid arthritis and biopsied tissue showed a reduction in inflammatory monocytes and macrophages, specifically CD68+ cells [16]. After 12 weeks, IL-1α, IL-1β, IL-6, and TNF-α were reduced and clinical symptoms improved[16]. In later weeks, there was a decrease in macrophages, but not monocytes, suggesting that monocyte differentiation or adhesion to endothelial cells is disrupted by gold [16]. Using cultured

synoviocytes from human patients with rheumatoid arthritis, auranofin caused a dose-dependent suppression of the inflammation enzyme COX-2, from the suppression of NF-κB and its downstream cytokines IL-1β and PGE2 [17]. Auranofin has also been tested *in vitro* with MCF-7 breast cancer cells, causing more intracellular calcium, a pathway for apoptosis[18]. These studies suggest possible mechanisms for the action of gold and inform which biomarkers and cells will be studied in this chapter.

GST and auranofin are gold complexes where gold has an oxidation state of I. Gold in the III oxidation state is a strong oxidizer, which may be responsible for the side effects of gold complexes, mediated by T-cell sensitization[19], [20]. It is known that Au(III) acts as an oxidizing agent when in contact with proteins, displaying nonspecific binding with proteins that have available sulfur groups, itself reducing to Au(I)[21]. Au^+ is unstable in physiological conditions, being easily converted to Au(III) or Au^0 [22]. Gold targets thiol groups and most serum gold will bind to albumin[22], [23]. In gold (I) disodium thiomalate, the gold is in the I oxidation state, but mononuclear phagocytes oxidize the Au(I) to Au(III) [20]. However, gold remains in the III oxidation state when binding to DNA, changing the DNA conformation[21].

Nanoparticles can serve as a comparison to the nanocrystalline films used here. In a 2011 study, gold nanoparticles in hydrogels showed properties of bacterial inhibition against Gram positive and Gram negative species *in vitro* [24]. However, the gold nanoparticles showed cytotoxic effects on human cell lines *in vitro*, linked to a two-fold increase in intracellular ROS levels [24]. Here, silver nanoparticles in hydrogels did not show any cytotoxicity to human cells at the concentrations studied[24]. In contrast, in silver-gold alloyed nanoparticles, a lower concentration of silver reduced the cytotoxicity towards human gingival fibroblasts *in vitro*[25].

Gold nanoparticles reduced the release of IL-8 and IL-6, but silver increased IL-8, indicating activation of the studied cell species, human mesenchymal stem cells, *in vitro* [26]. Silver had an effect on the viability of these cells in a concentration dependent manner[26]. Gold nanoparticles had a limited effect, which may be attributed to size, as small nanoparticles can enter the nucleus[26]. Including gold with silver in nanoparticles appeared to decrease the biological activity of the silver, as was found in other studies [26]. Gold nanoparticles reduced expression and production of TNF-α, IL-1β, COX-2 and fibrosis via the NF-κB pathway in rat models of arthritis [27], [28].

In Chapter 4, contrary to expectations, nanocrystalline silver-gold films had comparable biological properties to the silver-only films. Previous work by Unrau showed the trend of higher gold alloy combinations leading to more grain boundaries from smaller grain sizes[29]. This trend was not clearly seen in this work with the Novel sputtering conditions, but an animal study provides the opportunity to

compare anti-inflammatory properties of a range of grain sizes and to examine other properties that may play a role in anti-inflammatory properties. There is a range of total silver or gold content, ammonia soluble silver, total deposition, percentage silver release in solution, and grain size in the films studied, all of which may be relevant for controlling inflammation and promoting healing. The goal of this study is to correlate the inflammation and healing outcomes to the chemical, physical, and biological data collected in Chapter 4.

Methods

Dressing Fabrication

As described previously, silver or silver-gold coatings were sputtered onto an HDPE mesh substrate using an in-house sputtering system. Three targets are used: 65% gold and 35% gold, with the balance silver, and a pure silver target. Standard and Novel sputtering conditions as described previously were used to make films. Dressings for this study are made by sandwiching two layers of coated HDPE with one layer of gauze.

Animal Study

The protocol to be used for the animal study is adapted from the protocol developed by Patricia Nadworny[2]. Figure 5-1 displays a timeline and summary of procedures to take place during the study.

Day -21 to Day -14:
Animals acclimatize to environment.

Day -14:
Animals shaved on left side. First application of DNCB.

Day -7:
Second application of DNCB.

Day -3: Third application of DNCB. Fentanyl patches applied.

Day 0:
Final application of DNCB. Pigs weighed. Biopsies, blood sample, and dressings applied 4 hours after DNCB application.

Day 2:
Biopsies taken. New dressings applied.

Day 3: Pigs weighed. Biopsies and blood samples taken. Pigs euthanized.

Figure 5-1 Timeline of procedures for dermal inflammation animal study.

Animal Acquisition and Care

This study was approved by the University of Alberta Animal Care and Use Committee and MedStar Health Research Institute (MHRI) Institutional Animal Care and Use Committee. All animal procedures

will be conducted at the Burn and Surgical Research Laboratory at Medstar Health Research Institute in Washington DC. The approved protocol can be found in Appendix B. Twenty-four Large White/Landrace swine (15-25 kg) will be used in this study. All animals are to be healthy and without significant wounds or scars on their backs. The animals are housed in individual pens with a 12 hour light/dark cycle, where they are allowed to acclimatize seven days prior to starting experiments. Three animals will be used for each experimental and control group. The animals will receive antibiotic-free water and standard hog ration ad libitum up until Day 0 of the experiment as per facility procedure. Animals will be fasted for 12 hours prior to procedures requiring anesthetic on Days 0, 2, and 3. Table 5-1 lists the Control and Experimental groups for the study.

Table 5-1 Control and Experimental groups, with codes and descriptions for groups in the dermal inflammation animal study.

Group	Code	Description
Negative Control, Sham	NC	No DNCB application, treated with saline-soaked gauze
Positive Control	PC	Treated with saline soaked gauze
Standard Silver Dressing	Ag100S	100% Silver, Standard Sputtering Conditions
Novel Silver Dressing	Ag100N	100% Silver, Novel Sputtering Conditions
Standard Low Gold Dressing	Ag65S	65% Silver, 35% Gold, Standard Sputtering Conditions
Novel Low Gold Dressing	Ag65N	65% Silver, 35% Gold, Novel Sputtering Conditions
Standard High Gold Dressing	Ag35S	35% Silver, 65% Gold, Standard Sputtering Conditions
Novel High Gold Dressing	Ag35N	35% Silver, 65% Gold, Novel Sputtering Conditions

Sensitization to DNCB for Inflammatory Reaction

Inflammation will be induced using a 10% solution of DNCB in 4:1 acetone:olive oil. On Day -14, the hair on the backs of all 24 pigs will be shaved using electric clippers and surgically prepared as per facility protocol. Baseline punch biopsies will be taken from a site distant to the studied area to serve as a baseline for uninjured skin. From each pig, three biopsies are to be flash frozen and three will be preserved in formalin. Baseline blood samples will also be collected at the same time as biopsies. The areas for observation will be outlined on each flank with a surgical marker, an area approximately 15 by 25 cm on each side of each pig's back. Then, the DNCB solution will be painted over the outlined areas for 21 pigs. This procedure will be repeated on Days -7, -3, and 0. On Day -3, pigs will be given fentanyl patches on shaved skin away from the rash, to avoid discomfort during the final application and treatment. The remaining three pigs, which will be part of the negative control group (NC), will not have DNCB

application, but will be painted with a saline solution and will receive fentanyl patches at Day -3. Images will be taken of the rash area on Days -14, -7, -3, and 0.

Surgical Procedures

On Day 0, all pigs will be weighed. On Day 0, the biopsy procedure will occur 2 hours ± 30 minutes after the final DNCB application. Pigs will be placed under general anesthetic via isoflurane inhalation and ketamine injection according to facility protocol. Further details of anesthetic and analgesic administration, including doses, can be found in the protocol in Appendix B. Animal care staff will assess and monitor pigs under anesthesia according to facility procedures. Heart rate and oxygen saturation will be monitored by an oxygen clip to the ear. Depth of anesthesia will be monitored regularly. Vital signs will be recorded at a minimum interval of every 17 minutes.

Visual observations and photographs are taken of the rash area on each procedure day. Scores of erythema and edema will be made on Days 0, 2, and 3 [2]. Pigs will be scored on the bleeding of past biopsies on Days 2 and 3 when biopsies are taken. Scores will be made by three independent observers and averaged. Weight changes from Day 0 to 3 are also recorded. Pigs will be monitored daily for changes in appearance and behaviour. On Day 0, 2, and 3, biopsies and blood samples are taken. Dressings are changed on Day 2. Erythema scoring is displayed in Table 5-2, edema scoring is displayed in Table 5-3, and biopsy bleeding scoring is displayed in Table 5-4.

Table 5-2 Semi-quantitative erythema scoring for rashes created on pigs.

Score	Description
0	No redness, as compared to a negative control on Day 0
1	Barely visible redness
2	Moderate redness
3	Severe, bright red
4	Dark red/purple coloration

Table 5-3 Semi-quantitative edema scoring for rashes created on pigs.

Score	Description
0	No swelling, as compared to a negative control on Day 0
1	Mildly raised tissue covering parts of the rash
2	Moderately raised and firm tissue covering parts of the rash
3	Swelling and hardness of tissue over most of the rash
4	Hard raised tissue over the entire rash area

Table 5-4 Semi-quantitative scoring of biopsy bleeding for animals in study.

Score	Description
0	No bleeding
1	Minimal bleeding
2	Moderate bleeding
3	Severe bleeding

Treatment and Sampling

Blood samples for serum analysis will be collected into sodium citrate, SST, and Paxgene tubes. The volume taken from each pig will be under 12 mL. Biopsy locations are to be taken as shown below in Figure 5-2. Six samples will be taken on each side of the pig on each procedure day with a 4 mm full thickness biopsy punch. Biopsies from subsequent days will be spaced a minimum of 4 cm from the previous days biopsies to limit the effect from past biopsies, but still be well within the bounds of the rash.
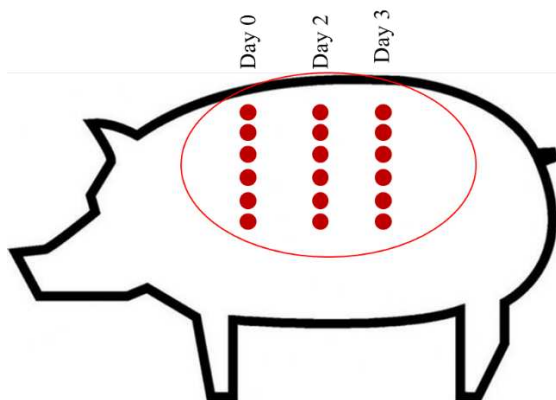
Figure 5-2 Biopsy sampling locations for dermal model, six per day per side, within rash boundary (indicated by red oval).

Biopsies from each day will be randomly assigned for analysis. Three biopsies will be placed in 4% formalin at room temperature to preserve for staining and imaging. Three biopsies will be snap-frozen in liquid nitrogen and then kept at -80°C until use for protein and gene analysis.

Calcium alginate dressings will be used to reach hemostasis once biopsies are taken. The positive and negative controls will be treated with a sterile dressing of HDPE and gauze, saturated with 0.9% sodium chloride in sterile water. Nanocrystalline silver or silver-gold dressings will be moistened with sterile water and placed over the entire rash and secured. New fentanyl patches may be applied as needed. Dressings will be replaced on Day 2 after biopsies are taken and observations are made.

Sample Analysis

All samples for tissue staining and imaging will be placed in 4% formalin at the time of biopsy acquisition. They will be rinsed with PBS before being placed in 70% ethanol and stored at 4°C. At the time of sectioning, the tissue samples will be dehydrated in alcohol and xylene, oriented and embedded in paraffin, and sectioned at a thickness of 5 μm. Paraffinized samples will be deparaffinized and rehydrated at the time of staining.

Histopathology

For histopathological analysis, sections will be stained with hematoxylin and eosin following standard procedures. Hematoxylin stains cell nuclei and eosin stains the extracellular matrix. Images will be taken of the slides at 20x and 100x magnification at various depths using an optical microscope with an attached digital camera. Images will be taken to show the epidermis, upper and lower dermis, and the epidermis-dermis junction.

Immunohistochemistry

Tissue samples after 48 and 72 hours of treatment will be analyzed for the presence of TGF-β, Il-4 and TNF-α. These biomarkers have been chosen to represent three aspects of the healing process. TGF-β is a growth factor involved in wound healing, IL-4 is an anti-inflammatory cytokine that suppresses immune functions, and TNF-α is a pro-inflammatory cytokine produced by macrophages. For antigen retrieval, samples will be incubated with proteinase K, then hydrogen peroxide, then serum and antibodies appropriate to the biomarker. All slides will also be incubated with DAB (3,3′-Diaminobenzidine) to stain cell nuclei. Images will be taken at 20x and 100x magnification with a microscope with fluorescence imaging.

Apoptosis Detection

Detection of apoptotic cells in sectioned tissue samples can be determined using a commercially available In Situ Cell Death Detection Kit. This kit identifies genomic DNA strand breakages that occur during apoptosis with fluorescein labels by incubating with a TUNEL (Terminal deoxynucleotidyl transferase (TdT) dUTP Nick-End Labeling) reaction mixture. After dewaxing, rehydration, and proteinase K treatment, the enzyme-nucleotide labelling solution will be applied according to kit instructions. Apoptotic cells will be detected at a green wavelength of 515 to 565 nm by a fluorescence imaging microscope.

SIMS

Time-of-Flight secondary ion mass spectrometry (ToF-SIMS) can be used to detect the presence, depth, and concentration of various gold and silver species from paraffinized tissue samples. The analysis will be performed for tissue samples which include the epidermis and dermis.

ToF-SIMS will be performed with a detection instrument with a reactive ion beam to identify gold and silver species based on mass. Instrument software will provide the summed intensity, total counts and maximum intensity of each mass-selected species across the image. Optical images will also be taken parallel to the ToF-SIMS images to corroborate with tissue structures.

Table 5-5 shows the species of interest for SIMS analysis and the atomic weights that will be used to identify them. Silver has two isotopes while gold has one isotope. It is not expected to see gold oxide, as it is known to be unstable, but gold chloride is expected to be present. Multi-atom silver clusters were found in tissues after the application of nanocrystalline silver wound dressings, so gold clusters may be expected as well for Ag65 and Ag35 groups.

Table 5-5 Weights used in SIMS analysis[30]

Species	Isotopes	Atomic Weights for Analysis
Silver Compounds		
Ag	Ag: 107, 109	107, 109
AgO	Ag: 107, 109; O: 16	123, 125
Ag_2O	Ag: 107, 109; O: 16	230, 232, 234
AgCl	Ag: 107, 109; Cl: 35, 37	142, 144, 146
$AgNO_3$	Ag: 107, 109; N: 14, 15; O:16	169, 170, 171, 172
Silver Clusters		
Ag_2	Ag: 107, 109	214, 216, 218
Ag_3	Ag: 107, 109	321, 323, 325, 327
Ag_4	Ag: 107, 109	428, 430, 432, 434, 436
Ag_5	Ag: 107, 109	535, 537, 539, 541, 543, 545

Species	Isotopes	Atomic Weights for Analysis
Ag$_6$	Ag: 107, 109	642, 644, 646, 648, 650, 652, 654
Ag$_7$	Ag: 107, 109	749, 751, 753, 755, 757, 759, 761, 763
Gold Compounds		
Au	Au:197	197
Au2O	Au: 197; O: 16	410
Au2O3	Au: 197; O: 16	442
AuCl	Au:197; Cl: 35, 37	232, 234
AuCl3	Au: 197; Cl: 35, 37	302, 304, 306, 308
Gold Clusters		
Au2	Au:197	394
Au3	Au:197	591
Au4	Au:197	788
Au5	Au:197	985
Au6	Au:197	1182
Au7	Au:197	1379

Gene Expression

RNA is extracted and isolated from powdered snap-frozen tissue samples and serum samples and measured by RT-PCR. Primers sequences for the encoded biomarker will amplify the segment of interest containing the gene for the cytokine during replication cycles and add a fluorescent tag which can be read by spectrophotometry[31]. The markers of interest are IFN-γ, IL-1β, IL-2, IL-4, IL-6, IL-8, IL-10, IL-12, TNF-α, and TGF-β1. Each biomarker is explained further in Table 5-6.

Table 5-6 Biomarkers for Study

Biomarker	Definition and Importance
IFN-γ	Interferon gamma. Secreted by T cells and natural killer cells with roles in innate immunity, cell proliferation and apoptosis, and macrophage activation[32].
IL-1β	Interleukin 1β. Mediates apoptosis and is involved in the acute inflammatory response [33].
IL-2	Interleukin 2. Stimulates proliferation of T lymphocytes and induces the secretion of other cytokines such as IFN- γ, IL-4, and TNF [34]. Enhances the immune effects of T and B cells[34].
IL-4	Interleukin 4. Produced by mast cells and basophils, responsible for regulation and suppression of initial immune responses to support tissue repair[35].
IL-6	Interleukin 6. Involved in acute immune response, including signalling the proliferation and differentiation effects on immune cells[36].

Biomarker	Definition and Importance
IL-8	Interleukin 8. Proinflammatory cytokine with targeted effects on neutrophils, particularly their attraction and activation[37].
IL-10	Interleukin 10. Anti-inflammatory cytokine, limits immune response to prevent tissue damage[38]
IL-12	Interleukin 12. Causes differentiation of T-cells, implicated in auto-immunity[39]. Increases production of IFN- γ[39].
TNF-α	Tumor Necrosis Factor alpha. Inflammatory cytokine secreted during acute inflammation for cell signalling, which may lead to apoptosis or necrosis[40].
TGF-β1	Transforming Growth Factor Beta. Part of the inflammatory response by regulating and inhibiting T cells[41]. Participates in tissue healing by granulation tissue formation and re-epithelization[42].

ELISA

ELISA is an enzyme immunoassay. Cytokine antigens are bound to an enzyme-labeled antibody which is then absorbed on the wall of a plastic plate which is read by a spectrophotometer[43]. Multiple methods are available for performing ELISA analysis. A kit will be purchased to perform the assay on a panel of pro and anti-inflammatory cytokines, which will be those listed above in Table 5-6.

Statistics

Two-way ANOVA is used to assess the effects of material type and sputtering condition for the six experimental dressings, with Tukey's post-hoc tests if significance is found from the ANOVA tests. For comparisons with the negative or positive control groups, unpaired t-tests are used. Significance is defined as $p < 0.05$.

Predicted Results

Predictions of the results will be given in this section to discuss anticipated trends.

Erythema and Edema Scoring

The DNCB sensitization process is expected to give all animals a maximum score for both edema and erythema on Day 0. Positive control (PC) pigs are expected to see minimal improvement over the three days, as only a saline soaked gauze bandage will be applied. Negative control (NC) pigs will have the lowest possible scores for both erythema and edema at all time points. Previous work shows that

nanocrystalline silver decreased erythema and edema, most dramatically reducing edema over the Day 0 control less than one day after treatment application [30]. In this study, dressing changes and wound observation will take place only on Day 2, not on Day 1. On Day 2, it is expected that Ag100N, Ag100S and Ag65N groups will have a low edema score and moderately low erythema. These dressings have the highest silver content, which is already proven to promote wound healing, unlike gold which is not yet proven in this application. By Day 3, the scores for these groups are predicted to decrease, especially the score for erythema.

The total silver and gold deposition of Ag35N is greater than that for Ag100N or Ag65N. However, there is limited evidence suggesting that the inclusion of gold could slow healing, therefore the scoring predictions for Day 2 are moderate for both edema and erythema [44], [45]. On Day 3, the scores are predicted to remain moderate as healing is not yet complete. Ag35S is expected to have the worst performance for wound healing of the experimental groups, followed by Ag65S, which will be reflected in the scores for erythema and edema. This is because of the low combined deposition of both silver and gold in these dressings.

Based on these predictions, a sample dataset has been generated for the purposes of visualizing expected trends, shown in Figures 5-3 and 5-4.
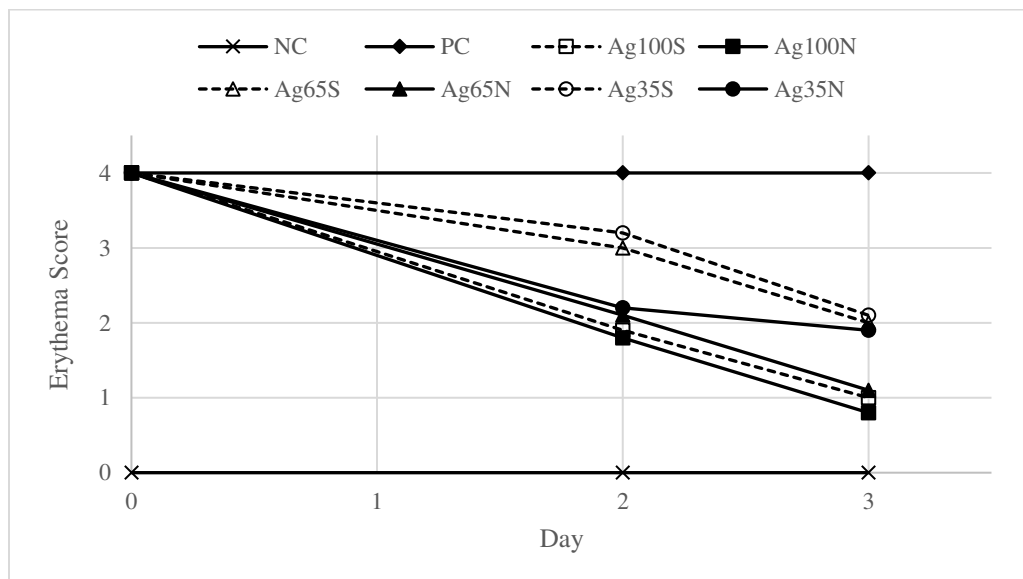
Figure 5-3 Predicted erythema scoring.
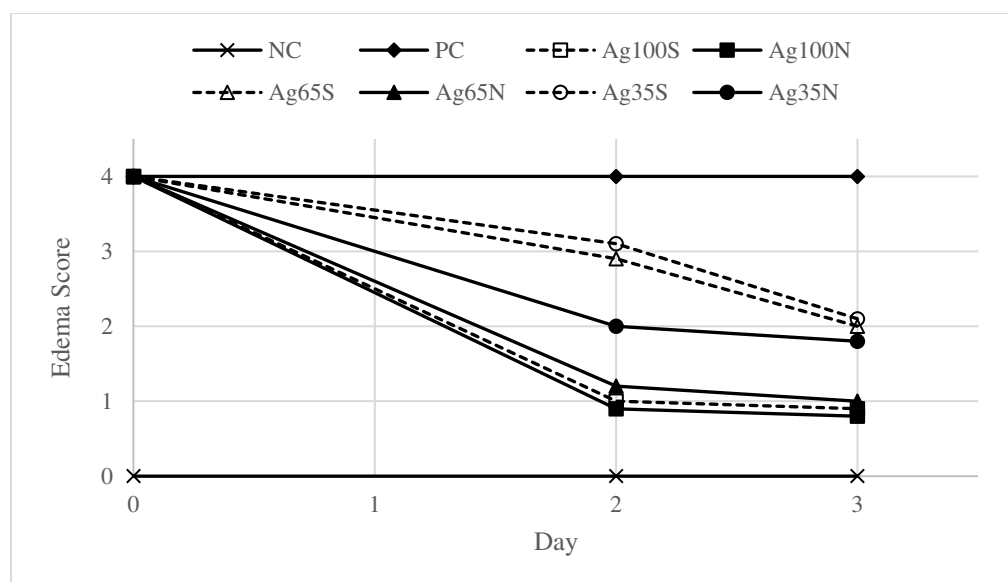
Figure 5-4 Predicted edema scoring.

Histopathology

For the negative controls (NC) with no DNCB application, the H&E staining will show normal skin with a well-defined epidermis and dermis and low cellularity for all days[30]. All animals treated with DNCB will show an extreme inflammatory reaction on Day 0, which will continue on Days 2 and 3 for positive saline controls (PC) [30]. It is expected to see an influx of inflammatory cells and red blood cells with evidence of edema and a delaminated epidermis[30].

By Day 2, it is expected that Ag100N, Ag100S, and Ag65N groups will have the formation of a new epidermis, with near normal tissue and few inflammatory cells by Day 3. This is expected to occur to a lesser extent for the other experimental groups, where healing is expected to be slower. The addition of gold is expected from other studies to cause more cytotoxicity and a greater fibrotic reaction over silver, although this likely depends on the gold and silver species used in those experiments, and may not be reflected in the healing process that might be seen here[24], [25], [26].

Immunohistochemistry

The most intense staining for TGF-β will be for positive controls. Experimental samples are expected to have minimal staining at Day 2 and will be comparable to negative controls at Day 3, if healing is near completion. Healed tissue is expected to have very little staining for TNF-α by Day 3. Positive control pigs will have intense staining localized to cells. Minor TNF- α staining will be seen on Day 2 for experimental groups, with more staining for groups still with significant inflammation. Positive control

pigs will have light staining for IL-4. It is expected to see cell specific staining for experimental groups, with the most intense staining on Day 2.

Apoptosis

It is expected that there would be few apoptotic cells seen in the negative control group (NC) as there is no wound. For the positive controls there is apoptosis expected in the epidermis and upper dermis from previous studies[2]. It is known that nanocrystalline silver treatment results in targeted apoptosis of inflammatory cells, particularly in the dermis[2]. It is expected that this will be seen for the Ag100S and Ag100N pigs. Ag100N may have a greater effect in this area than Ag100S because there is more silver in Ag100N, and more is released in solution. See Chapter 4 for more details on the physical properties of the dressings.

It is difficult to predict what the combined effect of silver and gold will be in the Ag65 and Ag35 groups. The gold based drug auranofin has been implicated in increasing apoptosis of human cancer cells *in vitro* by increasing intracellular calcium levels [18]. It appears also that the size of gold nanoparticles effects the pathway of cell death, so the amount of apoptosis versus necrosis may depend on the size of clusters released, which can be observed with SIMS[46].

SIMS

From previous work, it is expected that the silver and gold deposition will primarily be in the epidermis, with minimal penetration to the dermis [30]. Silver chlorides and silver oxides were more likely to penetrate deeper into the dermis, while silver clusters remained in a thin layer on the surface of the epidermis[30].

The total silver and gold deposited in the tissues will likely be related to both the total silver and gold contained in each dressing and the ease of release. It was shown in Chapter 4 that Standard samples released a greater percentage of their silver in solution, but Novel samples released a greater total by weight. Novel samples also have the greatest total silver and gold, particularly the Ag35 Novel samples. It is therefore likely to see the most silver or gold deposition in tissues for Ag35N, followed by Ag65N and Ag100N, then Ag35S. Silver chloride is more likely to form over gold chloride because silver is more reactive than gold. Still, some gold chloride would be expected, particularly in groups where there is significantly more gold than silver. Gold oxide is not likely to be seen as it tends to be unstable. Gold and silver oxides and chlorides will likely be seen in the dermis and epidermis. Standard samples have a greater percentages of ammonia soluble silver, although Novel samples have a greater raw amount. This

will be reflected in the amount of silver oxides and chlorides. Silver clusters are expected to be seen from previous work but the formation and stability of gold clusters in the epidermis is uncertain[30].

mRNA and ELISA

The gene expression and protein production will follow similar trends, so the expected results for mRNA and ELISA analysis will be discussed together. Tables 5-7 and 5-8 show general trends in biomarkers as compared to the Negative Control (non-DNCB) pigs at each time period. The symbol '-' or '--' indicates a decrease compared to the negative control, '+' or '++' indicates an increase, and 0 indicates a similar level. Discussion of each biomarker and trends will follow. For most biomarkers, the positive control (PC) and Ag100 groups are based on previously published work[30]. Ag35 and Ag65 will follow trends that reflect literature sources and predicted healing timelines. Ag65 is expected to have more similarities to the predictions for Ag100, while Ag35 will more often follow literature assumptions of the activity of gold.

Table 5-7 Biomarker predicted relative comparison to Negative Control, Day 2

Biomarker	NC	PC	Ag100S	Ag100N	Ag65S	Ag65N	Ag35S	Ag35N
IFN-γ	0	0	+	+	0	+	0	0
IL-1β	0	0	++	++	++	++	++	++
IL-2	0	+	+	+	+	+	+	+
IL-4	0	0	+	+	+	+	+	+
IL-6	0	+	+	+	+	+	+	+
IL-8	0	+	+	+	0	0	0	0
IL-10	0	+	+	+	+	+	+	+
IL-12	0	0	0	0	0	0	0	0
TNF-α	0	+	++	++	+	+	+	+
TGF-β1	0	+	+	+	+	+	+	+

Table 5-8 Biomarker predicted relative comparison to Negative Control, Day 3

Biomarker	NC	PC	Ag100S	Ag100N	Ag65S	Ag65N	Ag35S	Ag35N
IFN-γ	0	++	0	0	+	0	+	+
IL-1β	0	0	0	0	+	0	+	+
IL-2	0	+	0	0	0	0	0	0
IL-4	0	++	0	0	+	0	+	+
IL-6	0	+	0	0	+	0	+	+

Biomarker	NC	PC	Ag100S	Ag100N	Ag65S	Ag65N	Ag35S	Ag35N
IL-8	0	+	0	0	0	0	0	0
IL-10	0	+	0	0	+	0	+	+
IL-12	0	0	--	--	-	-	-	-
TNF-α	0	0	--	--	-	-	-	-
TGF-β1	0	+	-	-	0	0	0	0

IL-1β: IL-1β is particularly important in the acute inflammatory phase. Nanocrystalline silver has previously caused a significant increase in this biomarker. Therefore, it is expected that early in the healing process, there would be a significant increase for the first two days, followed by a return to normal (NC) levels by Day 3 as healing is mostly complete. There is expected to be some elevation in levels for pigs where acute inflammation is still predicted to be ongoing by Day 3 such as Ag35S and Ag65S.

IL-2: IL-2 is expected to be upregulated initially in all groups that have had DNCB application. As healing progresses, the levels will return to baseline [11].

IL-4 and IFN- γ: IL-4 works to suppress the initial immune response to initiate tissue healing, but may still remain elevated if the immune response is ongoing, especially in positive controls, but also in the Ag35 groups which are expected to have a slower healing response. IFN-γ is also expected to follow similar trends to IL-4.

IL-6 and IL-8: IL-6 and IL-8 are closely related in function and therefore in trends. Both are pro-inflammatory cytokines. Nanocrystalline silver reduced IL-6 and IL-8 from the high levels caused by DNCB inflammation[2]. Gold has been shown in some cases to reduce the release of IL-6 and IL-8 after inflammation, although some sources suggest increased levels[11], [15], [16]. Therefore, levels are elevated on Day 2, but as healing progresses, the levels will drop.

IL-10: IL-10 is an anti-inflammatory cytokine that sees increased production in response to inflammation. As healing progresses, the levels will return to baseline. Nanocrystalline silver has been previously shown to increase IL-10 levels and there is some evidence to suggest that gold will do the same[30], [44].

IL-12: There are expected to be few changes in IL-12 initially. IL-12 is more involved in chronic inflammation and autoimmunity. If healing progresses quickly and inflammation is limited, then IL-12 will not be increased over baseline. While it is uncertain the effect gold will have on IL-12, although it has been seen that nanocrystalline silver suppressed IL-12 production by Day 3[30].

TNF-α: DNCB inflammation is expected to increase levels of TNF-α, which will be decreased by Day 3 with application of silver and gold as studies have suggested that both materials reduce levels of TNF-α [16], [27], [28].

TGF-β1: On Day 2, all groups are expected to have upregulated TGF- β1. As healing nears completion for experimental groups on Day 3, the levels will drop[30].

References

[1] L. Lossi, L. D'Angelo, P. De Girolamo, and A. Merighi, "Anatomical features for an adequate choice of experimental animal model in biomedicine: II. Small laboratory rodents, rabbit, and pig," *Annals of Anatomy - Anatomischer Anzeiger*, vol. 204, pp. 11–28, Mar. 2016, doi: 10.1016/j.aanat.2015.10.002.

[2] P. L. Nadworny, J. Wang, E. E. Tredget, and R. E. Burrell, "Anti-inflammatory activity of nanocrystalline silver in a porcine contact dermatitis model," *Nanomedicine: Nanotechnology, Biology and Medicine*, vol. 4, no. 3, pp. 241–251, Sep. 2008, doi: 10.1016/j.nano.2008.04.006.

[3] P. L. Nadworny, B. K. Landry, J. Wang, E. E. Tredget, and R. E. Burrell, "Does nanocrystalline silver have a transferable effect?," *Wound Repair and Regeneration*, vol. 18, no. 2, Art. no. 2, 2010, doi: 10.1111/j.1524-475X.2010.00579.x.

[4] F.-R. F. Fan and A. J. Bard, "Chemical, Electrochemical, Gravimetric, and Microscopic Studies on Antimicrobial Silver Films," *J. Phys. Chem. B*, vol. 106, no. 2, Art. no. 2, Jan. 2002, doi: 10.1021/jp012548d.

[5] P. E. Lipsky and M. Ziff, "Inhibition of antigen- and mitogen-induced human lymphocyte proliferation by gold compounds.," *J Clin Invest*, vol. 59, no. 3, pp. 455–466, Mar. 1977.

[6] M. Harth, C. R. Stiller, N. R. St C Sinclair, J. Evans, D. McGirr, and R. Zuberi, "Effects of a gold salt on lymphocyte responses.," *Clin Exp Immunol*, vol. 27, no. 2, pp. 357–364, Feb. 1977.

[7] K. Ugai, M. Ziff, and P. E. Lipsky, "Gold-induced changes in the morphology and functional capabilities of human monocytes," *Arthritis Rheum*, vol. 22, no. 12, pp. 1352–1360, Dec. 1979, doi: 10.1002/art.1780221206.

[8] B. H. Littman and R. E. Hall, "Effects of gold sodium thiomalate on functional correlates of human monocyte maturation," *Arthritis Rheum*, vol. 28, no. 12, pp. 1384–1392, Dec. 1985, doi: 10.1002/art.1780281211.

[9] B. H. Littman and P. Schwartz, "Gold inhibition of the production of the second complement component by lymphokine-stimulated human monocytes," *Arthritis Rheum*, vol. 25, no. 3, pp. 288–296, Mar. 1982, doi: 10.1002/art.1780250306.

[10] S. Hirohata, K. Nakanishi, T. Yanagida, M. Kawai, H. Kikuchi, and K. Isshi, "Synergistic Inhibition of Human B Cell Activation by Gold Sodium Thiomalate and Auranofin," *Clinical Immunology*, vol. 91, no. 2, pp. 226–233, May 1999, doi: 10.1006/clim.1999.4686.

[11] J. Lampa, L. Klareskog, and J. Rönnelid, "Effects of gold on cytokine production in vitro; increase of monocyte dependent interleukin 10 production and decrease of interferon-gamma levels.," *The Journal of Rheumatology*, vol. 29, no. 1, pp. 21–28, Jan. 2002.

[12] A. Lorber, W. H. Jackson, and T. M. Simon, "Assessment of immune response during chrysotherapy. Comparison of gold sodium thiomalate vs. auranofin," *Scand J Rheumatol*, vol. 10, no. 2, pp. 129–137, 1981, doi: 10.3109/03009748109095285.

[13] B. Wolach, J. E. DeBoard, T. D. Coates, R. L. Baehner, and L. A. Boxer, "Correlation of in vitro and in vivo effects of gold compounds on leukocyte function: possible mechanisms of action," *J Lab Clin Med*, vol. 100, no. 1, pp. 37–44, Jul. 1982.

[14] D. T. Walz, M. J. DiMartino, D. E. Griswold, A. P. Intoccia, and T. L. Flanagan, "Biologic actions and pharmacokinetic studies of auranofin," *The American Journal of Medicine*, vol. 75, no. 6, Part 1, pp. 90–108, Dec. 1983, doi: 10.1016/0002-9343(83)90481-3.

[15] N.-H. Kim, M.-Y. Lee, S.-J. Park, J.-S. Choi, M.-K. Oh, and I.-S. Kim, "Auranofin blocks interleukin-6 signalling by inhibiting phosphorylation of JAK1 and STAT3," *Immunology*, vol. 122, no. 4, pp. 607–614, 2007, doi: 10.1111/j.1365-2567.2007.02679.x.

[16] G. Yanni, M. Nabil, M. R. Farahat, R. N. Poston, and G. S. Panayi, "Intramuscular gold decreases cytokine expression and macrophage numbers in the rheumatoid synovial membrane.," *Ann Rheum Dis*, vol. 53, no. 5, pp. 315–322, May 1994.

[17] R. Yamada *et al.*, "Auranofin inhibits interleukin-1β-induced transcript of cyclooxygenase-2 on cultured human synoviocytes," *European Journal of Pharmacology*, vol. 385, no. 1, pp. 71–79, Nov. 1999, doi: 10.1016/S0014-2999(99)00707-4.

[18] E. Varghese and D. Büsselberg, "Auranofin, an Anti-Rheumatic Gold Compound, Modulates Apoptosis by Elevating the Intracellular Calcium Concentration ([Ca2+]i) in MCF-7 Breast Cancer Cells," *Cancers*, vol. 6, no. 4, Art. no. 4, Dec. 2014, doi: 10.3390/cancers6042243.

[19] S. L. Best and P. J. Sadler, "Gold drugs: Mechanism of action and toxicity," *Gold Bull*, vol. 29, no. 3, pp. 87–93, Sep. 1996, doi: 10.1007/BF03214741.

[20] C. Goebel, M. Kubicka-Muranyi, T. Tonn, J. Gonzalez, and E. Gleichmann, "Phagocytes render chemicals immunogenic: oxidation of gold(I) to the T cell-sensitizing gold(III) metabolite generated by mononuclear phagocytes," *Arch Toxicol*, vol. 69, no. 7, pp. 450–459, Jun. 1995, doi: 10.1007/s002040050198.

[21] P. Calamai *et al.*, "Biological properties of two gold(III) complexes: AuCl3 (Hpm) and AuCl2 (pm)," *Journal of Inorganic Biochemistry*, vol. 66, no. 2, Art. no. 2, May 1997, doi: 10.1016/S0162-0134(96)00190-0.

[22] T. Zou, C. T. Lum, C.-N. Lok, J.-J. Zhang, and C.-M. Che, "Chemical biology of anticancer gold(III) and gold(I) complexes," *Chem. Soc. Rev.*, vol. 44, no. 24, pp. 8786–8801, Nov. 2015, doi: 10.1039/C5CS00132C.

[23] M. B. Harbut *et al.*, "Auranofin exerts broad-spectrum bactericidal activities by targeting thiol-redox homeostasis," *Proceedings of the National Academy of Sciences*, vol. 112, no. 14, pp. 4453–4458, Apr. 2015, doi: 10.1073/pnas.1504022112.

[24] E. Marsich *et al.*, "Biological response of hydrogels embedding gold nanoparticles," *Colloids and Surfaces B: Biointerfaces*, vol. 83, no. 2, pp. 331–339, Apr. 2011, doi: 10.1016/j.colsurfb.2010.12.002.

[25] S. Grade, J. Eberhard, J. Jakobi, A. Winkel, M. Stiesch, and S. Barcikowski, "Alloying colloidal silver nanoparticles with gold disproportionally controls antibacterial and toxic effects," *Gold Bull*, vol. 47, no. 1, pp. 83–93, May 2014, doi: 10.1007/s13404-013-0125-6.

[26] D. Mahl *et al.*, "Silver, gold, and alloyed silver–gold nanoparticles: characterization and comparative cell-biologic action," *J Nanopart Res*, vol. 14, no. 10, p. 1153, Sep. 2012, doi: 10.1007/s11051-012-1153-5.

[27] M. A. Khan and M. J. Khan, "Nano-gold displayed anti-inflammatory property via NF-kB pathways by suppressing COX-2 activity," *Artificial Cells, Nanomedicine, and Biotechnology*, vol. 46, no. sup1, pp. 1149–1158, Oct. 2018, doi: 10.1080/21691401.2018.1446968.

[28] T. G. de Carvalho *et al.*, "Spherical neutral gold nanoparticles improve anti-inflammatory response, oxidative stress and fibrosis in alcohol-methamphetamine-induced liver injury in rats," *International Journal of Pharmaceutics*, vol. 548, no. 1, Art. no. 1, Sep. 2018, doi: 10.1016/j.ijpharm.2018.06.008.

[29] K. R. Unrau, "Activity of Nanocrystalline Gold and Silver Alloys," ERA. Accessed: May 27, 2022. [Online]. Available: https://era.library.ualberta.ca/items/e0ac4715-3e00-4814-ab41-19700ce1d802

[30] P. L. Nadworny, "Biological activity of nanostructured silver," ERA. Accessed: Jul. 11, 2022. [Online]. Available: https://era.library.ualberta.ca/items/1d6adcfa-166d-45fb-bddc-37823fbff14d

[31] E. M. Wagner, "Monitoring Gene Expression: Quantitative Real-Time RT-PCR," in *Lipoproteins and Cardiovascular Disease: Methods and Protocols*, L. A. Freeman, Ed., Totowa, NJ: Humana Press, 2013, pp. 19–45. doi: 10.1007/978-1-60327-369-5_2.

[32] G. Tau and P. Rothman, "Biologic functions of the IFN-γ receptors," *Allergy*, vol. 54, no. 12, pp. 1233–1251, Dec. 1999, doi: 10.1034/j.1398-9995.1999.00099.x.

[33] R. M. Friedlander, V. Gagliardini, R. J. Rotello, and J. Yuan, "Functional role of interleukin 1 beta (IL-1 beta) in IL-1 beta-converting enzyme-mediated apoptosis.," *Journal of Experimental Medicine*, vol. 184, no. 2, pp. 717–724, Aug. 1996, doi: 10.1084/jem.184.2.717.

[34] R. Thorpe, "2. - Interleukin-2," in *Cytokines*, A. R. Mire-Sluis and R. Thorpe, Eds., in Handbook of Immunopharmacology. , San Diego: Academic Press, 1998, pp. 19–33. doi: 10.1016/B978-012498340-3/50003-8.

[35] P. Choi and H. Reiser, "IL-4: role in disease and regulation of production," *Clin Exp Immunol*, vol. 113, no. 3, pp. 317–319, Sep. 1998, doi: 10.1046/j.1365-2249.1998.00690.x.

[36] R. J. Simpson, A. Hammacher, D. K. Smith, J. M. Matthews, and L. D. Ward, "Interleukin-6: structure-function relationships.," *Protein Sci*, vol. 6, no. 5, pp. 929–955, May 1997.

[37] M. C. Cesta *et al.*, "The Role of Interleukin-8 in Lung Inflammation and Injury: Implications for the Management of COVID-19 and Hyperinflammatory Acute Respiratory Distress Syndrome," *Front. Pharmacol.*, vol. 12, Jan. 2022, doi: 10.3389/fphar.2021.808797.

[38] S. S. Iyer and G. Cheng, "Role of Interleukin 10 Transcriptional Regulation in Inflammation and Autoimmune Disease," *Crit Rev Immunol*, vol. 32, no. 1, pp. 23–63, 2012.

[39] L. Sun, C. He, L. Nair, J. Yeung, and C. E. Egwuagu, "Interleukin 12 (IL-12) Family Cytokines: Role in Immune Pathogenesis and Treatment of CNS Autoimmune Disease," *Cytokine*, vol. 75, no. 2, pp. 249–255, Oct. 2015, doi: 10.1016/j.cyto.2015.01.030.

[40] H. T. Idriss and J. H. Naismith, "TNFα and the TNF receptor superfamily: Structure-function relationship(s)," *Microscopy Research and Technique*, vol. 50, no. 3, pp. 184–195, 2000, doi: 10.1002/1097-0029(20000801)50:3<184::AID-JEMT2>3.0.CO;2-H.

[41] M. A. Travis and D. Sheppard, "TGF-β Activation and Function in Immunity," *Annu Rev Immunol*, vol. 32, pp. 51–82, 2014, doi: 10.1146/annurev-immunol-032713-120257.

[42] H. Ramirez, S. B. Patel, and I. Pastar, "The Role of TGFβ Signaling in Wound Epithelialization," *Adv Wound Care (New Rochelle)*, vol. 3, no. 7, pp. 482–491, Jul. 2014, doi: 10.1089/wound.2013.0466.

[43] M. Alhajj, M. Zubair, and A. Farhana, "Enzyme Linked Immunosorbent Assay," in *StatPearls*, Treasure Island (FL): StatPearls Publishing, 2024. Accessed: May 07, 2024. [Online]. Available: http://www.ncbi.nlm.nih.gov/books/NBK555922/

[44] T. Shanmugasundaram, M. Radhakrishnan, V. Gopikrishnan, K. Kadirvelu, and R. Balagurunathan, "In vitro antimicrobial and in vivo wound healing effect of actinobacterially synthesised nanoparticles of silver, gold and their alloy," *RSC Advances*, vol. 7, no. 81, pp. 51729–51743, 2017, doi: 10.1039/C7RA08483H.

[45] S. Kumar *et al.*, "Carbohydrate-Coated Gold–Silver Nanoparticles for Efficient Elimination of Multidrug Resistant Bacteria and in Vivo Wound Healing," *ACS Appl. Mater. Interfaces*, vol. 11, no. 46, pp. 42998–43017, Nov. 2019, doi: 10.1021/acsami.9b17086.

[46] Y. Pan *et al.*, "Size-dependent cytotoxicity of gold nanoparticles," *Small*, vol. 3, no. 11, pp. 1941–1949, Nov. 2007, doi: 10.1002/smll.200700378.

Chapter 6 : Properties of Nanocrystalline Silver Solutions

Introduction

In support of the study of viscous silver treatments for silver release in the peritoneal cavity, the properties of aqueous nanocrystalline silver solutions are studied in this chapter. As previously described, nanocrystalline silver solutions made from sputtered films have exceptional wound healing and anti-inflammatory properties as seen in animal models [1]. Previous work has studied the effect of dissolving nanocrystalline silver films in aqueous solutions of varying solvent pH [2]. This work suggested that a higher starting pH of the solvent during dissolution (~pH 9) led to greater anti-inflammatory properties of the resulting solution, and lower starting pH during dissolution (~pH 4-6) results in greater antimicrobial activity[2]. However, the result of changing the final pH of the solution after dissolution has not been studied.

pH is significant in this study for its role in polymer degradation and in interactions with bacteria cells. The extracellular environment has an effect on the intracellular environment of cells, where an increase in extracellular pH also increases the intracellular pH[3]–[5]. Acidic pH appears to stimulate bacterial growth and impair the host inflammatory response[6]. Peritoneal fluid is slightly basic under normal conditions (pH 7.49), but is slightly acidic in infection cases (pH 6.75) [7]. In a more acidic wound environment, there is an increase in TNF-α and NF-κB, which are key inducers of inflammation [8]. However, wound failure is in some cases correlated with alkaline pH [9]. It is also known that the pH of the peritoneal cavity flushing solution, icodextrin, is acidic (between pH 5 and 6). Icodextrin is commonly used in abdominal surgery and is known to be safe, but not necessarily effective, in preventing adhesions[10].

In this chapter, nanocrystalline silver solutions are made from nanocrystalline silver solid films. This chapter details the processes of making and characterizing solutions, including methods for changing the concentration and pH of these solutions. The purpose of these tests is to understand the extent to which pH and concentration will affect the biological properties of the solutions, and to demonstrate methods that can be used in future experiments to make viscous solutions of varying properties.

Methods

Films

Films used in this chapter were made using an in-house sputtering apparatus as described in Chapter 2 using a pure silver target. Based on previous results, all films used in this section have the same parameters: 4.5% oxygen, 1.8A current controlled process, with water injected at a rate of 15 µL/min, indicated as Novel conditions in Chapter 3. The chamber pressure is maintained at 40 mTorr, and the total gas flow rate is a 400 sccm argon-oxygen mixture. These parameters were chosen because results in Chapter 3 showed that this reproducibly creates a dressing with high silver deposition and strong antibacterial properties.

Solutions

As described previously, the standard nanocrystalline silver solutions were created by soaking nanocrystalline silver films in distilled water at a ratio of 2 square inches per 7.5 mL and placed in a 37°C incubator. Solutions were acidified with nitric acid and diluted for analysis by AAS. Ammonia soluble silver was not measured in the solutions but was measured in the films by dissolution in ammonium hydroxide, then diluted for analysis by AAS.

Changes to the standard process were made with the aim of adjusting the concentration of the standard 6 hour solution. This was first attempted by changing the time of dissolution from 6 hours to 2 or 24 hours. Then, different ratios of dressing to water were used. The standard ratio was 2 square inches in 7.5 mL distilled water, which was decreased to 1 square inch or increased to 4 square inches in the same volume in the same size container. The third method was to use standard 6 hour, 2 square inch solutions and dilute with additional water, or concentrate by evaporation.

Solutions of potassium phosphate monobasic and dibasic were used to adjust the pH of the silver solutions. Potassium phosphates were chosen as non-irritating additives that would not produce adverse effects when placed in the abdominal cavity. The pH of solutions was measured using a calibrated Thermo Scientific Orion Dual Star pH/ISE meter. Calibration was performed according to manufacturer protocol. For the potassium phosphate pH adjustments, 1 M solutions of monobasic and dibasic were made, then added in various ratios to the silver solutions and the resulting pH was measured and recorded. No precipitation of silver or other particles was observed, but it is known that phosphate can form complexes with silver in solution.

Log Reductions

The standard procedure for log reductions is described in Chapter 2 but is briefly outlined here. Nanocrystalline silver solutions were made by dissolution of the solid film in water at 37°C. Adjustments for concentration or pH were made after the films were removed. 1.8 mL of the silver solution was combined with 200 μL of an inoculum of *Pseudomonas aeruginosa* or *Staphylococcus aureus* in log phase in tryptic soy broth. This solution was incubated for 1 hour at 37°C. The activity of silver was stopped with STS then diluted, plated, incubated overnight, and counted.

Statistics

Statistics were performed as previously described, with use of unpaired two sample t-tests with Welch's correction and one-way or two-way ANOVA tests with Tukey's post-hoc tests. Analysis was performed using Microsoft Excel or R.

Results

Baseline Properties

The baseline properties of the silver film and solutions are given in Table 6-1 and 6-2. Table 6-1 gives the results of chemical digests for total silver and ammonia soluble silver. Six hour dissolutions were performed on the films and are displayed in Table 6-2. The values obtained aligned with the measurements seen in previous experiments in Chapters 3 and 4.

Table 6-1 Measurements of total silver and ammonia soluble silver for solid nanocrystalline silver films.

Total Silver (mg/in^2)	Ammonia Soluble Silver (mg/in^2)	Percent Ammonia Soluble Silver (%)
4.53 ± 0.27	1.70 ± 0.10	37.7 ± 2.9

Table 6-2 Measurements of silver concentration and pH of nanocrystalline silver solutions.

Silver released in solution (mg/L)	Silver released in solution (mg/in^2)	Percent released (%)	Solution pH
38.9 ± 6.1	0.14 ± 0.02	3.07 ± 0.33	9.67 ± 0.05

Log reductions from the Novel condition solutions are shown here from data collected for Chapter 3. Table 6-3 shows log reductions with a 10% inoculum in silver solution and Table 6-4 shows the log reductions with a 2.5% inoculum in silver solution. While log reductions with the 10% inoculum do not

reach the threshold for bactericidal activity, the 2.5% ratio exceeds a log reduction of three, in most cases reaching a total kill, even with a larger strength of inoculum.

Table 6-3 Log reductions with 10% inoculum in nanocrystalline silver solution.

	S. aureus	P. aeruginosa
Inoculum Size (CFU/mL)	2.33E+07	1.70E+08
Cells in solution (CFU)	4.67E+06	3.40E+07
Novel	0.99±0.11	0.53±0.12

Table 6-4 Log reductions with 2.5% inoculum in nanocrystalline silver solution.

	S. aureus	P. aeruginosa
Inoculum Size (CFU/mL)	5.17E+08	1.00E+10
Cells in solution (CFU)	2.58E+07	5.00E+08
Novel	>5	>6
	4.89	>6
	>5	>6
	>5	>6
	4.89	>6
	>5	>6
Average	>5	>6

Time Effect on Concentration

To increase the concentration of the silver solutions, the amount of time the film was left in solution was increased to 24 hours from the standard 6 hours. For comparison, the time in solution was also decreased to 2 hours. The results of silver release in solution are shown below in Figure 6-1. Data points are an average of three independent solutions, with standard deviation represented as the error bars. There was not a significant difference between 6 and 24 hours of dissolution for release of silver, but there was between 2 and 6 hours. These trends suggest that the amount of silver dissolved from the dressing was

limited after 6 hours. It was unclear at this point if this was due to a saturation of the solution or the strong binding of silver in the film limiting how much was readily released.
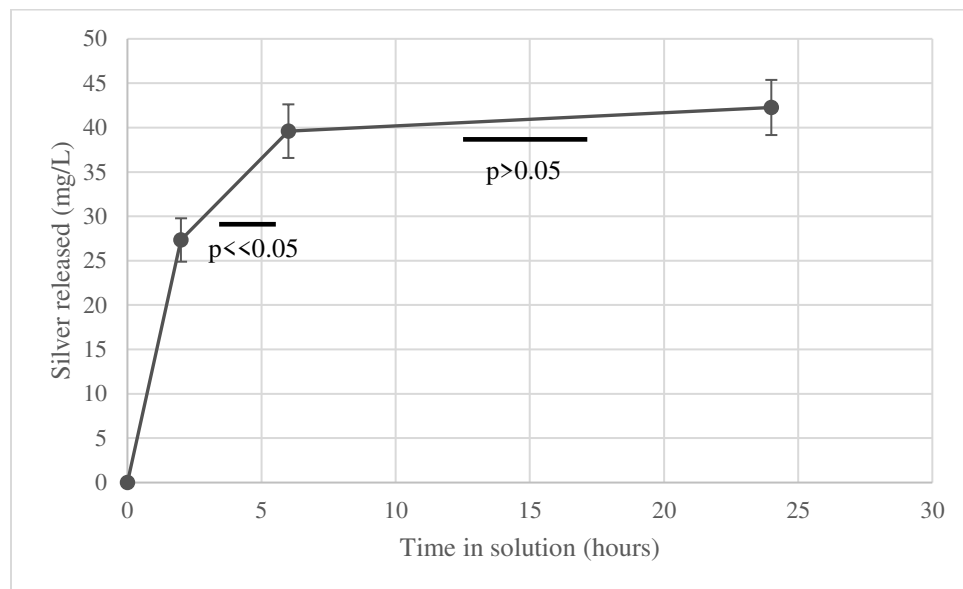
Figure 6-1 Effect of time of dissolution on silver solution concentration, up to 24 hours.

As can be seen in Table 6-5 below, the one-way ANOVA confirmed that time in solution has an effect, but this appears to be carried by the early time comparison from 2 to 6 hours. To assess composition, once the film was removed from solution, an ammonium hydroxide dissolution was carried out to measure ammonia soluble silver. There was not a significant effect of dissolution time on the amount of ammonia soluble silver remaining in the film, suggesting that additional dissolution time does not change the chemical composition of the dressing. The results have limited application because the ammonia soluble silver remaining in some samples is more than the original amount measured prior to dissolution (1.7 mg/in^2). This may be due to measurement error as this phenomenon was not seen in Chapter 3 with similar tests.

Table 6-5 ANOVA p-values values for effect of dissolution time on solution concentration and film composition.

Time in solution (hrs)	Silver concentration in solution (mg/L)	Ammonia soluble silver remaining (mg/in^2)
2	27.3±2.4	1.4±0.1
6	39.6±3.0	2.0±0.5
24	42.3±3.1	1.7±0.4
ANOVA	p=1.5E-03	p=0.33

Size Effect on Concentration

Another potential method to increase the concentration of the silver solutions was to increase the size of film in solution for the standard 6 hour dissolution at 37°C. For comparison, the size of film was also decreased to 1 in^2. The results of silver release in solution using these conditions are shown below in Figure 6-2. The silver concentration does not increase linearly with the size of film, but in a similar trend to time in solution (Figure 6-1), the effect of size decreases with increasing size. There is a significant increase in the silver released from 1 in^2 to 2 in^2, but not from from 2 in^2 to 4 in^2, but this may be partially due to the variability of the measurements in the 4 in^2 group.
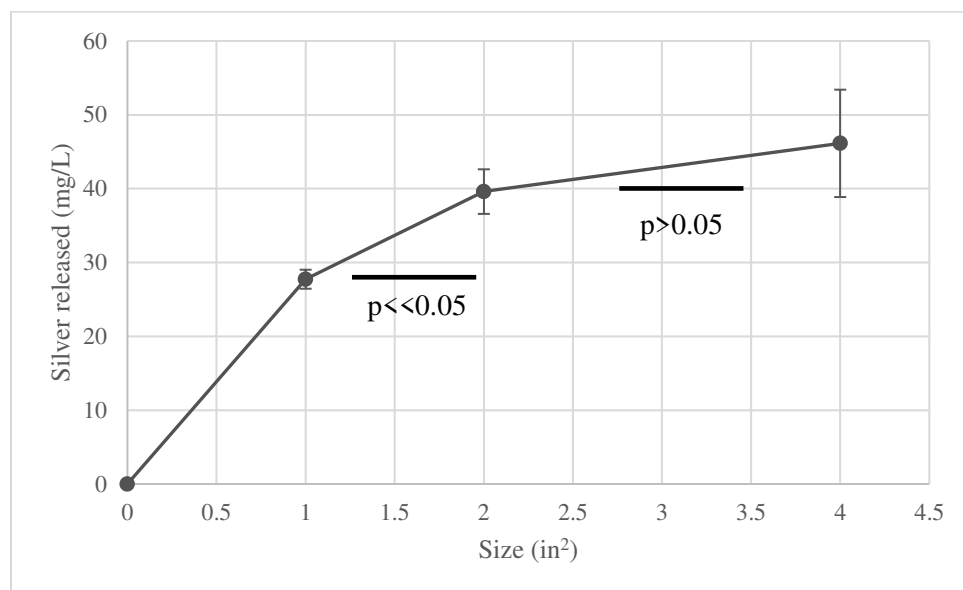
Figure 6-2, Effect of film size on silver solution concentration after 6 hour dissolution.

Table 6-6 shows the one-way ANOVA results from the size-concentration study. With the ANOVA test, the effect of film size was shown to be significant. The total silver released per square inch of dressing decreased with more dressing in the solution, suggesting that the limitations with silver release may be more related to the saturation of the solution than the binding of silver in the film. Silver has limited solubility in water. The ammonia soluble silver in the film was measured after dissolution to assess dressing composition and is also shown in Table 6-6. As in the tests displayed in Table 6-5, the remaining ammonia soluble silver appears to be greater than the initial amount measured previously for some samples.

Table 6-6 Silver solution concentration and ammonia soluble silver remaining in film after dissolution for three film sizes, with p-values from one-way ANOVA.

Film size (in²)	Silver concentration in solution (mg/L)	Ammonia soluble silver remaining (mg/in²)
1	27.7±1.3	2.2±0.2
2	39.6±3.0	2.0±0.5
4	46.1±7.3	1.4±0.4
ANOVA p-value	7.50 E-03	p=0.15

Dilution Effect on Silver Concentration

With the lack of significant results from increasing time and size, concentrations were altered by diluting and evaporating silver solutions. The evaporation of the solution was performed by placing a flask of silver solution on a hot plate and heating to between 60 and 80°C. Evaporation to 44% of the original volume, from 45 mL to 20 mL took approximately 20 minutes. It was observed that while heating took place, the solution changed from colourless to a pink, red, or yellow colour. This phenomenon was also recognized in un-heated solutions that had some exposure to the environment.

Figure 6-3 displays the experimental and predicted concentrations of the diluted and concentrated silver solutions. Experimental data points are an average of three samples, all made from the same initial silver solution. The predicted concentrations are made from calculations based on the concentration of the undiluted (Normal) solution. While the experimental and predicted concentrations for the Dilute solution are similar, there is a wider gap for the Concentrated solution. The experimental value is lower than predicted, which may suggest that the silver is adhering to the side of the glassware.
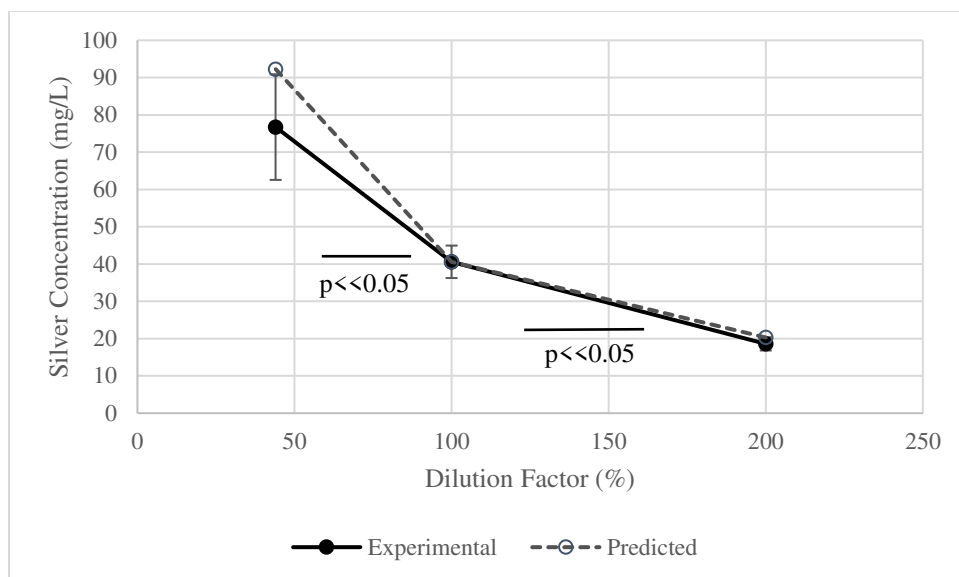
Figure 6-3 Experimental and predicted effects of dilution on solution concentration of silver.

Table 6-7 shows the analysis comparing Concentrated and Dilute solutions to the Normal (undiluted) solution. The one-way ANOVA test confirms that the dilution/concentration has an effect on the resulting concentration. In a t-test comparison, both the Dilute and Concentrated solutions are significantly different than the Normal concentration. Table 6-7 also shows the pH measured for each solution. In a one-way ANOVA test for pH it was shown that changing the concentration does not have a significant effect on pH.

Table 6-7 Silver solution concentration and pH, with p-values of one-way ANOVA and t-tests to Normal concentration.

	Silver concentration (mg/L)	p-value for t-test to normal	pH
Dilute (200% volume)	18.6±1.8	4.33E-06	8.93±0.38
Normal (100% volume)	40.6±4.4	N/A	9.41±0.15
Concentrated (44% volume)	76.7±14.2	4.94E-04	9.15±0.19
ANOVA p-value	2.6 E-08		0.17

Dilution Effect on Log Reductions

A log reduction was performed on the Dilute and Concentrated samples with *S. aureus*. Only one organism was used as it was sufficient to compare the bactericidal activity. *S. aureus* is a good candidate for this as it showed significant differences between Standard and Novel nanocrystalline silver solutions

in Chapter 3. Table 6-8 shows that the log reductions from Normal and Concentrated solutions reached the threshold for bactericidal activity (log reduction >3), but not all Dilute solutions were above this. One-way ANOVA was performed. The results of the ANOVA and t-tests are displayed in Table 6-9 and demonstrate a significant effect of concentration on the bactericidal capacity. All comparisons between groups were statistically significant according to t-tests.

Table 6-8 Log reductions of solutions with varying silver concentrations.

Condition	Log Reduction	Silver Concentration (mg/L)
Dilute	2.96±0.19	19.7±1.6
Normal	4.12±0.33	44.1±2.9
Concentrated	5.71±0.36	72.0±11.7

Table 6-9 ANOVA and t-test p-values for log reductions with Dilute, Concentrated, and unaltered or Normal solutions.

Comparison	p-value
Dilute-Normal	8.25E-03
Normal-Concentrated	4.87E-03
Dilute-Concentrated	3.50E-04
ANOVA	1.15E-04

pH Effect on Log Reductions

The pH of the silver solutions may influence their biological properties. The average pH of the silver solutions was measured to be 9.67 with a standard deviation of 0.05, taken from 12 independently made solutions for 6 hours with two square inches of dressing in 7.5 mL of water, the standard time and concentration ratio used previously.

Potassium phosphate was used to change the pH for additional experiments. 1 molar stock solutions of potassium phosphate monobasic and dibasic were made for this purpose. Varying ratios of potassium phosphate monobasic and dibasic were added to the silver solutions. Table 6-10 shows the results of pH adjustments. These tests used 15 mL silver solutions. pH measurements performed one week later confirmed that the pH of these solutions was stable in this time period. This confirmed an ability to make solutions with a stable pH in the desired range.

Table 6-10 pH values of nanocrystalline silver solutions, with and without potassium phosphate additions.

Initial pH	Potassium Phosphate Monobasic Added (µL)	Potassium Phosphate Dibasic Added (µL)	New pH
9.22	350	300	**6.77**
9.67	500	500	**7.02**
9.69	500	250	**6.55**
9.36	700	50	**5.65**
9.77	750	0	**4.91**
9.71	1000	0	**4.66**
9.64	5000	0	**4.30**

To confirm that there were no interactions between the potassium phosphate solutions and silver, 9 mL of nanocrystalline silver solution was added to 1 mL of potassium phosphate monobasic, dibasic, or 500 µL of each. Theoretically, 0.39 mg was added to the solution as measured from the original solution by AAS. When adding silver to potassium phosphate dibasic, particulates formed, as seen by a cloudy solution. This was not seen for potassium phosphate monobasic, and there was a small amount of cloudiness seen for the 50:50 combination of monobasic and dibasic. Despite variable particulate formation, the measured silver was very similar for all three categories, which was 0.52 mg, with a standard deviation of 0.003 mg.

For log reductions comparing solution pH, three modified silver solutions were made with acidic, neutral and basic pH. The target for the Acidic pH was 5, the Neutral pH target was 7, and the Basic pH target was 9. To adjust the pH, the Acidic pH had 1mL of potassium monobasic added. The Neutral pH had 500 µL of potassium phosphate monobasic and 500 µL of potassium phosphate dibasic added. The Basic pH of approximately pH 9 had 1 mL of water added to 9 mL of silver solution, to keep the silver concentration changes consistent across all samples while preserving the original pH. Two sets of log reductions were performed with both *P. aeruginosa* and *S. aureus*. Each set of experiments was separated by an interval of 8 months.

In the first set of log reductions (Trial 1), shown in Table 6-11, the log reductions shown are between 1.5 and 3.5, with most not reaching the bactericidal threshold. These log reductions are of a lower magnitude than those obtained for the concentration study, in Table 8, but the silver concentrations seen here are lower than for previous log reductions. These results show a trend in log reductions with varying pH. However, these trends are not the same for *P. aeruginosa* and *S. aureus*. The log reduction trends towards increasing with increasing pH for *P. aeruginosa* but decreasing with increasing pH for *S. aureus*. From

one way ANOVA tests displayed in Table 6-12, the effect of pH was significant for both bacteria. The comparisons between groups did not show a significant difference between Basic and Neutral for *P. aeruginosa*, or Acidic and Neutral for *S. aureus*.

Table 6-11 Log reductions of pH-adjusted solutions for *P. aeruginosa* and *S. aureus*, Trial 1.

		P. aeruginosa		*S. aureus*	
Inoculum Size		8.33E+08 CFU/mL		5.00E+08 CFU/mL	
Silver concentration		26.7 mg/L		26.7 mg/L	
	pH	Log reduction	Average	Log reduction	Average
Acidic	4.81	1.89	2.20±0.27	2.79	2.47±0.33
		2.40		2.48	
		2.30		2.13	
Neutral	6.91	3.00	3.01±0.21	2.12	2.37±0.37
		3.22		2.79	
		2.80		2.20	
Basic	9.23	2.74	3.00±0.40	1.44	1.57±0.13
		3.47		1.57	
		2.80		1.70	

Table 6-12 ANOVA and t-test p-values for log reductions with *P. aeruginosa* and *S. aureus* on pH-adjusted solutions, Trial 1.

	P. aeruginosa	*S. aureus*
Acidic-Neutral	0.015	0.74
Neutral-Basic	0.99	0.023
Acidic-Basic	0.045	0.011
p-value ANOVA	0.027	0.018

Another log reduction was performed to confirm the trends seen, several months after the first trial, and the data is shown in Table 6-13. The inoculum strength was higher, as was the concentration of silver used. For *P. aeruginosa*, the trend was the same as before, with greater separation between groups than the first trial. The Acidic silver solution had an unexpectedly small log reduction of less than 1, with increasing log reductions with increasing pH. For *S. aureus*, trends could not be clearly seen because total kills (no surviving colonies) could not be calculated as a discrete number. Two of three Acidic samples

had total kills, compared to one and none for Neutral and Basic. That suggests that there may be a decreasing trend in log reductions with increasing pH, although this cannot be confirmed by the data available. Table 6-14 shows the ANOVA results and t-test p-values for the *P. aeruginosa* samples. All comparisons are significant (p<0.05) with a significant effect for pH, where the pH was much smaller than seen in Trial 1.

Table 6-13 Log reductions of pH-adjusted solutions for *P. aeruginosa* and *S. aureus*, Trial 2.

		P. aeruginosa		*S. aureus*	
Inoculum Size		5.50E+09 CFU/mL		1.17E+09 CFU/mL	
Silver Concentration		89.2 mg/L		78.0 mg/L	
	pH	Log reduction	Average	Log reduction	Average
Acidic	4.81	1.10	0.96±0.13	Total kill (>5.8)	>4
		0.92		Total kill (>5.8)	
		0.86		3.72	
Neutral	6.68	2.54	3.21±0.66	Total kill (>5.8)	>5
		3.24		4.77	
		3.85		5.85	
Basic	8.35	4.44	4.81±0.61	5.54	5.14±0.70
		4.48		4.34	
		5.52		5.54	

Table 6-14 ANOVA and t-test p-values for log reductions with *P. aeruginosa* and *S. aureus* on pH-adjusted solutions, Trial 2.

	p-value, *P. aeruginosa*	p-value, *S. aureus*
Acidic-Neutral	4.32E-03	N/A
Neutral-Basic	3.60E-02	N/A
Acidic-Basic	4.38E-04	N/A
ANOVA	3.16E-04	N/A

Concentration of Repeated Solutions

A 2 in^2 piece of film was placed in 7.5 mL of water, incubated for 6 hours, then removed and placed into a fresh 7.5 mL of water for another 6 hours. The silver concentrations of both solutions were measured by AAS. This test was performed in two independent trials with film samples of the same production batch but performed several months apart. Data is shown in Table 6-15 and Table 6-16. Between the two trials, the silver concentration increased almost four-fold. This is expected to be to the age of the film.

In Trial 1, the second dissolution (Solution 2) generated almost as much silver release as Solution 1, and the difference between the silver concentrations of Solution 1 and Solution 2 was not significant. In Trial 2, the solutions also did not have a significant difference in the silver released.

Table 6-15 Silver concentrations of repeat solutions after 6 hour dissolution, Trial 1.

	Solution silver concentration (mg/L)
Solution 1	26.9±1.2
Solution 2	21.2±3.5
T-test p-value	p=0.092

Table 6-16 Silver concentrations of repeat solutions after 6 hour dissolution, Trial 2.

	Solution silver concentration (mg/L)
Solution 1	83.6±7.9
Solution 2	90.2±16.7
T-test p-value	p=0.66

Figure 6-4 shows the XRD spectra of a sample of Novel film (Original), a sample after soaking in one solution (Solution 1), and a sample after soaking twice (Solution 2). Two sets of Solution 1 and Solution 2 films were analyzed and compared against a spectrum from a film that had not been placed in water. The peak placements are the same for Solution 1 and 2 samples compared to Original. The silver oxide peak, found at approximately 33°2θ, appears to change shape after time in solution, developing a double peak most clearly seen in Solution 2B. This double peak may indicate a new species may have been formed on the surface from the dissolution and atmospheric exposure.
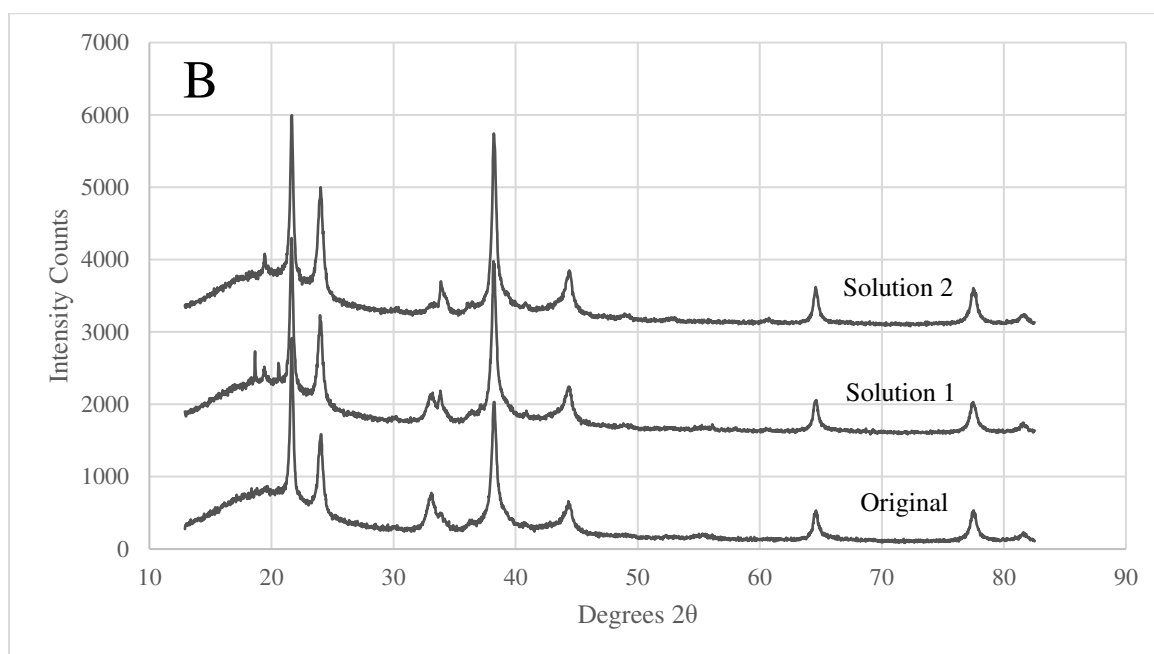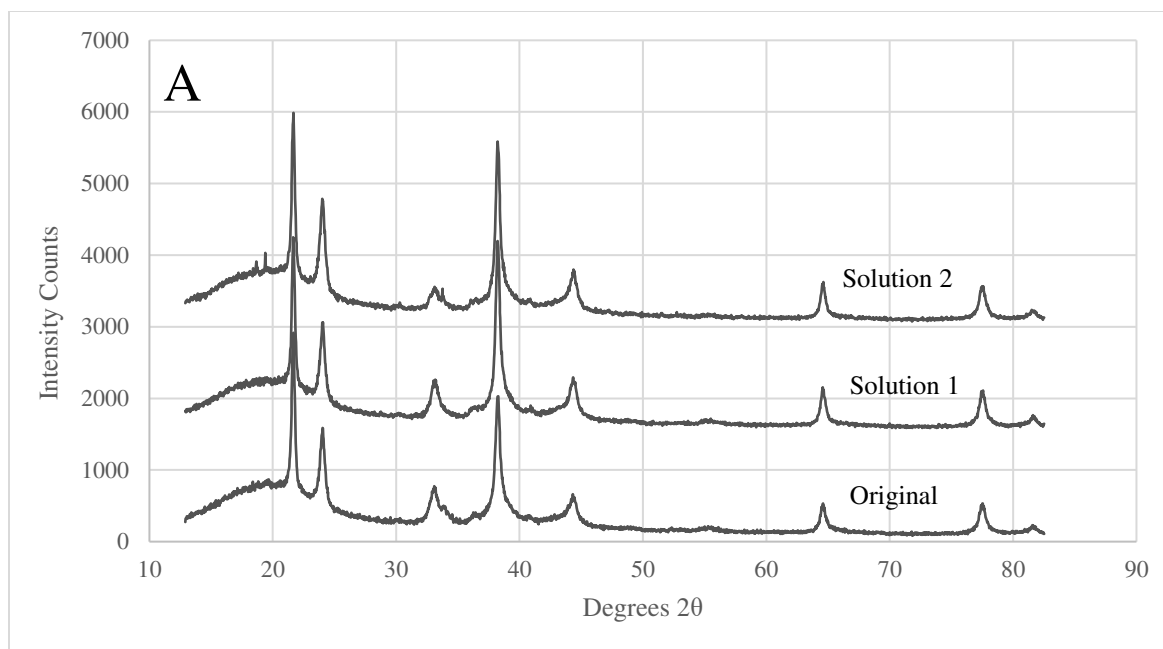
Figure 6-4 XRD spectra of repeat solutions for Trial 2. A and B represent two samples for Solution 1 and Solution 2.

Discussion

The purpose of this chapter was to better understand the properties of nanocrystalline silver solutions and how they may be modified to be used as anti-adhesion treatments. The first goal was to find a reliable method of increasing the concentration of the nanocrystalline silver-based solutions. To assess the impact of time on final solution concentration, the time was increased up to 24 hours. There was not a significant difference in the final concentration beyond 6 hours, suggesting that for practical use, any time between 6 and 24 hours could be appropriate for making the solutions due to the semi-equilibrating nature of the films. Therefore, the time of dressing dissolution was increased to approximately 18 hours (overnight) to facilitate ease of use in future experiments.

Size was also assessed. While the increase from 1 in^2 in 7.5 mL to 2 in^2 did result in significantly more silver, the increase to 4 in^2 was not significant. The suitability of the 7.5 mL to 2 in^2 ratio was confirmed. The observations from the changes in film size and time in solution suggested that there is a plateau of silver release at a certain point, likely due to saturation of silver in solution. In subsequent experiments to make large volumes of solution, without changing the ratio, the silver concentration in solution increased. Without changing any of the film's properties, the primary difference was the type of container used and the freedom of the films to interact with the water rather than adhering to one side of the container. Increasing the size of container increased the silver concentration from 40.4 mg/L to 53.6 mg/L in 15 mL solutions. Shaking further increased the silver extracted from 50.8 mg/L to 61.6 mg/L in 75 mL solutions. Later tests with silver films showed that the solution concentration could be as much as 90 mg/L, refuting the idea that the solution would be saturated at 40 mg/L. It is possible that the increased age of the film may contribute to surface degradation, increasing the release in solution.

In experiments with film time in solution and size, the ammonia soluble silver remaining in the dressing was measured. There was a large amount of variation in the ammonia soluble silver measured. In Chapter 3, there was also a large amount of variation, but all samples had less ammonia soluble silver measured in the film after time in solution than the average pre-solution quantity. Here, some samples had a larger amount of ammonia soluble which could be simply due to measurement variability or could be related to interactions between the water and the film surface during dissolution that forms more ammonia soluble species.

When film size and time did not prove to significantly increase the amount of silver extracted, another method was used to reliably change the silver concentration. Diluting the solution resulted in a predicted decrease in concentration. However, evaporating a portion of the water in the solution did not increase the

concentration as much as predicted, although this may be due to silver adhering to the sides of the container. The colour change to yellow, pink, or red, which was seen especially in heated solutions, is similar to colour changes seen in nanoparticle synthesis. The phenomenon of surface plasmon resonance means that changes in size distribution and shape of particles alter the oscillation of electrons and the wavelength of absorption, changing the perceived colour of the solution[11]. Here, the heating of the solution encouraged interaction of the silver species and agglomeration into nanoparticles, as signalled by the colour shift. However, keeping the solutions at 4°C can stabilize the solutions for storage, causing no further agglomeration or colour change[11]. This would suggest that the biological activity of the Concentrated solutions may have been reduced, as the silver was not in the same form as the Normal or Dilute solutions.

Because pH is known to be relevant for biological effects, the pH was modified, choosing chemicals that are considered to be safe in small quantities as additives to food and non-irritants. Potassium phosphate is a food safe additive. Sodium hydroxide is also commonly used as a pH adjustment agent in consumable products. The silver solutions began at a basic pH, typically between 9 and 9.5. After successfully modifying the pH, log reductions were performed. It was expected from literature that a more acidic pH could increase the antibacterial properties, however this was not consistently the case. This trend was seen for log reductions with *S. aureus*, but the opposite for *P. aeruginosa*. The magnitude of the log reductions was also not consistent across the multiple trials for concentration or pH. There is evidence of the effectiveness of nanocrystalline silver solutions as antibacterial agents, but the extent is variable, and is likely due to concentration of silver, silver species, and inoculum strength. This may be indicative of variable biological properties *in vivo*.

In tests using solutions, in trials that took place several months apart, the silver concentration increased almost four-fold. Most likely this effect is due to the age of the film. Limited data suggests that the amount of ammonia soluble silver may have decreased over time, from 1.7 mg/in^2 initially to 1.4 mg/in^2 three years after production when stored at 4°C. It is possible that oxygen is being released from the films over time which may affect the stability of the silver remaining. More research is needed to study the effect of film aging, particularly its effect on solution release properties.

Conclusion

This chapter highlighted challenges in making aqueous solutions with a consistent concentration or finding a reliable method of altering the concentration or pH. The inconsistency may be related to the dissolution conditions or the age of the dressing. In future tests, given the consistent concentration of

silver despite changing dissolution characteristics means that the dissolution characteristics can be changed for practical constraints without significantly changing the solution properties. Still, log reductions have shown that both pH and silver concentration can have an effect on biological properties. The magnitude of log reductions is highly dependent on the ratio of silver to inoculum and the concentration of the silver solution. The biological effect of pH appears to be dependent on the organism tested. The effect of dressing age on solution properties needs to be explored further, particularly as a greater concentration of silver in solution could be beneficial for medical applications.

References

[1] P. L. Nadworny, J. Wang, E. E. Tredget, and R. E. Burrell, "Anti-inflammatory activity of nanocrystalline silver-derived solutions in porcine contact dermatitis," *J. Inflamm.*, vol. 7, no. 1, Art. no. 1, Feb. 2010, doi: 10.1186/1476-9255-7-13.

[2] P. L. Nadworny, "Biological activity of nanostructured silver," ERA. Accessed: Jul. 11, 2022. [Online]. Available: https://era.library.ualberta.ca/items/1d6adcfa-166d-45fb-bddc-37823fbff14d

[3] M. Kos *et al.*, "Carbon dioxide differentially affects the cytokine release of macrophage subpopulations exclusively via alteration of extracellular pH," *Surg. Endosc. Interv. Tech.*, vol. 20, no. 4, pp. 570–576, Apr. 2006, doi: 10.1007/s00464-004-2175-6.

[4] M. A. West, J. Baker, and J. Bellingham, "Kinetics of Decreased LPS-Stimulated Cytokine Release by Macrophages Exposed to CO2," *J. Surg. Res.*, vol. 63, no. 1, pp. 269–274, Jun. 1996, doi: 10.1006/jsre.1996.0259.

[5] M. A. West, D. J. Hackam, J. Baker, J. L. Rodriguez, J. Bellingham, and O. D. Rotstein, "Mechanism of decreased in vitro murine macrophage cytokine release after exposure to carbon dioxide: relevance to laparoscopic surgery.," *Ann. Surg.*, vol. 226, no. 2, pp. 179–190, Aug. 1997.

[6] M. M. P. J. Reijnen, E. M. Skrabut, V. A. Postma, J. W. Burns, and H. van Goor, "Polyanionic Polysaccharides Reduce Intra-abdominal Adhesion and Abscess Formation in a Rat Peritonitis Model," *J. Surg. Res.*, vol. 101, no. 2, pp. 248–253, Dec. 2001, doi: 10.1006/jsre.2001.6288.

[7] H.-P. Simmen and J. Blaser, "Analysis of pH and pO2 in abscesses, peritoneal fluid, and drainage fluid in the presence or absence of bacterial infection during and after abdominal surgery," *Am. J. Surg.*, vol. 166, no. 1, pp. 24–27, Jul. 1993, doi: 10.1016/S0002-9610(05)80576-8.

[8] A. Bellocq *et al.*, "Low Environmental pH Is Responsible for the Induction of Nitric-oxide Synthase in Macrophages," *J. Biol. Chem.*, vol. 273, no. 9, pp. 5086–5092, Feb. 1998, doi: 10.1074/jbc.273.9.5086.

[9] H. H. Leveen *et al.*, "Chemical acidification of wounds. An adjuvant to healing and the unfavorable action of alkalinity and ammonia.," *Ann. Surg.*, vol. 178, no. 6, pp. 745–753, Dec. 1973.

[10] F. Catena, L. Ansaloni, S. Di Saverio, A. D. Pinna, and On Behalf of the World Society of Emergency Surgery, "P.O.P.A. Study: Prevention of Postoperative Abdominal Adhesions by Icodextrin 4% Solution After Laparotomy for Adhesive Small Bowel Obstruction. A Prospective Randomized Controlled Trial," *J. Gastrointest. Surg.*, vol. 16, no. 2, Art. no. 2, Feb. 2012, doi: 10.1007/s11605-011-1736-y.

[11] P. Mendis, R. M. de Silva, K. M. N. de Silva, L. A. Wijenayaka, K. Jayawardana, and M. Yan, "Nanosilver rainbow: a rapid and facile method to tune different colours of nanosilver through the controlled synthesis of stable spherical silver nanoparticles," *RSC Adv.*, vol. 6, no. 54, pp. 48792–48799, 2016, doi: 10.1039/C6RA08336F.

Chapter 7 : Viscous Polymer Solutions with Nanocrystalline Silver

Introduction

Hyaluronic acid (HA) and carboxymethylcellulose (CMC), as sodium salts, will be used to create viscous solutions. These two polymers were chosen because they are natural, biodegradable, hydrophilic, miscible, and non-toxic[1]. They are commonly used in adhesion applications as a film, solution, gel, or spray, both alone or in combination with other polymers [2], [3], [4], [5], [6], [7], [8], [9]. Figure 7-1 shows a diagram of the structure of these two polysaccharides; A is CMC and B is HA [10]. Both are anionic at physiological pH and form weak binding interactions with each other[10]. The average chain length (n) is 400 units for CMC and 5000 units for HA
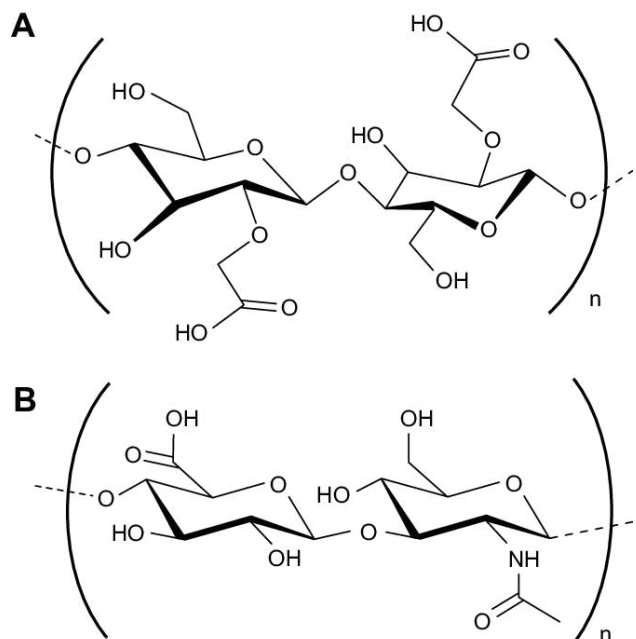
Figure 7-1 Structure of polymers used in this chapter. A is carboxymethyl cellulose (CMC), B is hyaluronic acid (HA)[10].

Hyaluronic acid forms a two-stranded helix with multiple hydrogen bonds per unit[11]. HA has a number of biological functions, depending on the size of the molecules and their location in the body. High molecular weight HA functions as a lubricant and shock absorber, as well as having anti-inflammatory and immunosuppressive capabilities[12]. This further points to its suitability as an adhesion barrier material, given that adhesions are developed through an inflammatory process. However, small fragments with a molecular weight around 1000 Da will induce inflammatory cytokines and stimulate the production

of PAI-1, which could contribute to adhesion formation[12], [13]. Fragments smaller than this stimulate fibroblast production and collagen synthesis, which could either contribute to healing or the strengthening of adhesions[12]. Carboxymethyl cellulose gels were effective against *Pseudomonas aeruginosa* and *Staphylococcus aureus* infected wounds in rats and improved wound healing in part by reducing the inflammation in the wound area [14]. There are a large number of studies describing CMC's incorporation into films, dressings, or hydrogels for a variety of healing applications[1]. CMC treatment accelerated wound healing and collagen deposition in mice[15]. In combination, HA and CMC stimulated repair of human corneal epithelial cells in *in vitro* tests without significant toxic effects, having benefits for cell migration and wound closure [16]. When used as a method of adhesion prevention, HA-CMC did not interfere with healing of intestinal anastomoses, and reduced the incidence and severity of adhesions[5].

One criticism of these materials is that HA normally degrades rapidly and is absorbed quickly without a stabilizing or crosslinking agent[17]. However, higher viscosity solutions, which corresponds to higher molecular weight or higher concentration, have a longer retention in the abdominal cavity[3], [18], [19]. Similarly, the adhesion and abscess prevention capacity of HA or CMC in rats appeared to be dependent on viscosity, not the type of polymer itself[3]. In this experiment, we will be using a range of concentrations for HA and CMC based on literature values and practical constraints [3], [10]. It was found that in combined solutions of HA and CMC, HA contributed most of the viscosity [10]. Still, the low-shear viscosity of combined HA and CMC was increased over the average sum of individual components [10].

When the viscoelastic properties of hyaluronan in aqueous solutions were studied over a pH range, the complex viscosity was relatively stable from a pH of approximately 3 to 11[20]. Additionally, changes to viscoelastic properties that occur outside that pH range are reversible[20]. Another study indicates that degradation of HA occurs outside of pH 4 to 11, starting early after the solution is generated, as studied by molecular weight and radius of gyration. Degradation was higher at pH above this range, compared to pH below the range[21].This indicates that within the pH range studied, our polymer solutions should have a relatively stable viscosity.

There are additional factors that effect polymer degradation. In hydrogel combinations of CMC and HA, a greater concentration ratio of HA increased the degradation time[18]. Even without including CMC, increasing HA concentration in solution increases the time for degradation[4], [22]. A higher viscosity or molecular weight also increased the retention time[18], [22]. Temperature also plays a role, as HA

degraded faster at room temperature than at refrigerator temperature (~4°C) [22]. Temperature increased hydrolysis, causing an earlier onset of mass loss[23].

The key to the adhesion prevention treatments in this study is the incorporation of nanocrystalline silver. When sodium hyaluronate gel was mixed with a growth factor, the combination was better at preventing adhesions than either alone[2]. Depending on the molecular interactions between the solutes, there has been found to be more drug diffusion and release when the drug has less interactions with the surrounding polymer [24]. For gels using poly(lactic-co-glycolic acid) (PLGA), a higher viscosity polymer resulted in a slower drug release[25]. In Pluronic gels, lower concentrations of the polymer degraded faster, resulting in faster drug release[26]. Higher viscosity polymers allow for less drug diffusion [27]. Diffusion also depends on the microenvironment within the gel which is created by the concentration of components [24], [28].

In polymer-water-drug systems, it has been found for a multiple combinations of polymers and drugs that the drug release was independent of the original drug concentration, and was instead diffusion and degradation controlled [28], [29]. The degradation and mass loss of the polymer mostly corresponds to drug release, with only a small amount attributed to drug diffusion [26], [30]. The phases of drug release tend to start with a burst release of drug from the surface of the material, then a slower, constant release followed by a phase of constant, but faster, release, which can also be seen as a secondary burst [23], [30], [31]. The burst release follows first order kinetics, followed by sustained zero order kinetics[30], [31].

It appears that when there is a larger distribution in the molecular weight of the polymer, there is a faster first phase release[30]. Using a model drug agent released from PLGA gels, smaller molecular weight polymer samples had a slower release during the initial burst phase, but released the same total amount after 24 hours as the higher molecular weight samples, and *in vivo*, the release of the low molecular weight polymer was the highest [32]. Another group working with PLGA found that there was a faster release from lower molecular weight polymers and increased burst release[23]. While molecular weight variation is not in the scope of this chapter, this observation points to the differences in drug release that can depend on release conditions, polymer characteristics, and drug type. pH can also change the release profile. The mechanism of release from PLGA microspheres was the same at pH 7.4 and 2.4, but at pH 2.4 the burst release reached a plateau faster [29]. Degradation products can also create acidic microenvironments within the gel that increase degradation[29]. It should be noted that *in vitro* tests do not necessarily reflect the release that will take place *in vivo*, where there is more release *in vivo* [32]. *In vivo,* one research group found that there was no lag phase as was noticed *in vitro,* and there was a faster hydrolysis rate *in vivo*, leading to more degradation and diffusion[27].

The purpose of this chapter is to develop viscous solutions containing nanocrystalline silver. These solutions were characterized through *in vitro* procedures to assess silver release and degradation, as affected by polymer concentration and solution pH.

Methods

Material Fabrication

Nanocrystalline silver films used in this chapter were made using an in-house sputtering apparatus as described in Chapter 2 using a pure silver target. Based on previous results, all dressings used in this section have the same parameters: 4.5% oxygen, 1.8A current, and water injected at a rate of 15 µL/min. The chamber pressure is maintained at 40 mTorr, and the total gas flow rate is a 400 sccm argon-oxygen mixture. These parameters were chosen because Chapter 3 and Chapter 4 show that this reproducibly creates a dressing with high silver deposition and strong antibacterial properties.

Viscous Solutions

Sodium hyaluronate (NaHA or HA) and sodium carboxymethylcellulose (NaCMC or CMC) were purchased from Sigma Aldrich and were used to increase the viscosity of the silver solutions. These two components were mixed into silver solutions in combinations from a range of 0.5% to 2.0% using a magnetic stir bar and plate. Viscosity was measured using a Brookfield cone and plate rheometer (RVDNX CP, CPA-51Z spindle). HA-CMC solutions are shear thinning liquids, so a range of shear rates were used for measurement. The range was from 3.84 to 384 1/s, or 1 to 100 rpm.

Measuring Silver Release and Degradation

After viscous silver solutions were made, 2 mL samples of each solution were loaded into dialysis cassettes (Thermo Scientific, molecular weight cutoff 10 000) in triplicate. These were submerged in 100 mL PBS in 600 mL beakers on an incubator-shaker at 37°C and 60 rpm. At predetermined time intervals, a 5 mL sample of the PBS was removed, acidified with 5 mL nitric acid, and diluted with 10 mL water for AAS analysis for silver quantity. Samples taken were replaced with fresh PBS.

For one series of tests, samples were also taken after 2 and 4 hours for log reductions. 1.8 mL of the PBS was combined with 200 µL of bacterial inoculum for an incubation period of 1 or 3 hours. After the incubation period, the activity of silver was stopped with STS, then diluted, plated, incubated overnight, and counted. The full log reduction procedure can be found in Chapter 2.

At the end of the experiment, a final sample for silver analysis was taken. The viscous solution was removed from the dialysis cassette and the viscosity measured as previously described to estimate the degradation of the polymers during the course of the experiment.

Equation 7-1 Percent viscosity reduction calculation.

$$\frac{\text{Initial viscosity} - \text{Final viscosity}}{\text{Initial viscosity}} \times 100\% = \text{Percent reduction}$$

Measuring and Adjusting pH

The pH of the viscous solutions was adjusted using potassium phosphate and sodium hydroxide. For a 10 mL viscous solution, the appropriate mass of NaHA and NaCMC are added to 9 mL of silver solution, mixed, then 1 mL of additional chemicals are added to obtain the desired pH. The targets for final pH of these solutions were 5, 7, and 9. pH was measured with a calibrated Thermo Scientific Orion Dual Star pH/ISE meter. The degradation of the polymer and release of silver were measured over a three day test in PBS as described previously.

Log Reductions

Viscous solutions are brought into direct contact with a bacterial inoculum (*S. aureus*) to measure the log reduction. To simulate the peritoneal fluid in the peritoneal cavity, the bacterial culture is grown in BCS. A gel was made with 0.5% HA and 0.5% CMC. The concentration of the silver solution was measured with AAS. In a 15 mL conical tube, 2 mL of the gel was added to 7.5 mL BCS. 500 µL of *S. aureus* inoculum in log phase in BCS was added to this tube and mixed by inversion. The solution was incubated in a stationary incubator for two hours at 37°C. After one hour, each tube was inverted to mix the contents. After 2 hours total (one additional hour after mixing), each tube is mixed vigorously and a log reduction performed as previously described.

Statistics

Unpaired two sample t-tests with Welch's correction were used to compare sample groups if only comparisons between two groups were being performed. For comparisons with multiple factors, one-way or two-way ANOVA with Tukey's post-hoc tests were used. The results of Tukey's post-hoc tests can be found in Appendix A. Analysis was performed using Microsoft Excel or R.

Results: Initial Trial

Before beginning studies for silver release and degradation, trial solutions were made and the viscosity measured to inform the conditions to be used. As seen in Figure 7-2, all solutions display shear thinning behaviour, with viscosity decreasing as the shear rate increases. This shear thinning behavior is seen most significantly with the 1% HA 1% CMC gel. This test also demonstrated that there was not a significant difference in viscosity between 0.5% HA:1% CMC and 1% HA: 0.5% CMC.
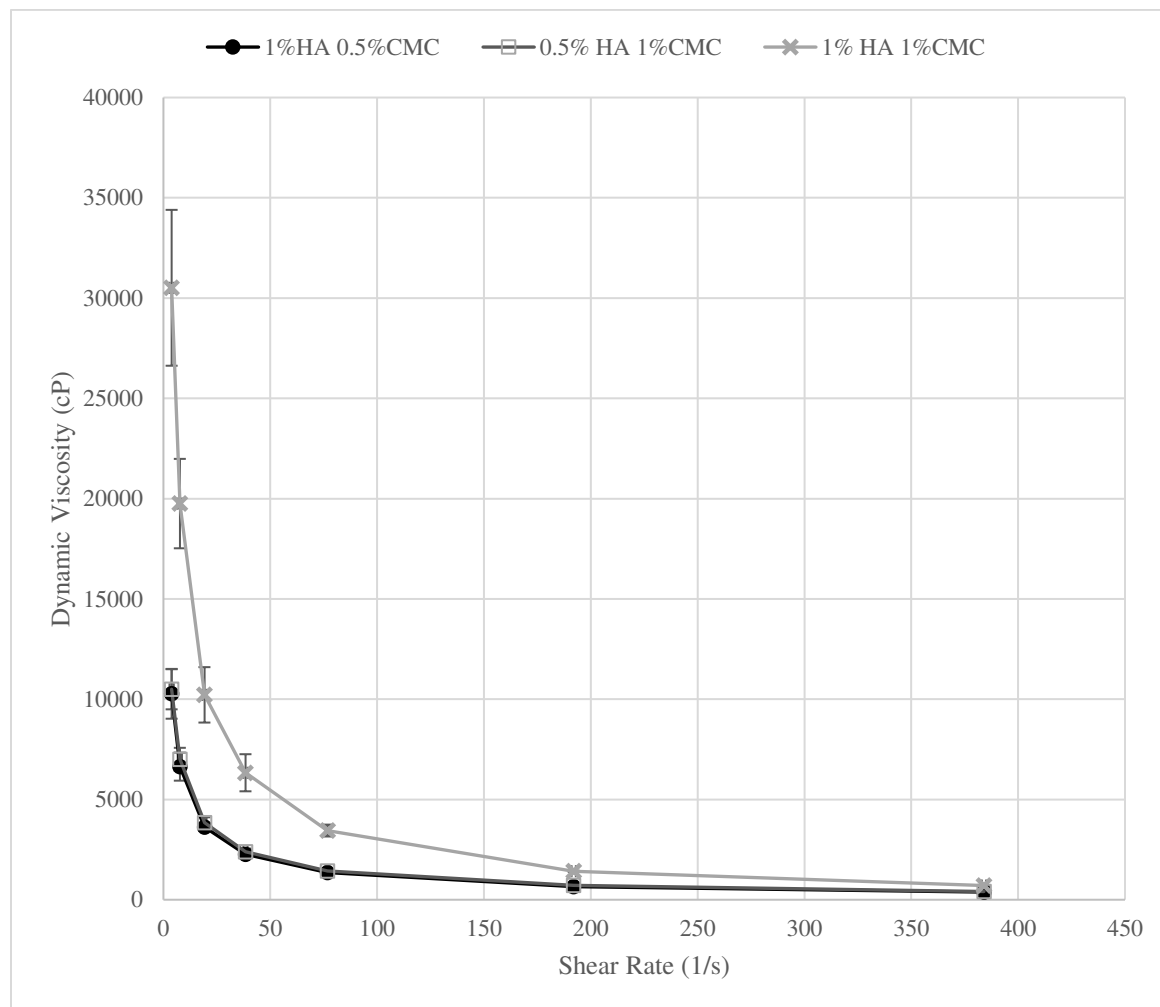
Figure 7-2 Dynamic viscosity of HA-CMC solutions, measured in cP at shear rates from 3.84 to 384 1/s.

Results: Composition Study

Two tests were performed as part of the composition study. Details and abbreviations are given in Table 7-1. The purpose of these tests was to assess the differences in viscosity, silver release, and degradation of

polymer gels with different compositions. All gels were made with an aqueous solution of nanocrystalline silver soaked in distilled water at 37°C for approximately 18 hours.

Table 7-1 Compositions of polymer solutions used for studying the effect of polymer composition, separated into two tests, with abbreviations for each sample group. Concentrations are given in w/v%.

Test 1	Test 2
0.5% HA, 0.5% CMC (Low viscosity, T1L)	0.25% HA, 0.5% CMC (Low viscosity, T2L)
0.5% HA, 1% CMC (Mid viscosity, T1M)	0.5% HA, 0.5% CMC (Mid viscosity, T2M)
0.5% HA, 1% CMC (Control, no silver, T1C)	
1% HA, 1% CMC (High viscosity, T1H)	0.5% HA, 1% CMC (High viscosity, T2H)

Test 1

For Test 1, three gel solutions were made with different polymer concentrations. They are indicated as 'Low viscosity', 'Mid viscosity', and 'High viscosity' or T1L, T1M, and T1H. Triplicate 2 mL samples of each solution were loaded into dialysis cassettes for three days in PBS of pH 7 on an incubator-shaker at 37°C and 60 rpm. The starting concentration of the silver solution was found to be 20 mg/L. The same silver solution was used for each gel in the test. For Test 1, a control solution (T1C) containing 0.5% HA and 1% CMC was made using distilled water without nanocrystalline silver.

At the start of the experiment, the viscosity of each solution was measured three times at each chosen shear rate (representing a range from 1 to 100 rpm) and the averages and standard deviations are shown in Figure 7-3 below. As is expected for a shear thinning fluid, all solutions had an exponential decrease in viscosity with increasing shear rate. For T1M and T1H, the viscosity could not be measured above 20 rpm (76.8 1/s) at the beginning of the experiment because this exceeded the maximum torque for the apparatus.
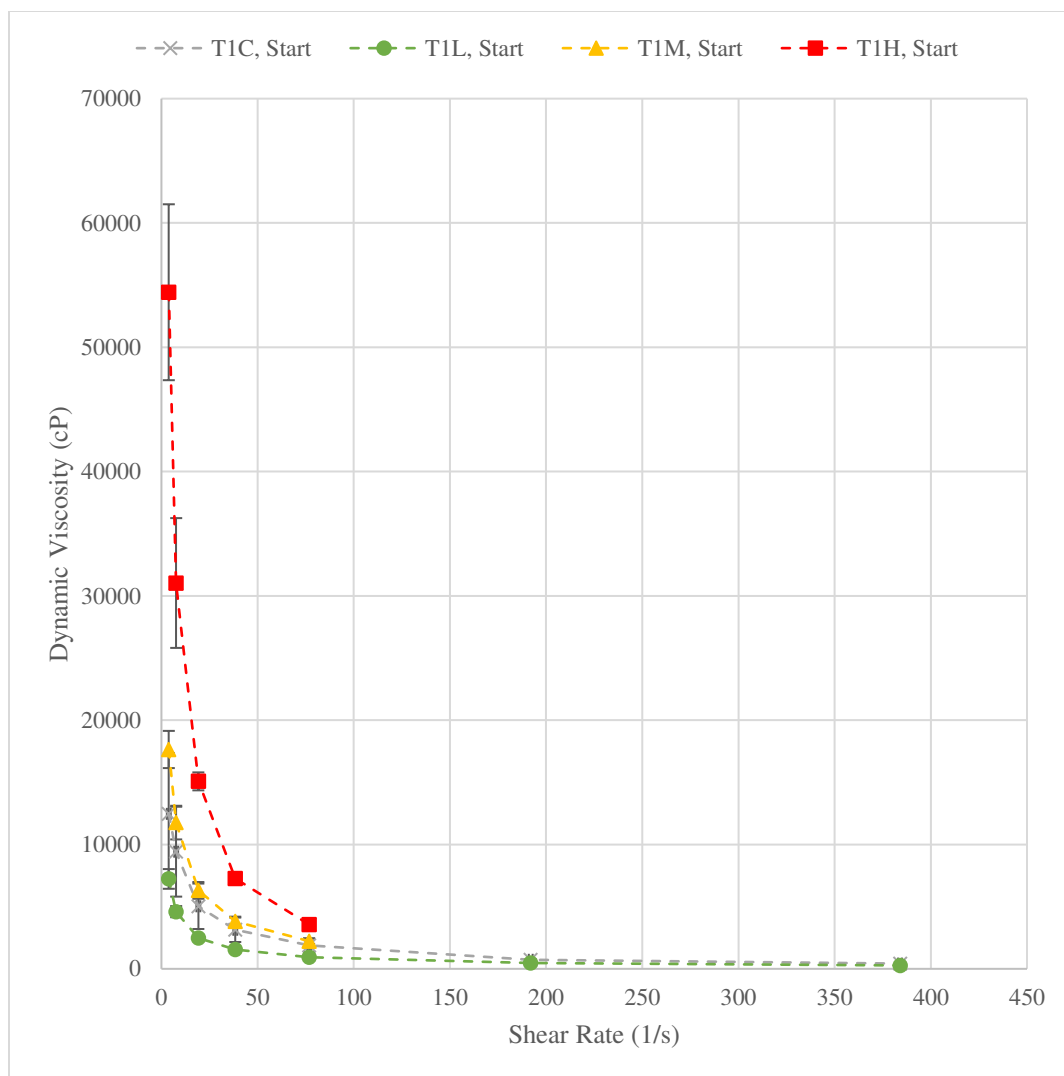
Figure 7-3 Dynamic viscosity curves for samples in Test 1 before degradation.

After three days in PBS, the gels were removed from the dialysis cassettes and the viscosity measured. Figure 7-4 shows the viscosity at each shear rate as an average of three measurements, with standard deviations. The viscosity had clearly decreased from the initial measurements, but the shear thinning properties were still present.
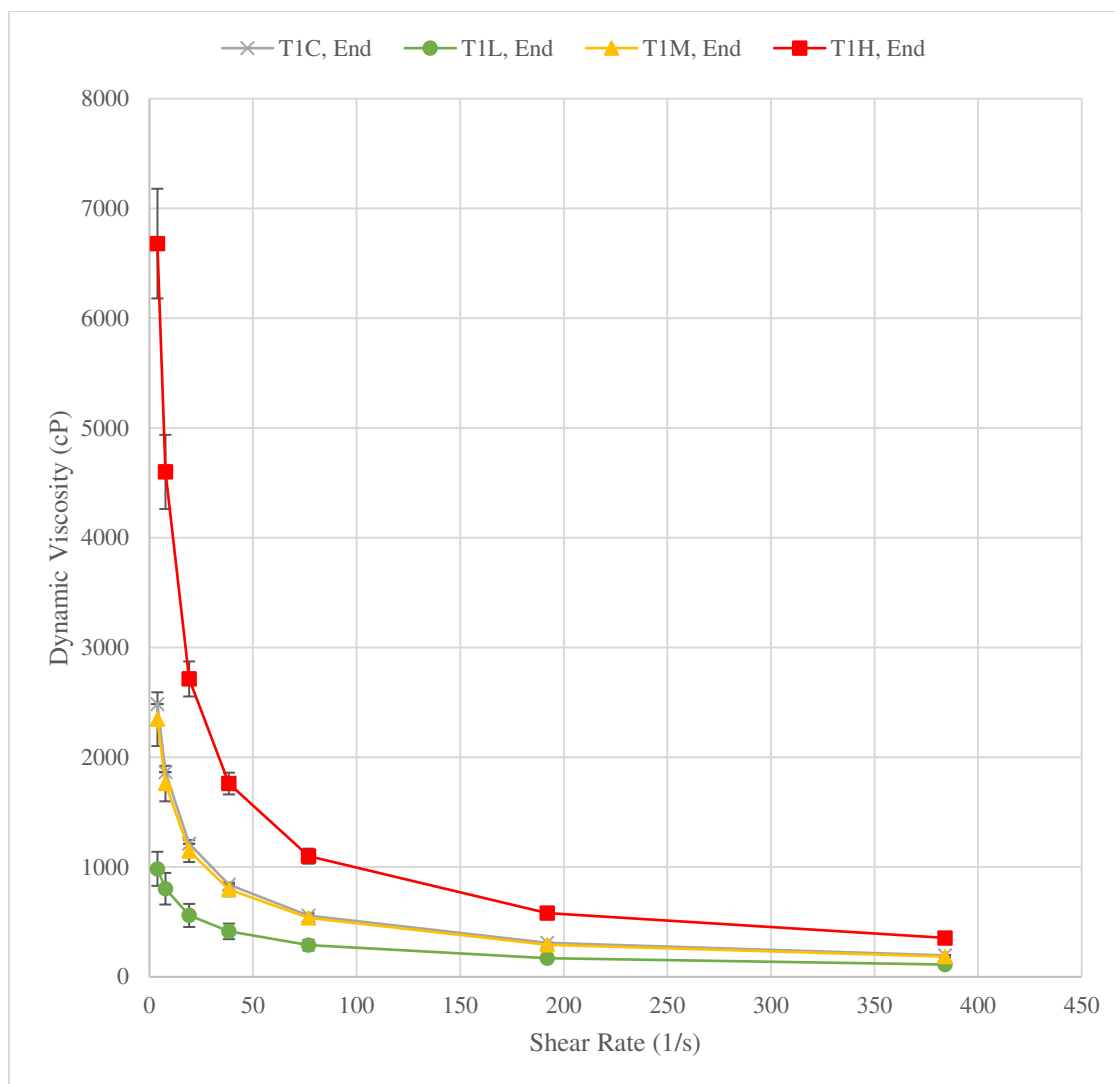
Figure 7-4 Dynamic viscosity curves after 3 days degradation in PBS for samples in Test 1.

ANOVA and post-hoc tests were performed for the three silver solution groups (T1L, T1M, T1H) at 5, 10, and 20 rpm, corresponding to the three middle shear rates tested: 19.2, 38.4, and 76.8 1/s. ANOVA results are shown in Table 7-2. ANOVA results confirm that the experimental methods caused a significant change in viscosity over the three days. It also showed that polymer composition, as expected, had a significant effect on viscosity measured. There is a significant effect for each of these factors ($p \ll 0.05$) and a significant interaction effect ($p \ll 0.05$) at each shear rate. Using Tukey's post hoc tests, there is a significant ($p \ll 0.05$) difference between all composition groups at the beginning of the test. There are also significant differences between the composition groups after the test, except for comparisons between T1M and T1L, and T1M and T1H at 20 rpm. There is not a significant difference for T1L before and after at 20 rpm, but there is a significant difference at 5 and 10 rpm.

Table 7-2 ANOVA p-values for Test 1 for the effects of time and polymer concentration (composition). Grouped by shear rate for viscosity measurement.

Effect	p-value at 5 rpm (19.2 1/s)	p-value at 10 rpm (38.4 1/s)	p-value at 20 rpm (76.8 1/s)
Before-After	3.8E-13	3.91E-13	3.09E-13
Composition	2.97E-12	5.65E-12	6.47E-12
Interaction	1.80E-10	1.73E-09	1.12E-08

At 2 and 4 hours, PBS samples were taken to perform log reductions, indicated as "2 hour release" and "4 hour release" respectively. Data is displayed in Figure 7-5 and Figure 7-6, as an average of three samples, with standard deviation error bars. Samples of T1C were included as controls. There were no significant differences in log reduction between any of the experimental groups or when compared to the control group with no silver. None of the samples reached the level of bactericidal, which is a log reduction of 3, and in many cases, the bacterial load increased. The 4 hour release did not show significant differences in between any groups. The effect of increased incubation time of 1 versus 3 hours was minimal, but still significant for T1L, T1M, and T1H ($p<0.05$).
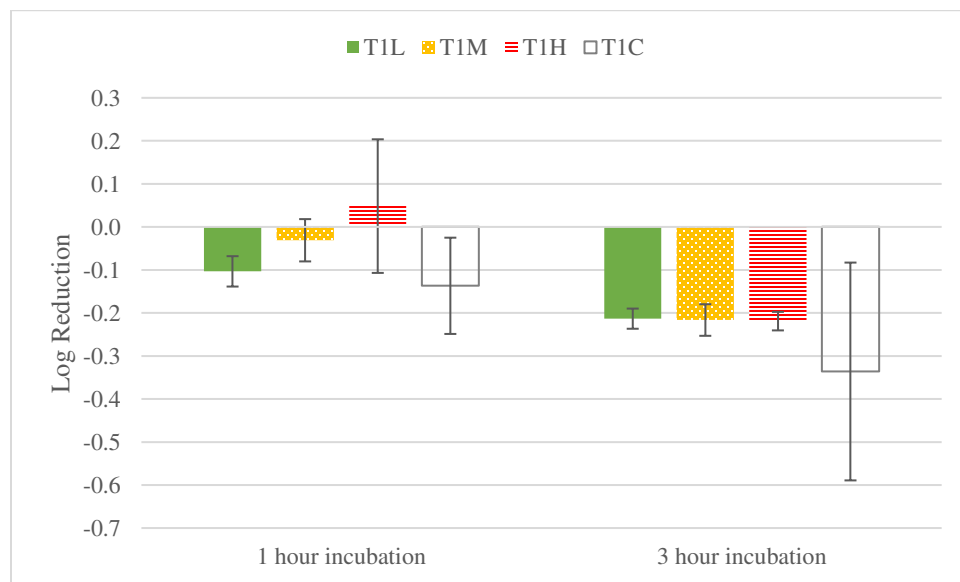
Figure 7-5 Log reductions using *S. aureus* with PBS samples after 2 hours of silver release from polymer samples.
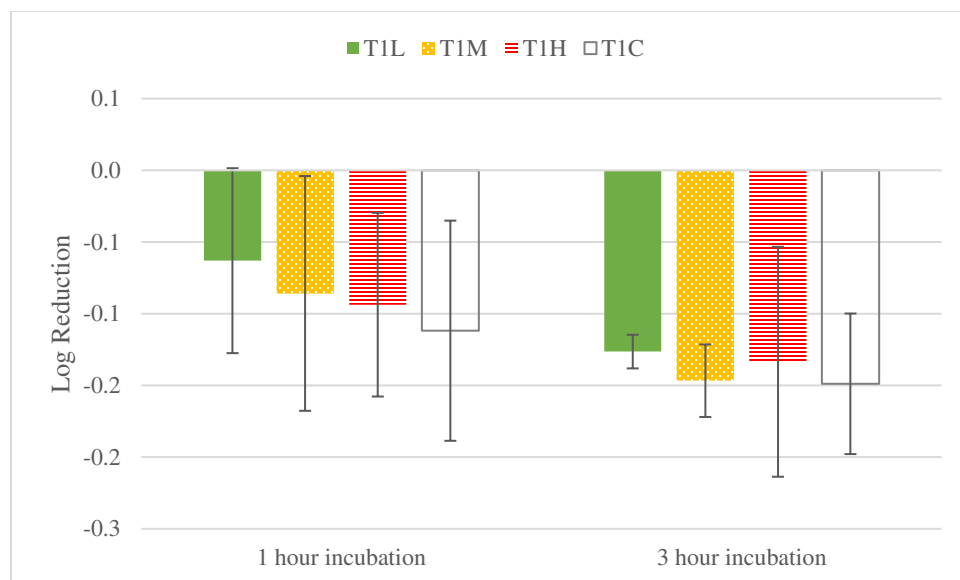
Figure 7-6 Log reductions using *S. aureus* with PBS after 4 hours of silver release from polymer samples.

The average percent change in viscosity over three days at three mid-range shear rates was calculated as a measure of polymer degradation and is displayed in Figure 7-10. The percent change is marginally higher for the lower viscosity samples. In the ANOVA test, displayed in Table 7-3, shear rate and composition effects are both statistically significant. The interaction effect is not significant. From post-hoc tests, most comparisons between groups were not significant. There was not a significant difference in viscosity reduction between the composition groups, despite the significant ANOVA effects.
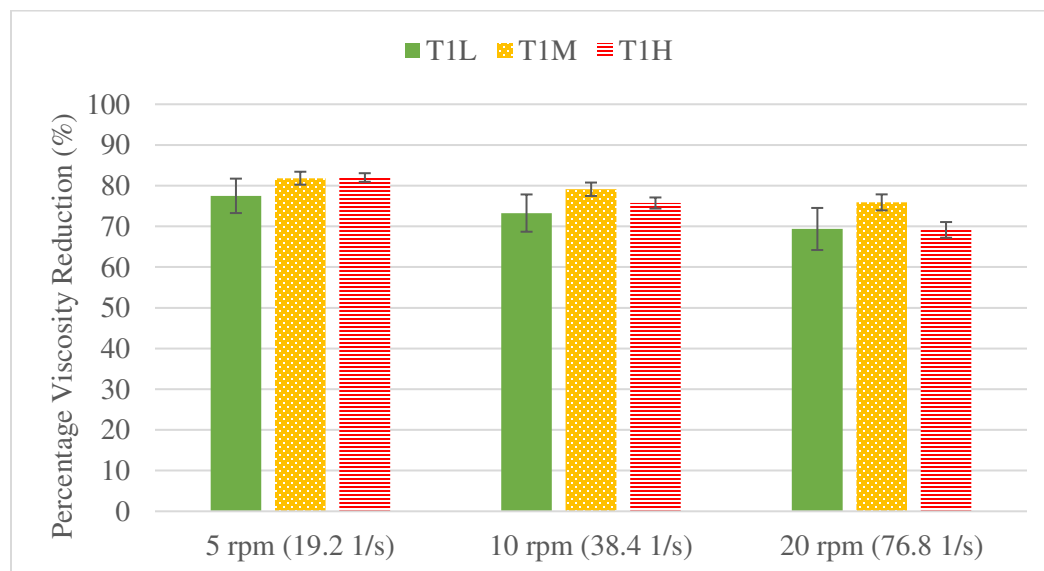
Figure 7-7 Percent viscosity reduction at three shear rates, Test 1.

Table 7-3 ANOVA p-values for effect of shear rate and gel composition on percent viscosity reduction, Test 1.

Effect	p-value
Shear Rate	2.59E-05
Composition	3.54E-03
Interaction	0.41

Test 1 also included a comparison of T1M to T1C to test the effect of silver on the parameters studied. T1C is a control group of the same composition but made using distilled water instead of nanocrystalline silver solution. Figure 7-8 shows the initial viscosities and Figure 7-9 shows the percent viscosity reduction of these two groups. There are no significant differences between T1M and T1C for the initial viscosity or the percent viscosity reduction. While T1C appears to have a lower starting viscosity and percent viscosity reduction than T1M, there was more variability in T1C and the differences were not significant.
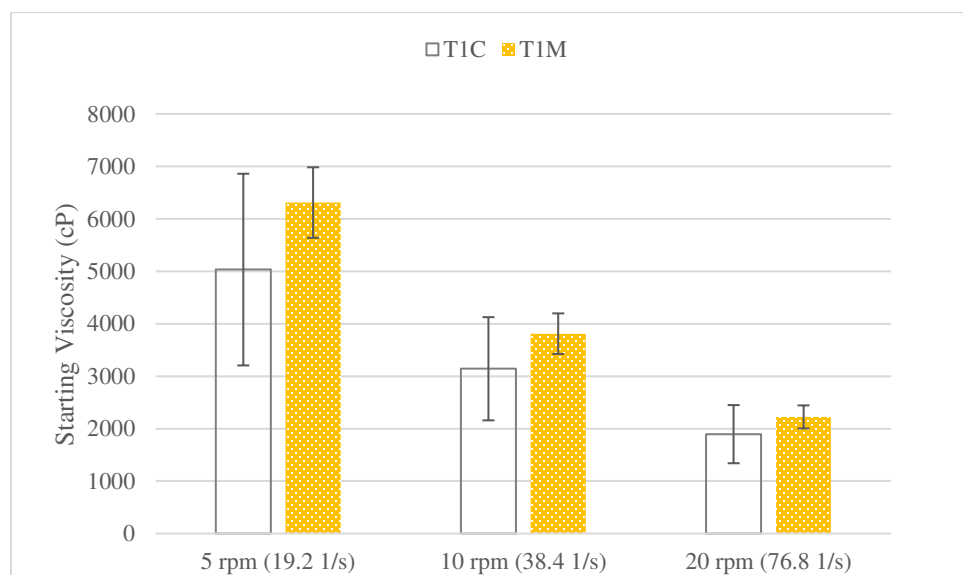
Figure 7-8 Comparison of starting viscosities for control and silver-containing gels with 0.5% HA and 1% CMC.
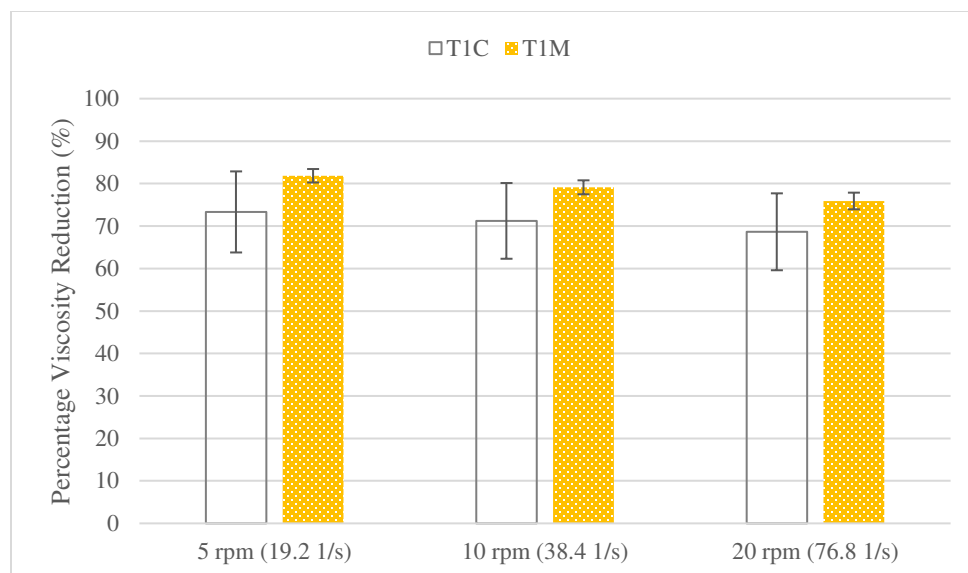
Figure 7-9 Comparison of percent viscosity reduction for control and silver-containing gels with 0.5% HA and 1% CMC.

The silver release profile is shown below in Figure 7-10. At 1, 2, 4, 8, 24, 48, and 72 hours, 5 mL samples are taken of the PBS surrounding each gel sample, acidified, and analyzed for silver concentration by AAS. T1C was sampled at the same intervals, confirming that no silver was measured in that solution. Data points for the three silver-containing gels are shown as an average of three samples with standard deviations as error bars. The trend is the same for all three samples: rapid initial release over the first few hours, then a slowing increase, towards a plateau in silver release from 48 to 72 hours. Approximately 27% of the initial 0.16 mg loaded into each gel was released into the surrounding PBS after 72 hours.
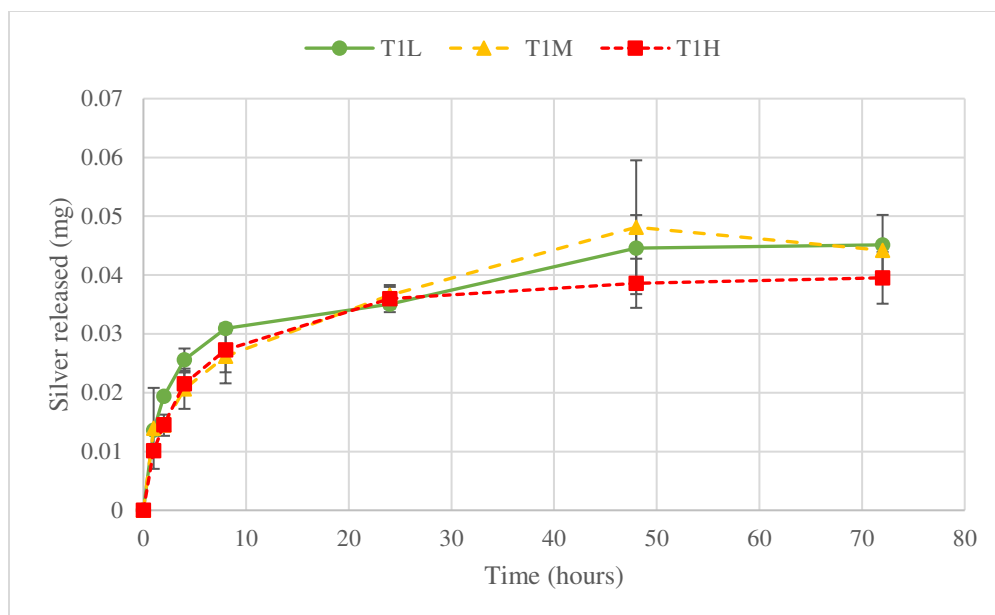
Figure 7-10 Silver released over time from silver-containing polymer gels into 100mL PBS, Test 1.

ANOVA was performed for silver release in Test 1 and the p-values shown in Table 7-4. Both time and composition were identified as significant effects. Within each composition group, release after 4 hours is significantly greater than the release measured at 1 or 2 hours. This is expected due to the shape of the release profile. For T1M samples, the comparison between 4 and 8 hours was significant. Otherwise, significant differences within composition groups were not seen after 4 hours. Between composition groups, there were no significant differences at any time point, despite the significance of the composition effect.

Table 7-4 ANOVA p-values for the effect of time and gel composition on silver release from polymer gels into PBS, Test 1.

Effect	p-value
Time	5.48E-22
Composition	1.35E-02
Interaction	0.48

Test 2

To gather more information on the effect of composition on degradation and release, another composition test was performed. PBS at a pH of 7.4 was used to better reflect the physiological conditions inside the peritoneal cavity. The compositions selected for Test 2 built on experience with Test 1. T2L is 0.25% HA and 0.5% CMC, T2M is 0.5% HA and 0.5% CMC, and T2H is 0.5% HA and 1% CMC. T1H was found to

be too viscous to easily dissolve the polymer by mixing or to be administered to the dialysis cassette through an 18 gauge needle. This limited the practical use of a gel of this viscosity. This composition was removed from study, with the addition of a lower concentration sample, 0.25% HA 0.5% CMC (T2L). Log reductions were not performed for Test 2. The remaining parameters were the same as Test 1 including test duration, range of shear rates, and sampling intervals.

Figure 7-11 shows the starting viscosities for the samples in Test 2. Data points are an average of four measurements of the same gel before loading into dialysis cassettes. The shear thinning trend is present, but the range of viscosities is much smaller than for Test 1. In Test 1, most data points are under 20 000 cP, but in Test 2, most data points fall beneath 6000 cP.
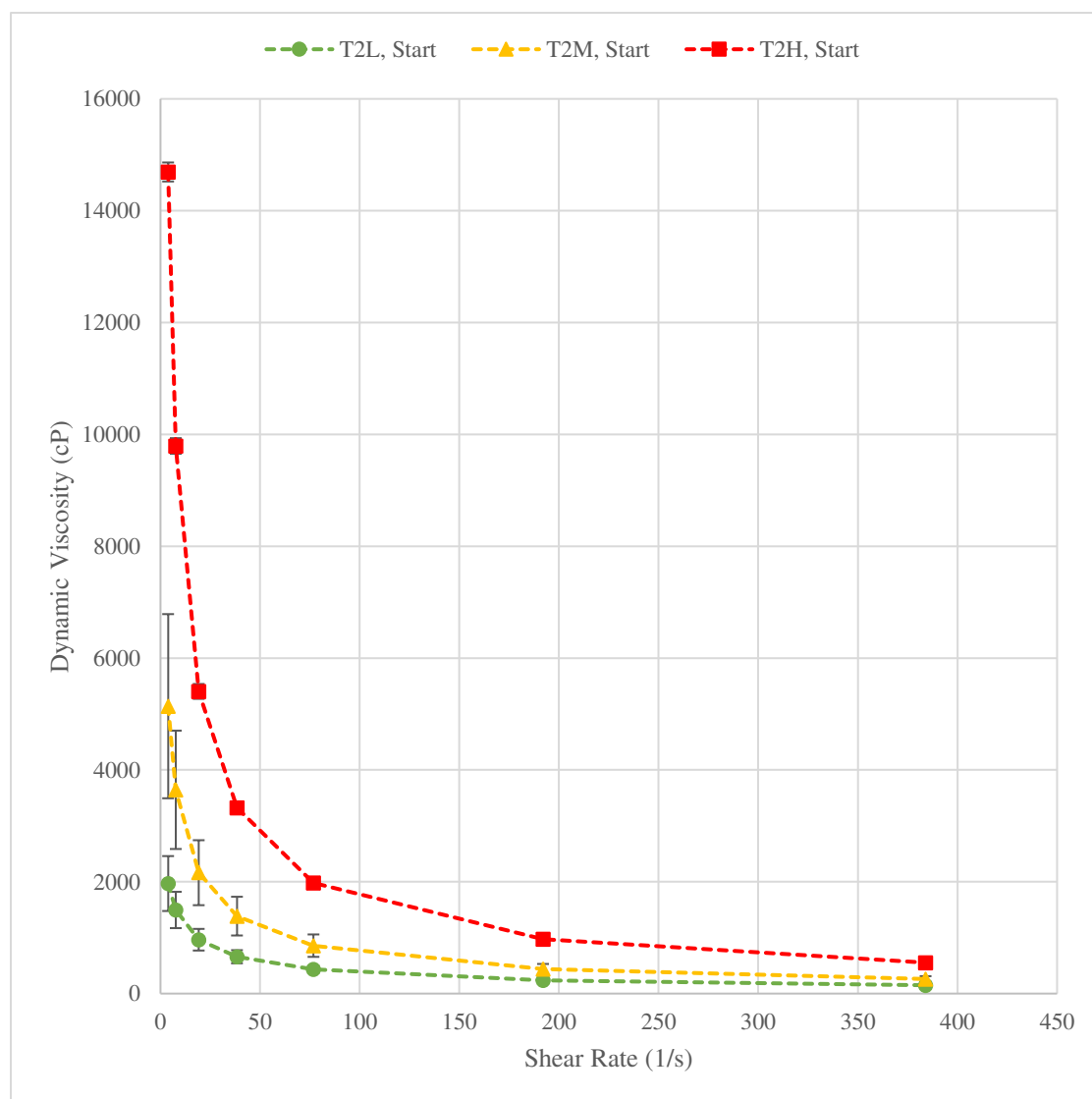
Figure 7-11 Starting viscosity curve for viscous solutions in Test 2.

Figure 7-12 shows the viscosity profile of the gels after three days in PBS. Data points are an average of three samples. The profiles are very similar to the initial viscosity curves, but for lower viscosity. As anticipated, shear thinning behaviour is still seen, although it is less strong after degradation, especially for T2L.
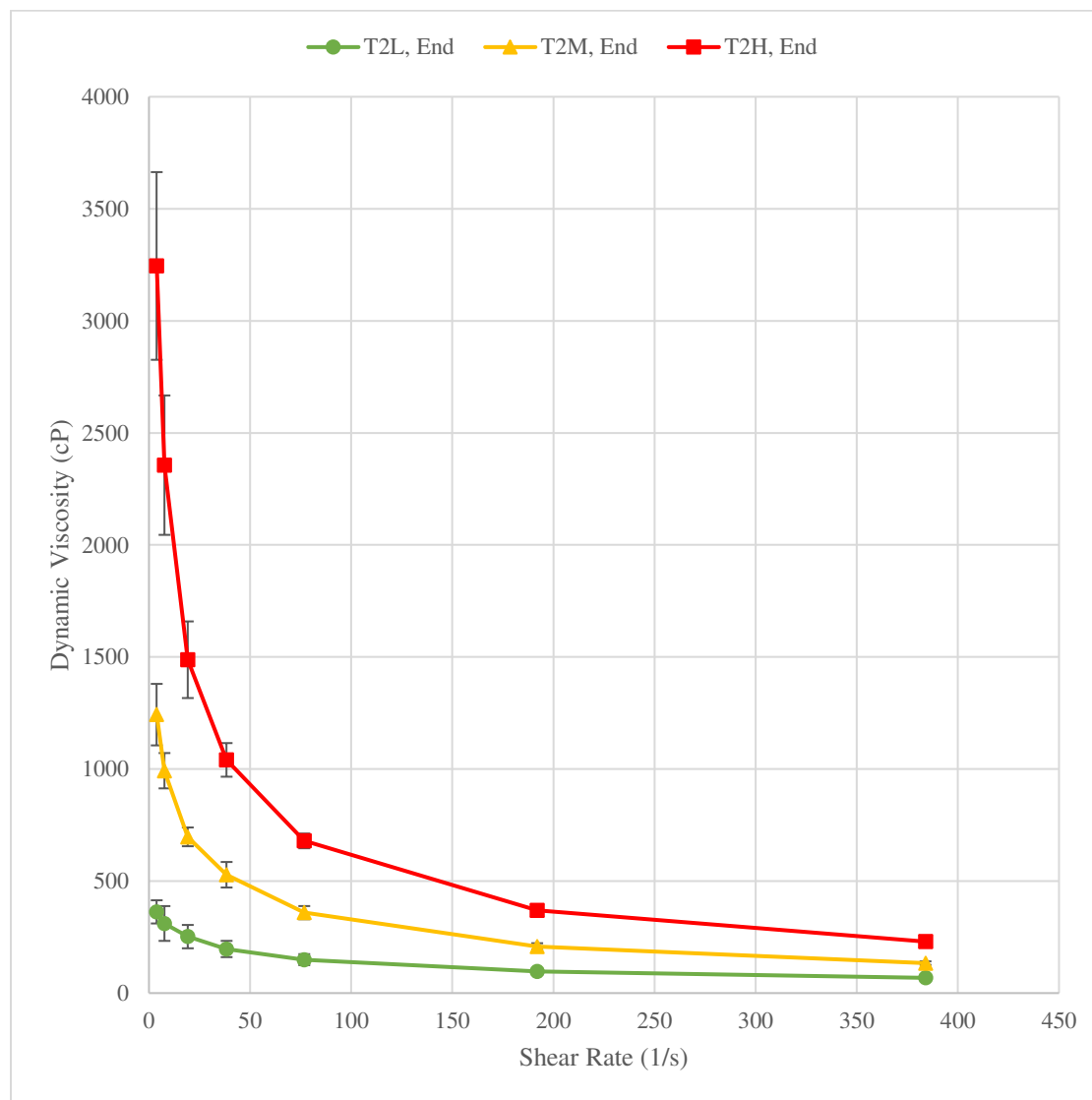
Figure 7-12 Viscosity curves for gel samples after 3 days degradation in PBS for Test 2.

ANOVA results for Test 2 viscosities are displayed in Table 7-5. The trends of significance in ANOVA are the same as for Test 1. There is a significant effect of time and composition individually and a significant interaction effect. Test 2 has significant p-values for all factors, but they are much smaller than those for Test 1. In post-hoc tests, there are fewer significant comparisons than for Test 1. Still, comparisons of before and after within the T2M and T2H groups are significant at all shear rates. For T2L, at 5 rpm, there is not a significant difference between viscosity before and after. At 10 rpm, the difference approaches

significance (p=0.069) and the difference reaches significance at 20 rpm (p=0.049). At the beginning of the test, composition groups were significantly different from each other at all shear rates. In the after groups, T2M and T2H are only significantly different at 20 rpm (p=0.030) but approach significance at 5 rpm and 10 rpm (p=0.083, p=0.051).

Table 7-5 ANOVA p-values for effect of time and composition on viscosity, Test 2, grouped by shear rate.

Effect	p-value at 5 rpm (19.2 1/s)	p-value at 10 rpm (38.4 1/s)	p-value at 20 rpm (76.8 1/s)
Before-After	3.92E-03	2.98E-03	3.16E-03
Composition	1.38E-03	1.08E-03	6.52E-04
Interaction	5.01E-04	3.78E-04	2.29E-04

Figure 7-13 displays the percent viscosity reduction for Test 2 at the three middle shear rates used for analysis. Percent viscosity reduction is overall lower for Test 2 than for Test 1. Percent viscosity reduction does not appear to follow a consistent trend by composition, with the lowest percent viscosity reduction being found for T2M.
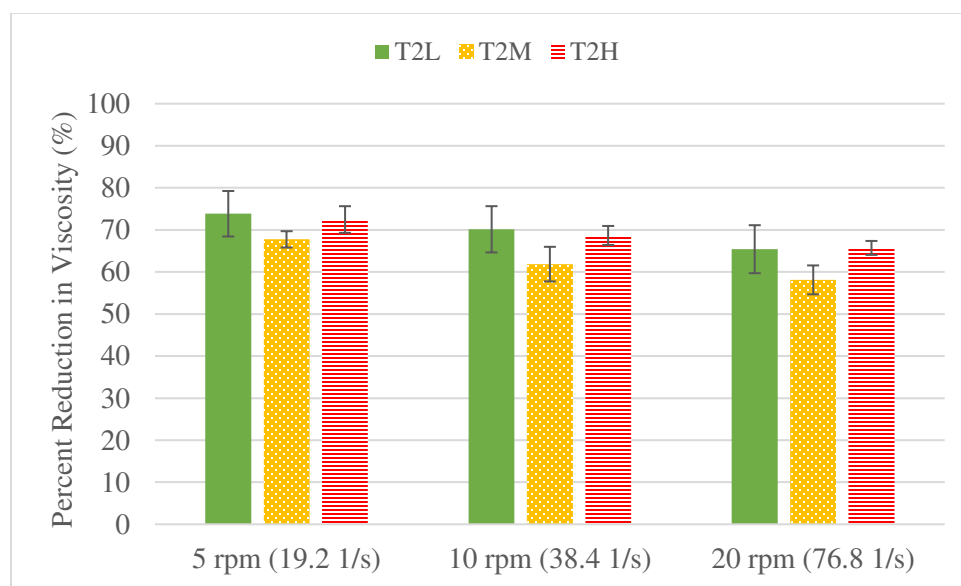
Figure 7-13 Percent viscosity reduction at three shear rates for samples with three polymer concentrations, Test 2.

Table 7-6 shows the ANOVA effects for viscosity reduction. The effect of shear rate is of a lower magnitude than for Test 1, but it is of a similar magnitude of effect for composition and the interaction terms. In Test 2, as for Test 1, both shear rate and composition have a significant effect on the calculated viscosity reduction, but the interaction term is not significant. In post-hoc tests, there was not a significant

difference between composition groups. The p-values for comparisons between T2L and T2H were especially high, demonstrating their similarity.

Table 7-6 ANOVA p-values for effect of shear rate and gel composition on percent viscosity reduction, Test 2.

Effect	p-value
Shear Rate	1.35E-03
Composition	2.09E-03
Interaction	0.97

Figure 7-14 and 7-15 display the silver release for Test 2, with Figure 7-15 focused on the first eight hours. In comparison to Test 1, there is a more noticeable plateau after 8 hours for Test 2, except for the unusually high measurement of T2L at 48 hours, but there is a large amount of variation at that sampling point. The percentage of total silver released after 72 hours was 25% to 28% of the initial 0.12 mg loaded into each gel. At 8 hours, T2L, T2M, and T2H had already released 26.9%, 27.6%, and 26.2% of the total silver loaded.
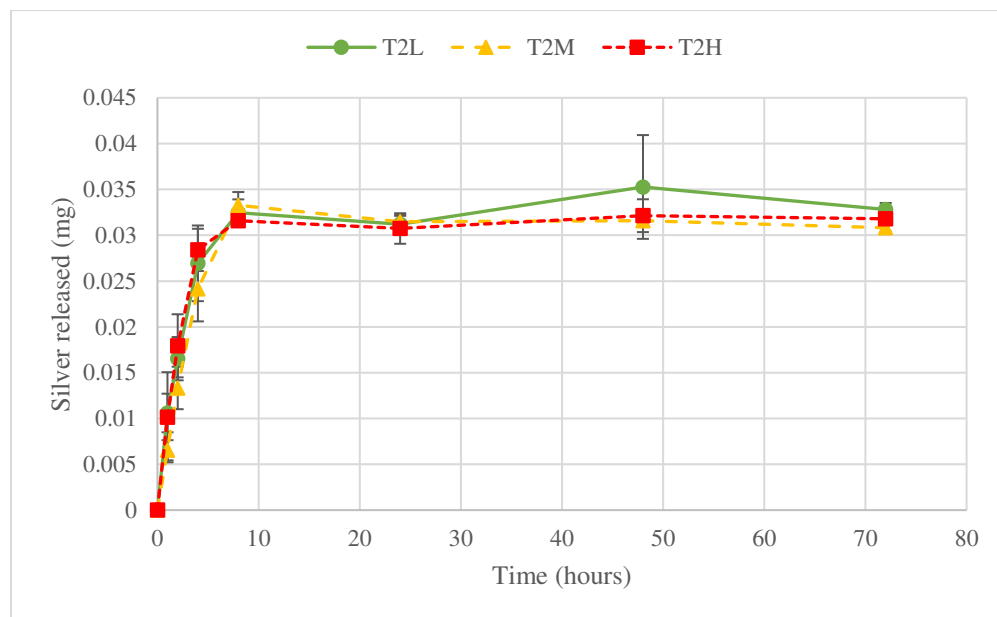
Figure 7-14 Silver released from polymer gels into 100 mL PBS over time, Test 2.
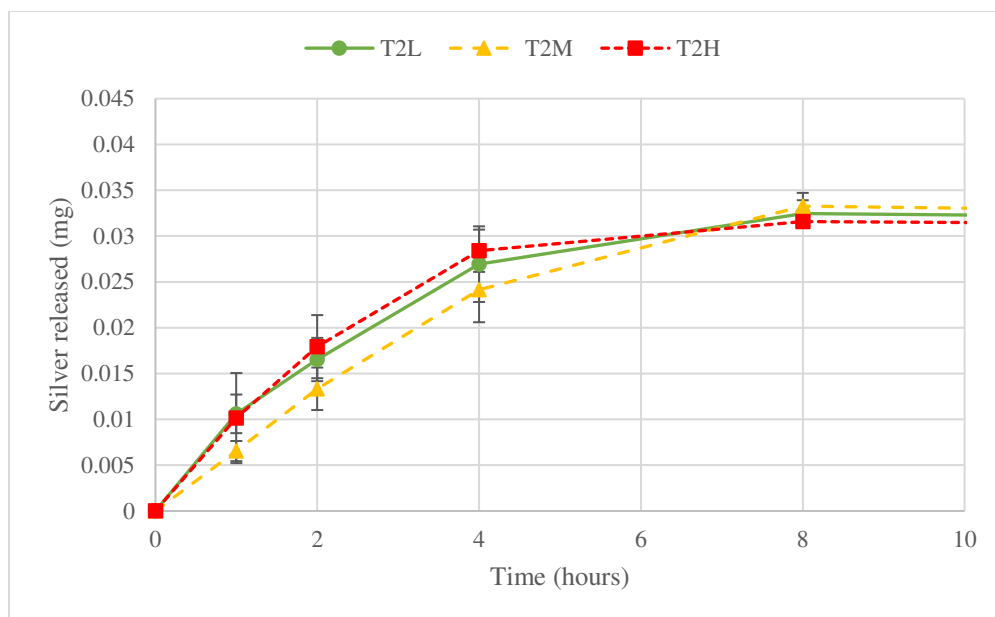
Figure 7-15 Silver released from polymer gels into 100 mL PBS in first eight hours, Test 2.

Table 7-7 shows the ANOVA results. Time is a very significant effect, which is to be expected, but composition is also a significant effect, despite the similarities between groups seen in Figure 7-14. In post-hoc tests, the same comparisons are significant as were for Test 1. Comparisons of silver release within composition groups at 1 and 2 hours were significant compared to measurements at 4 hours and beyond. Other relevant comparisons after 2 hours were not significant for high and low viscosity samples. For T2M samples, the comparison between 4 and 8 hours was significant. It can be seen in Figure 15 that there is a greater increase from 4 to 8 hours for T2M than for any other sample.

Table 7-7 ANOVA p-values for effect of time and gel composition on silver release from polymer gels into PBS, Test 2.

Effect	p-value
Time	3.11E-25
Composition	2.55E-02
Interaction	0.49

Discussion: Composition Study

Table 7-8 displays the starting viscosities at three shear rates for Test 1 and 2 samples. Test 1 provided an initial range of viscosities for study. However, the limitations of high viscosity solutions such as the 1% HA-1% CMC are due to the difficulty of properly mixing and the difficulty in loading and applying the gel. A challenge of measuring a wide range of viscosities, depending on shear rate, was found in using the

same spindle for all samples to ensure consistency. At times, the maximum torque was exceeded, so the measurements at the highest shear rates were less reliable. Viscosities measured at the lowest shear rates had the most variation between samples and measurements. For these reasons, the viscosities at 5 rpm, 10 rpm, and 20 rpm were used for statistical analysis. Test 2 provided a more accurate test environment with the pH of the PBS being increased to 7.4, and the range of compositions was adjusted to what would be more applicable if used as an adhesion treatment.

Table 7-8 Starting viscosities for Test 1 and 2 samples at three shear rates, ordered by polymer concentration.

	Composition	Viscosity at 5 rpm (cP)	Viscosity at 10 rpm (cP)	Viscosity at 20 rpm (cP)
T2L	0.25% HA, 0.5% CMC	963 ± 194	659 ± 117	432 ± 67
T1L	0.5% HA, 0.5% CMC	2485 ± 149	1550 ± 86	941 ± 49
T2M	0.5% HA, 0.5% CMC	2162 ± 581	1385 ± 346	857 ± 200
T1M	0.5% HA, 1% CMC	6310 ± 672	3811 ± 387	2224 ± 220
T2H	0.5% HA, 1% CMC	5403 ± 133	3322 ±77	1981 ± 38
T1H	1% HA, 1% CMC	15080 ± 723	7257 ± 287	3562 ± 59

The viscosity curves seen in this study agree with what is expected from literature. Other work with HA has confirmed that there is no permanent damage to the polymer from the high shear rates of rheometer measurement[33]. However, at high shear rates, with time, the polymer chains will align, causing the viscosity to decrease with constant shear rate [33]. Semi-dilute HA solutions, 0.5 wt% to 1 wt%, display Newtonian behaviour at high shear rates due to the alignment of chains[33]. In this experiment, at high shear rates and low polymer concentrations, the viscosity curve begins to plateau around 200 1/s shear rate. For high molecular weight hyaluronic acid, shear thinning behaviour is seen with an exponential curve, but this is less significant with lower concentrations and lower molecular weights[19]. CMC also has reversible pseudoplastic properties in CMC-only solutions, where increasing shear rates disrupt hydrogen bonding between chains, decreasing the measured viscosity [34]. Low concentrations of CMC (0.2%-0.8%) display two regions of shear thinning, separated by a plateau[35]. It is also seen that CMC solutions above 1% initially display shear thickening behaviour below a critical shear rate of approximately 1 1/s [35]. It is suggested that these low shear rates increase viscosity by entangling polymer coils[35].

No change in viscosity was found after a minimum of two months for CMC solutions of a wide range of concentrations studied by Lopez and Richtering, suggesting good stability for the gels under ambient

conditions [36]. The combined viscosity of CMC with other polymers is greater than the calculated average due to electrostatic interactions between unlike molecules[34]. This was likely seen in this current experiment when combining HA and CMC, particularly for T1H.

The percent viscosity reduction for samples in Test 1 and 2 is shown in Table 7-9. After three days, the viscosity of the gels decreased between 65% and 85%. The lowest viscosity reduction in this study was T2M and this condition also had the lowest percent viscosity reduction in Test 1 (T1L). Test 1 samples had an overall greater percent reduction viscosity compared to samples from Test 2, which is notable given that the Test 1 samples had a higher initial viscosity. Still, considering the results for both tests together, there does not appear to be a trend according to composition. At low concentrations, there are less significant differences before and after, despite a percent viscosity reduction of at least 50%. However, the minimal shear thinning behaviour seen in viscosity curves for lower concentration samples, especially after the experiment, is expected from literature[19].

Table 7-9 Percent viscosity reduction after three days in PBS at three shear rates for Test 1 and 2.

	Composition	Viscosity Reduction, 5 rpm (%)	Viscosity Reduction, 10 rpm (%)	Viscosity Reduction, 20 rpm (%)
T2L	0.25% HA, 0.5% CMC	73.84 ± 5.41	70.14 ± 5.50	65.41 ± 5.70
T1L	0.5% HA, 0.5% CMC	77.50 ± 4.23	73.26 ± 4.58	69.36 ± 5.17
T2M	0.5% HA, 0.5% CMC	67.74 ± 1.94	61.86 ± 4.11	58.11 ± 3.44
T1M	0.5% HA, 1% CMC	81.84 ± 1.59	79.12 ±1.64	75.90 ± 1.96
T2H	0.5% HA, 1% CMC	72.47 ± 3.17	68.67 ± 2.26	65.71 ±1.66
T1H	1% HA, 1% CMC	82.01 ± 1.06	75.74 ± 1.36	69.14 ± 1.93

Table 7-10 shows the percent of initial silver released after 2, 8, and 72 hours. The maximum silver released in Test 1 was up to 0.05 mg, or 30% of loaded silver. Test 2 only saw a maximum release of up to 0.035 mg. It is possible that the increase in pH of the PBS is the reason for the limited release. At 24 hours, for both Test 1 and 2, the amount released was just above 0.03 mg, but in Test 1, the release continued to increase, while it plateaued in Test 2. As can be seen in Figure 7-16, there are limited correlations to be discerned between starting viscosity and percentage of silver released. However, the 1% HA-1% CMC group (T1H), which had an initial viscosity at 10 rpm double the next highest group, appears to have the lowest percent release. It is expected from literature that the higher the starting viscosity, the less degradation and slower silver release[18], [19]. This group, despite a high percent degradation, still had an ending viscosity comparable to the initial viscosities of lower concentration

samples. So, much of the silver is likely still bound to the polymer for all these gels. It is also notable that only polymer segments less than 10kDa could be released from the dialysis cassettes into the surrounding PBS.

Table 7-10 Percent silver release into PBS, sampled at 2, 8, and 72 hours for Test 1 and 2 samples.

	Composition	**Silver Release at 2 hours (%)**	**Silver Release at 8 hours (%)**	**Silver Release at 72 hours (%)**
T2L	0.25% HA, 0.5% CMC	13.70 ± 1.96	26.91 ± 1.20	27. 19 ± 0.60
T1L	0.5% HA, 0.5% CMC	12.06 ± 0.25	19.24 ± 0.50	28.07 ± 3.17
T2M	0.5% HA, 0.5% CMC	11.05 ± 1.92	27.58 ± 1.20	25.53 ± 0.44
T1M	0.5% HA, 1% CMC	9.00 ± 1.12	16.29 ± 2.87	27.49 ± 0.70
T2H	0.5% HA, 1% CMC	14.87 ± 2.85	26.19 ± 0.17	26.36 ± 1.16
T1H	1% HA, 1% CMC	9.04 ± 0.26	16.96 ± 2.36	24.59 ± 2.74
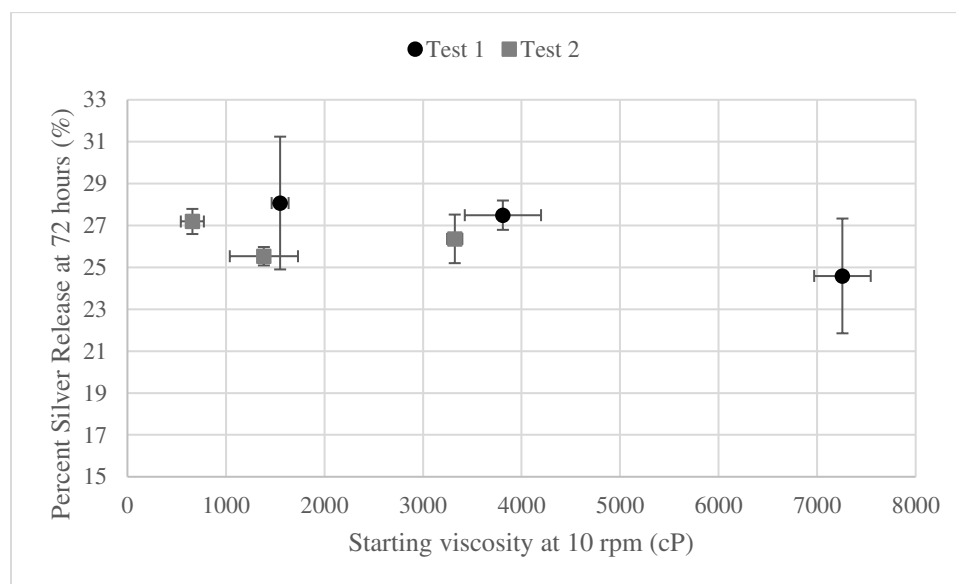
Figure 7-16 Percent silver released after 72 hours plotted against starting viscosity at 10 rpm.

In a 2022 study, modified hyaluronic acid and methylcellulose hydrogels were studied in *in vitro* and *in vivo* studies[37]. In a pH 7.4 environment, the release profile was similar to what was seen in the present study, achieving up to 42% release after approximately 3 days with a 10 wt% gel[37]. The hydrogels did not reach a log reduction of 1 with *S. aureus* or *E. coli*, which agrees with the results seen here[37]. In a 2008 release kinetics study, 4-20 mg/mL of dexamethasone was mixed into 1% or 2.3% sodium hyaluronate[38]. No change in viscosity was observed with the inclusion of the drug[38]. Release into PBS or BSS (balanced salt solution) saw comparable kinetics for drug release [38]. This study saw a

release profile characterized by a moderate burst release initially, where 50% of the drug was released in the first six hours, then release slowed after 24 hours, with steady state reached after 48 hours[38]. Over three days, 90% of the dexamethasone was retrieved, with a full replacement of the surrounding fluid[38]. The volume of surrounding fluid apparently did not affect the release rate, with the standard fluid volume being 0.2 mL with 0.2 mL of gel[38]. The kinetic profile of the two concentrations of HA were nearly identical[38].

The release profiles seen in literature are similar what is seen in the present study, however the percentage of total silver released is lower than may be expected, and there is a difference in percentage composition and release conditions[23], [30], [31]. In regard to the low percentage of silver released, it is possible that not all the silver thought to be added was actually added. Silver might have adhered to the beaker in which it was mixed, or the polymers may have swelled such that less than 2 mL of the initial silver solution is included in 2 mL of the final gel. There is no direct evidence seen for these confounding variables, so it may be suggested that the cause of low percentage silver release is strong binding of the silver to the polymer, even as it became fragmented, particularly given that only fragments below 10 kDa could be released from the dialysis cassette.

The inclusion of silver in the gel does not appear to have had an effect on the viscosity or degradation in this experiment. In some cases, the inclusion of drugs or other compounds can increase or decrease the viscosity depending whether it disrupts or supports hydrogen bonding, but nanocrystalline silver does not participate in hydrogen bonding, and should therefore not have an effect [11]. While there were no significant differences in initial viscosity or degradation rate, there were trends suggesting that the control gel may have a lower viscosity and slower degradation. The significance is affected by the increased variability in the control sample. However, if this is true, then the inclusion of silver may increase initial viscosity and degradation over time, but more data would be needed to support this claim.

In the log reductions performed, the silver released from the gels after 2 hours and 4 hours was insufficient to see significant bactericidal capacity, compared to a control gel containing no silver. The amount of silver released into the PBS by this point was measured between 0.02 and 0.03 mg. This can be compared to log reductions in previous chapters with nanocrystalline silver solutions containing a total of 0.08 mg of silver, where log reductions could reach the minimum of 3, especially when given a longer incubation time with the inoculum. It is expected that the reaction of silver with the chloride ions in PBS may be inactivating some of its effects. Knowing that PBS, or other environments high in chloride ions, can limit the effectiveness of silver means that not all the silver released will be biologically active silver.

Table 7-11 shows the results of adding a silver containing gel (0.5% HA, 0.5% CMC) directly to a bacterial inoculum in BCS for two hours to see if the low log reductions seen previously are due to limited contact of silver with bacteria because of release. The log reductions in Table 7-11 are still low in magnitude but are higher than log reductions for samples from silver released in PBS, shown in Figures 7-5 and 7-6. Even when mixed, most of the silver is inside the gel instead of on the surface, which would still limit the contact of silver with the bacteria.

Table 7-11 Log reductions with viscous silver solution, concentration 0.5% HA and 0.5% CMC w/v in aqueous nanocrystalline silver solution.

	P. aeruginosa		*S. aureus*	
Inoculum Size	2.08E+08		1.48E+04	
Silver Concentration	73.2 mg/L		73.2 mg/L	
	Log reduction	Average	Log reduction	Average
	0.64	0.58±0.06	0.65	0.38±0.20
	0.62		0.17	
	0.51		0.35	
	0.57		0.35	

Results: pH Study

The polymer composition used here for degradation and release tests is 0.5% HA and 0.5% CMC. Solutions are made with 90% aqueous nanocrystalline silver solution and 10% pH-altering additive by volume. Table 7-12 shows the results of additives on pH from experiments used to choose the right combination for use in degradation and release experiments. 'Unaltered' uses 10% distilled water instead of another additive. The conditions used for Tests 3 and 4 and the resulting pH are also shown in Table 7-12. The goal of Test 4 was to have an acidic, neutral, and basic solution, although the pH of the unaltered gel was higher than anticipated (pH 7.66) and the pH of the 1E-04 mol/L NaOH gel was lower than expected (pH 8.02). `

Table 7-12 Description of pH modifications and resulting pH, including samples used for Tests 3 and 4.

Composition	Description	pH	Test Use
0.5% HA, 1% CMC	Unaltered	5.25	
0.5% HA, 1% CMC	10% potassium phosphate monobasic	7.20	
0.5% HA, 1% CMC	10% potassium phosphate dibasic	8.09	
0.5% HA, 0.5% CMC	10% potassium phosphate monobasic	5.01	
0.5% HA, 0.5% CMC	Unaltered	6.08	
0.5% HA, 0.5% CMC	5E-05 mol/L sodium hydroxide	6.29	
0.5% HA, 0.5% CMC	2E-04 mol/L sodium hydroxide	9.85	
0.5% HA, 0.5% CMC	10% potassium phosphate monobasic	5.01	Test 3
0.5% HA, 0.5% CMC	1E-04 mol/L sodium hydroxide	8.75	Test 3
0.5% HA, 0.5% CMC	10% potassium phosphate monobasic	4.9	
0.5% HA, 0.5% CMC	Unaltered	6.8	
0.5% HA, 0.5% CMC	1E-04 mol/L sodium hydroxide	7.6	
0.5% HA, 0.5% CMC	10% potassium phosphate monobasic	5.02	Test 4
0.5% HA, 0.5% CMC	Unaltered	7.66	Test 4
0.5% HA, 0.5% CMC	1E-04 mol/L sodium hydroxide	8.02	Test 4

Test 3

Figure 7-17 displays the initial viscosity curves for Test 3. Each data point represents only one measurement because of available gel for sampling, so statistical comparisons could not be performed. The starting viscosity is in a range anticipated from measurements made of T1L and T2M, which have the same composition. Initially, it appears that the acidic gel (pH 5.01) has a higher starting viscosity than the basic gel (pH 8.75).
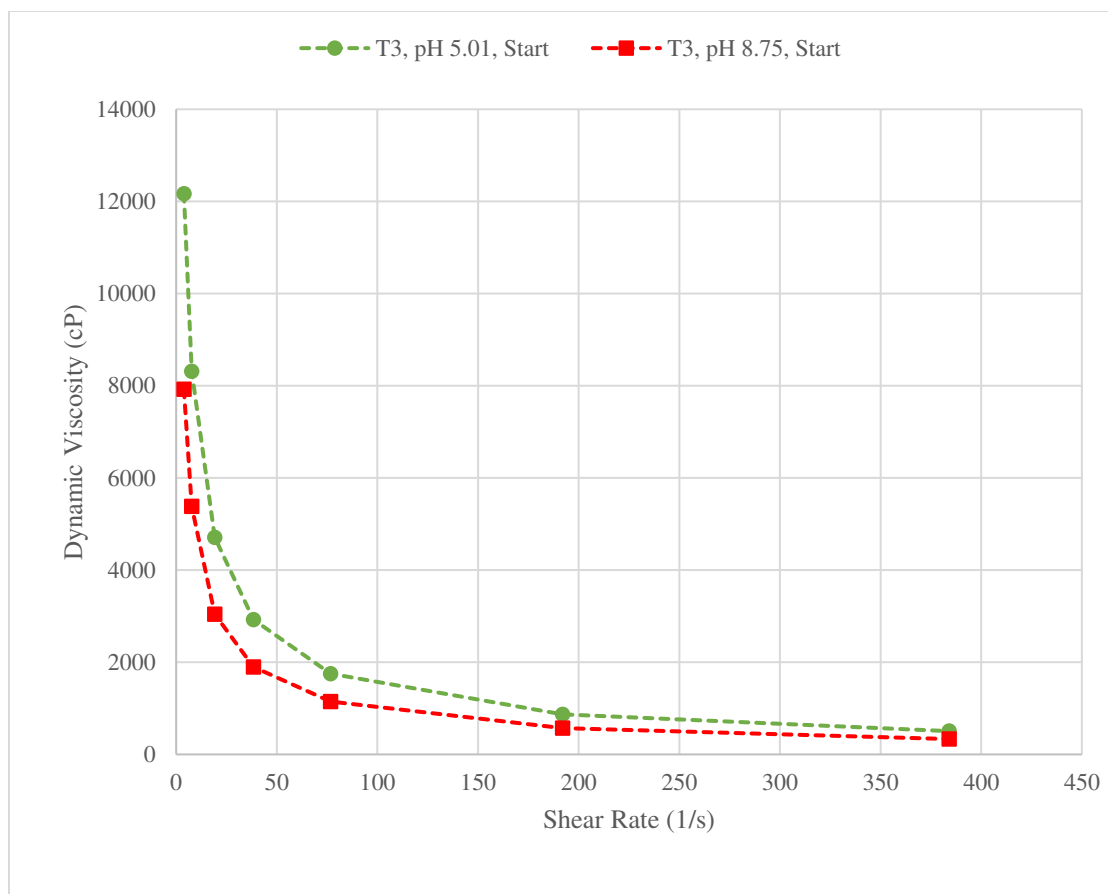
Figure 7-17 Starting viscosity curve for viscous solutions of concentration 0.5% HA and 0.5% CMC with modified pH, Test 3.

Due to the difference in sample size for viscosity measurements before and after the test, ANOVA was performed separately for viscosity measurements before and after. The results are shown in Table 7-13. According to the ANOVA test results, while the effect of shear rate was significant, the pH was not found to have a significant effect. However, the lack of replication limits the scope of this analysis.

Table 7-13 ANOVA p-values for effect of shear rate and pH on starting viscosities, Test 3.

Effect	p-value
Shear rate	4.57E-02
pH	7.07E-02

Figure 7-18 shows the ending viscosity curves for Test 3. Data points are the average of six measurements, two each from three independent samples. The shear thinning behaviour can be seen strongly. pH 5.01 had a lower viscosity than pH 8.75, suggesting greater polymer degradation over time. Table 7-14 shows the ANOVA values. Both pH and rpm had a significant effect, although the interaction

term was not significant. In Figure 7-18, the viscosity values appear to be close together, but the ANOVA suggests a significant difference. However, in post-hoc tests, the only shear rate at which there is a significant difference was at 5 rpm (p=2.06E-03).
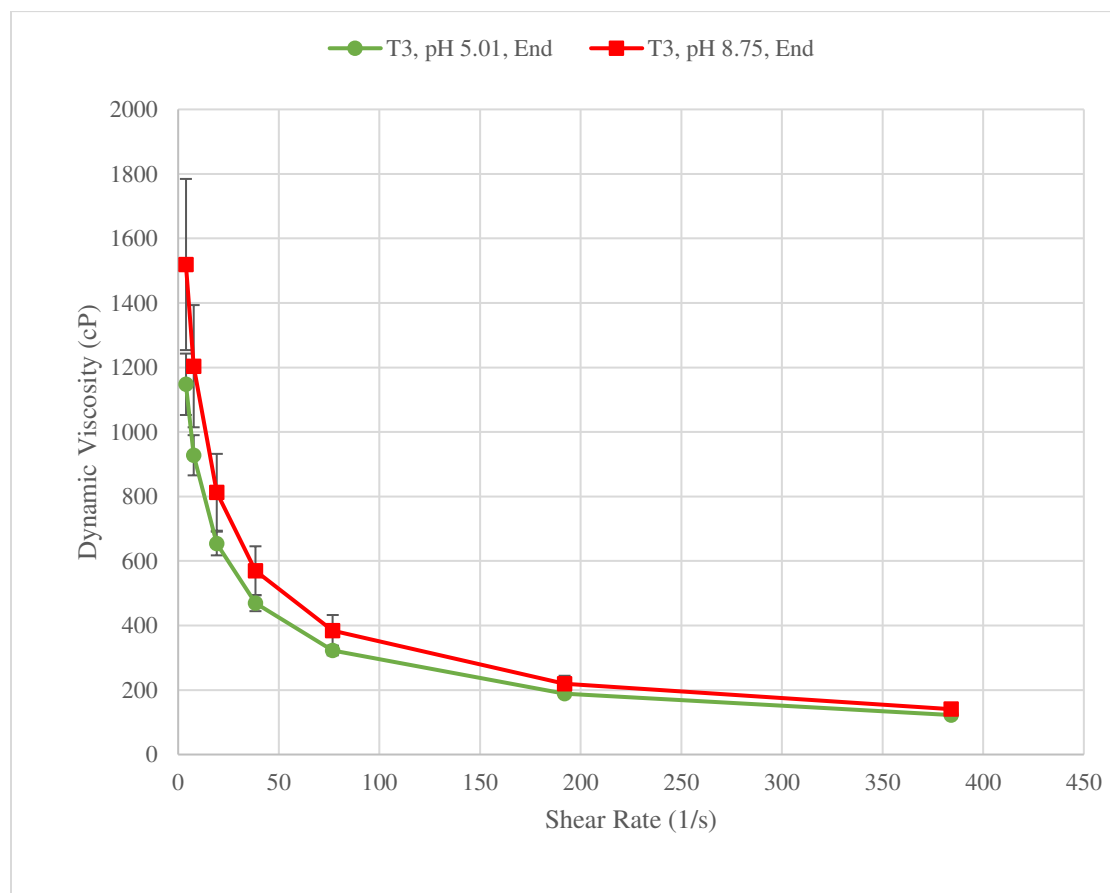
Figure 7-18 Viscosity curves after 3 days degradation in PBS, Test 3.

Table 7-14 ANOVA p-values for effect of shear rate and pH on ending viscosities, Test 3.

Effect	p-value
Shear rate	2.30E-14
pH	2.20E-05
Interaction	0.20

Figure 7-19 displays the percent viscosity reduction for Test 3 at three shear rates and Table 7-15 shows the ANOVA results for this data. Both rpm and pH had a significant effect, but not a significant interaction effect. At all shear rates, there was a significant difference between the pH groups in percent viscosity reduction. Within pH groups, only the comparison from 5 rpm to 20 rpm for pH 8.75 had a significant difference. This means that the percent viscosity reduction was relatively constant across shear

rates. The pH 5.01 samples had the highest viscosity reduction of all samples seen across the three tests thus far.
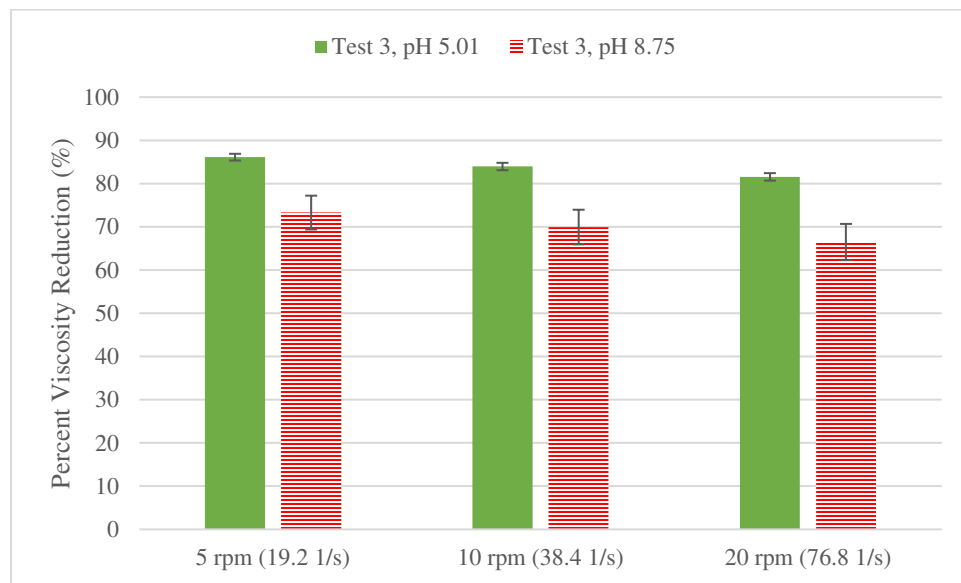
Figure 7-19 Percent viscosity reduction after 3 days in PBS at three shear rates, Test 3.

Table 7-15 ANOVA p-values for effect of shear rate and pH on viscosity reduction, Test 3.

Effect	p-value
Shear rate	2.06E-04
pH	5.52E-15
Interaction	0.64

Figure 7-20 shows the silver release for Test 3. Each data point is an average of three samples. From post-hoc tests, there were no significant differences between the pH groups at any time point. There is less plateau between 24 and 72 hours than had been seen in Test 1 or 2. Still, the trends of significance were similar to Test 1 and 2. There are significant differences between time points up to 4 hours, but not beyond. There was not a significant difference in silver release for either pH between 24 and 72 hours. As shown in Table 7-16, the only significant effect was time, not pH.
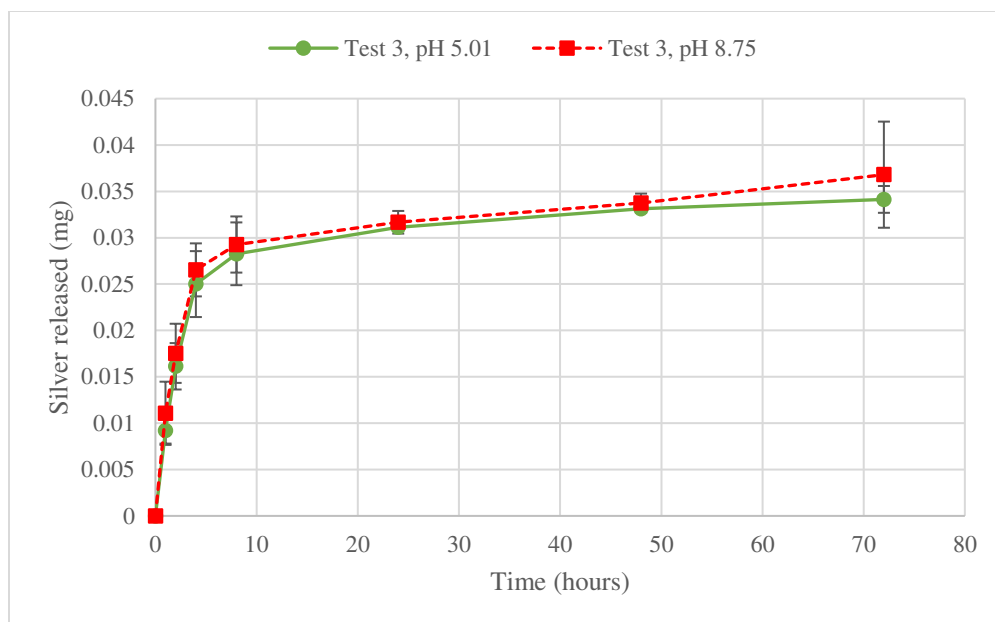
Figure 7-20 Silver released from gels into 100 mL PBS over time, Test 3.

Table 7-16 ANOVA p-values for effect of time and pH on silver release, Test 3.

Effect	p-value
Time	2.87E-15
pH	0.12
Interaction	0.99

Test 4

Test 4 includes an "unaltered" condition, which was expected to have a pH between 6 and 7 from previous tests (displayed in Table 7-12). The resulting pH for the three samples developed are 5.02, 7.66, and 8.02 as seen in Table 12. The low pH condition resulted in a very similar pH that was seen in Test 3, but the high pH condition with 1E-04 mol/L NaOH was lower than expected.

Figure 7-21 shows the viscosity curve for starting viscosities of Test 4 samples. Data points are an average of two measurements. The viscosities across all samples are lower than what was seen for the previous three tests. The high (basic) and low (acidic) pH groups seem to have marginally higher starting viscosities than the unaltered. The similarity between high and low pH groups is unexpected as the pH groups in Test 3 had a difference of approximately 1000 cP at 10 rpm (38.4 1/s). Table 7-17 shows the ANOVA values. While the effect for pH is shown to be significant by ANOVA, at the three middle shear rates (5, 10, and 20 rpm), there are no significant differences between pH groups, except for between pH 7.66 to pH 8.02 at 5 rpm (p=0.048)

154
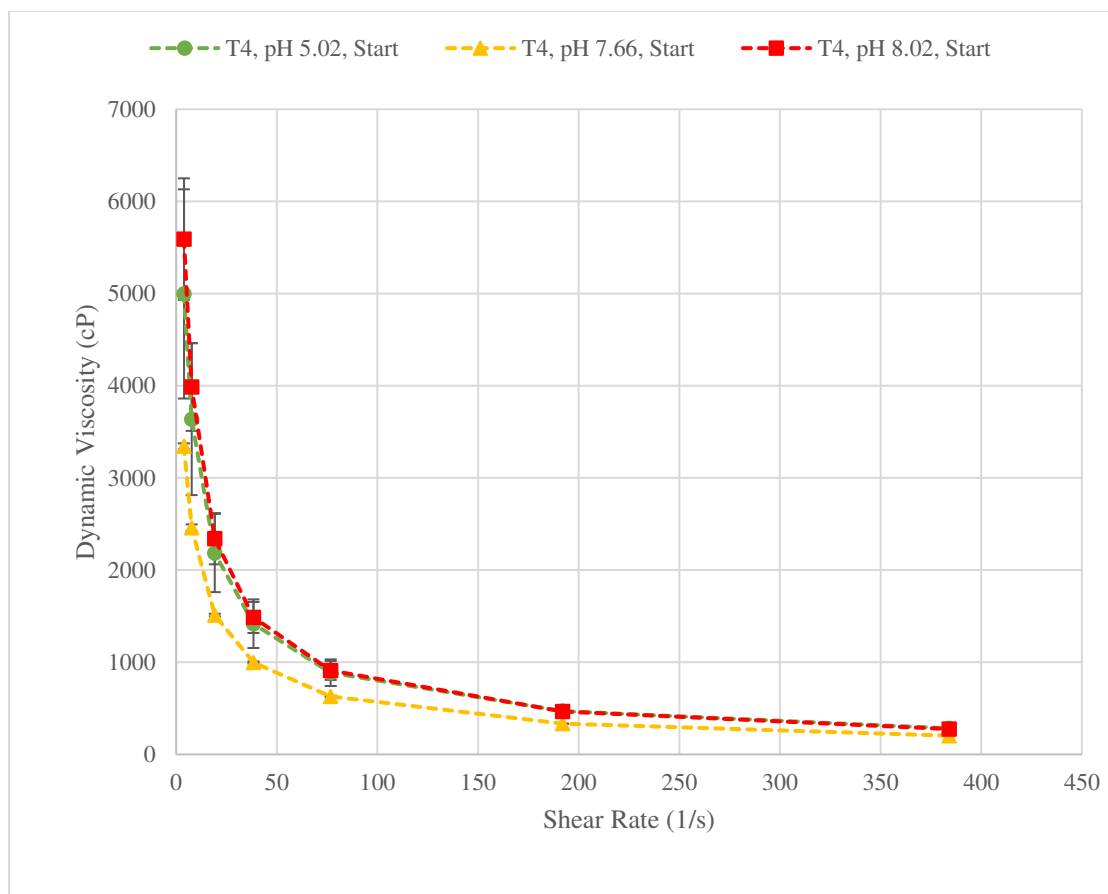
Figure 7-21 Starting viscosity curve for viscous solutions, Test 4.

Table 7-17 ANOVA p-values for effect of shear rate and pH on starting viscosities, Test 4.

Effect	p-value
Shear rate	1.22E-05
pH	3.32E-03
Interaction	0.47

Figure 7-22 shows the viscosity curves after the three day experiment. Data points are an average of five measurements. Despite starting at a lower viscosity than Test 3, the ending viscosities are higher than was seen for Test 3, meaning less degradation occurred over the course of the experiment. Still, they are not dissimilar trends to what was seen for the equivalent composition in Test 1 or 2. In these measurements, a greater distinction between pH groups was seen than at the beginning of the test. In Test 3, the high pH (8.02) group had a higher ending viscosity than low pH (5.02), and that trend is seen here also.
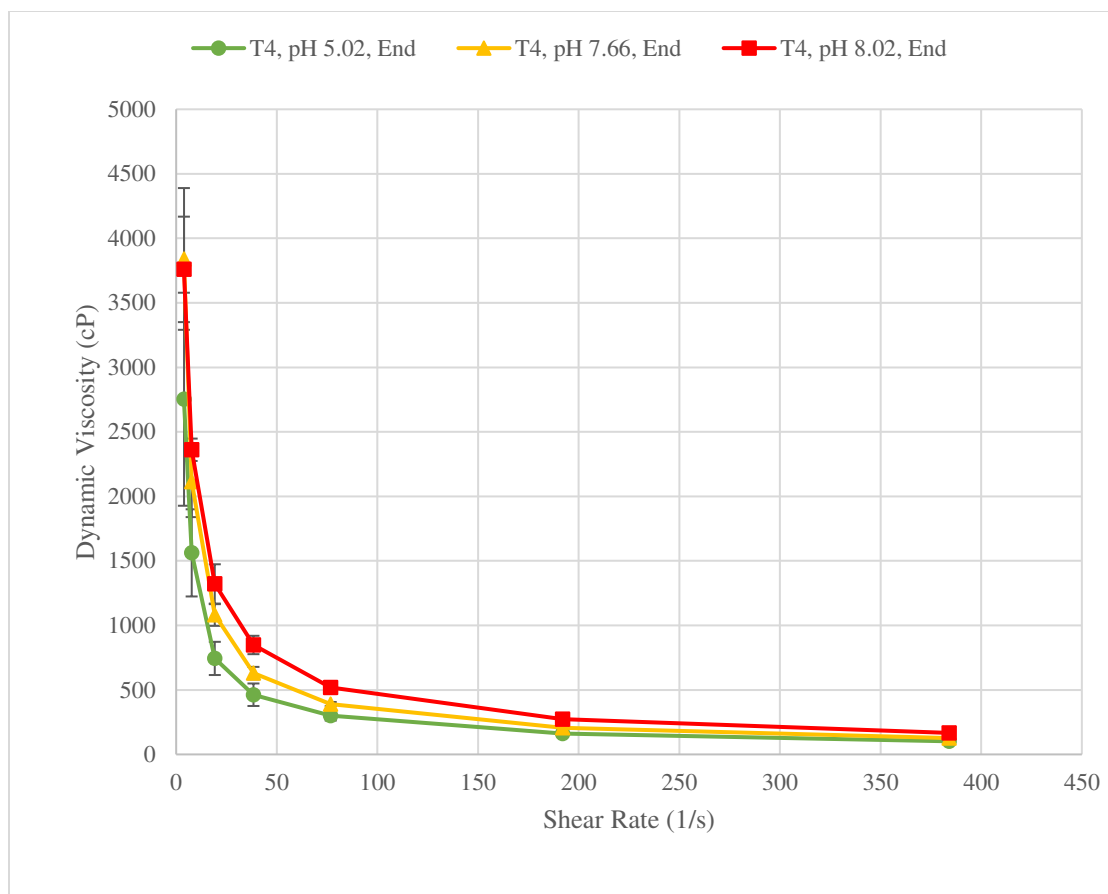
Figure 7-22 Viscosity curves after 3 days degradation in PBS, Test 4.

Table 7-18 shows the ANOVA results for end of test viscosities for Test 4. The shear rate, pH, and interaction effects are all significant. The ending viscosities in Test 3 did not have a significant interaction effect. In post-hoc tests, there was a significant difference between low pH (5.02) and high (pH 8.02) pH groups at all shear rates. The only significant difference between pH 7.66 and pH 8.02 groups was at 5 rpm, and there were differences between pH 7.66 and pH 5.02 at 5 rpm and 10 rpm.

Table 7-18 ANOVA p-values for effect of shear rate and pH on ending viscosities, Test 4.

Effect	p-value
Shear rate	7.43E-21
pH	9.31E-15
Interaction	2.60E-04

Figure 7-23 shows the percent viscosity reduction at three shear rates with Table 7-19 showing the ANOVA results. The percent viscosity reduction values are lower than was seen in previous tests, most likely due to the unusually low viscosities measured at the beginning of the test. The acidic pH group was

156

significantly higher viscosity reduction than 7.66 pH or 8.02 pH, but was still lower than expected. Unlike the previous tests, there was not a significant effect of shear rate on the viscosity reduction. The low and high pH groups had especially consistent values across all rpm. As expected, pH 5.02 had a significant difference to the higher pH groups at each shear rate. The pH 7.66 and 8.02 groups had a significant difference only at 5 rpm.
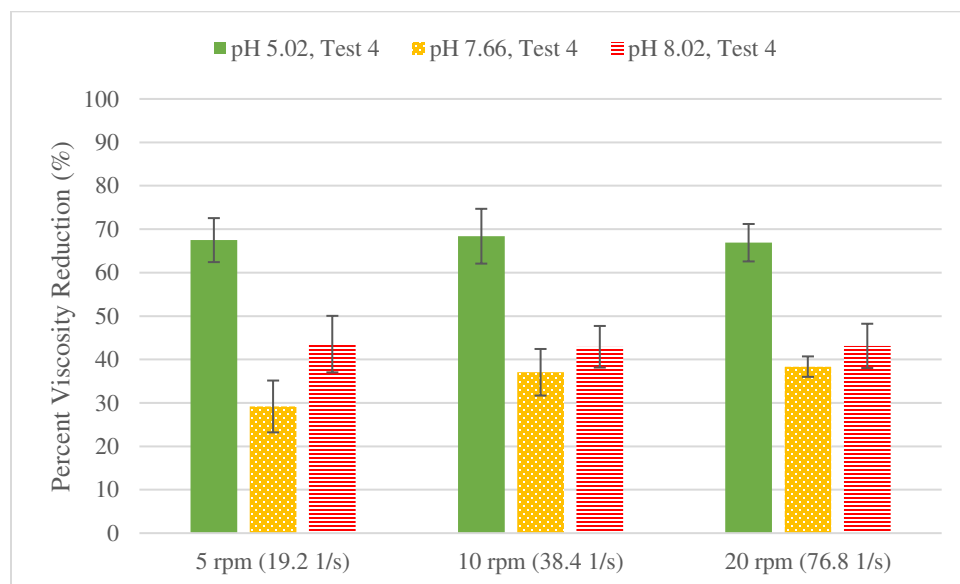
Figure 7-23 Percent viscosity reduction at three shear rates, Test 4.

Table 7-19 ANOVA p-values for effect of shear rate and pH on percent viscosity reduction, Test 4.

Effect	p-value
Shear rate	0.27
pH	1.33E-18
Interaction	0.18

Figure 7-24 shows the silver released over time and Table 7-20 shows the corresponding ANOVA results. The starting silver in each gel was 0.099 mg, compared to 0.12 mg in Test 3, but a larger total amount of silver was released in Test 4. This may be due to the lower starting viscosities. There is more of a plateau seen here after 8 hours than was seen for Test 3. In Test 3, the basic pH group released marginally more silver than the acidic pH group, this was true as well here, although the middle pH group (7.66) exceeded all. By 72 hours, there were no significant differences between pH groups. Differing from previous tests, there was not a significant increase from 1 to 2 hours in any group, nor from 2 to 4 hours. From 4 to 8 hours, only the Low pH group had a significant increase. As with Test 3, only time had a significant effect on silver release, not pH.
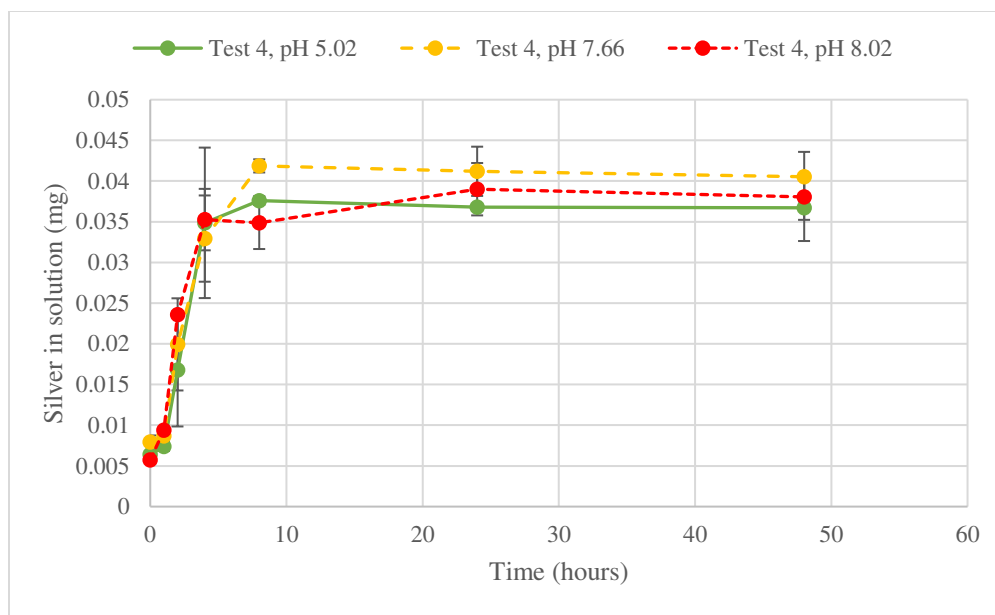
Figure 7-24 Silver released from gels into 100 mL PBS over time, Test 4.

Table 7-20 ANOVA p-values for effect of time and pH on silver release, Test 4.

Effect	p-value
Time	2.38E-22
pH	0.27
Interaction	0.43

Discussion: pH Study

For the pH study, two tests (Test 3 and Test 4) were conducted with the same polymer composition for all groups (0.5% HA, 0.5% CMC). Table 7-21 displays the initial viscosities measured for Test 3 and 4 at three shear rates. It was expected that the viscosity would not change significantly with pH. There was variation between samples, but there was not a consistent trend with pH, as can be seen in Figure 7-25. The potential trend of decreasing viscosity with increasing pH seen in Test 3 was not seen in Test 4. Overall, the viscosities measured in Test 3 were higher than Test 4.

Table 7-21 Starting viscosities for Test 3 and 4 at three shear rates, ordered by increasing pH

	pH	Viscosity at 5 rpm (cP)	Viscosity at 10 rpm (cP)	Viscosity at 20 rpm (cP)
Test 3	5.01	4712	2713	1750
Test 4	5.02	2185 ± 424	1419 ± 264	887 ± 145
Test 4	7.66	1512 ± 14	997 ± 11	629 ± 7
Test 4	8.02	2341 ± 278	1486 ± 168	911± 103
Test 3	8.75	3045	1895	1147
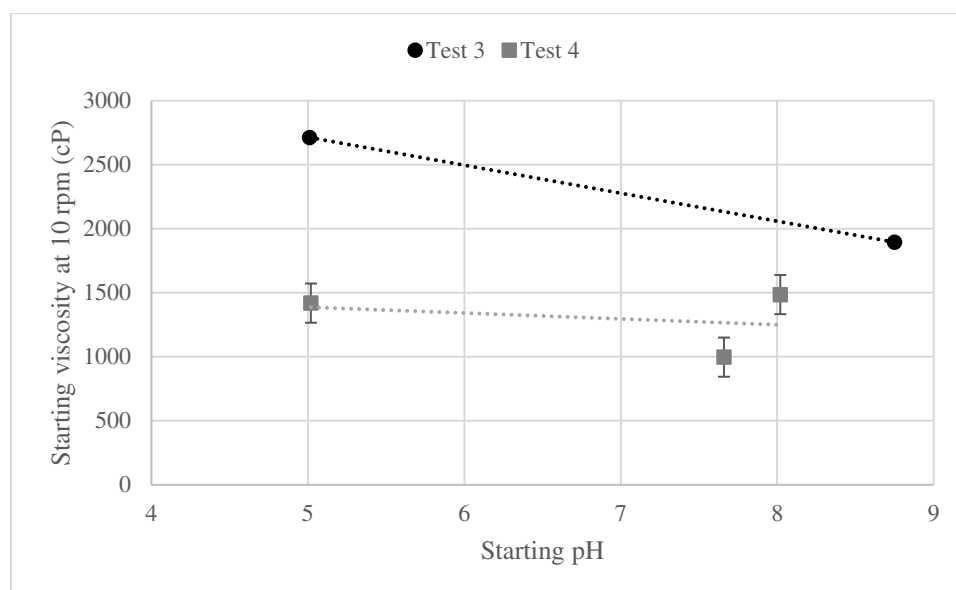
Figure 7-25 Starting viscosity at 10 rpm plotted against pH for Test 3 and 4

Temperature at measurement of viscosity or time of mixing was not controlled or measured during this study but may be partially responsible for the differences in viscosity between different tests of similar composition. Some work suggests that at the polymer concentrations that were used in this present study, the differences in viscosity between 25 and 37°C should have only a marginal effect on relative viscosity[33]. However, in solutions of CMC only, a 1% solution could decrease by approximately 50% in measured viscosity between 20 and 40°C at 50 rpm[34]. Changes in viscosity with temperature are more significant with lower temperatures[39]. The difference in apparent viscosity from 30 to 40°C is minimal, but there is a significant difference from 10 to 20°C [39]. Higher temperature solutions also display more Newtonian behaviour, and less shear thinning [39].

Table 7-22 and Figure 7-26 display percent viscosity by starting pH. Figure 26 demonstrates the trend in percent viscosity reduction at 10 rpm with pH. There appears to be a trend of decreasing percent viscosity

reduction with increasing starting pH, but more samples with a greater range of pH would be needed to confirm this. The viscosity reduction for Test 4 samples overall is much less than expected. While it is possible that a high pH was the cause of low degradation, this effect was not seen for Test 3 at pH 8.75.

Table 7-22 Percent viscosity reduction at three shear rates for Test 3 and 4.

	pH	Viscosity Reduction At 5 rpm (%)	Viscosity Reduction At 10 rpm (%)	Viscosity Reduction At 20 rpm (%)
Test 3	5.01	86.12 ± 0.78	83.95 ± 0.86	81.56 ± 0.87
Test 4	5.02	67.49 ± 5.07	68.39 ± 6.31	66.89 ± 4.31
Test 4	7.66	29.18 ± 5.97	37.05 ± 5.37	38.35 ± 2.35
Test 4	8.02	43.54 ± 6.51	42.92 ± 4.79	43.12 ± 5.10
Test 3	8.75	73.30 ± 3.91	69.94 ± 4.01	69.15 ± 1.97
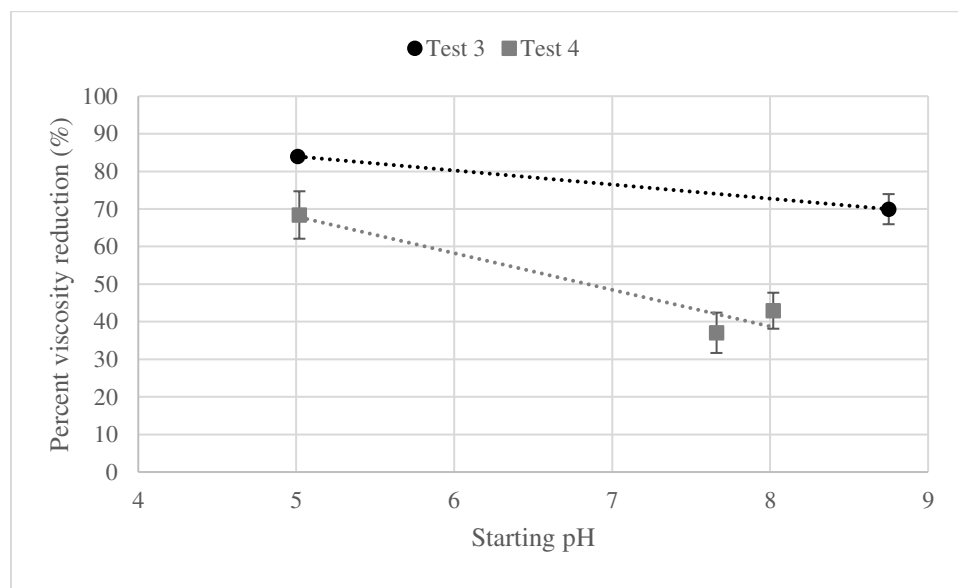
Figure 7-26 Percent viscosity reduction at 10 rpm plotted against pH for Test 3 and 4.

There is a pH dependence of polymer structure and shape, even at constant ionic strength[40]. CMC is found to form dense aggregates at low pH (pH 1.6), but are uniformly distributed with little entanglement at pH 7[40]. The dense aggregates resulted in a lower bulk viscosity, as it is easier to orient large molecules to the flow of applied shear stress[40]. It was also seen that the effect of shear thinning was less pronounced above the pKa of the polymer, which is 3.65 for CMC [40]. Above its pKa, CMC chains are negatively charged, with more repulsive forces increasing sample viscosity and decreasing the degree or shear thinning behaviour[40].

HA solutions of concentration 0.05% to 0.5% were modified with phosphate buffers and NaOH in a 2008 study [21]. At all pH values, there was Newtonian fluid behaviour for low concentrations of HA [21]. For 0.5% HA solutions, at high pH (approximately 13), there is such disruption in intermolecular bonds that the viscosity is very low and the profile is of Newtonian flow, with some of this effect also seen at very low pH (pH 1-2) [21]. At pH 7 there is minimal rupture of chains[21]. In an earlier study, it was seen that below 1.5, the disruption of HA chains was irreversible, but around pH 5, there is a reversible decrease in intrinsic viscosity[41]. HCl can be used to lower the pH below the pKa of NaCMC (pKa= 3.65), decreasing the charge density and facilitating interactions between CMC chains[36]. The addition of 0.5 M NaOH (resulting in pH 13.5) decreased viscosity and 0.5 M HCl (resulting in pH 0.5) increased viscosity, by decreasing available bonds, or decreasing the charge density[36]. The pKa of HA is approximately 3.

Independent of pH there may be an effect of adding certain ions to the polymer solution on viscosity. The addition of salts decreases the solubility of polyelectrolytes like CMC, but chains are more likely to aggregate, which could increase the viscosity [36]. NaOH bonds with available blocks on the cellulose backbone, preventing these blocks from interacting with other CMC chains[36]. The addition of HCl to the HA solutions caused a decrease in viscosity due to electrostatic repulsions causing a more compact conformation of the HA coils[39]. Another study of CMC gels found that sodium, chloride, and hydrogen ions had the effect of decreasing the viscosity. However, this effect was only seen if the CMC was dissolved in water after the ions had been added by shielding CMC from intermolecular interactions with itself [34]. This lower viscosity may be due to incomplete dissolution as salts slow the dissolution process[36]. This may account for some of the differences in viscosity between Tests 3 and 4, where the point at which the pH modifying ingredient was added was not recorded or intentionally controlled.

Table 7-23 and Figure 7-27 show the percent silver release for Test 3 and 4. The percent release at 72 hours, especially for Test 4, was higher than was seen for Test 1 and 2, even for the pH 7.66 group. This may be due to the low initial viscosity of Test 4 samples. There does not appear to be a significant trend of increasing or decreasing silver release with pH, as can be seen in the trends of percent silver release with pH shown in Figure 7-27. There was unexpectedly a delay in release for the first two hours for Test 4.

Table 7-23 Percent silver release into PBS at 2, 8, and 72 hours for Test 3 and 4.

	pH	Silver Release at 2 hours (%)	Silver Release at 8 hours (%)	Silver Release at 72 hours (%)
Test 3	5.01	13.19 ± 2.04	23.11 ± 2.77	27.90 ± 1.18
Test 4	5.02	7.46 ± 0.57	35.15 ± 9.32	37.03 ± 4.13
Test 4	7.66	8.74 ± 0.42	33.20 ± 5.34	40.86 ± 3.08
Test 4	8.02	9.48 ± 0	35.55 ± 3.81	38.37 ± 2.85
Test 3	8.75	14.33 ± 2.61	23.93 ± 2.48	30.09 ± 4.68
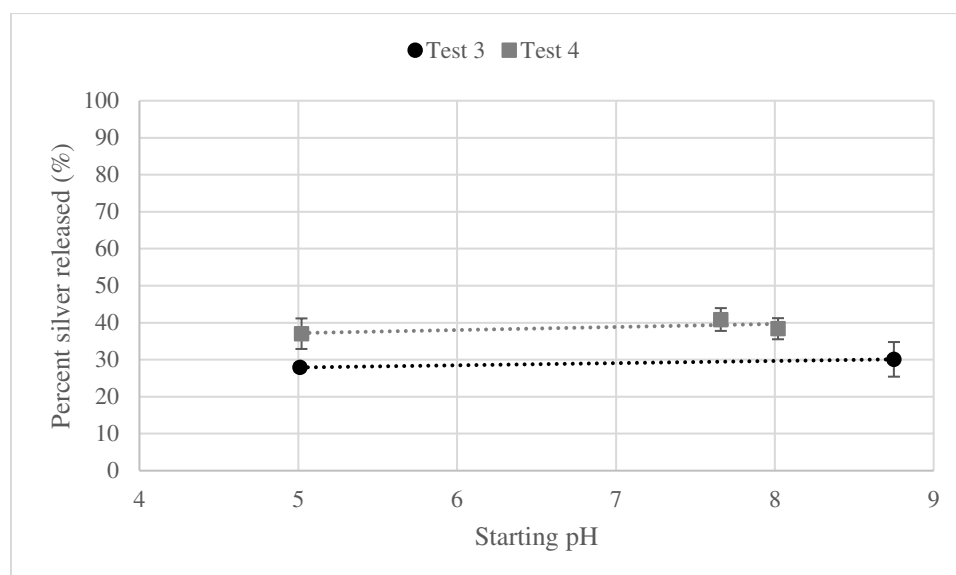
Figure 7-27 Percent silver released after 72 hours plotted against starting pH for Test 3 and 4.

In CMC and gelatin hydrogels, the uptake of drugs into gels and their release from such, is dependent on polymer ratio, amount of cross linking agent included, and total polymer concentration[42]. Release of drugs is dependent on the strength of electrostatic binding between the polymer and the drugs[42]. In the case of our study, silver was primarily found in positively charged forms. At the pH studied, the polymers were above their pKa value, therefore negatively charged and available for electrostatic interactions with positively charged silver. The release profile of the silver was not changed by the inclusion of ions or the changes in pH at the concentrations used.

Discussion: Silver Measurement Accuracy

After the four tests for the composition and pH studies were completed, a small experiment was performed to determine if the chloride in PBS would interfere with the accuracy of the silver measurements by AAS. After a 6-hour dissolution of nanocrystalline silver film, a set amount of this

solution was added to PBS and acidified with nitric acid for AAS as is standard practice. It was found that the measurement given by AAS did not agree with the expected value from the initial dissolution. Following this, solutions of silver nitrate in PBS with a range of concentrations from 0.01 mg/L to 30 mg/L were created, acidified with nitric acid, and analyzed by AAS. The results are shown in Figure 7-28. For the solutions in PBS, the AAS measured silver concentration could not be compared to known silver concentration or the measured concentrations for silver nitrate in water. Up to 0.1 mg/L, the AAS results appeared to correspond with the known amount of silver added, but above this, the results could not be interpreted. Therefore, the AAS measurements of silver in PBS may not be accurate and limit the ability to interpret the AAS results from this chapter.
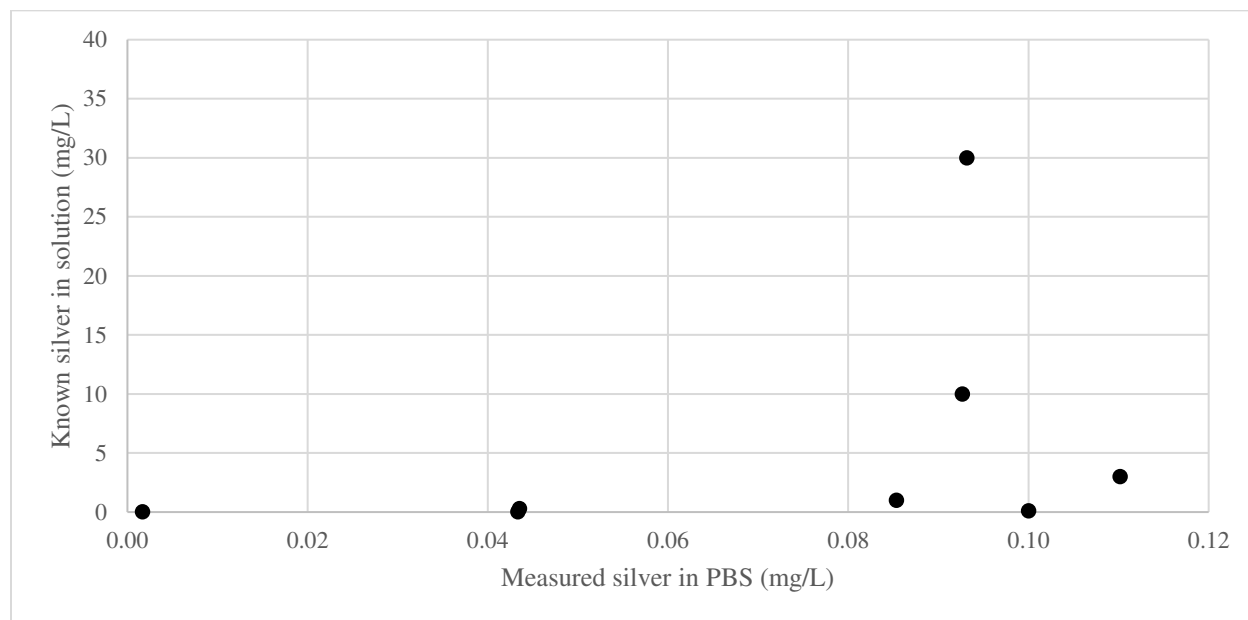
Figure 7-28 Silver measured in PBS versus actual silver concentration

Further literature search confirms that precipitating agents like chloride will cause a variation in AAS measurements which cannot be corrected using silver nitrate [43], [44]. This is because solid particulates are inconsistently atomized for analysis by AAS, meaning that some silver is still bound to chloride in solid form and won't be detected at the characteristic wavelength of 328 nm [43]. The decrease in absorption at this wavelength means a decrease in silver measured. This decrease is dependent on the ratio of chloride to silver and the time after the solution was made but could be less than 5% or greater than 30%[43]. Neither of these factors is controlled in the experiments in this chapter and in addition, the described study did not use a chloride to silver ratio that is similar to what was used here.

In another study, 10 to 100 ppm silver was added to various simulated biological media, including PBS with and without protein addition[45]. In addition to observing chloride precipitation, they found that

ionic silver was forming complexes with organic material, which would prevent chloride precipitation[45]. In this chapter, no experiments accounted for the possible effect of polymer segments released from the dialysis cassette forming complexes which could shield from precipitation, increasing solubility. No discernable white particulates were observed in the experiments in this chapter, but because of the likely low concentration of silver, very little precipitate would be formed.

Conclusion

There does not appear to be one composition group that was significantly better than any other for silver release or degradation. From the literature, it would be expected that higher viscosity polymers (like T1H) would degrade slower. However, this was not directly seen in terms of percentage of viscosity lost, although the ending viscosity was still higher than lower concentration samples. Therefore, for future animal studies, the composition of 0.5% HA-0.5% CMC will be used. Silver release followed trends expected from literature, however the uncertain accuracy of AAS to measure silver in a chloride containing environment may indicate that the quantity of silver released is not known. Future studies may use a more refined method to measure silver or indirectly measure the amount of silver released by observing a biological effect.

Although the focus of anti-adhesion treatments is on anti-inflammatory properties, not anti-bacterial activity, the possible contamination of the abdominal cavity during surgery would make an anti-bacterial agent useful for this application. The low log reductions seen here may not translate to poor anti-bacterial properties *in vivo*, where the bacterial load could be lower in the abdominal cavity.

In the present study, it is likely that the pH range studied for clinical relevance was not low or high enough to see a major effect on viscosity, degradation, or silver release. This pH range was above the pKa of both polymers, so changes in electrostatic interactions are unlikely. For animal studies, the unaltered pH group will be used.

References

[1] V. Kanikireddy, K. Varaprasad, T. Jayaramudu, C. Karthikeyan, and R. Sadiku, "Carboxymethyl cellulose-based materials for infection control and wound healing: A review," *International Journal of Biological Macromolecules*, vol. 164, pp. 963–975, Dec. 2020, doi: 10.1016/j.ijbiomac.2020.07.160.

[2] G. Wei, C. Zhou, G. Wang, L. Fan, K. Wang, and X. Li, "Keratinocyte Growth Factor Combined with a Sodium Hyaluronate Gel Inhibits Postoperative Intra-Abdominal Adhesions," *Int J Mol Sci*, vol. 17, no. 10, p. 1611, Sep. 2016, doi: 10.3390/ijms17101611.

[3] M. M. P. J. Reijnen, E. M. Skrabut, V. A. Postma, J. W. Burns, and H. van Goor, "Polyanionic Polysaccharides Reduce Intra-abdominal Adhesion and Abscess Formation in a Rat Peritonitis Model," *Journal of Surgical Research*, vol. 101, no. 2, pp. 248–253, Dec. 2001, doi: 10.1006/jsre.2001.6288.

[4] Y. Yeo *et al.*, "In situ cross-linkable hyaluronic acid hydrogels prevent post-operative abdominal adhesions in a rabbit model," *Biomaterials*, vol. 27, no. 27, pp. 4698–4705, Sep. 2006, doi: 10.1016/j.biomaterials.2006.04.043.

[5] S. Yamaner, M. Kalayci, U. Barbaros, E. Balik, and T. Bulut, "Does Hyaluronic Acid-Carboxymethylcellulose (HA-CMC) Membrane Interfere With the Healing of Intestinal Suture Lines and Abdominal Incisions?," *Surg Innov*, vol. 12, no. 1, pp. 37–41, Mar. 2005, doi: 10.1177/155335060501200106.

[6] J. S. Park *et al.*, "An Assessment of the Effects of a Hyaluronan-Based Solution on Reduction of Postsurgical Adhesion Formation in Rats: A Comparative Study of Hyaluronan-Based Solution and Two Film Barriers," *Journal of Surgical Research*, vol. 168, no. 1, pp. 49–55, Jun. 2011, doi: 10.1016/j.jss.2009.09.025.

[7] C. J. J. M. Sikkink, B. de Man, R. P. Bleichrodt, and H. van Goor, "Auto-Cross-Linked Hyaluronic Acid Gel Does Not Reduce Intra-Abdominal Adhesions or Abscess Formation in a Rat Model of Peritonitis," *Journal of Surgical Research*, vol. 136, no. 2, pp. 255–259, Dec. 2006, doi: 10.1016/j.jss.2006.06.021.

[8] K. Kramer, N. Senninger, H. Herbst, and W. Probst, "Effective Prevention of Adhesions With Hyaluronate," *Archives of Surgery*, vol. 137, no. 3, pp. 278–282, Mar. 2002, doi: 10.1001/archsurg.137.3.278.

[9] Z. Cohen *et al.*, "Prevention of Postoperative Abdominal Adhesions by a Novel, Glycerol/Sodium Hyaluronate/Carboxymethylcellulose-Based Bioresorbable Membrane: A Prospective, Randomized, Evaluator-Blinded Multicenter Study," *Dis Colon Rectum*, vol. 48, no. 6, pp. 1130–1139, Jun. 2005, doi: 10.1007/s10350-004-0954-8.

[10] P. A. Simmons and J. G. Vehige, "Investigating the potential benefits of a new artificial tear formulation combining two polymers," *Clin Ophthalmol*, vol. 11, pp. 1637–1642, Sep. 2017, doi: 10.2147/OPTH.S135550.

[11] Y. Zhu and S. Granick, "Biolubrication: Hyaluronic Acid and the Influence on Its Interfacial Viscosity of an Antiinflammatory Drug," *Macromolecules*, vol. 36, no. 4, pp. 973–976, Feb. 2003, doi: 10.1021/ma025988r.

[12] R. Stern, A. A. Asari, and K. N. Sugahara, "Hyaluronan fragments: An information-rich system," *European Journal of Cell Biology*, vol. 85, no. 8, pp. 699–715, Aug. 2006, doi: 10.1016/j.ejcb.2006.05.009.

[13] A. J. Esposito, S. J. Heydrick, M. R. Cassidy, J. Gallant, A. F. Stucchi, and J. M. Becker, "Substance P is an early mediator of peritoneal fibrinolytic pathway genes and promotes intra-abdominal adhesion formation," *Journal of Surgical Research*, vol. 181, no. 1, pp. 25–31, May 2013, doi: 10.1016/j.jss.2012.05.056.

[14] T. W. Wong and N. A. Ramli, "Carboxymethylcellulose film for bacterial wound infection control and healing," *Carbohydrate Polymers*, vol. 112, pp. 367–375, Nov. 2014, doi: 10.1016/j.carbpol.2014.06.002.

[15] P. Basu, U. Narendrakumar, R. Arunachalam, S. Devi, and I. Manjubala, "Characterization and Evaluation of Carboxymethyl Cellulose-Based Films for Healing of Full-Thickness Wounds in Normal and Diabetic Rats," *ACS Omega*, vol. 3, no. 10, pp. 12622–12632, Oct. 2018, doi: 10.1021/acsomega.8b02015.

[16] J. S. Lee, S. U. Lee, C.-Y. Che, and J.-E. Lee, "Comparison of cytotoxicity and wound healing effect of carboxymethylcellulose and hyaluronic acid on human corneal epithelial cells," *Int J Ophthalmol*, vol. 8, no. 2, pp. 215–221, Apr. 2015, doi: 10.3980/j.issn.2222-3959.2015.02.01.

[17] J. Zhou, C. Elson, and T. D. G. Lee, "Reduction in postoperative adhesion formation and re-formation after an abdominal operation with the use of N, O - carboxymethyl chitosan," *Surgery*, vol. 135, no. 3, pp. 307–312, Mar. 2004, doi: 10.1016/j.surg.2003.07.005.

[18] J. E. Lee *et al.*, "Oxaliplatin-loaded chemically cross-linked hydrogels for prevention of postoperative abdominal adhesion and colorectal cancer therapy," *International Journal of Pharmaceutics*, vol. 565, pp. 50–58, Jun. 2019, doi: 10.1016/j.ijpharm.2019.04.065.

[19] J. Kim, J.-Y. Chang, Y.-Y. Kim, M.-J. Kim, and H.-S. Kho, "Effects of molecular weight of hyaluronic acid on its viscosity and enzymatic activities of lysozyme and peroxidase," *Archives of Oral Biology*, vol. 89, pp. 55–64, May 2018, doi: 10.1016/j.archoralbio.2018.02.007.

[20] I. Gatej, M. Popa, and M. Rinaudo, "Role of the pH on Hyaluronan Behavior in Aqueous Solution," *Biomacromolecules*, vol. 6, no. 1, pp. 61–67, Jan. 2005, doi: 10.1021/bm040050m.

[21] A. Maleki, A.-L. Kjøniksen, and B. Nyström, "Effect of pH on the Behavior of Hyaluronic Acid in Dilute and Semidilute Aqueous Solutions," *Macromolecular Symposia*, vol. 274, no. 1, pp. 131–140, 2008, doi: 10.1002/masy.200851418.

[22] P. Snetkov, K. Zakharova, S. Morozkina, R. Olekhnovich, and M. Uspenskaya, "Hyaluronic Acid: The Influence of Molecular Weight on Structural, Physical, Physico-Chemical, and Degradable Properties of Biopolymer," *Polymers (Basel)*, vol. 12, no. 8, p. E1800, Aug. 2020, doi: 10.3390/polym12081800.

[23] M. Ochi, B. Wan, Q. Bao, and D. J. Burgess, "Influence of PLGA molecular weight distribution on leuprolide release from microspheres," *International Journal of Pharmaceutics*, vol. 599, p. 120450, Apr. 2021, doi: 10.1016/j.ijpharm.2021.120450.

[24] B. Pose-Vilarnovo *et al.*, "Modulating drug release with cyclodextrins in hydroxypropyl methylcellulose gels and tablets," *Journal of Controlled Release*, vol. 94, no. 2, pp. 351–363, Feb. 2004, doi: 10.1016/j.jconrel.2003.10.002.

[25] J. Araújo, E. Vega, C. Lopes, M. A. Egea, M. L. Garcia, and E. B. Souto, "Effect of polymer viscosity on physicochemical properties and ocular tolerance of FB-loaded PLGA nanospheres," *Colloids and Surfaces B: Biointerfaces*, vol. 72, no. 1, Art. no. 1, Aug. 2009, doi: 10.1016/j.colsurfb.2009.03.028.

[26] B. C. Anderson, N. K. Pandit, and S. K. Mallapragada, "Understanding drug release from poly(ethylene oxide)-b-poly(propylene oxide)-b-poly(ethylene oxide) gels," *Journal of Controlled Release*, vol. 70, no. 1, pp. 157–167, Jan. 2001, doi: 10.1016/S0168-3659(00)00341-2.

[27] Y. Fang, N. Zhang, Q. Li, J. Chen, S. Xiong, and W. Pan, "Characterizing the release mechanism of donepezil-loaded PLGA microspheres in vitro and in vivo," *Journal of Drug Delivery Science and Technology*, vol. 51, pp. 430–437, Jun. 2019, doi: 10.1016/j.jddst.2019.03.029.

[28] M. G. Lara, M. V. L. B. Bentley, and J. H. Collett, "In vitro drug release mechanism and drug loading studies of cubic phase gels," *International Journal of Pharmaceutics*, vol. 293, no. 1, pp. 241–250, Apr. 2005, doi: 10.1016/j.ijpharm.2005.01.008.

[29] B. S. Zolnik and D. J. Burgess, "Effect of acidic pH on PLGA microsphere degradation and release," *Journal of Controlled Release*, vol. 122, no. 3, pp. 338–344, Oct. 2007, doi: 10.1016/j.jconrel.2007.05.034.

[30] S. H. S. Koshari *et al.*, "Design of PLGA-Based Drug Delivery Systems Using a Physically-Based Sustained Release Model," *Journal of Pharmaceutical Sciences*, vol. 111, no. 2, pp. 345–357, Feb. 2022, doi: 10.1016/j.xphs.2021.09.007.

[31] G. Acharya *et al.*, "A study of drug release from homogeneous PLGA microstructures," *Journal of Controlled Release*, vol. 146, no. 2, pp. 201–206, Sep. 2010, doi: 10.1016/j.jconrel.2010.03.024.

[32] R. B. Patel, L. Solorio, H. Wu, T. Krupka, and A. A. Exner, "Effect of injection site on in situ implant formation and drug release in vivo," *Journal of Controlled Release*, vol. 147, no. 3, pp. 350–358, Nov. 2010, doi: 10.1016/j.jconrel.2010.08.020.

[33] A. Maleki, A.-L. Kjøniksen, and B. Nyström, "Anomalous Viscosity Behavior in Aqueous Solutions of Hyaluronic Acid," *Polym. Bull.*, vol. 59, no. 2, pp. 217–226, Sep. 2007, doi: 10.1007/s00289-007-0760-2.

[34] X. H. Yang and W. L. Zhu, "Viscosity properties of sodium carboxymethylcellulose solutions," *Cellulose*, vol. 14, no. 5, pp. 409–417, Oct. 2007, doi: 10.1007/s10570-007-9137-9.

[35] A. Benchabane and K. Bekkour, "Rheological properties of carboxymethyl cellulose (CMC) solutions," *Colloid Polym Sci*, vol. 286, no. 10, pp. 1173–1180, Sep. 2008, doi: 10.1007/s00396-008-1882-2.

[36] C. G. Lopez and W. Richtering, "Oscillatory rheology of carboxymethyl cellulose gels: Influence of concentration and pH," *Carbohydrate Polymers*, vol. 267, p. 118117, Sep. 2021, doi: 10.1016/j.carbpol.2021.118117.

[37] L. Long *et al.*, "Injectable multifunctional hyaluronic acid/methylcellulose hydrogels for chronic wounds repairing," *Carbohydrate Polymers*, vol. 289, p. 119456, Aug. 2022, doi: 10.1016/j.carbpol.2022.119456.

[38] M. S. Spitzer *et al.*, "Sodium hyaluronate gels as a drug-release system for corticosteroids: release kinetics and antiproliferative potential for glaucoma surgery," *Acta Ophthalmologica*, vol. 86, no. 8, pp. 842–848, 2008, doi: 10.1111/j.1755-3768.2007.01149.x.

[39] A. García-Abuín, D. Gómez-Díaz, J. M. Navaza, L. Regueiro, and I. Vidal-Tato, "Viscosimetric behaviour of hyaluronic acid in different aqueous solutions," *Carbohydrate Polymers*, vol. 85, no. 3, pp. 500–505, Jun. 2011, doi: 10.1016/j.carbpol.2011.02.028.

[40] I. Dogsa, M. Tomšič, J. Orehek, E. Benigar, A. Jamnik, and D. Stopar, "Amorphous supramolecular structure of carboxymethyl cellulose in aqueous solution at different pH values as determined by rheology, small angle X-ray and light scattering," *Carbohydrate Polymers*, vol. 111, pp. 492–504, Oct. 2014, doi: 10.1016/j.carbpol.2014.04.020.

[41] E. Gura, M. Hückel, and P.-J. Müller, "Specific degradation of hyaluronic acid and its rheological properties," *Polymer Degradation and Stability*, vol. 59, no. 1, pp. 297–302, Jan. 1998, doi: 10.1016/S0141-3910(97)00194-8.

[42] G. Buhus, M. Popa, and J. Desbrieres, "Hydrogels Based on Carboxymethylcellulose and Gelatin for Inclusion and Release of Chloramphenicol," *Journal of Bioactive and Compatible Polymers*, vol. 24, no. 6, pp. 525–545, Nov. 2009, doi: 10.1177/0883911509349687.

[43] R. F. Lee and W. F. Pickering, "Effect of precipitate and complex formation on the determination of silver by atomic-absorption spectroscopy," *Talanta*, vol. 18, no. 11, pp. 1083–1094, Nov. 1971, doi: 10.1016/0039-9140(71)80220-5.

[44] P. Bermejo-Barrera, A. Moreda-Piñeiro, and A. Bermejo-Barrera, "Study of chemical modifiers for direct determination of silver in sea water by ETA-AAS with deuterium background correction," *Talanta*, vol. 43, no. 1, pp. 35–44, Jan. 1996, doi: 10.1016/0039-9140(95)01702-X.

[45] K. Loza, C. Sengstock, S. Chernousova, M. Köller, and M. Epple, "The predominant species of ionic silver in biological media is colloidally dispersed nanoparticulate silver chloride," *RSC Advances*, vol. 4, no. 67, pp. 35290–35297, 2014, doi: 10.1039/C4RA04764H.

Chapter 8 : Nanocrystalline Silver Treatments in Animal Model of Surgical Adhesions

Introduction

As detailed in Chapter 1, there has been extensive research on adhesion formation and treatment using rat models. The rat is a small and easy to care for species that is commonly used in surgical models. Rabbits have also been used as adhesion models, particularly in developing adhesions involving the uterine horn [1], [2], [3], [4]. Pigs are less commonly used but are an ideal model due to their similar size and wound healing processes in comparison to humans. In a 2015 study of the biodegradation of polymer scaffolds for adhesion prevention, both rats and pigs were used as models[5]. The scaffolds degraded faster *in vivo* than was seen *in vitro*, and the pig model saw faster degradation than the rat model, likely due to the differences in physiological environment[5]. Given that the results of the rat model were not the same as the more human-like pig model, this confirms the use of pigs instead of rats for more clinically applicable research. In a 2002 study with adult pigs, researchers created a peritoneal defect laparoscopically and covered the defect with mesh affixed with clips or Seprafilm® HA-CMC membrane[6]. Another porcine study used a laparotomy and used multiple membrane materials per animal to study inflammation, foreign body reaction, and adhesion formation, with second look laparotomies at 30 and 90 days[7]. Pigs have also been used as an animal models to study adhesion formation using different surgical techniques given their similarity to humans [8], [9], [10].

As discussed previously, hyaluronate (HA) and carboxymethylcellulose are water-soluble biodegradable polymers that will be used with nanocrystalline silver solutions to prevent adhesions[11]. Seprafilm® and other HA-CMC adhesion treatments have been extensively studied, demonstrating the potential benefits and safety[4], [6], [12], [13], [14], [15], [16], [17]. Seprafilm® is FDA approved as an adhesion barrier and will be used as a control group for comparison to the experimental groups.

The lack of toxic effects of implanted silver medical devices has already been extensively proven by the various technologies and applications including urinary catheters and orthopedic implants[18]. Silver coatings on catheters implanted in rats did not reduce cell viability compared to PDMS alone[19]. Silver coatings may reduce the incidence of infection, although the efficacy depends on the method of coating and species of silver, but in no case did it increase human cell death or infection rates[20], [21], [22]. Silver coated orthopedic megaprostheses showed decreased infection rates over titanium only[23]. Their implantation in rabbits for 12 weeks resulted in elevated silver levels in the blood but no pathologic or gross organ changes and no evidence of surrounding area inflammation[23]. Argyria is a condition related

to the buildup and precipitation of silver in cells due to excessive silver exposure. This is not considered life threatening and is rarely encountered[18]. This evidence supports the assumption that silver toxicity will not be a concern for implanted silver gels, which have a low concentration of silver.

Nanocrystalline silver is a commonly used wound and burn dressing, and the solutions derived from soaking the film in water have also shown significant anti-inflammatory capacity[24]. It follows that the silver species released from the film could also be encapsulated in a viscous gel-like solution for inflammation reduction and adhesion prevention. Not only is nanocrystalline silver an effective anti-inflammatory agent when applied directly, it also has significant effects when applied on the opposite side of the animal from the wound[24], [25], [26]. Given the beneficial effects of remote application, nanocrystalline silver wound dressings will also be applied externally to the surgical site on the animal where adhesions have been induced.

Methods

While there are multiple accepted scoring systems and variations on the technique of inducing adhesion formation, many studies follow a similar accepted procedure. Here, the cecum-sidewall procedure described in the literature primarily for rats has been adapted for pigs. A summary of procedures is provided below in Figure 8-1. SOP's are attached in Appendix B.

Premedication: Intramuscular injection of Medetomidine (3 mg/mL)/Butorphanol (10 mg/mL)/Ketamine (100 mg/mL). Atropine (0.4mg/mL) and Glycopyrrolate (0.2mg/mL) will be given pre-surgically as anti-cholinergics.

Reopen Abdominal Cavity: Make observations. Take samples of adhesion tissue, abdominal wall, and cecum.

12 hours before surgery: Animals fasted

Blood Sample: 5-10mL sample from jugular vein

Pain Relief: Trans-dermal fentanyl patches changed every 48 hours.

7 Days, End of Study: Weigh, Premedication, Anesthesia, Take Blood Sample

Animals weighed

Anesthesia: Inhalation of isoflurane.

Surgery (Day 0): Laparotomy (opening of abdominal cavity by midline incision. Abrasion of cecum. Excision of superficial layers of the corresponding abdominal wall. Treatment if indicated. Placement in close contact. Suture closed. Cover with bandages and tape.

Monitoring: Monitored daily for behaviour and appearance. Bandages changed and wound condition assessed on Day 2 and 4

Euthanasia: By barbiturate overdose under anesthesia

Figure 8-1 Summary and timeline of procedures for animal model of adhesions.

Animal Acquisition and Care

Yorkshire pigs will be acquired and given a minimum of 5 days to acclimate to new surroundings prior to surgery. Animals will be housed individually but have visual, olfactory, and auditory contact. Animals are monitored twice daily on weekdays and once daily on weekends and holidays. An inspection of each animal will be performed during the acclimation period by a veterinarian or veterinarian technician. Animals are selected for the study based on cage side and clinical observations and inspection. Animals with health problems that would interfere with animal wellbeing or study outcomes will be excluded from the study. Five animals are allocated for each group, with up to five additional animals for pilot testing of adhesion formation and scoring methods, or for unexpected complications with a study animal. Pigs will be 35-45 kg at the start of the study.

Groups

Table 8-1 Experimental and Control Groups for animal study with adhesions.

Group	Code	Description
Control Group 1	CG1	Sham surgery- laparotomy but no abrasion
Control Group 2	CG2	No treatment controls- abrasion with no treatment
Control Group 3	CG3	Comparison product group – treatment with Seprafilm®
Control Group 4	CG4	Vehicle controls – gel containing no silver
Experimental Group 1	EG1	Gel with silver treatment
Experimental Group 2	EG2	External silver dressing

Gels are made with 0.5% sodium hyaluronate and 0.5% sodium carboxymethyl cellulose in sterile distilled water and thoroughly mixed to ensure the polymers have dissolved. 20 mL of the appropriate gel is applied to the abdominal cavity of each animal in group EG1 and CG4.

For the group EG2, nanocrystalline silver is sputtered onto HDPE mesh using the Novel sputtering process and are cut into 12 by 6 inch pieces. Two film pieces are sandwiched with a layer of gauze, soaked in distilled water, and applied external to the surgical area after closure. Dressings will be changed on Day 2 and Day 4.

Surgical Procedures

Animals will be fasted for minimum of 12 hours prior to surgery. Water is allowed *ad libitum*. For all surgical procedures, animals are anesthetized and provided with an antibiotic. In preparation for surgery,

animals will be intubated, given an ear vein IV, and transferred to the surgical suite. Anesthesia is maintained with oxygen and isoflurane inhalation. When a suitable depth of anesthesia is reached, procedures may begin. The abdominal area will then be shaved and cleansed and a baseline blood sample will be taken. Vital signs are monitored at least every 17 minutes.

A 15 cm midline incision will be made into the abdominal cavity, carefully dividing tissue layers with a scalpel or electrocautery. When the peritoneum is reached, the surgeon will bluntly dissect. After the surgeon confirms no presence of adhesions, or records the presence of such, the terminal ileum and cecum will be mobilized. To create adhesions, abrasion with a sterile gauze pad will be performed on the parietal and parenchymal peritoneum using a laparotomy pad or dry sterile gauze pad over a set area of approximately 2 square inches, except the sham procedure group (CG1). Treatments will be applied directly to abraded surfaces in CG3, CG4, and EG1. The abdominal cavity will be closed in layers with appropriate Vicryl sutures or surgical clips. Animals in EG2 then have the incision area covered by a nanocrystalline silver wound dressing. All other animals have the incision area covered with a facility standard surgical dressing and a topical antibiotic.

On Day 2 and Day 4 post-surgery animals will have external dressings changed under anesthesia. Incision sites will also be assessed and photographed. On Day 7, under anesthesia, a blood sample will be collected, then the animals euthanized before re-opening the abdominal cavity to make observations and collect tissues samples of any present adhesions and abdominal wall.

At the end of each procedure except Day 7, animals will be disconnected from isoflurane and transitioned to ventilation with room air. The animals will be returned to their pens and kept on ventilation until breathing on their own. Regular monitoring will continue until animals are conscious and stable. Observation will continue to recognize surgical complications. Analgesia is provided immediately post-surgery on Day 0, with a continuous release fentanyl patch for three days, and additional post-surgical analgesia as needed.

Adhesion Scoring

On Day 7, adhesions will be scored according to the following scales presented in Tables 8-2 and 8-3. The Strength scoring in Table 8-3 is adapted from Hoffmann et al.[27].

Table 8-2 Semi-quantitative scoring for quantity of adhesions by observation seven days after surgery.

Score	Description
0	No adhesions
1	1-3
2	4-7
3	8-12
4	12+

Table 8-3 Semi-quantitative scoring for strength of adhesions by use of traction or dissection, seven days after adhesion-inducing surgery [27].

Score	Description
0	No adhesions
1	Gentle traction required to break adhesion
2	Blunt dissection required to break adhesion
3	Sharp dissection required to break adhesion

The final adhesion score for use in statistical analysis will be the sum of the Quantity and Strength Scores.

Sample Analysis

Histology

Tissue samples taken on Day 7 will be paraffin embedded and sectioned for histological analysis. H&E is used for observing tissue morphology and scoring fibrosis. Wright-Giemsa staining is used to stain inflammatory cells and may be used to semi-quantitatively score inflammation. Masson's Trichrome staining is used to stain collagen which may be used to observe and score fibrosis. Scoring for this study

is adapted from scores presented by Yilmaz et. al. and Wei et. al[28], [29]. Scoring categories are shown in Table 8-4. Qualitative observations will also be made of the tissue sections.

Table 8-4 Semi-quantitative scoring of inflammation and fibrosis in tissue samples of abdominal wall and adhesions.

Score	Inflammation	Fibrosis
0	No inflammation	No fibrosis
1	Mild: Giant cells, lymphocytes, and plasma cells	Thin bunches of cellular fibrosis
2	Moderate: Giant cells, lymphocytes, eosinophils, neutrophils	Wide areas of fibrosis with reduced vascularization
3	Severe: Massive infiltration of inflammatory cells, microabscesses present	Areas of fibrosis formed by thick bunch of collagen

ELISA

ELISA is performed on serum samples taken for the following markers: IFN-γ, IL-10, IL-12, IL-1β, IL-2, IL-4, IL-6, IL-8, TNF-α, TGF-β1. Descriptions of these biomarkers can be found in Chapter 5.

Statistics

Means and standard deviations are calculated for numerical scores and quantitative measurements in each experimental group. Comparisons between groups will be made using the Kruskal-Wallis test because the variable is not assumed to be normal because of a small sample set, so one-way ANOVA would not be appropriate. Dunn's test with the Holm's correction method accounts for the increased rate of false positives from repeated t-tests and will be used for multiple comparisons between groups. Significance is defined as $p<0.05$.

Pilot Study

As a pilot study to refine procedures, one animal underwent the procedure described for CG2. On Day 0, after preparation and anesthesia, a blood sample was taken under anesthesia before creating a 15 cm midline incision in layers until the abdominal cavity was reached. The cecum was isolated and abraded with dry gauze along with the abdominal wall in the same area. Pictures were taken throughout the process. The skin was stapled closed. The staple line was coated with a topical antibiotic and covered with

an adhesive bandage and secured with a neoprene vest. The pig was taken from the surgical room to recover. Notably, adhesions were seen after opening the abdominal cavity, before any intentional abrasion took place.

On Day 2 and Day 4 the vest and bandages were removed under anesthesia to observe the healing process. Figure 8-2 shows images of the pig during bandage changes. No edema or excessive tenderness was noticed. The bandages were replaced. It was decided that Day 2 and 4 bandage replacements were not necessary as no adverse effects were identified and these procedures subjected the pig to additional risks from anesthesia. Pigs will be monitored for changes in behaviour or appearance to alert staff to complications.
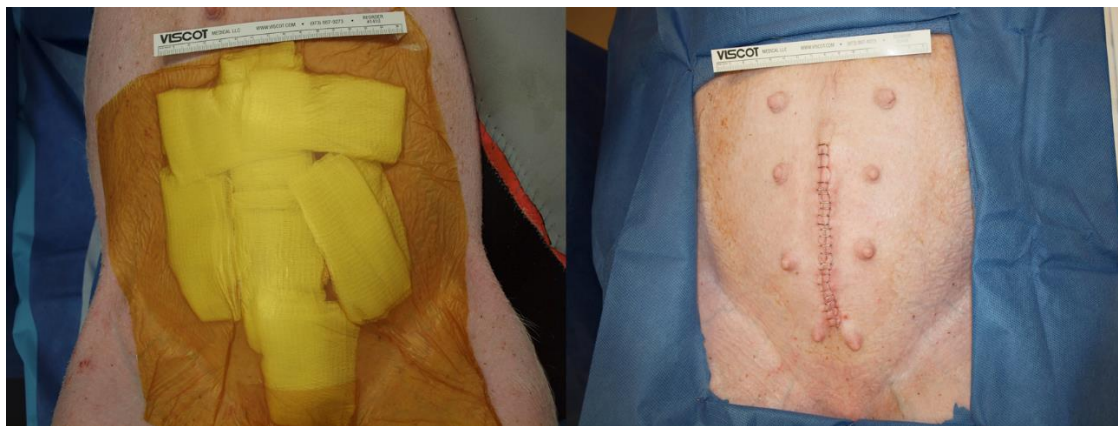
Figure 8-2 Images of external surgical area for pilot pig on Day 2.

On Day 7 the pig was anesthetized and a blood sample was taken. Then, the bandages were removed and the abdominal cavity was reopened along the original incision line. Adhesions were observed along the incision line. Adhesions were not found from the cecum to the abdominal wall but were found in multiple locations between segments of the bowel and the abdominal wall. This observation led to a change in the scoring criteria from adhesion severity to scoring by the quantity of adhesions. Most adhesions required sharp dissection to break, although some were broken accidentally by blunt dissection. Changes were suggested to the protocol to perform a laparoscopic procedure before reopening the abdominal cavity to observe adhesions without breaking those present. Treatments will also be applied over a greater area in the abdominal cavity to prevent adhesion formation in the broader locations seen. Abrasion of the cecum and sidewall may need to be stronger in order to reliably produce adhesions in a fixed area.

Expected Results

Adhesion Scoring

Based on the pilot study and assumptions of the effectiveness of each treatment group, a simulated data set of scores for five pigs per group was created and is displayed in Table 8-5 for Adhesion Quantity and Table 8-6 for Adhesion Strength. The Adhesion Quantity score is the most important aspect of adhesion scoring, since reducing the incidence of adhesions at any strength is the primary goal. Even adhesions with a low strength score still have the potential to cause complications for patients.

Table 8-5 Predicted Adhesion Quantity scores.

	CG1	CG2	CG3	CG4	EG1	EG2
Pig 1	2	3	2	2	0	1
Pig 2	3	3	2	2	1	1
Pig 3	2	4	2	1	1	1
Pig 4	2	3	3	1	1	1
Pig 5	2	2	3	3	1	2
Average	**2.2**	**3.0**	**2.4**	**1.8**	**0.8**	**1.2**
Standard Deviation	0.45	0.71	0.55	0.84	0.45	0.45

Table 8-6 Predicted Adhesion Strength scores.

	CG1	CG2	CG3	CG4	EG1	EG2
Pig 1	2	2	2	2	0	1
Pig 2	3	3	2	2	1	1
Pig 3	2	3	2	1	1	1
Pig 4	2	2	2	1	2	2
Pig 5	2	2	2	2	2	2
Average	**2.2**	**2.4**	**2.0**	**1.6**	**1.2**	**1.4**
Standard Deviation	0.45	0.55	0	0.55	0.84	0.55

Figure 8-3 displays the average predicted scores for Adhesion Quantity for each experimental and control group. EG1 is expected to reduce the number of adhesions, but given the large area for possible occurrence, it is expected that most pigs in this group may still have 1-3 adhesions (a Quantity score of 1). CG2 is expected to have the most adhesions, followed closely by CG1 and CG3. Despite no intentional abrasion, the sham surgery (CG1) will still have a large number of adhesions due to the trauma caused by the laparotomy. With this predicted data, the Kruskal-Wallis test is significant with p=0.00133. The

comparisons from CG2 to EG1 and CG2 to EG2 are significant according to the Dunn's post-hoc test with Holm's correction.
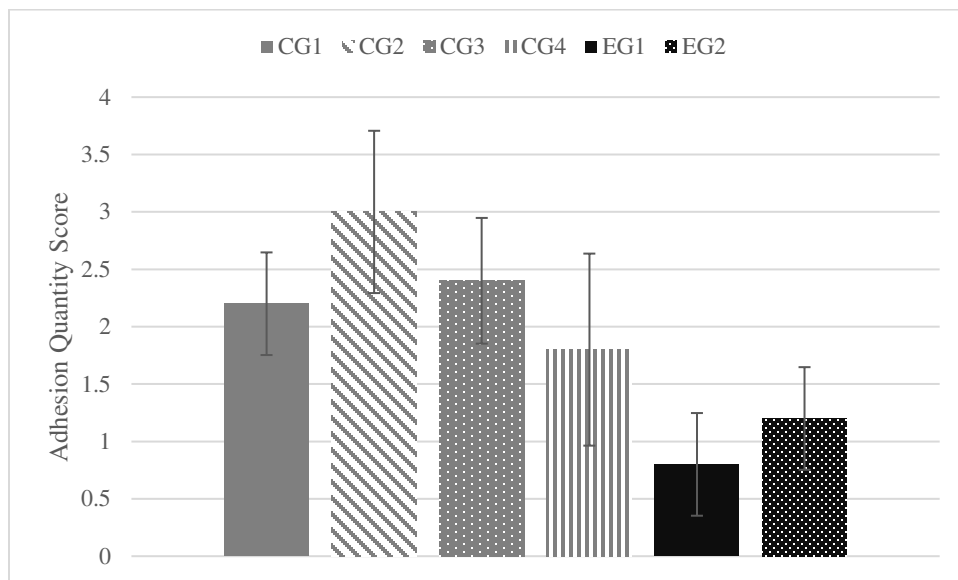
Figure 8-3 Predicted Adhesion Quantity scores.

Figure 8-4 displays the average predicted Adhesion Strength scores for each group. The Kruskal-Wallis test is significant for this predicted data set with a p-value of 0.023, but no comparisons reached significance after Holm's correction. It is expected that there would be no significant difference in adhesion strength among groups, as there is a smaller range of scores for Strength compared to Quantity.
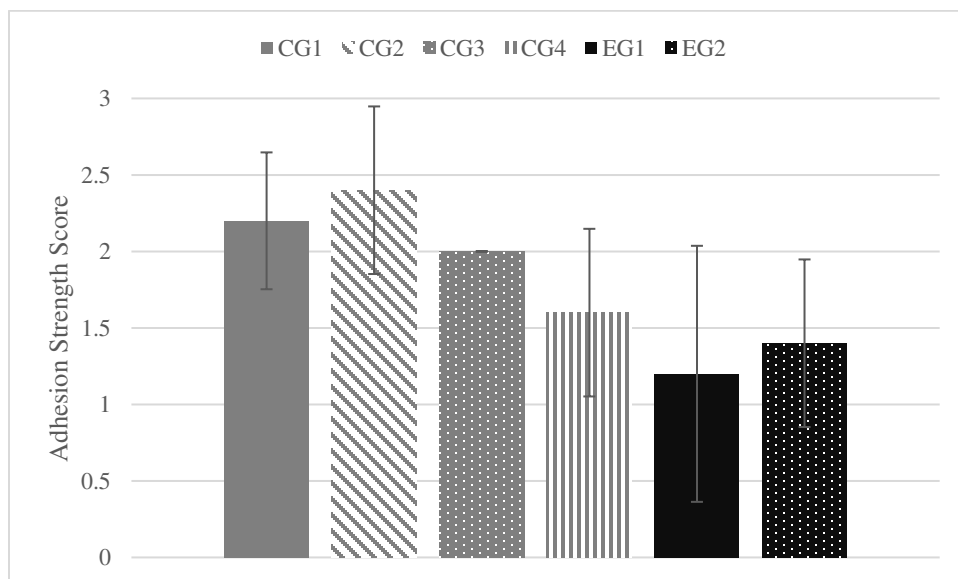
Figure 8-4 Predicted Adhesion Strength scores.

Figure 8-5 displays the predicted Adhesion Summary scores, which are the sum of the Quantity and Strength scores. As with the Quantity score, the Kruskal-Wallis test is significant with p=0.0023. The comparisons from CG2 to EG1 and CG2 to EG2 are significant according to Dunn's post-hoc test with Holm's correction.
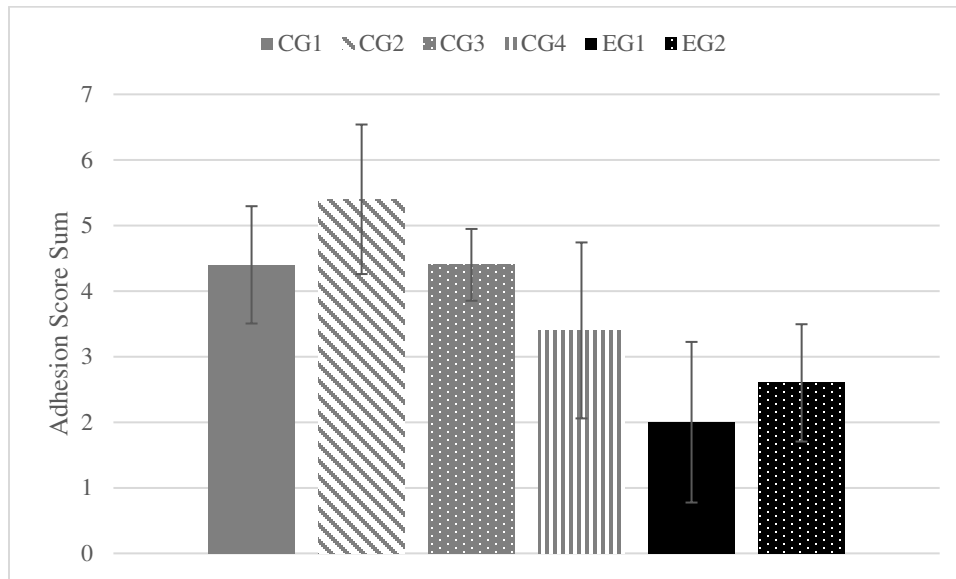
Figure 8-5 Predicted Adhesion Summary scores.

Sample Analysis

Histology

Evidence of inflammation and fibrosis will likely still be present after seven days, even as much of the healing process is complete. It is expected from other research that tissue with adhesions will look similar across any control or experimental group animal with moderate inflammation and severe fibrosis [4]. Sites of tissue injury without adhesions are still expected to have an inflammatory response with macrophages and neutrophils still remaining after one week, with minimal to moderate fibrosis [4].

In rats, HA-CMC barrier materials did not significantly reduce fibrosis or inflammation as seen by H&E staining[17]. Even three weeks after initial injury, fibrosis could be seen by thick collagen bands and irregular fibroblast proliferation and inflammation was seen by significant cellular infiltrates [17].

After 10 days, H&E staining of sub-mesothelial tissue did not show significant differences in inflammation for rabbits treated with polymer gels, but control groups had increased collagen deposition over experimental treatments [1]. This suggests that the inflammation scores may be similar, but fibrosis

could be distinguished between some experimental and control groups. In a rat study after seven days with a growth factor in a polymer gel, there was some reduction seen in inflammation for the experimental group and differences could be seen in collagen structure[12].

ELISA

In control groups, it is expected that inflammatory biomarkers such as IFN-γ and IL-2 will still be elevated but will be returned to normal levels in the experimental treatment groups. IL-1β and TNF-α are involved in the acute inflammatory response and will likely not be elevated in any group after one week, as their most important role in adhesion healing are in the first few days[30]. IL-6 and IL-8 similarly will be decreasing after the first few days but may still be elevated in control animals where there is still a significant inflammatory reaction. IL-12 by one week should have similar levels to Day 0 in most groups, except where inflammation is still severe.

IL-4 and IL-10 are anti-inflammatory and will be elevated where healing is still taking place to suppress the initial immune reaction. This is also the case for TGF-β1 where it assists with tissue healing and promotes ECM production [31]. Studies of adhesion formation suggest that adhesion fibroblasts will have increased levels of IL-10 and TGF-β1, which should be seen after seven days especially in animals with many adhesions [32].

References

[1]   D. Akerberg, C. Grunditz, M. Posaric-Bauden, K. Isaksson, R. Andersson, and B. Tingstedt, "The influence on abdominal adhesions and inflammation in rabbits after exposure to differently charged polypeptides," vol. 2012, Jul. 2012, doi: 10.4236/jbise.2012.58055.

[2]   R. A. Lang, P. M. Grüntzig, C. Weisgerber, C. Weis, E. K. Odermatt, and M. H. Kirschner, "Polyvinyl alcohol gel prevents abdominal adhesion formation in a rabbit model," *Fertil. Steril.*, vol. 88, no. 4, Supplement, Art. no. 4, Supplement, Oct. 2007, doi: 10.1016/j.fertnstert.2007.01.108.

[3]   R. E. Leach, J. W. Burns, E. J. Dawe, M. D. SmithBarbour, and M. P. Diamond, "Reduction of Postsurgical Adhesion Formation in the Rabbit Uterine Horn Model with Use of Hyaluronate/Carboxymethylcellulose Gel1 1Supported by Genzyme Corporation, Protocol No. 92-0902, Cambridge, Massachusetts.," *Fertil. Steril.*, vol. 69, no. 3, Art. no. 3, Mar. 1998, doi: 10.1016/S0015-0282(97)00573-6.

[4]   Y. Yeo *et al.*, "In situ cross-linkable hyaluronic acid hydrogels prevent post-operative abdominal adhesions in a rabbit model," *Biomaterials*, vol. 27, no. 27, Art. no. 27, Sep. 2006, doi: 10.1016/j.biomaterials.2006.04.043.

[5]   C. Wang, K. Zhang, H. Wang, S. Xu, and C. C. Han, "Evaluation of biodegradability of poly (DL-lactic-co-glycolic acid) scaffolds for post-surgical adhesion prevention: In vitro, in rats and in pigs," *Polymer*, vol. 61, pp. 174–182, Mar. 2015, doi: 10.1016/j.polymer.2015.02.001.

[6]   K. Kramer, N. Senninger, H. Herbst, and W. Probst, "Effective Prevention of Adhesions With Hyaluronate," *Arch. Surg.*, vol. 137, no. 3, Art. no. 3, Mar. 2002, doi: 10.1001/archsurg.137.3.278.

[7]   J. Jin *et al.*, "Human Peritoneal Membrane Controls Adhesion Formation and Host Tissue Response Following Intra-Abdominal Placement in a Porcine Model," *J. Surg. Res.*, vol. 156, no. 2, Art. no. 2, Oct. 2009, doi: 10.1016/j.jss.2009.04.010.

[8]   C. L. Garrard, R. H. Clements, L. Nanney, J. M. Davidson, and W. O. Richards, "Adhesion formation is reduced after laparoscopic surgery," *Surg. Endosc.*, vol. 13, no. 1, pp. 10–13, Jan. 1999, doi: 10.1007/s004649900887.

[9]   B. V. Pham *et al.*, "Pilot comparison of adhesion formation following colonic perforation and repair in a pig model using a transgastric, laparoscopic, or open surgical technique," *Endoscopy*, vol. 40, no. 8, pp. 664–669, Aug. 2008, doi: 10.1055/s-2008-1077436.

[10]   M. P. Diamond, K. Stecco, and A. J. Paulson, "Use of the PROACT™ System for reduction of postsurgical peritoneal adhesions," *Fertil. Steril.*, vol. 79, no. 1, pp. 198–202, Jan. 2003, doi: 10.1016/S0015-0282(02)04541-7.

[11]   V. Kanikireddy, K. Varaprasad, T. Jayaramudu, C. Karthikeyan, and R. Sadiku, "Carboxymethyl cellulose-based materials for infection control and wound healing: A review," *Int. J. Biol. Macromol.*, vol. 164, pp. 963–975, Dec. 2020, doi: 10.1016/j.ijbiomac.2020.07.160.

[12]   G. Wei, C. Zhou, G. Wang, L. Fan, K. Wang, and X. Li, "Keratinocyte Growth Factor Combined with a Sodium Hyaluronate Gel Inhibits Postoperative Intra-Abdominal Adhesions," *Int. J. Mol. Sci.*, vol. 17, no. 10, p. 1611, Sep. 2016, doi: 10.3390/ijms17101611.

[13]   M. M. P. J. Reijnen, E. M. Skrabut, V. A. Postma, J. W. Burns, and H. van Goor, "Polyanionic Polysaccharides Reduce Intra-abdominal Adhesion and Abscess Formation in a Rat Peritonitis Model," *J. Surg. Res.*, vol. 101, no. 2, pp. 248–253, Dec. 2001, doi: 10.1006/jsre.2001.6288.

[14]   S. Yamaner, M. Kalayci, U. Barbaros, E. Balik, and T. Bulut, "Does Hyaluronic Acid-Carboxymethylcellulose (HA-CMC) Membrane Interfere With the Healing of Intestinal Suture Lines and Abdominal Incisions?," *Surg. Innov.*, vol. 12, no. 1, pp. 37–41, Mar. 2005, doi: 10.1177/155335060501200106.

[15]   C. J. J. M. Sikkink, B. de Man, R. P. Bleichrodt, and H. van Goor, "Auto-Cross-Linked Hyaluronic Acid Gel Does Not Reduce Intra-Abdominal Adhesions or Abscess Formation in a Rat Model of Peritonitis," *J. Surg. Res.*, vol. 136, no. 2, pp. 255–259, Dec. 2006, doi: 10.1016/j.jss.2006.06.021.

[16]   Z. Cohen *et al.*, "Prevention of Postoperative Abdominal Adhesions by a Novel, Glycerol/Sodium Hyaluronate/Carboxymethylcellulose-Based Bioresorbable Membrane: A Prospective, Randomized,

Evaluator-Blinded Multicenter Study," *Dis. Colon Rectum*, vol. 48, no. 6, pp. 1130–1139, Jun. 2005, doi: 10.1007/s10350-004-0954-8.

[17] J. S. Park *et al.*, "An Assessment of the Effects of a Hyaluronan-Based Solution on Reduction of Postsurgical Adhesion Formation in Rats: A Comparative Study of Hyaluronan-Based Solution and Two Film Barriers," *J. Surg. Res.*, vol. 168, no. 1, pp. 49–55, Jun. 2011, doi: 10.1016/j.jss.2009.09.025.

[18] A. B. G. Lansdown, *Silver in Healthcare*. 2010. doi: 10.1039/9781849731799.

[19] F. Suska *et al.*, "In vivo evaluation of noble metal coatings," *J. Biomed. Mater. Res. B Appl. Biomater.*, vol. 92B, no. 1, pp. 86–94, 2010, doi: 10.1002/jbm.b.31492.

[20] P. Sioshansi, "New processes for surface treatment of catheters," *Artif. Organs*, vol. 18, no. 4, pp. 266–271, Apr. 1994, doi: 10.1111/j.1525-1594.1994.tb02193.x.

[21] M. K. Dasgupta, "Silver peritoneal catheters reduce bacterial colonization," *Adv. Perit. Dial. Conf. Perit. Dial.*, vol. 10, pp. 195–198, Jan. 1994.

[22] J. H. Crabtree, R. J. Burchette, R. A. Siddiqi, I. T. Huen, L. L. Hadnott, and A. Fishman, "The Efficacy of Silver-Ion Implanted Catheters in Reducing Peritoneal Dialysis-Related Infections," *Perit. Dial. Int.*, vol. 23, no. 4, pp. 368–374, Jul. 2003, doi: 10.1177/089686080302300410.

[23] G. Gosheger *et al.*, "Silver-coated megaendoprostheses in a rabbit model—an analysis of the infection rate and toxicological side effects," *Biomaterials*, vol. 25, no. 24, pp. 5547–5556, Nov. 2004, doi: 10.1016/j.biomaterials.2004.01.008.

[24] P. L. Nadworny, J. Wang, E. E. Tredget, and R. E. Burrell, "Anti-inflammatory activity of nanocrystalline silver-derived solutions in porcine contact dermatitis," *J. Inflamm.*, vol. 7, no. 1, Art. no. 1, Feb. 2010, doi: 10.1186/1476-9255-7-13.

[25] P. L. Nadworny, J. Wang, E. E. Tredget, and R. E. Burrell, "Anti-inflammatory activity of nanocrystalline silver in a porcine contact dermatitis model," *Nanomedicine Nanotechnol. Biol. Med.*, vol. 4, no. 3, Art. no. 3, Sep. 2008, doi: 10.1016/j.nano.2008.04.006.

[26] P. L. Nadworny, B. K. Landry, J. Wang, E. E. Tredget, and R. E. Burrell, "Does nanocrystalline silver have a transferable effect?," *Wound Repair Regen.*, vol. 18, no. 2, Art. no. 2, 2010, doi: 10.1111/j.1524-475X.2010.00579.x.

[27] N. Hoffmann *et al.*, "Choice of Hemostatic Agent Influences Adhesion Formation in a Rat Cecal Adhesion Model," *J. Surg. Res.*, vol. 155, pp. 77–81, Nov. 2008, doi: 10.1016/j.jss.2008.08.008.

[28] G. Wei *et al.*, "Gallic Acid Attenuates Postoperative Intra-Abdominal Adhesion by Inhibiting Inflammatory Reaction in a Rat Model," *Med. Sci. Monit. Int. Med. J. Exp. Clin. Res.*, vol. 24, pp. 827–838, Feb. 2018, doi: 10.12659/MSM.908550.

[29] H. G. Yilmaz, I. H. Tacyildiz, C. Keles, E. Gedik, and N. Kilinc, "Micronized purified flavonoid fraction may prevent formation of intraperitoneal adhesions in rats," *Fertil. Steril.*, vol. 84, pp. 1083–1088, Oct. 2005, doi: 10.1016/j.fertnstert.2005.03.076.

[30] A. H. Maciver, M. McCall, and A. M. James Shapiro, "Intra-abdominal adhesions: Cellular mechanisms and strategies for prevention," *Int. J. Surg.*, vol. 9, no. 8, pp. 589–594, Jan. 2011, doi: 10.1016/j.ijsu.2011.08.008.

[31] P. A. Lucas, D. J. Warejcka, H. E. Young, and B. Y. Lee, "Formation of Abdominal Adhesions Is Inhibited by Antibodies to Transforming Growth Factor-β1," *J. Surg. Res.*, vol. 65, no. 2, pp. 135–138, Oct. 1996, doi: 10.1006/jsre.1996.0355.

[32] R. T. Beyene, S. L. Kavalukas, and A. Barbul, "Intra-abdominal adhesions: Anatomy, physiology, pathophysiology, and treatment," *Curr. Probl. Surg.*, vol. 52, no. 7, pp. 271–319, Jul. 2015, doi: 10.1067/j.cpsurg.2015.05.001.

Chapter 9 : Conclusions

The purpose of this research was to study the chemical, physical, and *in vitro* biological properties of nanocrystalline silver and silver-gold materials to prepare for studying their effectiveness when applied to *in vivo* wound environments.

Chapter 3 demonstrated the effectiveness of Novel sputtering parameters in creating films for dressings. As expected, a higher current resulted in the most silver deposition, but with a lower percentage of silver oxide than Standard films. The sputtering parameters, particularly the oxygen concentration in argon gas and the current, were chosen to maximize the amount of silver deposition while maintaining the ammonia soluble silver in the range of approximately 40-50%. The Novel films created in this study had an average of 38% ammonia soluble silver. The role of oxygen is well understood for its effect on the resulting films, but it is unclear what the benefit of water when studying film properties. Water may have been effective in creating an ideal environment for dressing stability and this could be an area for further study. In solution, Novel samples released more silver in quantity, but not in percentage of total silver. Standard samples released more silver in water by percentage, which may relate to the bonding strength or the greater surface area seen in the SEM images. SEM also showed that when dissolved in solution, patches of the film structure were severely disrupted, but some areas were only affected minimally on the surface. The smaller grain size for Standard sample is likely related to the greater percentage of ammonia soluble silver (58%) compared to Novel samples. It will be seen in the future dermal model animal study if composition and grain size matters more to healing properties than just raw quantity of silver. An interesting observation from this work was that in some cases, after soaking the film in water the measured ammonia soluble silver was greater than before. The hypothesis for this phenomenon is that interactions with water are changing the compounds on the surface of the film. Both Standard and Novel samples had excellent log reductions, but Novel had better longevity. In the CZOI test, Novel samples had measurable zones after nine days, while 35.9% of the initial silver in the sample was still remaining versus 11.45% remaining for Standard.

In the *in vitro* experiments in Chapter 4, all nanocrystalline silver and silver-gold samples had good antibacterial properties, especially for short term log reductions, but the physical and chemical properties are of great interest. The unusual trends in grain size and unexpectedly high deposition for Ag35, especially preferentially for gold over silver, are interesting areas for further study. Grain size for Standard samples followed the expected trend of decreasing with increasing gold concentration. However, Ag65 Novel had an unexpectedly small grain size, disrupting the trend for Novel samples. This may be a

limitation of the number of samples and may not be seen with replication of the study. However, it is interesting that Ag65 Novel and Ag65 Standard had both a similar grain size and a similar percentage of ammonia soluble, suggesting that similarities in composition would result in similar grain size. Ag35 and Ag100 did not have similar ammonia soluble percentages between Standard and Novel samples and had significantly different grain sizes. More silver was released in solution by Ag35 than would be expected compared to Ag100 samples, as its release was greater than 35% of the silver released by Ag100. This is especially notable as less silver was sputtered onto Ag35 samples than nominal alloy composition would suggest. Ag65 and Ag35 samples released similar amount of silver into solution, which may be relevant for upcoming animal studies if Ag35 samples are able to release silver or gold more rapidly into the wound environment. However, release of silver into water is limited in its comparison to *in vivo* wound environments so further research is needed.

While gold has been used for modern medical applications for decades, there is limited research on the comparison of gold and silver in reducing inflammation *in vivo*, especially for an animal model that has a similar healing profile to humans. This demonstrates the need for further research to compare the effect of silver and gold in reducing dermal inflammation. This may have significant clinical applications for wound and burn dressings in the future. The most important metric from the dermal animal study is overall healing, as this matters most to patients and clinicians. However, the distinction between Standard and Novel conditions or even alloy composition may not be seen in edema and erythema scores, but instead will be seen in serum and tissue concentrations of cytokines. Another interesting outcome of this study will be to see the silver and gold compounds will be found in the tissue and what the spatial distribution is.

In the experiments in Chapter 6 with increasing the silver concentration in solution, it was found that the simple and rapid methods would not work. Increasing concentration in solution seems mostly to depend on film properties to release silver, not the properties of dissolution, although ensuring good contact of the water with the coated surface or the film is important. Heating the silver solution causes agglomeration as seen by the colour change seen in heated solutions. pH did not have a consistent effect on log reductions. These experiments also indicated that dressing age may be a source of further study as some dressing properties, particularly silver release into solution, seem to be impacted by dressing age.

In Chapter 7, the polymer in solution properties were as expected, with shear thinning properties and a viscosity decrease of between 65 and 80% depending on the sample and test. In Test 1, it appeared that the higher the initial viscosity, the greater the percentage viscosity drop, but this was not found in Test 2

with similar conditions. Only 25-40% of the silver was released at 72 hours when the test was completed, although AAS results were found to have uncertain accuracy. A final burst to release the remaining silver is expected from literature and would likely occur with more time. However, this study was limited in that the dialysis cassette kept the gel from spreading as it might *in vivo* and gel fragments above 10 000 Da were not released from the dialysis cassette. It is also possible that not all silver thought to be in solution was incorporated into the gel, or the silver binds to the polymers strongly and would not be released without further degradation of the polymers. Another challenge with this experiment that will also be present in experiments in the abdominal cavity, is the likely formation of silver chloride.

There were no consistent trends with pH for viscosity reduction or silver release. In the pH range used, there isn't an expected disruption of the polymer structure and therefore would not affect silver release. However, this information is still relevant as there may be future applications where pH is important to treatment or healing properties. Log reductions on a sample of silver released in PBS were not significantly different from control samples. It is likely because very little silver is released in the first few hours, which is when they were performed, and is the period of time post-surgery that is most important to prevent infection. In a separate experiment of log reductions combining BSA, silver gels, and a bacterial inoculum, the log reductions were still low. This is likely due to only a small amount of silver was available for contact with the bacteria. The gel sticks together even after shaking, and therefore most of the silver stays protected from contact with bacteria. In addition, the silver released would interact with the chloride and proteins found in BSA. This may mean that the antibacterial properties of silver are not likely to be relevant available for the gel applied in abdominal cavity but may still have an impact on inflammation while also providing a barrier to prevent adhesions from forming. The effectiveness of nanocrystalline silver in dressing form and gel form will be seen in the upcoming animal study. External application of nanocrystalline silver is expected to provide anti-inflammatory benefits and help prevent infection of the external surgical wound. The internal application of a HA-CMC silver gel will have less silver incorporated than the silver dressing but will be directly applied to also form a physical barrier between inflamed tissue surfaces.

Bibliography

Acharya, Ghanashyam, Crystal S. Shin, Kumar Vedantham, Matthew McDermott, Thomas Rish, Keith Hansen, Yourong Fu, and Kinam Park. 2010. "A Study of Drug Release from Homogeneous PLGA Microstructures." *Journal of Controlled Release*, Nanomedicine and Drug Delivery (NanoDDS'09), 146 (2): 201–6. https://doi.org/10.1016/j.jconrel.2010.03.024.

Akerberg, Daniel, Carl Grunditz, Monika Posaric-Bauden, Karolin Isaksson, Roland Andersson, and Bobby Tingstedt. 2012. "The Influence on Abdominal Adhesions and Inflammation in Rabbits after Exposure to Differently Charged Polypeptides" 2012 (July). https://doi.org/10.4236/jbise.2012.58055.

Albers, Christoph E., Wilhelm Hofstetter, Klaus A. Siebenrock, Regine Landmann, and Frank M. Klenke. 2013. "*In Vitro* Cytotoxicity of Silver Nanoparticles on Osteoblasts and Osteoclasts at Antibacterial Concentrations." *Nanotoxicology* 7 (1): 30–36. https://doi.org/10.3109/17435390.2011.626538.

Alhajj, Mandy, Muhammad Zubair, and Aisha Farhana. 2024. "Enzyme Linked Immunosorbent Assay." In *StatPearls*. Treasure Island (FL): StatPearls Publishing. http://www.ncbi.nlm.nih.gov/books/NBK555922/.

Allègre, Lucie, Isabelle Le Teuff, Salomé Leprince, Sophie Warembourg, Hubert Taillades, Xavier Garric, Vincent Letouzey, and Stephanie Huberlant. 2018. "A New Bioabsorbable Polymer Film to Prevent Peritoneal Adhesions Validated in a Post-Surgical Animal Model." *PLoS ONE* 13 (11): e0202285. https://doi.org/10.1371/journal.pone.0202285.

Anderson, Brian C, Nita K Pandit, and Surya K Mallapragada. 2001. "Understanding Drug Release from Poly(Ethylene Oxide)-b-Poly(Propylene Oxide)-b-Poly(Ethylene Oxide) Gels." *Journal of Controlled Release* 70 (1): 157–67. https://doi.org/10.1016/S0168-3659(00)00341-2.

Araújo, J., E. Vega, C. Lopes, M. A. Egea, M. L. Garcia, and E. B. Souto. 2009. "Effect of Polymer Viscosity on Physicochemical Properties and Ocular Tolerance of FB-Loaded PLGA Nanospheres." *Colloids and Surfaces B: Biointerfaces* 72 (1): 48–56. https://doi.org/10.1016/j.colsurfb.2009.03.028.

Araújo, Raimundo Fernandes de, Aurigena Antunes de Araújo, Jonas Bispo Pessoa, Franscisco Paulo Freire Neto, Gisele Ribeiro da Silva, Ana Luiza C. S. Leitão Oliveira, Thaís Gomes de Carvalho, et al. 2017. "Anti-Inflammatory, Analgesic and Anti-Tumor Properties of Gold Nanoparticles." *Pharmacological Reports* 69 (1): 119–29. https://doi.org/10.1016/j.pharep.2016.09.017.

Arnold, Peter B, Colleen W Green, Pamela A Foresman, and George T Rodeheaver. 2000. "Evaluation of Resorbable Barriers for Preventing Surgical Adhesions." *Fertility and Sterility* 73 (1): 157–61. https://doi.org/10.1016/S0015-0282(99)00464-1.

AshaRani, PV, Swaminathan Sethu, Hui Kheng Lim, Ganapathy Balaji, Suresh Valiyaveettil, and M. Prakash Hande. 2012. "Differential Regulation of Intracellular Factors Mediating Cell Cycle, DNA Repair and Inflammation Following Exposure to Silver Nanoparticles in Human Cells." *Genome Integrity* 3 (1): 2. https://doi.org/10.1186/2041-9414-3-2.

Avital, Shmuel, Thomas J. Bollinger, James D. Wilkinson, Floriano Marchetti, Michael D. Hellinger, and Laurence R. Sands. 2005. "Preventing Intra-Abdominal Adhesions With Polylactic Acid Film: An Animal Study." *Diseases of the Colon & Rectum* 48 (1): 153–57. https://doi.org/10.1007/s10350-004-0748-z.

Banakh, O, P.E Schmid, R Sanjinés, and F Lévy. 2002. "Electrical and Optical Properties of TiOx Thin Films Deposited by Reactive Magnetron Sputtering." *Surface and Coatings Technology* 151–152:272–75. https://doi.org/10.1016/S0257-8972(01)01605-X.

Basu, Poulami, Uttamchand Narendrakumar, Ruckmani Arunachalam, Sobita Devi, and Inderchand Manjubala. 2018. "Characterization and Evaluation of Carboxymethyl Cellulose-Based Films for Healing of Full-Thickness Wounds in Normal and Diabetic Rats." *ACS Omega* 3 (10): 12622–32. https://doi.org/10.1021/acsomega.8b02015.

Bayhan, Zulfu, Sezgin Zeren, Fatma Emel Kocak, Cengiz Kocak, Raziye Akcılar, Ertugrul Kargı, Cagrı Tiryaki, Faik Yaylak, and Aydın Akcılar. 2016. "Antiadhesive and Anti-Inflammatory Effects of

Pirfenidone in Postoperative Intra-Abdominal Adhesion in an Experimental Rat Model." *Journal of Surgical Research* 201 (2): 348–55. https://doi.org/10.1016/j.jss.2015.11.033.

Beer, Christiane, Rasmus Foldbjerg, Yuya Hayashi, Duncan S. Sutherland, and Herman Autrup. 2012. "Toxicity of Silver Nanoparticles—Nanoparticle or Silver Ion?" *Toxicology Letters* 208 (3): 286–92. https://doi.org/10.1016/j.toxlet.2011.11.002.

Bellocq, Agnès, Sidonie Suberville, Carole Philippe, France Bertrand, Joëlle Perez, Bruno Fouqueray, Gisèle Cherqui, and Laurent Baud. 1998. "Low Environmental pH Is Responsible for the Induction of Nitric-Oxide Synthase in Macrophages." *Journal of Biological Chemistry* 273 (9): 5086–92. https://doi.org/10.1074/jbc.273.9.5086.

Bello-Guerrero, Jorge Alberto, César Alberto Cruz-Santiago, and Javier Luna-Martínez. 2016a. "Pirfenidone vs Sodium Hyaluronate/Carboxymethyl Cellulose as Prevention of the Formation of Intra-Abdominal Adhesions After Colonic Surgery. A Randomized Study in an Experimental Model." *Cirugía Española (English Edition)* 94 (1): 31–37. https://doi.org/10.1016/j.cireng.2015.06.013.

Benchabane, Adel, and Karim Bekkour. 2008. "Rheological Properties of Carboxymethyl Cellulose (CMC) Solutions." *Colloid and Polymer Science* 286 (10): 1173–80. https://doi.org/10.1007/s00396-008-1882-2.

Berkesoglu, Mustafa, Yasemin Yuyucu Karabulut, Didem Derici Yildirim, Ozgur M. Turkmenoglu, and Musa M. Dirlik. 2020. "Topical Application of High-Dose Mesna Prevents Adhesion Formation: An Experimental Animal Study." *Journal of Surgical Research* 251 (July):152–58. https://doi.org/10.1016/j.jss.2020.01.027.

Bermejo-Barrera, P., A. Moreda-Piñeiro, and A. Bermejo-Barrera. 1996. "Study of Chemical Modifiers for Direct Determination of Silver in Sea Water by ETA-AAS with Deuterium Background Correction." *Talanta* 43 (1): 35–44. https://doi.org/10.1016/0039-9140(95)01702-X.

Best, Sabine L., and Peter J. Sadler. 1996. "Gold Drugs: Mechanism of Action and Toxicity." *Gold Bulletin* 29 (3): 87–93. https://doi.org/10.1007/BF03214741.

Betz, G. 1980. "Alloy Sputtering." *Surface Science* 92 (1): 283–309. https://doi.org/10.1016/0039-6028(80)90258-7.

Beyene, Robel T., Sandra L. Kavalukas, and Adrian Barbul. 2015. "Intra-Abdominal Adhesions: Anatomy, Physiology, Pathophysiology, and Treatment." *Current Problems in Surgery* 52 (7): 271–319. https://doi.org/10.1067/j.cpsurg.2015.05.001.

Biondo-Simões, Maria De Lourdes Pessole, Wagner Augusto Schiel, Mayara Arantes, Tatiane Da Silveira, Rogério Ribeiro Robes, and Flávio Daniel Saavedra Tomasich. 2016. "Comparison between Polypropylene and Polypropylene with Poliglecaprone Meshes on Intraperitoneal Adhesion Formation." *Revista Do Colégio Brasileiro de Cirurgiões* 43 (December):416–23. https://doi.org/10.1590/0100-69912016006002.

Boland, Genevieve M., and Ronald J. Weigel. 2006. "Formation and Prevention of Postoperative Abdominal Adhesions." *Journal of Surgical Research* 132 (1): 3–12. https://doi.org/10.1016/j.jss.2005.12.002.

Boonkaew, Benjawan, Margit Kempf, Roy Kimble, Pitt Supaphol, and Leila Cuttle. 2014. "Antimicrobial Efficacy of a Novel Silver Hydrogel Dressing Compared to Two Common Silver Burn Wound Dressings: Acticoat™ and PolyMem Silver®." *Burns* 40 (1): 89–96. https://doi.org/10.1016/j.burns.2013.05.011.

Borrazzo, E. C., M. F. Belmont, D. Boffa, and D. L. Fowler. 2004. "Effect of Prosthetic Material on Adhesion Formation after Laparoscopic Ventral Hernia Repair in a Porcine Model." *Hernia* 8 (2): 108–12. https://doi.org/10.1007/s10029-003-0181-6.

Bragg, P. D., and D. J. Rainnie. 1974. "The Effect of Silver Ions on the Respiratory Chain of *Escherichia Coli*." *Canadian Journal of Microbiology* 20 (6): 883–89. https://doi.org/10.1139/m74-135.

Bresson, Lucie, Eric Leblanc, Anne Sophie Lemaire, Teru Okitsu, and Feng Chai. 2017. "Autologous Peritoneal Grafts Permit Rapid Reperitonealization and Prevent Postoperative Abdominal

Adhesions in an Experimental Rat Study." *Surgery* 162 (4): 863–70. https://doi.org/10.1016/j.surg.2017.05.005.

Broek, Richard P. G. ten, Yama Issa, Evert J. P. van Santbrink, Nicole D. Bouvy, Roy F. P. M. Kruitwagen, Johannes Jeekel, Erica A. Bakkum, Maroeska M. Rovers, and Harry van Goor. 2013. "Burden of Adhesions in Abdominal and Pelvic Surgery: Systematic Review and Met-Analysis." *BMJ* 347 (October):f5588. https://doi.org/10.1136/bmj.f5588.

Brüggmann, Dörthe, Garri Tchartchian, Markus Wallwiener, Karsten Münstedt, Hans-Rudolf Tinneberg, and Andreas Hackethal. 2010. "Intra-Abdominal Adhesions." *Deutsches Ärzteblatt International* 107 (44): 769–75. https://doi.org/10.3238/arztebl.2010.0769.

Bryaskova, Rayna, Nelly Georgieva, Tonya Andreeva, and Rumiana Tzoneva. 2013. "Cell Adhesive Behavior of PVA-Based Hybrid Materials with Silver Nanoparticles." *Surface and Coatings Technology* 235 (November):186–91. https://doi.org/10.1016/j.surfcoat.2013.07.032.

Buhus, Gabriela, Marcel Popa, and Jacques Desbrieres. 2009. "Hydrogels Based on Carboxymethylcellulose and Gelatin for Inclusion and Release of Chloramphenicol." *Journal of Bioactive and Compatible Polymers* 24 (6): 525–45. https://doi.org/10.1177/0883911509349687.

Burke, L D, and P F Nugent. 1998. "The Electrochemistry of Gold: II the Electrocatalytic Behaviour of the Metal in Aqueous Media." *Gold Bulletin* 31 (2): 39–50. https://doi.org/10.1007/BF03214760.

Burrell, Robert. 2021. Personal Communication.

Burrell, Robert E., and Patricia Nadworny. 2010a. "Nanocrystalline Silver: Novel Structure and Activity." In *The Third International Conference on the Development of Biomedical Engineering in Vietnam*, edited by Vo Van Toi and Truong Quang Dang Khoa, 27:6–9. IFMBE Proceedings. Berlin, Heidelberg: Springer Berlin Heidelberg. https://doi.org/10.1007/978-3-642-12020-6_2.

Calamai, Paola, Stefania Carotti, Annalisa Guerri, Luigi Messori, Enrico Mini, Pierluigi Orioli, and Gian Paolo Speroni. 1997a. "Biological Properties of Two Gold(III) Complexes: AuCl3 (Hpm) and AuCl2 (Pm)." *Journal of Inorganic Biochemistry* 66 (2): 103–9. https://doi.org/10.1016/S0162-0134(96)00190-0.

Carvalho, Isabel, Nicolina Dias, Mariana Henriques, Sebastian Calderon V, Paulo Ferreira, Albano Cavaleiro, and Sandra Carvalho. 2020. "Antibacterial Effects of Bimetallic Clusters Incorporated in Amorphous Carbon for Stent Application." *ACS Applied Materials & Interfaces* 12 (22): 24555–63. https://doi.org/10.1021/acsami.0c02821.

Carvalho, Thaís Gomes de, Vinícius Barreto Garcia, Aurigena Antunes de Araújo, Luiz Henrique da Silva Gasparotto, Heloiza Silva, Gerlane Coelho Bernardo Guerra, Emilio de Castro Miguel, et al. 2018a. "Spherical Neutral Gold Nanoparticles Improve Anti-Inflammatory Response, Oxidative Stress and Fibrosis in Alcohol-Methamphetamine-Induced Liver Injury in Rats." *International Journal of Pharmaceutics* 548 (1): 1–14. https://doi.org/10.1016/j.ijpharm.2018.06.008.

Cassidy, Michael R., Alan C. Sherburne, Stanley J. Heydrick, and Arthur F. Stucchi. 2015. "Combined Intraoperative Administration of a Histone Deacetylase Inhibitor and a Neurokinin-1 Receptor Antagonist Synergistically Reduces Intra-Abdominal Adhesion Formation in a Rat Model." *Surgery* 157 (3): 581–89. https://doi.org/10.1016/j.surg.2014.09.031.

Catena, Fausto, Luca Ansaloni, Salomone Di Saverio, Antonio D. Pinna, and On Behalf of the World Society of Emergency Surgery. 2012a. "P.O.P.A. Study: Prevention of Postoperative Abdominal Adhesions by Icodextrin 4% Solution After Laparotomy for Adhesive Small Bowel Obstruction. A Prospective Randomized Controlled Trial." *Journal of Gastrointestinal Surgery* 16 (2): 382–88. https://doi.org/10.1007/s11605-011-1736-y.

Cavanagh, Marion H, Robert E Burrell, and Patricia L Nadworny. 2010. "Evaluating Antimicrobial Efficacy of New Commercially Available Silver Dressings." *International Wound Journal* 7 (5): 394–405. https://doi.org/10.1111/j.1742-481X.2010.00705.x.

Cesta, Maria Candida, Mara Zippoli, Carolina Marsiglia, Elizabeth Marie Gavioli, Flavio Mantelli, Marcello Allegretti, and Robert A. Balk. 2022. "The Role of Interleukin-8 in Lung Inflammation and Injury: Implications for the Management of COVID-19 and Hyperinflammatory Acute

Respiratory Distress Syndrome." *Frontiers in Pharmacology* 12 (January). https://doi.org/10.3389/fphar.2021.808797.

Charboneau, Alex J., John P. Delaney, and Greg Beilman. 2018. "Fucoidans Inhibit the Formation of Post-Operative Abdominal Adhesions in a Rat Model." *PLOS ONE* 13 (11): e0207797. https://doi.org/10.1371/journal.pone.0207797.

Choi, P, and H Reiser. 1998. "IL-4: Role in Disease and Regulation of Production." *Clinical and Experimental Immunology* 113 (3): 317–19. https://doi.org/10.1046/j.1365-2249.1998.00690.x.

Cohen, Zane, Anthony J. Senagore, Merril T. Dayton, Mark J. Koruda, David E. Beck, Bruce G. Wolff, Phillip R. Fleshner, et al. 2005. "Prevention of Postoperative Abdominal Adhesions by a Novel, Glycerol/Sodium Hyaluronate/Carboxymethylcellulose-Based Bioresorbable Membrane: A Prospective, Randomized, Evaluator-Blinded Multicenter Study." *Diseases of the Colon & Rectum* 48 (6): 1130–39. https://doi.org/10.1007/s10350-004-0954-8.

Corona, Roberta, Jasper Verguts, Ron Schonman, Maria Mercedes Binda, Karina Mailova, and Philippe Robert Koninckx. 2011. "Postoperative Inflammation in the Abdominal Cavity Increases Adhesion Formation in a Laparoscopic Mouse Model." *Fertility and Sterility* 95 (4): 1224–28. https://doi.org/10.1016/j.fertnstert.2011.01.004.

Crabtree, John H., Raoul J. Burchette, Rukhsana A. Siddiqi, Isan T. Huen, Linda L Hadnott, and Arnold Fishman. 2003. "The Efficacy of Silver-Ion Implanted Catheters in Reducing Peritoneal Dialysis-Related Infections." *Peritoneal Dialysis International* 23 (4): 368–74. https://doi.org/10.1177/089686080302300410.

Dasgupta, M K. 1994. "Silver Peritoneal Catheters Reduce Bacterial Colonization." *Advances in Peritoneal Dialysis Conference on Peritoneal Dialysis* 10 (January):195–98.

Diamond, Michael P, Kathy Stecco, and Amelia J Paulson. 2003. "Use of the PROACT™ System for Reduction of Postsurgical Peritoneal Adhesions." *Fertility and Sterility* 79 (1): 198–202. https://doi.org/10.1016/S0015-0282(02)04541-7.

Dogsa, Iztok, Matija Tomšič, Janez Orehek, Elizabeta Benigar, Andrej Jamnik, and David Stopar. 2014. "Amorphous Supramolecular Structure of Carboxymethyl Cellulose in Aqueous Solution at Different pH Values as Determined by Rheology, Small Angle X-Ray and Light Scattering." *Carbohydrate Polymers* 111 (October):492–504. https://doi.org/10.1016/j.carbpol.2014.04.020.

Dreger, Nathan Z., Zachary K. Zander, Yen-Hao Hsu, Derek Luong, Peiru Chen, Nancy Le, Trenton Parsell, et al. 2019. "Zwitterionic Amino Acid-Based Poly(Ester Urea)s Suppress Adhesion Formation in a Rat Intra-Abdominal Cecal Abrasion Model." *Biomaterials* 221 (November):119399. https://doi.org/10.1016/j.biomaterials.2019.119399.

Ellis, Harold, and Alison Crowe. 2009. "Medico-Legal Consequences of Post-Operative Intra-Abdominal Adhesions." *International Journal of Surgery* 7 (3): 187–91. https://doi.org/10.1016/j.ijsu.2009.04.004.

Ersoy, Eren, Vedat Ozturk, Aylin Yazgan, Mehmet Ozdogan, and Haldun Gundogdu. 2008. "Effect of Polylactic Acid Film Barrier on Intra-Abdominal Adhesion Formation." *Journal of Surgical Research* 147 (1): 148–52. https://doi.org/10.1016/j.jss.2007.09.005.

Esposito, Anthony J., Stanley J. Heydrick, Michael R. Cassidy, Joseph Gallant, Arthur F. Stucchi, and James M. Becker. 2013. "Substance P Is an Early Mediator of Peritoneal Fibrinolytic Pathway Genes and Promotes Intra-Abdominal Adhesion Formation." *Journal of Surgical Research* 181 (1): 25–31. https://doi.org/10.1016/j.jss.2012.05.056.

Falabella, Christine A., Mark M. Melendez, Lihui Weng, and Weiliam Chen. 2010. "Novel Macromolecular Crosslinking Hydrogel to Reduce Intra-Abdominal Adhesions." *Journal of Surgical Research* 159 (2): 772–78. https://doi.org/10.1016/j.jss.2008.09.035.

Fan, Fu-Ren F., and Allen J. Bard. 2002a. "Chemical, Electrochemical, Gravimetric, and Microscopic Studies on Antimicrobial Silver Films." *The Journal of Physical Chemistry B* 106 (2): 279–87. https://doi.org/10.1021/jp012548d.

Fang, Yicheng, Nan Zhang, Qi Li, Jianting Chen, Subin Xiong, and Weisan Pan. 2019. "Characterizing the Release Mechanism of Donepezil-Loaded PLGA Microspheres in Vitro and in Vivo." *Journal*

of Drug Delivery Science and Technology 51 (June):430–37. https://doi.org/10.1016/j.jddst.2019.03.029.

Feng, Bin, Tatsuya Yokoi, Akihito Kumamoto, Masato Yoshiya, Yuichi Ikuhara, and Naoya Shibata. 2016. "Atomically Ordered Solute Segregation Behaviour in an Oxide Grain Boundary." *Nature Communications* 7 (1): 11079. https://doi.org/10.1038/ncomms11079.

Ferland, R., D. Mulani, and P.K. Campbell. 2001. "Evaluation of a Sprayable Polyethylene Glycol Adhesion Barrier in a Porcine Efficacy Model." *Human Reproduction* 16 (12): 2718–23. https://doi.org/10.1093/humrep/16.12.2718.

Fitzpatrick, M. E*, A. T. Fry, P* Holdway, F. A. Kandil, J* Shackleton, and L. Suominen. 2005. "Determination of Residual Stresses by X-Ray Diffraction." Report/Guide. Teddington. September 2005. https://eprintspublications.npl.co.uk/2391/.

Foster, Deshka S., Clement D. Marshall, Gunsagar S. Gulati, Malini S. Chinta, Alan Nguyen, Ankit Salhotra, R. Ellen Jones, et al. 2020. "Elucidating the Fundamental Fibrotic Processes Driving Abdominal Adhesion Formation." *Nature Communications* 11 (1): 4061. https://doi.org/10.1038/s41467-020-17883-1.

Franková, Jana, Veronika Pivodová, Hana Vágnerová, Jana Juráňová, and Jitka Ulrichová. 2016. "Effects of Silver Nanoparticles on Primary Cell Cultures of Fibroblasts and Keratinocytes in a Wound-Healing Model." *Journal of Applied Biomaterials & Functional Materials* 14 (2): 137–42. https://doi.org/10.5301/jabfm.5000268.

Friedlander, R M, V Gagliardini, R J Rotello, and J Yuan. 1996. "Functional Role of Interleukin 1 Beta (IL-1 Beta) in IL-1 Beta-Converting Enzyme-Mediated Apoptosis." *Journal of Experimental Medicine* 184 (2): 717–24. https://doi.org/10.1084/jem.184.2.717.

Fu, Yan, Tao Gong, Jiaywei Tsauo, Mingchen Sang, He Zhao, Xiaowu Zhang, Jingui Li, and Xiao Li. 2021. "Nintedanib, a Multitarget Tyrosine Kinase Inhibitor, Suppresses Postoperative Peritoneal Adhesion Formation in a Rat Model." *Surgery* 170 (3): 806–12. https://doi.org/10.1016/j.surg.2021.03.055.

Fujii, Shoichi, Hiroshi Shimada, Hideyuki Ike, Chikara Kunisaki, Shigeo Ohki, Yasushi Ichikawa, Mitsuyoshi Ohta, Shigeru Yamagishi, and Shunichi Osada. 2009. "Reduction of Postoperative Abdominal Adhesion and Ileus by a Bioresorbable Membrane." *Hepato-Gastroenterology* 56 (91–92): 725–28.

Gaertner, Wolfgang B., Gonzalo F. Hagerman, Isaac Felemovicius, Margaret E. Bonsack, and John P. Delaney. 2008. "Two Experimental Models for Generating Abdominal Adhesions." *Journal of Surgical Research* 146 (2): 241–45. https://doi.org/10.1016/j.jss.2007.08.012.

García-Abuín, A., D. Gómez-Díaz, J. M. Navaza, L. Regueiro, and I. Vidal-Tato. 2011. "Viscosimetric Behaviour of Hyaluronic Acid in Different Aqueous Solutions." *Carbohydrate Polymers* 85 (3): 500–505. https://doi.org/10.1016/j.carbpol.2011.02.028.

Garrard, C. L., R. H. Clements, L. Nanney, J. M. Davidson, and W. O. Richards. 1999. "Adhesion Formation Is Reduced after Laparoscopic Surgery." *Surgical Endoscopy* 13 (1): 10–13. https://doi.org/10.1007/s004649900887.

Gatej, Iuliana, Marcel Popa, and Marguerite Rinaudo. 2005. "Role of the pH on Hyaluronan Behavior in Aqueous Solution." *Biomacromolecules* 6 (1): 61–67. https://doi.org/10.1021/bm040050m.

Goebel, Carsten, Malgorzata Kubicka-Muranyi, Torsten Tonn, José Gonzalez, and Ernst Gleichmann. 1995. "Phagocytes Render Chemicals Immunogenic: Oxidation of Gold(I) to the T Cell-Sensitizing Gold(III) Metabolite Generated by Mononuclear Phagocytes." *Archives of Toxicology* 69 (7): 450–59. https://doi.org/10.1007/s002040050198.

Goor, H. van. 2007. "Consequences and Complications of Peritoneal Adhesions." *Colorectal Disease: The Official Journal of the Association of Coloproctology of Great Britain and Ireland* 9 Suppl 2 (October):25–34. https://doi.org/10.1111/j.1463-1318.2007.01358.x.

Gosheger, Georg, Jendrik Hardes, Helmut Ahrens, Arne Streitburger, Horst Buerger, Michael Erren, Andreas Gunsel, Fritz H Kemper, Winfried Winkelmann, and Christof von Eiff. 2004. "Silver-Coated Megaendoprostheses in a Rabbit Model—an Analysis of the Infection Rate and

Toxicological Side Effects." *Biomaterials* 25 (24): 5547–56. https://doi.org/10.1016/j.biomaterials.2004.01.008.

Grade, Sebastian, Jörg Eberhard, Jurij Jakobi, Andreas Winkel, Meike Stiesch, and Stephan Barcikowski. 2014. "Alloying Colloidal Silver Nanoparticles with Gold Disproportionally Controls Antibacterial and Toxic Effects." *Gold Bulletin* 47 (1): 83–93. https://doi.org/10.1007/s13404-013-0125-6.

Grant, Hugh W., Michael C. Parker, Malcolm S. Wilson, Donald Menzies, Graham Sunderland, Jeremy N. Thompson, David N. Clark, Alastair D. Knight, Alison M. Crowe, and Harold Ellis. 2008. "Adhesions after Abdominal Surgery in Children." *Journal of Pediatric Surgery* 43 (1): 152–57. https://doi.org/10.1016/j.jpedsurg.2007.09.038.

Greenawalt, Keith E., M. Jude Colt, Rubina L. Corazzini, Megan C. Krauth, and Lena Holmdahl. 2011. "A Membrane Slurry Reduces Postoperative Adhesions in Rat Models of Abdominal Surgery." *Journal of Surgical Research* 168 (1): e25–30. https://doi.org/10.1016/j.jss.2010.02.009.

Greene, Arin K., Ian P. J. Alwayn, Vania Nose, Evelyn Flynn, David Sampson, David Zurakowski, Judah Folkman, and Mark Puder. 2005. "Prevention of Intra-Abdominal Adhesions Using the Antiangiogenic COX-2 Inhibitor Celecoxib." *Annals of Surgery* 242 (1): 140–46. https://doi.org/10.1097/01.sla.0000167847.53159.c1.

Grevious, Mark A., Mimis Cohen, Samir R. Shah, and Pedro Rodriguez. 2006. "Structural and Functional Anatomy of the Abdominal Wall." *Clinics in Plastic Surgery*, Abdominal Wall Reconstruction, 33 (2): 169–79. https://doi.org/10.1016/j.cps.2005.12.005.

Guisbiers, Grégory, Rubén Mendoza-Cruz, Lourdes Bazán-Díaz, J. Jesús Velázquez-Salazar, Rafael Mendoza-Perez, José Antonio Robledo-Torres, José-Luis Rodriguez-Lopez, Juan Martín Montejano-Carrizales, Robert L. Whetten, and Miguel José-Yacamán. 2016. "Electrum, the Gold–Silver Alloy, from the Bulk Scale to the Nanoscale: Synthesis, Properties, and Segregation Rules." *ACS Nano* 10 (1): 188–98. https://doi.org/10.1021/acsnano.5b05755.

Gura, E., M. Hückel, and P. -J. Müller. 1998. "Specific Degradation of Hyaluronic Acid and Its Rheological Properties." *Polymer Degradation and Stability*, Biodegradable Polymers and Macromolecules, 59 (1): 297–302. https://doi.org/10.1016/S0141-3910(97)00194-8.

Guthrie, Kathleen M., Ankit Agarwal, Dana S. Tackes, Kevin W. Johnson, Nicholas L. Abbott, Christopher J. Murphy, Charles J. Czuprynski, Patricia R. Kierski, Michael J. Schurr, and Jonathan F. McAnulty. 2012. "Antibacterial Efficacy of Silver-Impregnated Polyelectrolyte Multilayers Immobilized on a Biological Dressing in a Murine Wound Infection Model." *Annals of Surgery* 256 (2): 371–77. https://doi.org/10.1097/SLA.0b013e318256ff99.

Habib, SK, A Rizk, and IA Mousa. 1998. "Physical Parameters Affecting Deposition Rates of Binary Alloys in a Magnetron Sputtering System." *Vacuum* 49 (2): 153–60. https://doi.org/10.1016/S0042-207X(97)00158-9.

Harbut, Michael B., Catherine Vilchèze, Xiaozhou Luo, Mary E. Hensler, Hui Guo, Baiyuan Yang, Arnab K. Chatterjee, et al. 2015. "Auranofin Exerts Broad-Spectrum Bactericidal Activities by Targeting Thiol-Redox Homeostasis." *Proceedings of the National Academy of Sciences* 112 (14): 4453–58. https://doi.org/10.1073/pnas.1504022112.

Harris, Elizabeth S., Raymond F. Morgan, and Goerge T. Rodeheaver. 1995. "Analysis of the Kinetics of Peritoneal Adhesion Formation in the Rat and Evaluation of Potential Antiadhesive Agents." *Surgery* 117 (6): 663–69. https://doi.org/10.1016/S0039-6060(95)80010-7.

Harth, M, C R Stiller, N R St C Sinclair, J Evans, D McGirr, and R Zuberi. 1977. "Effects of a Gold Salt on Lymphocyte Responses." *Clinical and Experimental Immunology* 27 (2): 357–64.

Hasdemir, Pinar Solmaz, Mahmud Ozkut, Tevfik Guvenal, Melis Aylin Uner, Esat Calik, Semra Oruc Koltan, Faik Mumtaz Koyuncu, and Kemal Ozbilgin. 2017. "Effect of Pirfenidone on Vascular Proliferation, Inflammation and Fibrosis in an Abdominal Adhesion Rat Model." *Journal of Investigative Surgery* 30 (1): 26–32. https://doi.org/10.1080/08941939.2016.1215578.

Hellebrekers, B.W.J., G.C.M. Trimbos-Kemper, C.A. van Blitterswijk, E.A. Bakkum, and J.B.M.Z. Trimbos. 2000. "Effects of Five Different Barrier Materials on Postsurgical Adhesion Formation in the Rat." *Human Reproduction* 15 (6): 1358–63. https://doi.org/10.1093/humrep/15.6.1358.

Higo, Morihide, Yutaku Matsubara, Yuta Kobayashi, Masaru Mitsushio, Toshifumi Yoshidome, and Sadafumi Nakatake. 2020. "Formation and Decomposition of Gold Oxides Prepared by an Oxygen-Dc Glow Discharge from Gold Films and Studied by X-Ray Photoelectron Spectroscopy." *Thin Solid Films* 699 (April):137870. https://doi.org/10.1016/j.tsf.2020.137870.

Hirohata, Shunsei, Kyoko Nakanishi, Tamiko Yanagida, Mami Kawai, Hirotoshi Kikuchi, and Kunio Isshi. 1999. "Synergistic Inhibition of Human B Cell Activation by Gold Sodium Thiomalate and Auranofin." *Clinical Immunology* 91 (2): 226–33. https://doi.org/10.1006/clim.1999.4686.

Ho, P. S. 1978. "Effects of Enhanced Diffusion on Preferred Sputtering of Homogeneous Alloy Surfaces." *Surface Science* 72 (2): 253–63. https://doi.org/10.1016/0039-6028(78)90294-7.

Hoffmann, Nathan, Sameer Siddiqui, Shvetank Agarwal, Stephen Mckellar, Harold Kurtz, Matthew Gettman, and Mark Ereth. 2008a. "Choice of Hemostatic Agent Influences Adhesion Formation in a Rat Cecal Adhesion Model." *The Journal of Surgical Research* 155 (November):77–81. https://doi.org/10.1016/j.jss.2008.08.008.

Idriss, Haitham T., and James H. Naismith. 2000. "TNFα and the TNF Receptor Superfamily: Structure-Function Relationship(s)." *Microscopy Research and Technique* 50 (3): 184–95. https://doi.org/10.1002/1097-0029(20000801)50:3<184::AID-JEMT2>3.0.CO;2-H.

Ito, Tomoya, Yusuke Shintani, Laura Fields, Manabu Shiraishi, Mihai-Nicolae Podaru, Satoshi Kainuma, Kizuku Yamashita, et al. 2021. "Cell Barrier Function of Resident Peritoneal Macrophages in Post-Operative Adhesions." *Nature Communications* 12 (April):2232. https://doi.org/10.1038/s41467-021-22536-y.

Ivask, Angela, Amro ElBadawy, Chitrada Kaweeteerawat, David Boren, Heidi Fischer, Zhaoxia Ji, Chong Hyun Chang, et al. 2014. "Toxicity Mechanisms in Escherichia Coli Vary for Silver Nanoparticles and Differ from Ionic Silver." *ACS Nano* 8 (1): 374–86. https://doi.org/10.1021/nn4044047.

Iwasaki, Kenichi, Ali Reza Ahmadi, Le Qi, Melissa Chen, Wei Wang, Kenji Katsumata, Akihiko Tsuchida, James Burdick, Andrew M. Cameron, and Zhaoli Sun. 2019. "Pharmacological Mobilization and Recruitment of Stem Cells in Rats Stops Abdominal Adhesions After Laparotomy." *Scientific Reports* 9 (1): 7149. https://doi.org/10.1038/s41598-019-43734-1.

Iyer, Shankar Subramanian, and Genhong Cheng. 2012. "Role of Interleukin 10 Transcriptional Regulation in Inflammation and Autoimmune Disease." *Critical Reviews in Immunology* 32 (1): 23–63.

Javaherzadeh, Mojtaba, Ali Shekarchizadeh, Marjan Kafaei, Abass Mirafshrieh, Nariman Mosaffa, and Babak Sabet. 2016. "Effects of Intraperitoneal Administration of Simvastatin in Prevention of Postoperative Intra-Abdominal Adhesion Formation in Animal Model of Rat." *Bulletin of Emergency & Trauma* 4 (3): 156–60.

Jiang, Shichao, Wei Wang, Hede Yan, and Cunyi Fan. 2013. "Prevention of Intra-Abdominal Adhesion by Bi-Layer Electrospun Membrane." *International Journal of Molecular Sciences* 14 (6): 11861–70. https://doi.org/10.3390/ijms140611861.

Jin, Judy, Gabriela Voskerician, Shawn A. Hunter, Michael F. McGee, Leandro T. Cavazzola, Steve Schomisch, Karem Harth, and Michael J. Rosen. 2009a. "Human Peritoneal Membrane Controls Adhesion Formation and Host Tissue Response Following Intra-Abdominal Placement in a Porcine Model." *Journal of Surgical Research* 156 (2): 297–304. https://doi.org/10.1016/j.jss.2009.04.010.

Kanikireddy, Vimala, Kokkarachedu Varaprasad, Tippabattini Jayaramudu, Chandrasekaran Karthikeyan, and Rotimi Sadiku. 2020. "Carboxymethyl Cellulose-Based Materials for Infection Control and Wound Healing: A Review." *International Journal of Biological Macromolecules* 164 (December):963–75. https://doi.org/10.1016/j.ijbiomac.2020.07.160.

Karaca, Turgut, Ahmet Uğur Gözalan, Ömer Yoldaş, Bülent Çağlar Bilgin, and Ayla Tezer. 2013. "Effects of Tamoxifen Citrate on Postoperative Intra-Abdominal Adhesion in a Rat Model." *International Journal of Surgery* 11 (1): 68–72. https://doi.org/10.1016/j.ijsu.2012.11.015.

Khan, Mahmood Ahmad, and Mohd Jahir Khan. 2018. "Nano-Gold Displayed Anti-Inflammatory Property via NF-kB Pathways by Suppressing COX-2 Activity." *Artificial Cells, Nanomedicine, and Biotechnology* 46 (sup1): 1149–58. https://doi.org/10.1080/21691401.2018.1446968.

Kim, Jihoon, Ji-Youn Chang, Yoon-Young Kim, Moon-Jong Kim, and Hong-Seop Kho. 2018. "Effects of Molecular Weight of Hyaluronic Acid on Its Viscosity and Enzymatic Activities of Lysozyme and Peroxidase." *Archives of Oral Biology* 89 (May):55–64. https://doi.org/10.1016/j.archoralbio.2018.02.007.

Kim, Nam-Hoon, Mun-Yong Lee, Seon-Joo Park, Jeong-Sun Choi, Mi-Kyung Oh, and In-Sook Kim. 2007. "Auranofin Blocks Interleukin-6 Signalling by Inhibiting Phosphorylation of JAK1 and STAT3." *Immunology* 122 (4): 607–14. https://doi.org/10.1111/j.1365-2567.2007.02679.x.

Kishan, Alysha, Taneidra Buie, Canaan Whitfield-Cargile, Anupriya Jose, Laura Bryan, Noah Cohen, and Elizabeth Cosgriff-Hernandez. 2020. "In Vivo Performance of a Bilayer Wrap to Prevent Abdominal Adhesions." *Acta Biomaterialia* 115 (October):116–26. https://doi.org/10.1016/j.actbio.2020.08.021.

Kos, M., J. F. Kuebler, N. K. Jesch, G. Vieten, N. M. Bax, D. C. van der Zee, R. Busche, and B. M. Ure. 2006. "Carbon Dioxide Differentially Affects the Cytokine Release of Macrophage Subpopulations Exclusively via Alteration of Extracellular pH." *Surgical Endoscopy And Other Interventional Techniques* 20 (4): 570–76. https://doi.org/10.1007/s00464-004-2175-6.

Koshari, Stijn H. S., Xutao Shi, Linda Jiang, Debby Chang, Karthikan Rajagopal, Abraham M. Lenhoff, and Norman J. Wagner. 2022. "Design of PLGA-Based Drug Delivery Systems Using a Physically-Based Sustained Release Model." *Journal of Pharmaceutical Sciences* 111 (2): 345–57. https://doi.org/10.1016/j.xphs.2021.09.007.

Kramer, Klaus, Norbert Senninger, Hermann Herbst, and Wolfgang Probst. 2002a. "Effective Prevention of Adhesions With Hyaluronate." *Archives of Surgery* 137 (3): 278–82. https://doi.org/10.1001/archsurg.137.3.278.

Kumar, Satish, Rakesh Kumar Majhi, Abhishek Singh, Mitali Mishra, Ankit Tiwari, Saurabh Chawla, Puspendu Guha, et al. 2019. "Carbohydrate-Coated Gold–Silver Nanoparticles for Efficient Elimination of Multidrug Resistant Bacteria and in Vivo Wound Healing." *ACS Applied Materials & Interfaces* 11 (46): 42998–17. https://doi.org/10.1021/acsami.9b17086.

Lampa, Jon, Lars Klareskog, and Johan Rönnelid. 2002. "Effects of Gold on Cytokine Production in Vitro; Increase of Monocyte Dependent Interleukin 10 Production and Decrease of Interferon-Gamma Levels." *The Journal of Rheumatology* 29 (1): 21–28.

Landry, Breanne K., Patricia L. Nadworny, Oladipo E. Omotoso, Yadollah Maham, Jessica C. Burrell, and Robert E. Burrell. 2009. "The Kinetics of Thermal Instability in Nanocrystalline Silver and the Effect of Heat Treatment on the Antibacterial Activity of Nanocrystalline Silver Dressings." *Biomaterials* 30 (36): 6929–39. https://doi.org/10.1016/j.biomaterials.2009.09.003.

Lang, Reinhold Andreas, Patricia Mercedes Grüntzig, Christiane Weisgerber, Christine Weis, Erich Kurt Odermatt, and Martin Hartwig Kirschner. 2007a. "Polyvinyl Alcohol Gel Prevents Abdominal Adhesion Formation in a Rabbit Model." *Fertility and Sterility* 88 (4, Supplement): 1180–86. https://doi.org/10.1016/j.fertnstert.2007.01.108.

Fertility and Sterility 88 (4, Supplement): 1180–86. https://doi.org/10.1016/j.fertnstert.2007.01.108.

Lansdown, Alan B. G. 2010. *Silver in Healthcare*. https://doi.org/10.1039/9781849731799.

Lara, Marilisa G., M. Vitória L. B. Bentley, and John H. Collett. 2005. "In Vitro Drug Release Mechanism and Drug Loading Studies of Cubic Phase Gels." *International Journal of Pharmaceutics* 293 (1): 241–50. https://doi.org/10.1016/j.ijpharm.2005.01.008.

Lauder, Chris I. W., Giuseppe Garcea, Andrew Strickland, and Guy J. Maddern. 2011. "Use of a Modified Chitosan–Dextran Gel to Prevent Peritoneal Adhesions in a Rat Model." *Journal of Surgical Research* 171 (2): 877–82. https://doi.org/10.1016/j.jss.2010.06.028.

Lauder, Chris I. W., Andrew Strickland, and Guy J. Maddern. 2012. "Use of a Modified Chitosan–Dextran Gel to Prevent Peritoneal Adhesions in a Porcine Hemicolectomy Model." *Journal of Surgical Research* 176 (2): 448–54. https://doi.org/10.1016/j.jss.2011.10.029.

Leach, Richard E, James W Burns, Elizabeth J Dawe, Michelle D SmithBarbour, and Michael P Diamond. 1998a. "Reduction of Postsurgical Adhesion Formation in the Rabbit Uterine Horn Model with Use of Hyaluronate/ Carboxymethylcellulose Gel1 1Supported by Genzyme Corporation, Protocol No. 92-0902, Cambridge, Massachusetts." *Fertility and Sterility* 69 (3): 415–18. https://doi.org/10.1016/S0015-0282(97)00573-6.

Lee, Jee Eun, Sharif Md Abuzar, Yeji Seo, Hyeji Han, Youngbae Jeon, Eun Jung Park, Seung Hyuk Baik, and Sung-Joo Hwang. 2019. "Oxaliplatin-Loaded Chemically Cross-Linked Hydrogels for Prevention of Postoperative Abdominal Adhesion and Colorectal Cancer Therapy." *International Journal of Pharmaceutics* 565 (June):50–58. https://doi.org/10.1016/j.ijpharm.2019.04.065.

Lee, Jong Soo, Seung Uk Lee, Cheng-Ye Che, and Ji-Eun Lee. 2015. "Comparison of Cytotoxicity and Wound Healing Effect of Carboxymethylcellulose and Hyaluronic Acid on Human Corneal Epithelial Cells." *International Journal of Ophthalmology* 8 (2): 215–21. https://doi.org/10.3980/j.issn.2222-3959.2015.02.01.

Lee, R. F., and W. F. Pickering. 1971. "Effect of Precipitate and Complex Formation on the Determination of Silver by Atomic-Absorption Spectroscopy." *Talanta* 18 (11): 1083–94. https://doi.org/10.1016/0039-9140(71)80220-5.

Létoffé, Sylvie, Yongzheng Wu, Sophie E. Darch, Christophe Beloin, Marvin Whiteley, Lhousseine Touqui, and Jean-Marc Ghigo. n.d. "Pseudomonas Aeruginosa Production of Hydrogen Cyanide Leads to Airborne Control of Staphylococcus Aureus Growth in Biofilm and In Vivo Lung Environments." *mBio* 13 (5): e02154-22. https://doi.org/10.1128/mbio.02154-22.

Leveen, H H, G Falk, B Borek, C Diaz, Y Lynfield, B J Wynkoop, G A Mabunda, J L Rubricius, and G C Christoudias. 1973. "Chemical Acidification of Wounds. An Adjuvant to Healing and the Unfavorable Action of Alkalinity and Ammonia." *Annals of Surgery* 178 (6): 745–53.

Li, Hongbin, Xinjing Wei, Xiaotong Yi, Shize Tang, Jinmei He, Yudong Huang, and Feng Cheng. 2021. "Antibacterial, Hemostasis, Adhesive, Self-Healing Polysaccharides-Based Composite Hydrogel Wound Dressing for the Prevention and Treatment of Postoperative Adhesion." *Materials Science and Engineering: C* 123 (April):111978. https://doi.org/10.1016/j.msec.2021.111978.

Li, Jian, Jinhui Zhu, Ting He, Weida Li, Yue Zhao, Zaomei Chen, Junhui Zhang, Huaying Wan, and Rubing Li. 2017. "Prevention of Intra-Abdominal Adhesion Using Electrospun PEG/PLGA Nanofibrous Membranes." *Materials Science and Engineering: C* 78 (September):988–97. https://doi.org/10.1016/j.msec.2017.04.017.

Liau, S.y., D.c. Read, W.j. Pugh, J.r. Furr, and A.d. Russell. 1997. "Interaction of Silver Nitrate with Readily Identifiable Groups: Relationship to the Antibacterialaction of Silver Ions." *Letters in Applied Microbiology* 25 (4): 279–83. https://doi.org/10.1046/j.1472-765X.1997.00219.x.

Liebman, Shael M., Jacob C. Langer, Jean S. Marshall, and Stephen M. Collins. 1993. "Role of Mast Cells in Peritoneal Adhesion Formation." *The American Journal of Surgery* 165 (1): 127–30. https://doi.org/10.1016/S0002-9610(05)80415-5.

Lin, Long-Xiang, Fang Yuan, Hui-Hui Zhang, Ni-Na Liao, Jing-Wan Luo, and Yu-Long Sun. 2017. "Evaluation of Surgical Anti-Adhesion Products to Reduce Postsurgical Intra-Abdominal Adhesion Formation in a Rat Model." *PLOS ONE* 12 (2): e0172088. https://doi.org/10.1371/journal.pone.0172088.

Lipsky, P E, and M Ziff. 1977. "Inhibition of Antigen- and Mitogen-Induced Human Lymphocyte Proliferation by Gold Compounds." *Journal of Clinical Investigation* 59 (3): 455–66.

Littman, B. H., and R. E. Hall. 1985. "Effects of Gold Sodium Thiomalate on Functional Correlates of Human Monocyte Maturation." *Arthritis and Rheumatism* 28 (12): 1384–92. https://doi.org/10.1002/art.1780281211.

Littman, B. H., and P. Schwartz. 1982. "Gold Inhibition of the Production of the Second Complement Component by Lymphokine-Stimulated Human Monocytes." *Arthritis and Rheumatism* 25 (3): 288–96. https://doi.org/10.1002/art.1780250306.

Liu, J., T. Akahoshi, R. Namai, T. Matsui, and H. Kondo. 2000. "Effect of Auranofin, an Antirheumatic Drug, on Neutrophil Apoptosis." *Inflammation Research* 49 (9): 445–51. https://doi.org/10.1007/s000110050615.

Liu, Xin, Yunwei Wei, Xue Bai, Mingqi Li, Huimin Li, Lei Wang, Shuqian Zhang, et al. 2020. "Berberine Prevents Primary Peritoneal Adhesion and Adhesion Reformation by Directly Inhibiting TIMP-1." *Acta Pharmaceutica Sinica. B* 10 (5): 812–24. https://doi.org/10.1016/j.apsb.2020.02.003.

Long, Linyu, Cheng Hu, Wenqi Liu, Can Wu, Lu Lu, Li Yang, and Yunbing Wang. 2022. "Injectable Multifunctional Hyaluronic Acid/Methylcellulose Hydrogels for Chronic Wounds Repairing." *Carbohydrate Polymers* 289 (August):119456. https://doi.org/10.1016/j.carbpol.2022.119456.

Lopez, Carlos G., and Walter Richtering. 2021. "Oscillatory Rheology of Carboxymethyl Cellulose Gels: Influence of Concentration and pH." *Carbohydrate Polymers* 267 (September):118117. https://doi.org/10.1016/j.carbpol.2021.118117.

Lorber, A., W. H. Jackson, and T. M. Simon. 1981. "Assessment of Immune Response during Chrysotherapy. Comparison of Gold Sodium Thiomalate vs. Auranofin." *Scandinavian Journal of Rheumatology* 10 (2): 129–37. https://doi.org/10.3109/03009748109095285.

Lossi, Laura, Livia D'Angelo, Paolo De Girolamo, and Adalberto Merighi. 2016a. "Anatomical Features for an Adequate Choice of Experimental Animal Model in Biomedicine: II. Small Laboratory Rodents, Rabbit, and Pig." *Annals of Anatomy - Anatomischer Anzeiger* 204 (March):11–28. https://doi.org/10.1016/j.aanat.2015.10.002.

Loza, K., C. Sengstock, S. Chernousova, M. Köller, and M. Epple. 2014. "The Predominant Species of Ionic Silver in Biological Media Is Colloidally Dispersed Nanoparticulate Silver Chloride." *RSC Advances* 4 (67): 35290–97. https://doi.org/10.1039/C4RA04764H.

Lucas, Paul A., Debra J. Warejcka, Henry E. Young, and Bok Y. Lee. 1996. "Formation of Abdominal Adhesions Is Inhibited by Antibodies to Transforming Growth Factor-B1." *Journal of Surgical Research* 65 (2): 135–38. https://doi.org/10.1006/jsre.1996.0355.

Macarak, Edward J., Christine E. Lotto, Deepika Koganti, Xiaoling Jin, Peter J. Wermuth, Anna-Karin Olsson, Matthew Montgomery, and Joel Rosenbloom. 2018. "Trametinib Prevents Mesothelial-Mesenchymal Transition and Ameliorates Abdominal Adhesion Formation." *Journal of Surgical Research* 227 (July):198–210. https://doi.org/10.1016/j.jss.2018.02.012.

Maciver, Allison H., Michael McCall, and A. M. James Shapiro. 2011. "Intra-Abdominal Adhesions: Cellular Mechanisms and Strategies for Prevention." *International Journal of Surgery* 9 (8): 589–94. https://doi.org/10.1016/j.ijsu.2011.08.008.

Mahl, Dirk, Jörg Diendorf, Simon Ristig, Christina Greulich, Zi-An Li, Michael Farle, Manfred Köller, and Matthias Epple. 2012a. "Silver, Gold, and Alloyed Silver–Gold Nanoparticles: Characterization and Comparative Cell-Biologic Action." *Journal of Nanoparticle Research* 14 (10): 1153. https://doi.org/10.1007/s11051-012-1153-5.

Makarchian, Hamid Reza, Amir Kasraianfard, Pezhman Ghaderzadeh, Seyed Mohammad Reza Javadi, and Manoochehr Ghorbanpoor. 2017. "The Effectiveness of Heparin, Platelet-Rich Plasma (PRP), and Silver Nanoparticles on Prevention of Postoperative Peritoneal Adhesion Formation in Rats1." *Acta Cirúrgica Brasileira* 32 (January):22–27. https://doi.org/10.1590/s0102-865020170103.

Maleki, Atoosa, Anna-Lena Kjøniksen, and Bo Nyström. 2007. "Anomalous Viscosity Behavior in Aqueous Solutions of Hyaluronic Acid." *Polymer Bulletin* 59 (2): 217–26. https://doi.org/10.1007/s00289-007-0760-2.

Marsich, Eleonora, Andrea Travan, Ivan Donati, Andrea Di Luca, Monica Benincasa, Matteo Crosera, and Sergio Paoletti. 2011. "Biological Response of Hydrogels Embedding Gold Nanoparticles." *Colloids and Surfaces B: Biointerfaces* 83 (2): 331–39. https://doi.org/10.1016/j.colsurfb.2010.12.002.

Matsumura, Yoshinobu, Kuniaki Yoshikata, Shin-ichi Kunisaki, and Tetsuaki Tsuchido. 2003. "Mode of Bactericidal Action of Silver Zeolite and Its Comparison with That of Silver Nitrate." *Applied and Environmental Microbiology* 69 (7): 4278–81. https://doi.org/10.1128/AEM.69.7.4278-4281.2003.

McBride, W. H., K. Mason, H. R. Withers, and C. Davis. 1989. "Effect of Interleukin 1, Inflammation, and Surgery on the Incidence of Adhesion Formation and Death after Abdominal Irradiation in Mice." *Cancer Research* 49 (1): 169–73.

Mendis, Pramujitha, Rohini M. de Silva, K. M. Nalin de Silva, Lahiru A. Wijenayaka, Kalana Jayawardana, and Mingdi Yan. 2016. "Nanosilver Rainbow: A Rapid and Facile Method to Tune Different Colours of Nanosilver through the Controlled Synthesis of Stable Spherical Silver Nanoparticles." *RSC Advances* 6 (54): 48792–99. https://doi.org/10.1039/C6RA08336F.

Menzies, D., M. Parker, R. Hoare, and A. Knight. 2001. "Small Bowel Obstruction Due to Postoperative Adhesions: Treatment Patterns and Associated Costs in 110 Hospital Admissions." *Annals of The Royal College of Surgeons of England* 83 (1): 40–46.

Messori, L., F. Abbate, G. Marcon, P. Orioli, M. Fontani, E. Mini, T. Mazzei, S. Carotti, T. O'Connell, and P. Zanello. 2000. "Gold(III) Complexes as Potential Antitumor Agents: Solution Chemistry and Cytotoxic Properties of Some Selected Gold(III) Compounds." *Journal of Medicinal Chemistry* 43 (19): 3541–48. https://doi.org/10.1021/jm990492u.

Miranda, M. a. R., and J. M. Sasaki. 2018. "The Limit of Application of the Scherrer Equation." *Acta Crystallographica Section A: Foundations and Advances* 74 (1): 54–65. https://doi.org/10.1107/S2053273317014929.

Mollà, Meritxell, Julián Panés, Maria Casadevall, Azucena Salas, Carles Conill, Albert Biete, Donald C Anderson, D. Neil Granger, and Josep M Piqué. 1999. "Influence of Dose-Rate on Inflammatory Damage and Adhesion Molecule Expression after Abdominal Radiation in the Rat." *International Journal of Radiation Oncology*Biology*Physics* 45 (4): 1011–18. https://doi.org/10.1016/S0360-3016(99)00286-2.

Mommers, Elwin HH, Liu Hong, Audrey Jongen, and Nicole D Bouvy. 2019. "Baseline Performance of the Ischaemic Button Model for Induction of Adhesions in Laboratory Rats." *Laboratory Animals* 53 (1): 63–71. https://doi.org/10.1177/0023677218773116.

Moretti, Ana I. S., Francisco J. P. Souza Pinto, Vivian Cury, Marcia C. Jurado, Wagner Marcondes, Irineu T. Velasco, and Heraldo P. Souza. 2012. "Nitric Oxide Modulates Metalloproteinase-2, Collagen Deposition and Adhesion Rate after Polypropylene Mesh Implantation in the Intra-Abdominal Wall." *Acta Biomaterialia* 8 (1): 108–15. https://doi.org/10.1016/j.actbio.2011.08.004.

Mulley, Geraldine, A. Tobias A. Jenkins, and Nicholas R. Waterfield. 2014. "Inactivation of the Antibacterial and Cytotoxic Properties of Silver Ions by Biologically Relevant Compounds." *PLOS ONE* 9 (4): e94409. https://doi.org/10.1371/journal.pone.0094409.

Munireddy, Sanjay, Sandra L. Kavalukas, and Adrian Barbul. 2010. "Intra-Abdominal Healing: Gastrointestinal Tract and Adhesions." *Surgical Clinics of North America*, Wounds and Wound Management, 90 (6): 1227–36. https://doi.org/10.1016/j.suc.2010.08.002.

Musil, J, and J Vlček. 1998. "Magnetron Sputtering of Alloy-Based Films and Its Specifity | SpringerLink." *Czechoslovak Journal of Physics* 48:1209–24.

Nadworny, Patricia L. 2010a. "Biological Activity of Nanostructured Silver." ERA. Spring 2010. https://doi.org/10.7939/R3V35J.

Nadworny, Patricia L., Breanne K. Landry, JianFei Wang, Edward E. Tredget, and Robert E. Burrell. 2010a. "Does Nanocrystalline Silver Have a Transferable Effect?" *Wound Repair and Regeneration* 18 (2): 254–65. https://doi.org/10.1111/j.1524-475X.2010.00579.x.

Nadworny, Patricia L., JianFei Wang, Edward E. Tredget, and Robert E. Burrell. 2008a. "Anti-Inflammatory Activity of Nanocrystalline Silver in a Porcine Contact Dermatitis Model." *Nanomedicine: Nanotechnology, Biology and Medicine* 4 (3): 241–51. https://doi.org/10.1016/j.nano.2008.04.006.

———. 2010a. "Anti-Inflammatory Activity of Nanocrystalline Silver-Derived Solutions in Porcine Contact Dermatitis." *Journal of Inflammation* 7 (1): 13. https://doi.org/10.1186/1476-9255-7-13.

Nair, Satish K., Inder K. Bhat, and Amrit L. Aurora. 1974. "Role of Proteolytic Enzyme in the Prevention of Postoperative Intraperitoneal Adhesions." *Archives of Surgery* 108 (6): 849–53. https://doi.org/10.1001/archsurg.1974.01350300081019.

Nakada, T., Y. Ohkubo, and A. Kunioka. 1991. "Textured ZnO:Al Films for Solar Cells by DC-Magnetron Sputtering in Water Vapor Plasma." In *The Conference Record of the Twenty-Second IEEE Photovoltaic Specialists Conference - 1991*, 1389–92 vol.2. https://doi.org/10.1109/PVSC.1991.169435.

Nakada, Tokio, Yukinobu Ohkubo Yukinobu Ohkubo, and Akio Kunioka Akio Kunioka. 1991. "Effect of Water Vapor on the Growth of Textured ZnO-Based Films for Solar Cells by DC-Magnetron Sputtering." *Japanese Journal of Applied Physics* 30 (12R): 3344. https://doi.org/10.1143/JJAP.30.3344.

Nešović, Katarina, Ana Janković, Tamara Radetić, Maja Vukašinović-Sekulić, Vesna Kojić, Ljiljana Živković, Aleksandra Perić-Grujić, Kyong Yop Rhee, and Vesna Mišković-Stanković. 2019. "Chitosan-Based Hydrogel Wound Dressings with Electrochemically Incorporated Silver Nanoparticles – In Vitro Study." *European Polymer Journal* 121 (December):109257. https://doi.org/10.1016/j.eurpolymj.2019.109257.

Nguyen, Kathy C., Laura Richards, Andrey Massarsky, Thomas W. Moon, and Azam F. Tayabali. 2016. "Toxicological Evaluation of Representative Silver Nanoparticles in Macrophages and Epithelial Cells." *Toxicology in Vitro* 33 (June):163–73. https://doi.org/10.1016/j.tiv.2016.03.004.

Ochi, Masanori, Bo Wan, Quanying Bao, and Diane J. Burgess. 2021. "Influence of PLGA Molecular Weight Distribution on Leuprolide Release from Microspheres." *International Journal of Pharmaceutics* 599 (April):120450. https://doi.org/10.1016/j.ijpharm.2021.120450.

Oh, Jaewook, Kean G. Kuan, Leong U. Tiong, Markus I. Trochsler, Gregory Jay, Tannin A. Schmidt, Harry Barnett, and Guy J. Maddern. 2017. "Recombinant Human Lubricin for Prevention of Postoperative Intra-Abdominal Adhesions in a Rat Model." *Journal of Surgical Research* 208 (February):20–25. https://doi.org/10.1016/j.jss.2016.08.092.

Oncel, Mustafa, Necmi Kurt, Feza H. Remzi, Sibel S. Sensu, Selahattin Vural, Cem F. Gezen, Tarik G. Cincin, and Ergin Olcay. 2001. "The Effectiveness of Systemic Antibiotics in Preventing Postoperative, Intraabdominal Adhesions in an Animal Model." *Journal of Surgical Research* 101 (1): 52–55. https://doi.org/10.1006/jsre.2001.6245.

Pan, Yu, Sabine Neuss, Annika Leifert, Monika Fischler, Fei Wen, Ulrich Simon, Günter Schmid, Wolfgang Brandau, and Willi Jahnen-Dechent. 2007. "Size-Dependent Cytotoxicity of Gold Nanoparticles." *Small (Weinheim an Der Bergstrasse, Germany)* 3 (11): 1941–49. https://doi.org/10.1002/smll.200700378.

Panicker, S., I. M. Ahmady, C. Han, M. Chehimi, and A. A. Mohamed. 2020. "On Demand Release of Ionic Silver from Gold-Silver Alloy Nanoparticles: Fundamental Antibacterial Mechanisms Study." *Materials Today Chemistry* 16 (June):100237. https://doi.org/10.1016/j.mtchem.2019.100237.

Park, Jun Seok, Seong Jae Cha, Beom Gyu Kim, Yoo Shin Choi, Gui Young Kwon, Hyun Kang, and Seong Soo An. 2011. "An Assessment of the Effects of a Hyaluronan-Based Solution on Reduction of Postsurgical Adhesion Formation in Rats: A Comparative Study of Hyaluronan-Based Solution and Two Film Barriers." *Journal of Surgical Research* 168 (1): 49–55. https://doi.org/10.1016/j.jss.2009.09.025.

Parker, Michael C., Harold Ellis, Brendan J. Moran, Jeremy N. Thompson, Malcolm S. Wilson, Don Menzies, Alistair McGuire, et al. 2001. "Postoperative Adhesions: Ten-Year Follow-up of 12,584 Patients Undergoing Lower Abdominal Surgery." *Diseases of the Colon & Rectum* 44 (6): 822–29. https://doi.org/10.1007/BF02234701.

Pasaribu, Subur P., Mimpin Ginting, Indra Masmur, Jamaran Kaban, and Hestina. 2020. "Silver Chloride Nanoparticles Embedded in Self-Healing Hydrogels with Biocompatible and Antibacterial Properties." *Journal of Molecular Liquids* 310 (July):113263. https://doi.org/10.1016/j.molliq.2020.113263.

Patel, Ravi B., Luis Solorio, Hanping Wu, Tianyi Krupka, and Agata A. Exner. 2010. "Effect of Injection Site on in Situ Implant Formation and Drug Release in Vivo." *Journal of Controlled Release* 147 (3): 350–58. https://doi.org/10.1016/j.jconrel.2010.08.020.

Pedersen, Mie Østergaard, Agnete Larsen, Dan Sonne Pedersen, Meredin Stoltenberg, and Milena Penkowa. 2009. "Metallic Gold Reduces TNFα Expression, Oxidative DNA Damage and pro-Apoptotic Signals after Experimental Brain Injury." *Brain Research* 1271 (May):103–13. https://doi.org/10.1016/j.brainres.2009.03.022.

Percival, Steven L., Will Slone, Sara Linton, Tyler Okel, Linda Corum, and John G. Thomas. 2011. "The Antimicrobial Efficacy of a Silver Alginate Dressing against a Broad Spectrum of Clinically Relevant Wound Isolates." *International Wound Journal* 9 (3): 237–43. https://doi.org/10.1111/j.1742-481X.2011.00774.x.

Pham, B. V., K. Morgan, J. Romagnuolo, J. Glenn, S. Bazaz, C. Lawrence, and R. Hawes. 2008. "Pilot Comparison of Adhesion Formation Following Colonic Perforation and Repair in a Pig Model Using a Transgastric, Laparoscopic, or Open Surgical Technique." *Endoscopy* 40 (8): 664–69. https://doi.org/10.1055/s-2008-1077436.

Pierson, J. F., D. Wiederkehr, and A. Billard. 2005. "Reactive Magnetron Sputtering of Copper, Silver, and Gold." *Thin Solid Films* 478 (1): 196–205. https://doi.org/10.1016/j.tsf.2004.10.043.

Poehnert, D, L Grethe, L Maegel, D Jonigk, T Lippmann, A Kaltenborn, H Schrem, J Klempnauer, and M Winny. 2016. "Evaluation of the Effectiveness of Peritoneal Adhesion Prevention Devices in a Rat Model." *International Journal of Medical Sciences* 13 (7): 524–32. https://doi.org/10.7150/ijms.15167.

Poehnert, Daniel, Mahmoud Abbas, Hans-Heinrich Kreipe, Juergen Klempnauer, and Markus Winny. 2015. "High Reproducibility of Adhesion Formation in Rat with Meso-Stitch Approximation of Injured Cecum and Abdominal Wall." *International Journal of Medical Sciences* 12 (1): 1–6. https://doi.org/10.7150/ijms.8870.

Pose-Vilarnovo, Beatriz, Carmen Rodríguez-Tenreiro, José Fernando Rosa dos Santos, Juan Vázquez-Doval, Angel Concheiro, Carmen Alvarez-Lorenzo, and Juan J Torres-Labandeira. 2004. "Modulating Drug Release with Cyclodextrins in Hydroxypropyl Methylcellulose Gels and Tablets." *Journal of Controlled Release* 94 (2): 351–63. https://doi.org/10.1016/j.jconrel.2003.10.002.

Queirolo, G, M Dellagiovanna, and G De Santi. 1989. "Effect of the Sputtering Ambient Contamination on the Microstructure of Al–Si Films: Journal of Vacuum Science & Technology A: Vol 7, No 3." *Journal of Vacuum Science & Technology A* 7 (651). https://doi.org/10.1116/1.575860.

Ramamurthy, CH., M. Padma, I. Daisy mariya samadanam, R. Mareeswaran, A. Suyavaran, M. Suresh Kumar, K. Premkumar, and C. Thirunavukkarasu. 2013. "The Extra Cellular Synthesis of Gold and Silver Nanoparticles and Their Free Radical Scavenging and Antibacterial Properties." *Colloids and Surfaces B: Biointerfaces* 102 (February):808–15. https://doi.org/10.1016/j.colsurfb.2012.09.025.

Ramirez, Horacio, Shailee B. Patel, and Irena Pastar. 2014. "The Role of TGFβ Signaling in Wound Epithelialization." *Advances in Wound Care* 3 (7): 482–91. https://doi.org/10.1089/wound.2013.0466.

Rasool, Yusuf. 2009. "An Evaluation of the Anti-Inflammatory Activity and Mechanism of Action of Three Novel Auranofin Derivatives." Dissertation, University of Pretoria. https://repository.up.ac.za/handle/2263/22792.

Reijnen, M M P J, R P Bleichrodt, and H van Goor. 2003. "Pathophysiology of Intra-Abdominal Adhesion and Abscess Formation, and the Effect of Hyaluronan." *British Journal of Surgery* 90 (5): 533–41. https://doi.org/10.1002/bjs.4141.

Reijnen, Michel M. P. J., Eugene M. Skrabut, Victor A. Postma, James W. Burns, and Harry van Goor. 2001. "Polyanionic Polysaccharides Reduce Intra-Abdominal Adhesion and Abscess Formation in a Rat Peritonitis Model." *Journal of Surgical Research* 101 (2): 248–53. https://doi.org/10.1006/jsre.2001.6288.

Reissman, Petachia, Tiong-Ann-Teoh, Kevin Skinner, James W. Burns, and Steven D. Wexner. 1996. "Adhesion Formation After Laparoscopic Anterior Resection in a Porcine Model: A Pilot Study." *Surgical Laparoscopy Endoscopy & Percutaneous Techniques* 6 (2): 136.

Roduner, Emil. 2006. "Size Matters: Why Nanomaterials Are Different." *Chemical Society Reviews* 35 (7): 583–92. https://doi.org/10.1039/B502142C.

Ross, Joseph A., Nick Allan, Merle Olson, Crystal Schatz, P. Nick Nation, Justin Peter Gawaziuk, Japandeep Sethi, Song Liu, and Sarvesh Logsetty. 2020. "Comparison of the Efficacy of Silver-Based Antimicrobial Burn Dressings in a Porcine Model of Burn Wounds." *Burns* 46 (7): 1632–40. https://doi.org/10.1016/j.burns.2020.04.004.

Sant, S. B., K. S. Gill, and R. E. Burrell. 2007. "Nanostructure, Dissolution and Morphology Characteristics of Microcidal Silver Films Deposited by Magnetron Sputtering." *Acta Biomaterialia*, 2nd TMS Symposium on biological materials science, 3 (3): 341–50. https://doi.org/10.1016/j.actbio.2006.10.008.

———. 2009. "The Nature of Chemical Species in Novel Antimicrobial Silver Films Deposited by Magnetron Sputtering." *Philosophical Magazine A*, August. https://doi.org/10.1080/01418610208240020.

Scherrer, P. 1912. "Bestimmung der inneren Struktur und der Größe von Kolloidteilchen mittels Röntgenstrahlen." In *Kolloidchemie Ein Lehrbuch*, edited by Richard Zsigmondy, 387–409. Chemische Technologie in Einzeldarstellungen. Berlin, Heidelberg: Springer. https://doi.org/10.1007/978-3-662-33915-2_7.

Shanmugasundaram, Thangavel, Manikkam Radhakrishnan, Venugopal Gopikrishnan, Krishna Kadirvelu, and Ramasamy Balagurunathan. 2017. "In Vitro Antimicrobial and in Vivo Wound Healing Effect of Actinobacterially Synthesised Nanoparticles of Silver, Gold and Their Alloy." *RSC Advances* 7 (81): 51729–43. https://doi.org/10.1039/C7RA08483H.

Sheikpranbabu, Sardarpasha, Kalimuthu Kalishwaralal, Deepak Venkataraman, Soo Hyun Eom, Jongsun Park, and Sangiliyandi Gurunathan. 2009. "Silver Nanoparticles Inhibit VEGF-and IL-1β-Induced Vascular Permeability via Src Dependent Pathway in Porcine Retinal Endothelial Cells." *Journal of Nanobiotechnology* 7 (1): 8. https://doi.org/10.1186/1477-3155-7-8.

Shende, Pravin, Bhumi Oza, and R. S. Gaud. 2018. "Silver-Doped Titanium Dioxide Nanoparticles Encapsulated in Chitosan–PVA Film for Synergistic Antimicrobial Activity." *International Journal of Polymeric Materials and Polymeric Biomaterials* 67 (18): 1080–86. https://doi.org/10.1080/00914037.2017.1417290.

Sibbald, R. Gary, Jose Contreras-Ruiz, Patricia Coutts, Marjorie Fierheller, Arthur Rothman, and Kevin Woo. 2007. "Bacteriology, Inflammation, and Healing: A Study of Nanocrystalline Silver Dressings in Chronic Venous Leg Ulcers." *Advances in Skin & Wound Care* 20 (10): 549–58. https://doi.org/10.1097/01.ASW.0000294757.05049.85.

Sikkink, Cornelis J. J. M., Ben de Man, Robert P. Bleichrodt, and Harry van Goor. 2006. "Auto-Cross-Linked Hyaluronic Acid Gel Does Not Reduce Intra-Abdominal Adhesions or Abscess Formation in a Rat Model of Peritonitis." *Journal of Surgical Research* 136 (2): 255–59. https://doi.org/10.1016/j.jss.2006.06.021.

Simmen, Hans-Peter, and Jürg Blaser. 1993. "Analysis of pH and pO2 in Abscesses, Peritoneal Fluid, and Drainage Fluid in the Presence or Absence of Bacterial Infection during and after Abdominal Surgery." *The American Journal of Surgery* 166 (1): 24–27. https://doi.org/10.1016/S0002-9610(05)80576-8.

Simmons, Peter A, and Joseph G Vehige. 2017. "Investigating the Potential Benefits of a New Artificial Tear Formulation Combining Two Polymers." *Clinical Ophthalmology (Auckland, N.Z.)* 11 (September):1637–42. https://doi.org/10.2147/OPTH.S135550.

Simpson, R. J., A. Hammacher, D. K. Smith, J. M. Matthews, and L. D. Ward. 1997. "Interleukin-6: Structure-Function Relationships." *Protein Science : A Publication of the Protein Society* 6 (5): 929–55.

Sioshansi, P. 1994. "New Processes for Surface Treatment of Catheters." *Artificial Organs* 18 (4): 266–71. https://doi.org/10.1111/j.1525-1594.1994.tb02193.x.

Snetkov, Petr, Kseniia Zakharova, Svetlana Morozkina, Roman Olekhnovich, and Mayya Uspenskaya. 2020. "Hyaluronic Acid: The Influence of Molecular Weight on Structural, Physical, Physico-

Chemical, and Degradable Properties of Biopolymer." *Polymers* 12 (8): E1800. https://doi.org/10.3390/polym12081800.

Spitzer, Martin S., Efdal Yoeruek, Radoslaw T. Kaczmarek, Ana Sierra, Sabine Aisenbrey, Salvatore Grisanti, Karl U. Bartz-Schmidt, and Peter Szurman. 2008. "Sodium Hyaluronate Gels as a Drug-Release System for Corticosteroids: Release Kinetics and Antiproliferative Potential for Glaucoma Surgery." *Acta Ophthalmologica* 86 (8): 842–48. https://doi.org/10.1111/j.1755-3768.2007.01149.x.

Steensel, Sebastiaan van, Hong Liu, Elwin H. H. Mommers, Kaatje Lenaerts, and Nicole D. Bouvy. 2019. "Comparing Five New Polymer Barriers for the Prevention of Intra-Abdominal Adhesions in a Rat Model." *Journal of Surgical Research* 243 (November):453–59. https://doi.org/10.1016/j.jss.2019.05.043.

Stern, Robert, Akira A. Asari, and Kazuki N. Sugahara. 2006. "Hyaluronan Fragments: An Information-Rich System." *European Journal of Cell Biology* 85 (8): 699–715. https://doi.org/10.1016/j.ejcb.2006.05.009.

Sun, Lin, Chang He, Lekha Nair, Justine Yeung, and Charles E. Egwuagu. 2015. "Interleukin 12 (IL-12) Family Cytokines: Role in Immune Pathogenesis and Treatment of CNS Autoimmune Disease." *Cytokine* 75 (2): 249–55. https://doi.org/10.1016/j.cyto.2015.01.030.

Suska, Felicia, Sara Svensson, Anna Johansson, Lena Emanuelsson, Helen Karlholm, Mattias Ohrlander, and Peter Thomsen. 2010. "In Vivo Evaluation of Noble Metal Coatings." *Journal of Biomedical Materials Research Part B: Applied Biomaterials* 92B (1): 86–94. https://doi.org/10.1002/jbm.b.31492.

Tabibian, N., E. Swehli, A. Boyd, A. Umbreen, and J. H. Tabibian. 2017. "Abdominal Adhesions: A Practical Review of an Often Overlooked Entity." *Annals of Medicine and Surgery* 15 (March):9–13. https://doi.org/10.1016/j.amsu.2017.01.021.

Tarhan, Omer Ridvan, Ibrahim Barut, and Mekin Sezik. 2008. "An Evaluation of Normal Saline and Taurolidine on Intra-Abdominal Adhesion Formation and Peritoneal Fibrinolysis." *The Journal of Surgical Research* 144 (1): 151–57. https://doi.org/10.1016/j.jss.2007.09.006.

Tau, G., and P. Rothman. 1999. "Biologic Functions of the IFN-γ Receptors." *Allergy* 54 (12): 1233–51. https://doi.org/10.1034/j.1398-9995.1999.00099.x.

Thorpe, Robin. 1998. "2. - Interleukin-2." In *Cytokines*, edited by Anthony R. Mire-Sluis and Robin Thorpe, 19–33. Handbook of Immunopharmacology. San Diego: Academic Press. https://doi.org/10.1016/B978-012498340-3/50003-8.

Tjong, S. C., and Haydn Chen. 2004. "Nanocrystalline Materials and Coatings." *Materials Science and Engineering: R: Reports* 45 (1): 1–88. https://doi.org/10.1016/j.mser.2004.07.001.

Travis, Mark A., and Dean Sheppard. 2014. "TGF-β Activation and Function in Immunity." *Annual Review of Immunology* 32:51–82. https://doi.org/10.1146/annurev-immunol-032713-120257.

Trelewicz, Jason R., and Christopher A. Schuh. 2009. "Grain Boundary Segregation and Thermodynamically Stable Binary Nanocrystalline Alloys." *Physical Review B* 79 (9): 094112. https://doi.org/10.1103/PhysRevB.79.094112.

Truchetet, F., O. Guibon, and S. Meaume. 2012. "Clinicians' Rationale for Using a Silver Dressing: The French OMAg+E Observational Study." *Journal of Wound Care* 21 (12): 620–25. https://doi.org/10.12968/jowc.2012.21.12.620.

Tsai, Hungchun, Emily Hu, Kuoguang Perng, Minkar Chen, Jung-Chun Wu, and Yee-Shyi Chang. 2003. "Instability of Gold Oxide Au2O3." *Surface Science* 537 (1): L447–50. https://doi.org/10.1016/S0039-6028(03)00640-X.

Ugai, K., M. Ziff, and P. E. Lipsky. 1979. "Gold-Induced Changes in the Morphology and Functional Capabilities of Human Monocytes." *Arthritis and Rheumatism* 22 (12): 1352–60. https://doi.org/10.1002/art.1780221206.

Unrau, Kevin R. 2012a. "Activity of Nanocrystalline Gold and Silver Alloys." ERA. Spring 2012. https://doi.org/10.7939/R3M91X.

Varghese, Elizabeth, and Dietrich Büsselberg. 2014. "Auranofin, an Anti-Rheumatic Gold Compound, Modulates Apoptosis by Elevating the Intracellular Calcium Concentration ([Ca2+]i) in MCF-7 Breast Cancer Cells." *Cancers* 6 (4): 2243–58. https://doi.org/10.3390/cancers6042243.

Vediappan, Rajan Sundaresan, Catherine Bennett, Ahmed Bassiouni, Matthew Smith, John Finnie, Markus Trochsler, Alkis J. Psaltis, Sarah Vreugde, and Peter J. Wormald. 2020. "A Novel Rat Model to Test Intra-Abdominal Anti-Adhesive Therapy." *Frontiers in Surgery* 7 (April):12. https://doi.org/10.3389/fsurg.2020.00012.

Vediappan, Rajan Sundaresan, Catherine Bennett, Clare Cooksley, John Finnie, Markus Trochsler, Ryan D. Quarrington, Claire F. Jones, et al. 2021. "Prevention of Adhesions Post-Abdominal Surgery: Assessing the Safety and Efficacy of Chitogel with Deferiprone in a Rat Model." *PLOS ONE* 16 (1): e0244503. https://doi.org/10.1371/journal.pone.0244503.

Vimbela, Gina V, Sang M Ngo, Carolyn Fraze, Lei Yang, and David A Stout. 2017. "Antibacterial Properties and Toxicity from Metallic Nanomaterials." *International Journal of Nanomedicine* 12 (May):3941–65. https://doi.org/10.2147/IJN.S134526.

Vipond, M. N., S. A. Whawell, H. A. F. Dudley, and J. N. Thompson. 1990. "Peritoneal Fibrinolytic Activity and Intra-Abdominal Adhesions." *The Lancet*, Originally published as Volume 1, Issue 8698, 335 (8698): 1120–22. https://doi.org/10.1016/0140-6736(90)91125-T.

Vogels, Ruben R. M., Joanna W. A. M. Bosmans, Kevin W. Y. van Barneveld, Vincent Verdoold, Selwyn van Rijn, Marion J. J. Gijbels, John Penders, Stephanie O. Breukink, Dirk W. Grijpma, and Nicole D. Bouvy. 2015. "A New Poly(1,3-Trimethylene Carbonate) Film Provides Effective Adhesion Reduction after Major Abdominal Surgery in a Rat Model." *Surgery* 157 (6): 1113–20. https://doi.org/10.1016/j.surg.2015.02.004.

Wagner, Elke M. 2013. "Monitoring Gene Expression: Quantitative Real-Time RT-PCR." In *Lipoproteins and Cardiovascular Disease: Methods and Protocols*, edited by Lita A. Freeman, 19–45. Totowa, NJ: Humana Press. https://doi.org/10.1007/978-1-60327-369-5_2.

Walz, Donald T., Michael J. DiMartino, Don E. Griswold, Alfred P. Intoccia, and Thomas L. Flanagan. 1983. "Biologic Actions and Pharmacokinetic Studies of Auranofin." *The American Journal of Medicine*, Oral Gold Therapy in Rheumatoid Arthritis: Auranofin, 75 (6, Part 1): 90–108. https://doi.org/10.1016/0002-9343(83)90481-3.

Wang, Ai-Qin, Jun-Hong Liu, S. D. Lin, Tien-Sung Lin, and Chung-Yuan Mou. 2005. "A Novel Efficient Au–Ag Alloy Catalyst System: Preparation, Activity, and Characterization." *Journal of Catalysis* 233 (1): 186–97. https://doi.org/10.1016/j.jcat.2005.04.028.

Wang, Chenhong, Kuo Zhang, Heran Wang, Shanshan Xu, and Charles C. Han. 2015. "Evaluation of Biodegradability of Poly (DL-Lactic-Co-Glycolic Acid) Scaffolds for Post-Surgical Adhesion Prevention: In Vitro, in Rats and in Pigs." *Polymer* 61 (March):174–82. https://doi.org/10.1016/j.polymer.2015.02.001.

Weber, Birte, Ina Lackner, Melanie Haffner-Luntzer, Annette Palmer, Jochen Pressmar, Karin Scharffetter-Kochanek, Bernd Knöll, Hubert Schrezenemeier, Borna Relja, and Miriam Kalbitz. 2019. "Modeling Trauma in Rats: Similarities to Humans and Potential Pitfalls to Consider." *Journal of Translational Medicine* 17 (1): 305. https://doi.org/10.1186/s12967-019-2052-7.

Wei, Guangbing, Xin Chen, Guanghui Wang, Pengbo Jia, Qinhong Xu, Gaofeng Ping, Kang Wang, and Xuqi Li. 2015. "Inhibition of Cyclooxygenase-2 Prevents Intra-Abdominal Adhesions by Decreasing Activity of Peritoneal Fibroblasts." *Drug Design, Development and Therapy* 9 (June):3083–98. https://doi.org/10.2147/DDDT.S80221.

Wei, Guangbing, Yunhua Wu, Qi Gao, Cong Shen, Zilu Chen, Kang Wang, Junhui Yu, Xuqi Li, and Xuejun Sun. 2018a. "Gallic Acid Attenuates Postoperative Intra-Abdominal Adhesion by Inhibiting Inflammatory Reaction in a Rat Model." *Medical Science Monitor : International Medical Journal of Experimental and Clinical Research* 24 (February):827–38. https://doi.org/10.12659/MSM.908550.

Wei, Guangbing, Cancan Zhou, Guanghui Wang, Lin Fan, Kang Wang, and Xuqi Li. 2016. "Keratinocyte Growth Factor Combined with a Sodium Hyaluronate Gel Inhibits Postoperative Intra-Abdominal

Adhesions." *International Journal of Molecular Sciences* 17 (10): 1611. https://doi.org/10.3390/ijms17101611.

Weibel, M. -A., and G. Majno. 1973. "Peritoneal Adhesions and Their Relation to Abdominal Surgery: A Postmortem Study." *The American Journal of Surgery* 126 (3): 345–53. https://doi.org/10.1016/S0002-9610(73)80123-0.

Weissmüller, Jörg. 1994. "Alloy Thermodynamics in Nanostructures." *Journal of Materials Research* 9 (1): 4–7. https://doi.org/10.1557/JMR.1994.0004.

West, M A, D J Hackam, J Baker, J L Rodriguez, J Bellingham, and O D Rotstein. 1997. "Mechanism of Decreased in Vitro Murine Macrophage Cytokine Release after Exposure to Carbon Dioxide: Relevance to Laparoscopic Surgery." *Annals of Surgery* 226 (2): 179–90.

West, Michael A., Jeffrey Baker, and Janet Bellingham. 1996. "Kinetics of Decreased LPS-Stimulated Cytokine Release by Macrophages Exposed to CO2." *Journal of Surgical Research* 63 (1): 269–74. https://doi.org/10.1006/jsre.1996.0259.

Winny, Markus, Lavinia Maegel, Leonie Grethe, Torsten Lippmann, Danny Jonigk, Harald Schrem, Alexander Kaltenborn, Juergen Klempnauer, and Daniel Poehnert. 2016. "Adhesion Prevention Efficacy of Composite Meshes Parietex®, Proceed® and 4DryField® PH Covered Polypropylene Meshes in an IPOM Rat Model." *International Journal of Medical Sciences* 13 (12): 936–41. https://doi.org/10.7150/ijms.16215.

Wolach, B., J. E. DeBoard, T. D. Coates, R. L. Baehner, and L. A. Boxer. 1982. "Correlation of in Vitro and in Vivo Effects of Gold Compounds on Leukocyte Function: Possible Mechanisms of Action." *The Journal of Laboratory and Clinical Medicine* 100 (1): 37–44.

Wong, Kenneth K. Y., Stephanie O. F. Cheung, Liuming Huang, Jun Niu, Chang Tao, Chi-Ming Ho, Chi-Ming Che, and Paul K. H. Tam. 2009. "Further Evidence of the Anti-Inflammatory Effects of Silver Nanoparticles." *ChemMedChem* 4 (7): 1129–35. https://doi.org/10.1002/cmdc.200900049.

Wong, Tin Wui, and Nor Amlizan Ramli. 2014. "Carboxymethylcellulose Film for Bacterial Wound Infection Control and Healing." *Carbohydrate Polymers* 112 (November):367–75. https://doi.org/10.1016/j.carbpol.2014.06.002.

Wouters, Yves, Alain Galerie, and Jean-Pierre Petit. 1997. "Thermal Oxidation of Titanium by Water Vapour." *Solid State Ionics* 104 (1–2): 89–96. https://doi.org/10.1016/S0167-2738(97)00400-1.

Wright, J. Barry, Kan Lam, Andre G. Buret, Merle E. Olson, and Robert E. Burrell. 2002. "Early Healing Events in a Porcine Model of Contaminated Wounds: Effects of Nanocrystalline Silver on Matrix Metalloproteinases, Cell Apoptosis, and Healing." *Wound Repair and Regeneration* 10 (3): 141–51. https://doi.org/10.1046/j.1524-475X.2002.10308.x.

Yamada, Ryoji, Hajime Sano, Timothy Hla, Akira Hashiramoto, Wakako Fukui, Satoshi Miyazaki, Masataka Kohno, Yasunori Tsubouchi, Yoshiaki Kusaka, and Motoharu Kondo. 1999. "Auranofin Inhibits Interleukin-1β-Induced Transcript of Cyclooxygenase-2 on Cultured Human Synoviocytes." *European Journal of Pharmacology* 385 (1): 71–79. https://doi.org/10.1016/S0014-2999(99)00707-4.

Yamanaka, Mikihiro, Keita Hara, and Jun Kudo. 2005. "Bactericidal Actions of a Silver Ion Solution on Escherichia Coli, Studied by Energy-Filtering Transmission Electron Microscopy and Proteomic Analysis." *Applied and Environmental Microbiology* 71 (11): 7589–93. https://doi.org/10.1128/AEM.71.11.7589-7593.2005.

Yamaner, Sümer, Murat Kalayci, Umut Barbaros, Emre Balik, and Türker Bulut. 2005. "Does Hyaluronic Acid-Carboxymethylcellulose (HA-CMC) Membrane Interfere With the Healing of Intestinal Suture Lines and Abdominal Incisions?" *Surgical Innovation* 12 (1): 37–41. https://doi.org/10.1177/155335060501200106.

Yang, Xiao Hong, and Wei Ling Zhu. 2007. "Viscosity Properties of Sodium Carboxymethylcellulose Solutions." *Cellulose* 14 (5): 409–17. https://doi.org/10.1007/s10570-007-9137-9.

Yanni, G, M Nabil, M R Farahat, R N Poston, and G S Panayi. 1994. "Intramuscular Gold Decreases Cytokine Expression and Macrophage Numbers in the Rheumatoid Synovial Membrane." *Annals of the Rheumatic Diseases* 53 (5): 315–22.

Yeo, Yoon, Christopher B. Highley, Evangelia Bellas, Taichi Ito, Robert Marini, Robert Langer, and Daniel S. Kohane. 2006a. "In Situ Cross-Linkable Hyaluronic Acid Hydrogels Prevent Post-Operative Abdominal Adhesions in a Rabbit Model." *Biomaterials* 27 (27): 4698–4705. https://doi.org/10.1016/j.biomaterials.2006.04.043.

Yilmaz, Hatice Gulsen, Ibrahim Halil Tacyildiz, Celalettin Keles, Ercan Gedik, and Nihal Kilinc. 2005. "Micronized Purified Flavonoid Fraction May Prevent Formation of Intraperitoneal Adhesions in Rats." *Fertility and Sterility* 84 (October):1083–88. https://doi.org/10.1016/j.fertnstert.2005.03.076.

You, Chuangang, Chunmao Han, Xingang Wang, Yurong Zheng, Qiyin Li, Xinlei Hu, and Huafeng Sun. 2012. "The Progress of Silver Nanoparticles in the Antibacterial Mechanism, Clinical Application and Cytotoxicity." *Molecular Biology Reports* 39 (9): 9193–9201. https://doi.org/10.1007/s11033-012-1792-8.

Zhang, Ershuai, Boyi Song, Yuanjie Shi, Hui Zhu, Xiangfei Han, Hong Du, Chengbiao Yang, and Zhiqiang Cao. 2020. "Fouling-Resistant Zwitterionic Polymers for Complete Prevention of Postoperative Adhesion." *Proceedings of the National Academy of Sciences of the United States of America* 117 (50): 32046–55. https://doi.org/10.1073/pnas.2012491117.

Zhao, Xiaoye, Jianhai Yang, Yang Liu, Jushan Gao, Ke Wang, and Wenguang Liu. 2021. "An Injectable and Antifouling Self-Fused Supramolecular Hydrogel for Preventing Postoperative and Recurrent Adhesions." *Chemical Engineering Journal* 404 (January):127096. https://doi.org/10.1016/j.cej.2020.127096.

Zhou, Juan, Clive Elson, and Timothy D. G Lee. 2004. "Reduction in Postoperative Adhesion Formation and Re-Formation after an Abdominal Operation with the Use of N, O - Carboxymethyl Chitosan." *Surgery* 135 (3): 307–12. https://doi.org/10.1016/j.surg.2003.07.005.

Zhu, Yingxi, and Steve Granick. 2003. "Biolubrication: Hyaluronic Acid and the Influence on Its Interfacial Viscosity of an Antiinflammatory Drug." *Macromolecules* 36 (4): 973–76. https://doi.org/10.1021/ma025988r.

Zimmerman, Bevin. 2018. "Chapter 8 - Peritoneum, Retroperitoneum, Mesentery, and Abdominal Cavity." In *Boorman's Pathology of the Rat (Second Edition)*, edited by Andrew W. Suttie, 71–77. Boston: Academic Press. https://doi.org/10.1016/B978-0-12-391448-4.00008-3.

Zolnik, Banu S., and Diane J. Burgess. 2007. "Effect of Acidic pH on PLGA Microsphere Degradation and Release." *Journal of Controlled Release*, Proceedings of the Thirteenth International Symposium on Recent Advances in Drug Delivery Systems, 122 (3): 338–44. https://doi.org/10.1016/j.jconrel.2007.05.034.

Zou, Taotao, Ching Tung Lum, Chun-Nam Lok, Jing-Jing Zhang, and Chi-Ming Che. 2015. "Chemical Biology of Anticancer Gold(III) and Gold(I) Complexes." *Chemical Society Reviews* 44 (24): 8786–8801. https://doi.org/10.1039/C5CS00132C.

Appendix A: Tukey's Post-Hoc Tests

Tukey's Post-Hoc Test p-values from Chapter 4

	Total Silver	Ammonia Soluble Silver	Percent Ammonia Soluble Silver	Total Deposition
S:Ag100-N:Ag100	8.19E-13	2.81E-05	4.06E-03	2.34E-11
N:Ag35-N:Ag100	3.58E-13	7.26E-09	0.97	2.17E-07
S:Ag35-N:Ag100	7.31E-14	8.79E-09	0.05	3.49E-09
N:Ag65-N:Ag100	9.06E-08	0.11	0.97	1
S:Ag65-N:Ag100	3.02E-13	8.03E-08	0.14	6.42E-11
N:Ag35-S:Ag100	2.21E-02	8.14E-06	1.19E-03	8.86E-13
S:Ag35-S:Ag100	1.03E-06	1.17E-05	0.68	3.79E-05
N:Ag65-S:Ag100	3.44E-11	1.51E-03	1.44E-02	2.18E-11
S:Ag65-S:Ag100	6.12E-03	7.59E-04	0.34	0.58
S:Ag35-N:Ag35	7.83E-05	1	1.34E-02	4.09E-12
N:Ag65-N:Ag35	6.20E-12	5.00E-08	0.65	2.42E-07
S:Ag65-N:Ag35	0.97	4.14E-02	3.85E-02	1.24E-12
N:Ag65-S:Ag35	1.42E-12	6.39E-08	0.17	3.25E-09
S:Ag65-S:Ag35	2.22E-04	7.02E-02	0.99	3.54E-04
S:Ag65-N:Ag65	5.11E-12	1.01E-06	0.41	5.93E-11

	Silver Release	Percent silver release	Log reduction *S. aureus*	Grain Size
S:Ag100-N:Ag100	0.03	1.65E-05	6.35E-01	4.52E-04
N:Ag35-N:Ag100	1.17E-06	5.09E-02	9.99E-01	5.81E-03
S:Ag35-N:Ag100	3.45E-07	3.39E-05	4.08E-02	6.73E-09
N:Ag65-N:Ag100	3.66E-05	0.65	1.29E-01	8.78E-07
S:Ag65-N:Ag100	3.53E-06	2.87E-03	8.77E-01	6.23E-07
N:Ag35-S:Ag100	7.71E-05	1.61E-03	8.09E-01	0.59
S:Ag35-S:Ag100	1.52E-05	0.99	4.37E-01	8.40E-07
N:Ag65-S:Ag100	8.25E-03	3.00E-06	8.21E-01	2.08E-03
S:Ag65-S:Ag100	3.45E-04	2.74E-02	9.96E-01	1.18E-03
S:Ag35-N:Ag35	0.78	4.15E-03	6.97E-02	1.91E-07
N:Ag65-N:Ag35	7.41E-02	3.93E-03	2.11E-01	1.83E-04
S:Ag65-N:Ag35	0.88	0.54	9.68E-01	1.11E-04
N:Ag65-S:Ag35	8.25E-03	5.67E-06	9.78E-01	4.23E-04
S:Ag65-S:Ag35	0.23	7.43E-02	2.32E-01	7.25E-04
S:Ag65-N:Ag65	0.38	2.81E-04	5.61E-01	1

	Total Gold	Gold % of Total
S:Ag35-N:Ag35	1.22E-08	2.97E-03
N:Ag65-N:Ag35	3.70E-09	3.18E-09
S:Ag65-N:Ag35	1.22E-09	7.61E-09
N:Ag65-S:Ag35	7.25E-04	8.64E-09
S:Ag65-S:Ag35	1.09E-05	1.90E-08
S:Ag65-N:Ag65	3.52E-03	7.29E-03

P. aeruginosa CZOI	Day 1	Day 2	Day 3	Day 4
S:Ag35-N:Ag35	0.67	0.96	1	1
N:Ag65-N:Ag35	0.87	0.5	8.43E-02	0.14
S:Ag65-N:Ag35	0.94	0.68	0.56	8.13E-02
N:Ag65-S:Ag35	0.98	0.28	6.83E-02	0.14
S:Ag65-S:Ag35	0.94	0.42	0.48	8.13E-02
S:Ag65-N:Ag65	1	0.99	0.48	0.98

P. aeruginosa CZOI	Day 5	Day 6	Day 7
S:Ag35-N:Ag35	1	1	1
N:Ag65-N:Ag35	0.8	3.96E-05	0.53
S:Ag65-N:Ag35	0.12	0.75	1
N:Ag65-S:Ag35	0.8	3.96E-05	0.53
S:Ag65-S:Ag35	0.12	0.75	1
S:Ag65-N:Ag65	0.39	8.60E-05	0.53

S. aureus CZOI	Day 1	Day 2	Day 3	Day 4
S:Ag35-N:Ag35	0.98	0.72	1	0.92
N:Ag65-N:Ag35	0.72	0.99	0.52	0.43
S:Ag65-N:Ag35	0.82	0.84	0.65	0.99
N:Ag65-S:Ag35	0.5	0.84	0.65	0.19
S:Ag65-S:Ag35	0.61	0.3	0.77	0.99
S:Ag65-N:Ag65	1	0.72	1	0.29

S. aureus CZOI	Day 5	Day 6	Day 7
S:Ag35-N:Ag35	1	0.81	0.72
N:Ag65-N:Ag35	1.82E-04	3.59E-04	3.53E-05
S:Ag65-N:Ag35	1.92E-02	0.49	0.72
N:Ag65-S:Ag35	1.82E-04	1.60E-04	1.67E-05
S:Ag65-S:Ag35	1.92E-02	0.16	1
S:Ag65-N:Ag65	1.25E-02	1.63E-03	1.67E-05

Tukey's Post-Hoc Test p-values from Chapter 7

Test 1: Low, Mid, and High Viscosity. 1, 2, 4, 8, 24, 48, and 72 hour time points. 5, 10, and 20 rpm shear rates. Before and After test.

	Silver release		Silver release
fortyeight:High-eight:High	1	seventytwo:Mid-fortyeight:High	1
four:High-eight:High	0.99	twentyfour:Mid-fortyeight:High	1
one:High-eight:High	7.05E-11	two:Mid-fortyeight:High	3.37E-09
seventytwo:High-eight:High	1	one:High-four:High	7.50E-09
twentyfour:High-eight:High	1	seventytwo:High-four:High	0.98
two:High-eight:High	9.41E-06	twentyfour:High-four:High	1
eight:Low-eight:High	1	two:High-four:High	1.34E-03
fortyeight:Low-eight:High	0.96	eight:Low-four:High	0.91
four:Low-eight:High	0.77	fortyeight:Low-four:High	0.15
one:Low-eight:High	1.36E-10	four:Low-four:High	1
seventytwo:Low-eight:High	1	one:Low-four:High	1.52E-08
twentyfour:Low-eight:High	1	seventytwo:Low-four:High	0.84
two:Low-eight:High	1.03E-06	twentyfour:Low-four:High	1
eight:Mid-eight:High	1	two:Low-four:High	1.56E-04
fortyeight:Mid-eight:High	1	eight:Mid-four:High	0.71
four:Mid-eight:High	7.96E-02	fortyeight:Mid-four:High	0.99
one:Mid-eight:High	1.62E-12	four:Mid-four:High	0.87
seventytwo:Mid-eight:High	1	one:Mid-four:High	4.06E-11
twentyfour:Mid-eight:High	1	seventytwo:Mid-four:High	1
two:Mid-eight:High	7.50E-09	twentyfour:Mid-four:High	0.99
four:High-fortyeight:High	0.96	two:Mid-four:High	1.04E-06
one:High-fortyeight:High	3.39E-11	seventytwo:High-one:High	5.34E-11
seventytwo:High-fortyeight:High	1	twentyfour:High-one:High	2.41E-10
twentyfour:High-fortyeight:High	1	two:High-one:High	5.35E-02
two:High-fortyeight:High	4.06E-06	eight:Low-one:High	2.17E-11
eight:Low-fortyeight:High	1	fortyeight:Low-one:High	1.57E-12
fortyeight:Low-fortyeight:High	0.99	four:Low-one:High	7.01E-08
four:Low-fortyeight:High	0.60	one:Low-one:High	1
one:Low-fortyeight:High	6.43E-11	seventytwo:Low-one:High	1.41E-11
seventytwo:Low-fortyeight:High	1	twentyfour:Low-one:High	1.24E-10
twentyfour:Low-fortyeight:High	1	two:Low-one:High	0.25
two:Low-fortyeight:High	4.47E-07	seventytwo:Mid-fortyeight:High	1
eight:Mid-fortyeight:High	1	twentyfour:Mid-fortyeight:High	1
fortyeight:Mid-fortyeight:High	1	two:Mid-fortyeight:High	3.37E-09
four:Mid-fortyeight:High	4.18E-02	one:High-four:High	7.50E-09
one:Mid-fortyeight:High	1.35E-12	seventytwo:High-four:High	0.98
eight:Mid-one:High	7.95E-12	four:Low-two:High	1.12E-02
fortyeight:Mid-one:High	7.05E-11	one:Low-two:High	9.28E-02

	Silver release		Silver release
four:Mid-one:High	5.56E-06	seventytwo:Low-two:High	1.42E-06
one:Mid-one:High	0.97	twentyfour:Low-two:High	1.77E-05
seventytwo:Mid-one:High	2.19E-10	two:Low-two:High	1
twentyfour:Mid-one:High	8.50E-11	eight:Mid-two:High	6.85E-07
two:Mid-one:High	0.99	fortyeight:Mid-two:High	9.41E-06
twentyfour:High-seventytwo:High	1	four:Mid-two:High	0.29
two:High-seventytwo:High	6.86E-06	one:Mid-two:High	3.25E-04
eight:Low-seventytwo:High	1	seventytwo:Mid-two:High	3.31E-05
fortyeight:Low-seventytwo:High	0.98	twentyfour:Mid-two:High	1.16E-05
four:Low-seventytwo:High	0.71	two:Mid-two:High	0.79
one:Low-seventytwo:High	1.03E-10	fortyeight:Low-eight:Low	1
seventytwo:Low-seventytwo:High	1	four:Low-eight:Low	0.49
twentyfour:Low-seventytwo:High	1	one:Low-eight:Low	4.06E-11
two:Low-seventytwo:High	7.52E-07	seventytwo:Low-eight:Low	1
eight:Mid-seventytwo:High	1	twentyfour:Low-eight:Low	1
fortyeight:Mid-seventytwo:High	1	two:Low-eight:Low	2.66E-07
four:Mid-seventytwo:High	6.29E-02	eight:Mid-eight:Low	1
one:Mid-seventytwo:High	1.50E-12	fortyeight:Mid-eight:Low	1
seventytwo:Mid-seventytwo:High	1	four:Mid-eight:Low	2.73E-02
twentyfour:Mid-seventytwo:High	1	one:Mid-eight:Low	1.26E-12
two:Mid-seventytwo:High	5.55E-09	seventytwo:Mid-eight:Low	1
two:High-twentyfour:High	3.68E-05	twentyfour:Mid-eight:Low	1
eight:Low-twentyfour:High	1	two:Mid-eight:Low	2.05E-09
fortyeight:Low-twentyfour:High	0.80	four:Low-fortyeight:Low	2.73E-02
four:Low-twentyfour:High	0.95	one:Low-fortyeight:Low	1.98E-12
one:Low-twentyfour:High	4.73E-10	seventytwo:Low-fortyeight:Low	1
seventytwo:Low-twentyfour:High	1	twentyfour:Low-fortyeight:Low	0.91
twentyfour:Low-twentyfour:High	1	two:Low-fortyeight:Low	3.69E-09
two:Low-twentyfour:High	4.02E-06	eight:Mid-fortyeight:Low	1
eight:Mid-twentyfour:High	1	fortyeight:Mid-fortyeight:Low	0.96
fortyeight:Mid-twentyfour:High	1	four:Mid-fortyeight:Low	4.90E-04
four:Mid-twentyfour:High	0.20	one:Mid-fortyeight:Low	1.07E-12
one:Mid-twentyfour:High	2.73E-12	seventytwo:Mid-fortyeight:Low	0.82
seventytwo:Mid-twentyfour:High	1	twentyfour:Mid-fortyeight:Low	0.95
twentyfour:Mid-twentyfour:High	1	two:Mid-fortyeight:Low	3.71E-11
two:Mid-twentyfour:High	2.79E-08	one:Low-four:Low	1.44E-07
eight:Low-two:High	2.40E-06	seventytwo:Low-four:Low	0.38
fortyeight:Low-two:High	3.09E-08	twentyfour:Low-four:Low	0.87
one:Mid-four:Low	3.21E-10	four:Mid-fortyeight:Mid	7.96E-02
seventytwo:Mid-four:Low	0.94	one:Mid-fortyeight:Mid	1.62E-12

	Silver release		Silver release
twentyfour:Mid-four:Low	0.80	seventytwo:Mid-fortyeight:Mid	1
two:Mid-four:Low	1.04E-05	twentyfour:Mid-fortyeight:Mid	1
seventytwo:Low-one:Low	2.59E-11	two:Mid-fortyeight:Mid	7.50E-09
twentyfour:Low-one:Low	2.41E-10	one:Mid-four:Mid	2.06E-08
two:Low-one:Low	0.37	seventytwo:Mid-four:Mid	0.19
eight:Mid-one:Low	1.41E-11	twentyfour:Mid-four:Mid	9.28E-02
fortyeight:Mid-one:Low	1.36E-10	two:Mid-four:Mid	8.13E-04
four:Mid-one:Low	1.16E-05	seventytwo:Mid-one:Mid	2.60E-12
one:Mid-one:Low	0.91	twentyfour:Mid-one:Mid	1.72E-12
seventytwo:Mid-one:Low	4.29E-10	two:Mid-one:Mid	0.17
twentyfour:Mid-one:Low	1.64E-10	twentyfour:Mid-seventytwo:Mid	1
two:Mid-one:Low	1	two:Mid-seventytwo:Mid	2.52E-08
twentyfour:Low-seventytwo:Low	1	two:Mid-twentyfour:Mid	9.17E-09
two:Low-seventytwo:Low	1.58E-07	twentyfour:Mid-eight:Mid	1.00E+00
eight:Mid-seventytwo:Low	1	two:Mid-eight:Mid	6.32E-10
fortyeight:Mid-seventytwo:Low	1		
four:Mid-seventytwo:Low	1.76E-02		
one:Mid-seventytwo:Low	1.19E-12		
seventytwo:Mid-seventytwo:Low	1		
twentyfour:Mid-seventytwo:Low	1		
two:Mid-seventytwo:Low	1.25E-09		
two:Low-twentyfour:Low	1.93E-06		
eight:Mid-twentyfour:Low	1		
fortyeight:Mid-twentyfour:Low	1		
four:Mid-twentyfour:Low	0.12		
one:Mid-twentyfour:Low	1.98E-12		
seventytwo:Mid-twentyfour:Low	1		
twentyfour:Mid-twentyfour:Low	1		
two:Mid-twentyfour:Low	1.37E-08		
eight:Mid-two:Low	7.69E-08		
fortyeight:Mid-two:Low	1.03E-06		
four:Mid-two:Low	6.75E-02		
one:Mid-two:Low	2.71E-03		
seventytwo:Mid-two:Low	3.62E-06		
twentyfour:Mid-two:Low	1.27E-06		
two:Mid-two:Low	0.99		
fortyeight:Mid-eight:Mid	1		
four:Mid-eight:Mid	9.28E-03		
one:Mid-eight:Mid	1.14E-12		
seventytwo:Mid-eight:Mid	1.00E+00		

	Viscosity at 5 rpm	Viscosity at 10 rpm	Viscosity at 20rpm
Before:High-After:High	1.89E-12	3.79E-12	6.76E-06
After:Low-After:High	4.20E-04	4.57E-05	2.91E-02
Before:Low-After:High	0.98	0.81	0.98
After:Mid-After:High	6.17E-03	1.07E-03	0.18
Before:Mid-After:High	2.33E-06	5.18E-07	2.75E-03
After:Low-Before:High	5.27E-13	8.42E-13	1.90E-07
Before:Low-Before:High	1.66E-12	3.02E-12	3.11E-06
After:Mid-Before:High	7.60E-13	1.32E-12	5.15E-07
Before:Mid-Before:High	5.25E-11	1.57E-09	7.79E-03
Before:Low-After:Low	1.15E-03	2.42E-04	9.67E-02
After:Mid-After:Low	0.54	0.28	0.86
Before:Mid-After:Low	1.23E-08	1.87E-09	1.66E-05
After:Mid-Before:Low	1.89E-02	7.87E-03	0.48
Before:Mid-Before:Low	1.19E-06	1.72E-07	8.92E-04
Before:Mid-After:Mid	4.02E-08	6.96E-09	6.71E-05

	Percentage viscosity reduction		Percentage viscosity reduction
20rpm:High-10rpm:High	0.22	10rpm:Mid-5rpm:High	0.22
5rpm:High-10rpm:High	0.27	20rpm:Mid-5rpm:High	0.30
10rpm:Low-10rpm:High	0.98	5rpm:Mid-5rpm:High	1
20rpm:Low-10rpm:High	0.25	20rpm:Low-10rpm:Low	0.80
5rpm:Low-10rpm:High	1	5rpm:Low-10rpm:Low	0.72
10rpm:Mid-10rpm:High	0.89	10rpm:Mid-10rpm:Low	0.35
20rpm:Mid-10rpm:High	1.00	20rpm:Mid-10rpm:Low	0.97
5rpm:Mid-10rpm:High	0.30	5rpm:Mid-10rpm:Low	5.10E-02
5rpm:High-20rpm:High	1.42E-03	5rpm:Low-20rpm:Low	7.17E-02
10rpm:Low-20rpm:High	0.75	10rpm:Mid-20rpm:Low	1.94E-02
20rpm:Low-20rpm:High	1	20rpm:Mid-20rpm:Low	0.23
5rpm:Low-20rpm:High	6.02E-02	5rpm:Mid-20rpm:Low	1.97E-03
10rpm:Mid-20rpm:High	1.61E-02	10rpm:Mid-5rpm:Low	1.00
20rpm:Mid-20rpm:High	0.20	20rpm:Mid-5rpm:Low	1.00
5rpm:Mid-20rpm:High	1.63E-03	5rpm:Mid-5rpm:Low	0.70
10rpm:Low-5rpm:High	4.46E-02	20rpm:Mid-10rpm:Mid	0.92
20rpm:Low-5rpm:High	1.71E-03	5rpm:Mid-10rpm:Mid	0.97
5rpm:Low-5rpm:High	0.66	5rpm:Mid-20rpm:Mid	0.33

Test 2: Low, Mid, and High Viscosity. 1, 2, 4, 8, 24, 48, and 72 hour time points. 5, 10, and 20 rpm shear rates. Before and After test.

	Silver release		Silver release
fortyeight:High-eight:High	1	seventytwo:Mid-fortyeight:High	1
four:High-eight:High	0.99	twentyfour:Mid-fortyeight:High	1
one:High-eight:High	7.05E-11	two:Mid-fortyeight:High	3.37E-09
seventytwo:High-eight:High	1	one:High-four:High	7.50E-09
twentyfour:High-eight:High	1	seventytwo:High-four:High	0.98
two:High-eight:High	9.41E-06	twentyfour:High-four:High	1
eight:Low-eight:High	1	two:High-four:High	1.34E-03
fortyeight:Low-eight:High	0.96	eight:Low-four:High	0.91
four:Low-eight:High	0.77	fortyeight:Low-four:High	0.15
one:Low-eight:High	1.36E-10	four:Low-four:High	1
seventytwo:Low-eight:High	1	one:Low-four:High	1.52E-08
twentyfour:Low-eight:High	1	seventytwo:Low-four:High	0.84
two:Low-eight:High	1.03E-06	twentyfour:Low-four:High	1
eight:Mid-eight:High	1	two:Low-four:High	1.56E-04
fortyeight:Mid-eight:High	1	eight:Mid-four:High	0.71
four:Mid-eight:High	7.96E-02	fortyeight:Mid-four:High	0.99
one:Mid-eight:High	1.62E-12	four:Mid-four:High	0.87
seventytwo:Mid-eight:High	1	one:Mid-four:High	4.06E-11
twentyfour:Mid-eight:High	1	seventytwo:Mid-four:High	1
two:Mid-eight:High	7.50E-09	twentyfour:Mid-four:High	9.94E-01
four:High-fortyeight:High	0.96	two:Mid-four:High	1.04E-06
one:High-fortyeight:High	3.39E-11	seventytwo:High-one:High	5.34E-11
seventytwo:High-fortyeight:High	1	twentyfour:High-one:High	2.41E-10
twentyfour:High-fortyeight:High	1	two:High-one:High	5.35E-02
two:High-fortyeight:High	4.06E-06	eight:Low-one:High	2.17E-11
eight:Low-fortyeight:High	1	fortyeight:Low-one:High	1.57E-12
fortyeight:Low-fortyeight:High	0.99	four:Low-one:High	7.01E-08
four:Low-fortyeight:High	0.60	one:Low-one:High	1
one:Low-fortyeight:High	6.43E-11	seventytwo:Low-one:High	1.41E-11
seventytwo:Low-fortyeight:High	1	twentyfour:Low-one:High	1.24E-10
twentyfour:Low-fortyeight:High	1	two:Low-one:High	0.25
two:Low-fortyeight:High	4.47E-07	eight:Mid-one:High	7.95E-12
eight:Mid-fortyeight:High	1	fortyeight:Mid-one:High	7.05E-11
fortyeight:Mid-fortyeight:High	1	four:Mid-one:High	5.56E-06
four:Mid-fortyeight:High	4.18E-02	one:Mid-one:High	0.97
one:Mid-fortyeight:High	1.35E-12	seventytwo:Mid-one:High	2.19E-10
twentyfour:Mid-one:High	8.50E-11	eight:Mid-two:High	6.85E-07

	Silver release		Silver release
two:Mid-one:High	0.99	fortyeight:Mid-two:High	9.41E-06
twentyfour:High-seventytwo:High	1	four:Mid-two:High	0.29
two:High-seventytwo:High	6.86E-06	one:Mid-two:High	3.25E-04
eight:Low-seventytwo:High	1	seventytwo:Mid-two:High	3.31E-05
fortyeight:Low-seventytwo:High	0.98	twentyfour:Mid-two:High	1.16E-05
four:Low-seventytwo:High	0.71	two:Mid-two:High	0.79
one:Low-seventytwo:High	1.03E-10	fortyeight:Low-eight:Low	1
seventytwo:Low-seventytwo:High	1	four:Low-eight:Low	0.49
twentyfour:Low-seventytwo:High	1	one:Low-eight:Low	4.06E-11
two:Low-seventytwo:High	7.52E-07	seventytwo:Low-eight:Low	1
eight:Mid-seventytwo:High	1	two:Low-eight:Low	2.66E-07
fortyeight:Mid-seventytwo:High	1	eight:Mid-eight:Low	1
four:Mid-seventytwo:High	6.29E-02	fortyeight:Mid-eight:Low	1
one:Mid-seventytwo:High	1.50E-12	four:Mid-eight:Low	2.73E-02
seventytwo:Mid-seventytwo:High	1	one:Mid-eight:Low	1.26E-12
twentyfour:Mid-seventytwo:High	1	seventytwo:Mid-eight:Low	1
two:Mid-seventytwo:High	5.55E-09	twentyfour:Mid-eight:Low	1
two:High-twentyfour:High	3.68E-05	two:Mid-eight:Low	2.05E-09
eight:Low-twentyfour:High	1.00E+00	four:Low-fortyeight:Low	2.73E-02
fortyeight:Low-twentyfour:High	0.80	one:Low-fortyeight:Low	1.98E-12
four:Low-twentyfour:High	0.95	seventytwo:Low-fortyeight:Low	1
one:Low-twentyfour:High	4.73E-10	twentyfour:Low-fortyeight:Low	0.91
seventytwo:Low-twentyfour:High	1	two:Low-fortyeight:Low	3.69E-09
twentyfour:Low-twentyfour:High	1	eight:Mid-fortyeight:Low	1
two:Low-twentyfour:High	4.02E-06	fortyeight:Mid-fortyeight:Low	0.96
eight:Mid-twentyfour:High	1	four:Mid-fortyeight:Low	4.90E-04
fortyeight:Mid-twentyfour:High	1	one:Mid-fortyeight:Low	1.07E-12
four:Mid-twentyfour:High	0.20	seventytwo:Mid-fortyeight:Low	0.82
one:Mid-twentyfour:High	2.73E-12	twentyfour:Mid-fortyeight:Low	0.95
seventytwo:Mid-twentyfour:High	1	two:Mid-fortyeight:Low	3.71E-11
twentyfour:Mid-twentyfour:High	1	one:Low-four:Low	1.44E-07
two:Mid-twentyfour:High	2.79E-08	seventytwo:Low-four:Low	0.38
eight:Low-two:High	2.40E-06	twentyfour:Low-four:Low	0.87
fortyeight:Low-two:High	3.09E-08	two:Low-four:Low	1.47E-03
four:Low-two:High	1.12E-02	eight:Mid-four:Low	0.26
one:Low-two:High	9.28E-02	fortyeight:Mid-four:Low	0.77
seventytwo:Low-two:High	1.42E-06	four:Mid-four:Low	1
twentyfour:Low-two:High	1.77E-05	one:Mid-four:Low	3.21E-10

	Silver release		Silver release
two:Low-two:High	1	seventytwo:Mid-four:Low	0.94
twentyfour:Mid-four:Low	0.80	twentyfour:Mid-eight:Mid	1
two:Mid-four:Low	1.04E-05	two:Mid-eight:Mid	6.32E-10
seventytwo:Low-one:Low	2.59E-11	four:Mid-fortyeight:Mid	7.96E-02
twentyfour:Low-one:Low	2.41E-10	one:Mid-fortyeight:Mid	1.62E-12
two:Low-one:Low	0.37	seventytwo:Mid-fortyeight:Mid	1
eight:Mid-one:Low	1.41E-11	twentyfour:Mid-fortyeight:Mid	1
fortyeight:Mid-one:Low	1.36E-10	two:Mid-fortyeight:Mid	7.50E-09
four:Mid-one:Low	1.16E-05	one:Mid-four:Mid	2.06E-08
one:Mid-one:Low	0.91	seventytwo:Mid-four:Mid	0.19
seventytwo:Mid-one:Low	4.29E-10	twentyfour:Mid-four:Mid	9.28E-02
twentyfour:Mid-one:Low	1.64E-10	two:Mid-four:Mid	8.13E-04
two:Mid-one:Low	1	seventytwo:Mid-one:Mid	2.60E-12
twentyfour:Low-seventytwo:Low	1	twentyfour:Mid-one:Mid	1.72E-12
two:Low-seventytwo:Low	1.58E-07	two:Mid-one:Mid	0.17
eight:Mid-seventytwo:Low	1	twentyfour:Mid-seventytwo:Mid	1
fortyeight:Mid-seventytwo:Low	1	two:Mid-seventytwo:Mid	2.52E-08
four:Mid-seventytwo:Low	1.76E-02	two:Mid-twentyfour:Mid	9.17E-09
one:Mid-seventytwo:Low	1.19E-12	one:Mid-eight:Mid	1.14E-12
seventytwo:Mid-seventytwo:Low	1	seventytwo:Mid-eight:Mid	1
twentyfour:Mid-seventytwo:Low	1		
two:Mid-seventytwo:Low	1.25E-09		
two:Low-twentyfour:Low	1.93E-06		
eight:Mid-twentyfour:Low	1		
fortyeight:Mid-twentyfour:Low	1		
four:Mid-twentyfour:Low	0.12		
one:Mid-twentyfour:Low	1.98E-12		
seventytwo:Mid-twentyfour:Low	1		
twentyfour:Mid-twentyfour:Low	1		
two:Mid-twentyfour:Low	1.37E-08		
eight:Mid-two:Low	7.69E-08		
fortyeight:Mid-two:Low	1.03E-06		
four:Mid-two:Low	6.75E-02		
one:Mid-two:Low	2.71E-03		
seventytwo:Mid-two:Low	3.62E-06		
twentyfour:Mid-two:Low	1.27E-06		
two:Mid-two:Low	0.99		
fortyeight:Mid-eight:Mid	1		
four:Mid-eight:Mid	9.28E-03		

	Viscosity at 5 rpm	Viscosity at 10 rpm	Viscosity at 20rpm
Before:High-After:High	4.34E-08	5.37E-08	5.40E-08
After:Low-After:High	4.65E-03	1.46E-03	6.28E-04
Before:Low-After:High	0.46	0.25	0.15
After:Mid-After:High	8.27E-02	5.15E-02	3.02E-02
Before:Mid-After:High	0.13	0.23	0.30
After:Low-Before:High	2.14E-09	1.65E-09	1.19E-09
Before:Low-Before:High	1.19E-08	1.06E-08	8.63E-09
After:Mid-Before:High	5.82E-09	5.79E-09	4.83E-09
Before:Mid-Before:High	4.36E-07	4.07E-07	3.41E-07
Before:Low-After:Low	0.11	6.94E-02	4.89E-02
After:Mid-After:Low	0.54	0.32	0.23
Before:Mid-After:Low	7.83E-05	4.85E-05	3.14E-05
After:Mid-Before:Low	0.84	0.91	0.92
Before:Mid-Before:Low	5.79E-03	4.88E-03	3.90E-03
Before:Mid-After:Mid	8.97E-04	9.98E-04	8.41E-04

	Percentage viscosity reduction		Percentage viscosity reduction
20rpm:High-10rpm:High	0.99	10rpm:Mid-5rpm:High	7.90E-02
5rpm:High-10rpm:High	0.95	20rpm:Mid-5rpm:High	7.80E-03
10rpm:Low-10rpm:High	1	5rpm:Mid-5rpm:High	0.86
20rpm:Low-10rpm:High	0.98	20rpm:Low-10rpm:Low	0.86
5rpm:Low-10rpm:High	0.80	5rpm:Low-10rpm:Low	0.96
10rpm:Mid-10rpm:High	0.50	10rpm:Mid-10rpm:Low	0.27
20rpm:Mid-10rpm:High	8.13E-02	20rpm:Mid-10rpm:Low	3.37E-02
5rpm:Mid-10rpm:High	1	5rpm:Mid-10rpm:Low	1
5rpm:High-20rpm:High	0.51	5rpm:Low-20rpm:Low	0.25
10rpm:Low-20rpm:High	0.90	10rpm:Mid-20rpm:Low	0.97
20rpm:Low-20rpm:High	1	20rpm:Mid-20rpm:Low	0.42
5rpm:Low-20rpm:High	0.29	5rpm:Mid-20rpm:Low	1
10rpm:Mid-20rpm:High	0.95	10rpm:Mid-5rpm:Low	3.48E-02
20rpm:Mid-20rpm:High	0.37	20rpm:Mid-5rpm:Low	3.25E-03
5rpm:Mid-20rpm:High	1.00	5rpm:Mid-5rpm:Low	0.64
10rpm:Low-5rpm:High	1.00	20rpm:Mid-10rpm:Mid	0.96
20rpm:Low-5rpm:High	0.46	5rpm:Mid-10rpm:Mid	0.68
5rpm:Low-5rpm:High	1	5rpm:Mid-20rpm:Mid	0.14

Test 3: Low and High pH. 1, 2, 4, 8, 24, 48, and 72 hour time points. 5, 10, and 20 rpm shear rates.

	Silver release		Silver release
fortyeight:High-eight:High	0.78	two:Low-four:High	5.58E-03
four:High-eight:High	0.99	seventytwo:High-one:High	5.11E-10
one:High-eight:High	8.46E-07	twentyfour:High-one:High	6.89E-08
seventytwo:High-eight:High	0.11	two:High-one:High	0.26
twentyfour:High-eight:High	1	eight:Low-one:High	2.50E-06
two:High-eight:High	1.23E-03	fortyeight:Low-one:High	1.59E-08
eight:Low-eight:High	1	four:Low-one:High	9.84E-05
fortyeight:Low-eight:High	0.90	one:Low-one:High	1
four:Low-eight:High	0.82	seventytwo:Low-one:High	6.04E-09
one:Low-eight:High	1.19E-07	twentyfour:Low-one:High	1.19E-07
seventytwo:Low-eight:High	0.67	two:Low-one:High	0.62
twentyfour:Low-eight:High	1	twentyfour:High-seventytwo:High	0.60
two:Low-eight:High	2.47E-04	two:High-seventytwo:High	2.73E-07
four:High-fortyeight:High	0.14	eight:Low-seventytwo:High	4.11E-02
one:High-fortyeight:High	8.88E-09	fortyeight:Low-seventytwo:High	0.93
seventytwo:High-fortyeight:High	0.98	four:Low-seventytwo:High	1.14E-03
twentyfour:High-fortyeight:High	1	one:Low-seventytwo:High	1.00E-10
two:High-fortyeight:High	7.55E-06	seventytwo:Low-seventytwo:High	0.99
eight:Low-fortyeight:High	0.50	twentyfour:Low-seventytwo:High	0.45
fortyeight:Low-fortyeight:High	1	two:Low-seventytwo:High	6.44E-08
four:Low-fortyeight:High	3.35E-02	two:High-twentyfour:High	7.83E-05
one:Low-fortyeight:High	1.52E-09	eight:Low-twentyfour:High	0.96
seventytwo:Low-fortyeight:High	1	fortyeight:Low-twentyfour:High	1
twentyfour:Low-fortyeight:High	1	four:Low-twentyfour:High	0.22
two:Low-fortyeight:High	1.62E-06	one:Low-twentyfour:High	1.08E-08
one:High-four:High	1.72E-05	seventytwo:Low-twentyfour:High	1
seventytwo:High-four:High	6.47E-03	twentyfour:Low-twentyfour:High	1
twentyfour:High-four:High	0.60	two:Low-twentyfour:High	1.59E-05
two:High-four:High	2.54E-02	eight:Low-two:High	3.84E-03
eight:Low-four:High	1	fortyeight:Low-two:High	1.48E-05
fortyeight:Low-four:High	0.24	four:Low-two:High	0.11
one:Low-two:High	5.02E-02	seventytwo:Low-fortyeight:Low	1
seventytwo:Low-two:High	4.84E-06	twentyfour:Low-fortyeight:Low	1
two:Low-four:High	5.58E-03	two:Low-fortyeight:Low	3.12E-06
seventytwo:High-one:High	5.11E-10	one:Low-four:Low	1.18E-05
twentyfour:Low-two:High	1.44E-04	seventytwo:Low-four:Low	2.21E-02
two:Low-two:High	1	twentyfour:Low-four:Low	0.33
fortyeight:Low-eight:Low	0.67	two:Low-four:Low	2.92E-02

	Silver release			Silver release
four:Low-eight:Low	0.97	seventytwo:Low-one:Low		1.05E-09
one:Low-eight:Low	3.37E-07	twentyfour:Low-one:Low		1.82E-08
seventytwo:Low-eight:Low	0.40	two:Low-one:Low		0.18
twentyfour:Low-eight:Low	0.99	twentyfour:Low-seventytwo:Low		0.98
two:Low-eight:Low	7.80E-04	two:Low-seventytwo:Low		1.05E-06
four:Low-fortyeight:Low	6.11E-02	two:Low-twentyfour:Low		2.91E-05
one:Low-fortyeight:Low	2.66E-09			

	Viscosity After Test	Percent viscosity Reduction
20rpm:High-10rpm:High	2.94E-04	0.34
5rpm:High-10rpm:High	3.71E-06	0.37
10rpm:Low-10rpm:High	0.10	3.99E-08
20rpm:Low-10rpm:High	2.90E-06	1.67E-06
5rpm:Low-10rpm:High	0.23	1.70E-09
5rpm:High-20rpm:High	1.82E-11	4.12E-03
10rpm:Low-20rpm:High	0.22	2.82E-10
20rpm:Low-20rpm:High	0.56	8.22E-09
5rpm:Low-20rpm:High	5.46E-07	1.68E-11
10rpm:Low-5rpm:High	3.38E-09	7.88E-06
20rpm:Low-5rpm:High	6.66E-13	4.07E-04
5rpm:Low-5rpm:High	2.06E-03	2.49E-07
20rpm:Low-10rpm:Low	4.95E-03	0.71
5rpm:Low-10rpm:Low	3.04E-04	0.79
5rpm:Low-20rpm:Low	7.53E-09	0.10

Test 4: Low, Mid, and High pH. 1, 2, 4, 8, 24, 48, and 72 hour time points. 5, 10, and 20 rpm shear rates. Before and After test.

	Silver release		Silver release
fortyeight:High-eight:High	1	twentyfour:Mid-fortyeight:High	1
four:High-eight:High	0.18	two:Mid-fortyeight:High	2.60E-08
one:High-eight:High	5.25E-08	one:High-four:High	1.78E-03
seventytwo:High-eight:High	1	seventytwo:High-four:High	2.77E-02
twentyfour:High-eight:High	1	twentyfour:High-four:High	0.23
two:High-eight:High	3.51E-04	two:High-four:High	0.78
eight:Low-eight:High	1	eight:Low-four:High	0.23
fortyeight:Low-eight:High	1	fortyeight:Low-four:High	6.86E-02
four:Low-eight:High	1.06E-03	four:Low-four:High	0.93
one:Low-eight:High	9.48E-08	one:Low-four:High	3.13E-03
seventytwo:Low-eight:High	1	seventytwo:Low-four:High	7.18E-02
twentyfour:Low-eight:High	1	twentyfour:Low-four:High	3.91E-02
two:Low-eight:High	2.13E-06	two:Low-four:High	4.73E-02
eight:Mid-eight:High	1	eight:Mid-four:High	0.54
fortyeight:Mid-eight:High	0.98	fortyeight:Mid-four:High	2.23E-03
four:Mid-eight:High	1.43E-02	four:Mid-four:High	1
one:Mid-eight:High	3.73E-07	one:Mid-four:High	1.10E-02
seventytwo:Mid-eight:High	0.99	seventytwo:Mid-four:High	3.91E-03
twentyfour:Mid-eight:High	0.95	twentyfour:Mid-four:High	1.26E-03
two:Mid-eight:High	7.21E-07	two:Mid-four:High	1.95E-02
four:High-fortyeight:High	1.36E-02	seventytwo:High-one:High	4.55E-09
one:High-fortyeight:High	2.05E-09	twentyfour:High-one:High	7.48E-08
seventytwo:High-fortyeight:High	1	two:High-one:High	0.45
twentyfour:High-fortyeight:High	1	eight:Low-one:High	7.48E-08
two:High-fortyeight:High	1.23E-05	fortyeight:Low-one:High	1.37E-08
eight:Low-fortyeight:High	1	four:Low-one:High	0.25
fortyeight:Low-fortyeight:High	1	one:Low-one:High	1
four:Low-fortyeight:High	3.86E-05	seventytwo:Low-one:High	1.45E-08
one:Low-fortyeight:High	3.62E-09	twentyfour:Low-one:High	6.82E-09
seventytwo:Low-fortyeight:High	1	two:Low-one:High	1
twentyfour:Low-fortyeight:High	1	eight:Mid-one:High	4.20E-07
two:Low-fortyeight:High	7.48E-08	fortyeight:Mid-one:High	3.21E-10
eight:Mid-fortyeight:High	0.98	four:Mid-one:High	3.38E-02
fortyeight:Mid-fortyeight:High	1	one:Mid-one:High	1
four:Mid-fortyeight:High	6.30E-04	seventytwo:Mid-one:High	5.59E-10
one:Mid-fortyeight:High	1.37E-08	twentyfour:Mid-one:High	1.85E-10
seventytwo:Mid-fortyeight:High	1	two:Mid-one:High	1

	Silver release		Silver release
twentyfour:High-seventytwo:High	1	four:Mid-two:High	1
two:High-seventytwo:High	2.85E-05	one:Mid-two:High	0.85
eight:Low-seventytwo:High	1	seventytwo:Mid-two:High	3.06E-06
fortyeight:Low-seventytwo:High	1	twentyfour:Mid-two:High	9.16E-07
four:Low-seventytwo:High	8.94E-05	two:Mid-two:High	0.93
one:Low-seventytwo:High	8.11E-09	fortyeight:Low-eight:Low	1
seventytwo:Low-seventytwo:High	1	four:Low-eight:Low	1.50E-03
twentyfour:Low-seventytwo:High	1	one:Low-eight:Low	1.35E-07
two:Low-seventytwo:High	1.72E-07	seventytwo:Low-eight:Low	1
eight:Mid-seventytwo:High	1	twentyfour:Low-eight:Low	1
fortyeight:Mid-seventytwo:High	1	two:Low-eight:Low	3.06E-06
four:Mid-seventytwo:High	1.42E-03	eight:Mid-eight:Low	1
one:Mid-seventytwo:High	3.09E-08	fortyeight:Mid-eight:Low	0.96
seventytwo:Mid-seventytwo:High	1	four:Mid-eight:Low	1.95E-02
twentyfour:Mid-seventytwo:High	1	one:Mid-eight:Low	5.34E-07
two:Mid-seventytwo:High	5.91E-08	seventytwo:Mid-eight:Low	0.99
two:High-twentyfour:High	4.99E-04	twentyfour:Mid-eight:Low	0.92
eight:Low-twentyfour:High	1	two:Mid-eight:Low	1.03E-06
fortyeight:Low-twentyfour:High	1	four:Low-fortyeight:Low	2.77E-04
four:Low-twentyfour:High	1.50E-03	one:Low-fortyeight:Low	2.45E-08
one:Low-twentyfour:High	1.35E-07	seventytwo:Low-fortyeight:Low	1
seventytwo:Low-twentyfour:High	1	twentyfour:Low-fortyeight:Low	1
twentyfour:Low-twentyfour:High	1	two:Low-fortyeight:Low	5.34E-07
two:Low-twentyfour:High	3.06E-06	eight:Mid-fortyeight:Low	1
eight:Mid-twentyfour:High	1	fortyeight:Mid-fortyeight:Low	1
fortyeight:Mid-twentyfour:High	0.96	four:Mid-fortyeight:Low	4.14E-03
four:Mid-twentyfour:High	1.95E-02	one:Mid-fortyeight:Low	9.48E-08
one:Mid-twentyfour:High	5.34E-07	seventytwo:Mid-fortyeight:Low	1
seventytwo:Mid-twentyfour:High	0.99	twentyfour:Mid-fortyeight:Low	1
twentyfour:Mid-twentyfour:High	0.92	two:Mid-fortyeight:Low	1.82E-07
two:Mid-twentyfour:High	1.03E-06	one:Low-four:Low	0.35
eight:Low-two:High	4.99E-04	seventytwo:Low-four:Low	2.94E-04
fortyeight:Low-two:High	8.94E-05	twentyfour:Low-four:Low	1.36E-04
four:Low-two:High	1	two:Low-four:Low	0.92
one:Low-two:High	0.58	eight:Mid-four:Low	7.55E-03
seventytwo:Low-two:High	9.49E-05	fortyeight:Mid-four:Low	5.26E-06
twentyfour:Low-two:High	4.35E-05	four:Mid-four:Low	1
two:Low-two:High	0.99	one:Mid-four:Low	0.63
eight:Mid-two:High	2.65E-03	seventytwo:Mid-four:Low	9.63E-06
fortyeight:Mid-two:High	1.67E-06	twentyfour:Mid-four:Low	2.88E-06

	Silver release		Silver release
two:Mid-four:Low	0.76	one:Mid-two:Low	1
seventytwo:Low-one:Low	2.60E-08	seventytwo:Mid-two:Low	1.94E-08
twentyfour:Low-one:Low	1.22E-08	twentyfour:Mid-two:Low	6.07E-09
two:Low-one:Low	1	two:Mid-two:Low	1
eight:Mid-one:Low	7.65E-07	fortyeight:Mid-eight:Mid	0.74
fortyeight:Mid-one:Low	5.59E-10	four:Mid-eight:Mid	7.86E-02
four:Mid-one:Low	5.45E-02	one:Mid-eight:Mid	3.06E-06
one:Mid-one:Low	1	seventytwo:Mid-eight:Mid	0.85
seventytwo:Mid-one:Low	9.80E-10	twentyfour:Mid-eight:Mid	0.62
twentyfour:Mid-one:Low	3.21E-10	two:Mid-eight:Mid	5.94E-06
two:Mid-one:Low	1	four:Mid-fortyeight:Mid	8.94E-05
twentyfour:Low-seventytwo:Low	1	one:Mid-fortyeight:Mid	2.05E-09
two:Low-seventytwo:Low	5.67E-07	seventytwo:Mid-fortyeight:Mid	1
eight:Mid-seventytwo:Low	1	twentyfour:Mid-fortyeight:Mid	1
fortyeight:Mid-seventytwo:Low	1	two:Mid-fortyeight:Mid	3.83E-09
four:Mid-seventytwo:Low	4.37E-03	one:Mid-four:Mid	0.15
one:Mid-seventytwo:Low	1.01E-07	seventytwo:Mid-four:Mid	1.62E-04
seventytwo:Mid-seventytwo:Low	1	twentyfour:Mid-four:Mid	4.91E-05
twentyfour:Mid-seventytwo:Low	1	two:Mid-four:Mid	0.23
two:Mid-seventytwo:Low	1.93E-07	seventytwo:Mid-one:Mid	3.62E-09
two:Low-twentyfour:Low	2.60E-07	twentyfour:Mid-one:Mid	1.16E-09
eight:Mid-twentyfour:Low	1	two:Mid-one:Mid	1
fortyeight:Mid-twentyfour:Low	1	twentyfour:Mid-seventytwo:Mid	1
four:Mid-twentyfour:Low	2.11E-03	two:Mid-seventytwo:Mid	6.82E-09
one:Mid-twentyfour:Low	4.67E-08	two:Mid-twentyfour:Mid	2.17E-09
seventytwo:Mid-twentyfour:Low	1		
twentyfour:Mid-twentyfour:Low	1		
two:Mid-twentyfour:Low	8.93E-08		
eight:Mid-two:Low	1.76E-05		
fortyeight:Mid-two:Low	1.08E-08		
four:Mid-two:Low	0.41		

Appendix B: Animal Study Protocols

MEDSTAR HEALTH RESEARCH INSTITUTE
INSTITUTIONAL ANIMAL CARE AND USE COMMITTEE (IACUC) PROTOCOL

☒ **Initial** ☐ **Amendment**

If this is a Renewal (new application after end of 3rd year) please list old protocol number(s):
(*Approval for protocols is granted for 3 years. And all protocols will undergo an annual review. After 3 years, the protocol must to be resubmitted on a new form)

I.   Protocol Information

MHRI IACUC Protocol #	2023-025	
Protocol Title:	Anti-inflammatory activity of nanocrystalline silver and silver-gold dresssings and derived solutions in a porcine model of dermatitis.	

Principal Investigator (PI):		Jeffrey W. Shupp, MD
Inst./Dept./Sect.:	MedStar Health Research Institute/Burn Research	
Address:	108 Irving Street, NW, George Hyman Research Building, Room 304	
Office phone:	202-877-7738	Email: jeffrey.w.shupp@medstar.net
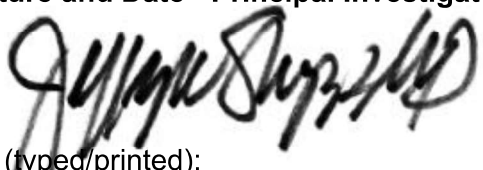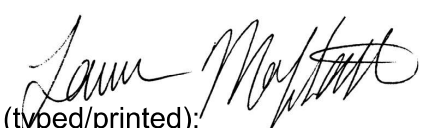
Co- investigator(Co-I): (If applicable)		Lauren T. Moffatt, Ph.D.
Address:	108 Irving St NW, Rm 304, Washington, DC 20010	
Office phone:	202-877-2064	E mail: Lauren.T.Moffatt@medstar.net

Emergency Contact Information:

Name	Office number	After hours/emergency number
Jeffrey Shupp, MD	202-877-7738	202-774-6799
Lauren Moffatt, Ph.D.	202-877-2064	202-674-8497

II. Study Type (Check all that apply): ☒ Drug   ☐ Device   ☐ Training   ☐Breeding
☒ **Procedure** ☒ **Pilot** ☐ Other: Specify

Hazard Use (x-rays, radioisotopes, biohazards, etc.)	
☐ **Biological Hazard** (Bio-safety Approval required) ☐ ABSL1 ☐ ABSL2 ☐ **Radiation Hazard** (Radiation Safety Approval required)	☒ **Other hazardous material(s) (specify):** dinitrochlorobenzene (DCNB) ☐ None

Signature and Date - Principal Investigator (PI): Name (typed/printed): Date: 24OCT2023	Signature and Date Co-Investigator (Co-I): (If applicable) Name (typed/printed): Date: 24OCT2023

PI ☒ Co-I ☐	NAME:	JEFFREY W. SHUPP, MD	EMAIL:		jeffrey.w.shupp@medstar.net
Yes ☒ No ☐	Relevant AALAS training modules completed				
Briefly describe training plan or qualifications:	Senior researcher and attending burn surgeon of more than 10 years with previous experience with the procedures on this protocol and at least 15 years of experience with this species.				
Role on Protocol	Perform all aspects of the protocol including dermatitis induction and sampling procedures. Teach and train less senior members of the team.				
YES ☒ NO ☐	Enrolled in the MedStar Health Occupational Health Program				

PI ☐ Co-I ☐	NAME:	BONNIE C. CARNEY, PHD	EMAIL:		BONNIE.C.CARNEY@MEDSTAR.NET
Yes ☒ No ☐	Relevant AALAS training modules completed				
Briefly describe training plan or qualifications:	Senior researcher with 8 years of experience with the procedures on this protocol and at least 8 years of experience with this species. Certified Surgical First Assistant (CSFA).				
Role on Protocol	Perform all aspects of the protocol including dermatitis induction and sampling procedures. Teach and train less senior members of the team.				
YES ☒ NO ☐	Enrolled in the MedStar Health Occupational Health Program				

PI ☐ Co-I ☒	NAME:	LAUREN T. MOFFATT, PHD	EMAIL:		LAUREN.T.MOFFATT@MEDSTAR.NET
Yes ☒ No ☐	Relevant AALAS training modules completed				
Briefly describe training plan or qualifications:	Senior researcher with about 10 years of experience with the procedures on this protocol and at least 10 years of experience with this species.				
Role on Protocol	Perform all aspects of the protocol. Teach and train less senior members of the team.				
YES ☒ NO ☐	Enrolled in the MedStar Health Occupational Health Program				

PI ☐ Co-I ☐	NAME:	ERIKS ZIEDINS, BS	EMAIL:		ERIKS.E.ZIEDINS@MEDSTAR.NET
Yes ☒ No ☐	Relevant AALAS training modules completed				
Briefly describe training plan or qualifications:	Over 1 year of experience working with this species and has familiarity with these procedures. Has been previously trained on monitoring during procedures, anesthesia and equipment setup and operation, blood and tissue collection, and assisting with surgical procedures.				
Role on Protocol	Perform all aspects of the protocol. Can conduct dermatitis induction procedures under the supervision of Dr. Carney, Dr. Shupp, or one of the surgeons on the protocol.				
YES ☒ NO ☐	Enrolled in the MedStar Health Occupational Health Program				

PI ☐ Co-I ☐	NAME:	MELISSA M. MCLAWHORN RN, BSN	EMAIL:	MELISSA.M.MCLAWHORN@MEDSTAR.NET
Yes ☒ No ☐	Relevant AALAS training modules completed			
Briefly describe training plan or qualifications:	Registered Nurse (RN). Four years of experience with working with animals and clinical experience in assiting with similar biopsy and wound exam procedures and in the OR.			
Role on Protocol	Monitor animal during procedures. Assist with procedures. Participate in terminal timepoint training exercises.			
YES ☒ NO ☐	Enrolled in the MedStar Health Occupational Health Program			
PI ☐ Co-I ☐	NAME:	EDWARD J. KELLEY, MD	EMAIL:	EDWARD.J.KELLY@MEDSTAR.NET
Yes ☒ No ☐	Relevant AALAS training modules completed			
Briefly describe training plan or qualifications:	PGY5 surgical resident physician. ~2.5 years experience working with pigs and similar duration of proficiency in the listed procedures. Clinical experience in anesthesia and surgical procedures.			
Role on Protocol	Perform all aspects of the protocol. Teach and train less senior members of the team.			
YES ☒ NO ☐	Enrolled in the MedStar Health Occupational Health Program			
PI ☐ Co-I ☐	NAME:	TARYN E. TRAVIS, MD	EMAIL:	TARYN.E.TRAVIS@MEDSTAR.NET
Yes ☒ No ☐	Relevant AALAS training modules completed			
Briefly describe training plan or qualifications:	Attending general and burn surgeon. Ten years of experience with working with animals. About 8 years of experience working with pigs. Clinical expertise in anesthesia, wound care, and surgical procedures.			
Role on Protocol	Perform all aspects of the protocol. Teach and train less senior members of the team.			
YES ☒ NO ☐	Enrolled in the MedStar Health Occupational Health Program			
PI ☐ Co-I ☐	Name:	CAMERON D'ORIO	EMAIL:	CAMERON.S.D'ORIO@MEDSTAR.NET
Yes ☒ No ☐	Relevant AALAS training modules completed			
Briefly describe training plan or qualifications:	About 9 months experience working with this species. Has been previously trained on monitoring during procedures, anesthesia and equipment setup and operation, sample collection, and assisting with surgical procedures.			
Role on Protocol	Perform all aspects of the protocol. Can conduct dermatitis induction procedures under the supervision of Dr. Carney, Dr. Shupp, or one of the surgeons on the protocol.			
YES ☒ NO ☐	Enrolled in the MedStar Health Occupational Health Program			
PI ☐ Co-I ☐	NAME:	DAVON LEE, BS	EMAIL:	DAVON.LEE@MEDSTAR.NET
Yes ☒ No ☐	Relevant AALAS training modules completed			

Briefly describe training plan or qualifications:	Medical student. About 6 months experience working with this species. Will be trained by senior team members on all aspects of the protocol.			
Role on Protocol	Collect and process samples and data. Record monitoring data during procedures. Can assist with surgical procedures after appropriate training.			
YES ☒ NO ☐	Enrolled in the MedStar Health Occupational Health Program			

PI ☐ Co-I ☐	NAME:	SHAWN TEJIRAM, MD	EMAIL:	SHAWN.TEJIRAM@MEDSTAR.NET
Yes ☒ No ☐	Relevant AALAS training modules completed			
Briefly describe training plan or qualifications:	Attending general surgeon and burn surgeon. About 5 years of experience conducting experiments with this species and ~8 years human clinical experience in OR and clinic settings with the same procedures and skin conditions.			
Role on Protocol	Perform all aspects of the protocol. Teach and train less senior members of the team.			
YES ☒ NO ☐	Enrolled in the MedStar Health Occupational Health Program			

PI ☐ Co-I ☐	NAME:	THARUN POTLURI, BS	EMAIL:	TP600@GEORGETOWN.EDU
Yes ☒ No ☐	Relevant AALAS training modules completed			
Briefly describe training plan or qualifications:	About 1 year of experience conducting experiments with animals. Minimal experience with pigs. Will be trained on skills for this protocol by senior team members.			
Role on Protocol	Perform all aspects of the protocol commensurate with training, except the dermatitis induction procedures. Can assist with procedures under the supervision of Dr. Shupp, Dr. Carney or one of the surgeons on the protocol.			
YES ☒ NO ☐	Enrolled in the MedStar Health Occupational Health Program			

PI ☐ Co-I ☐	NAME:	ARJUN KAUSHIK, MS	EMAIL:	ARJUN.KAUSHIK@MEDSTAR.NET
Yes ☒ No ☐	Relevant AALAS training modules completed			
Briefly describe training plan or qualifications:	About 1 year of experience conducting experiments with animals. Only about 3 months experience working with pigs. Has been previously trained on monitoring during pig procedures, anesthesia and equipment setup and operation, and assisting with surgical procedures. Will be further trained by senior team members on protocol-specific skills.			
Role on Protocol	Perform all aspects of the protocol commensurate with training. Can conduct dermatitis induction procedures under the supervision of Dr. Carney, Dr. Shupp, or one of the surgeons on the protocol.			
YES ☒ NO ☐	Enrolled in the MedStar Health Occupational Health Program			

PI ☐ Co-I ☐	NAME:	SHANE MATHEW, MD	EMAIL:	SHANE.MATHEW@MEDSTAR.NET
Yes ☒ No ☐	Relevant AALAS training modules completed			

Briefly describe training plan or qualifications:	PGY3 surgical resident physician. About 3 months of experience working with pigs. Can conduct monitoring during pig procedures, anesthesia and equipment setup and operation, vascular access including cut downs, foley insertion, sample collection, and wound creation procedures.			
Role on Protocol	**Perform all aspects of the protocol after appropriate training and documentation.**			
YES ☒ NO ☐	Enrolled in the MedStar Health Occupational Health Program			
PI ☐ Co-I ☐	NAME:	CORINNE BOGLE, BS	EMAIL:	CMB449@GEORGETOWN.EDU
Yes ☒ No ☐	Relevant AALAS training modules completed			
Briefly describe training plan or qualifications:	Medical student. About 2 months worth of experience conducting experiments with animals. Minimal experience with pigs. Will be trained on skills for this protocol by senior team members.			
Role on Protocol	Monitor animal during procedures. Can assist with surgical procedures under the supervision of Dr. Shupp, Dr. Carney or one of the surgeons on the protocol.			
YES ☒ NO ☐	Enrolled in the MedStar Health Occupational Health Program			
PI ☐ Co-I ☐	NAME:	DESIREE PINTO, MD	EMAIL:	DESIREE.PINTO@MEDSTAR.NET
Yes ☒ No ☐	Relevant AALAS training modules completed			
Briefly describe training plan or qualifications:	PGY4 surgical resident physician. Only a few months of experience working with pigs. Has been previously trained on monitoring during pig procedures, anesthesia and equipment setup and operation, vascular access, and wound creation procedures. Will be further trained by senior team members on protocol-specific skills.			
Role on Protocol	**Perform all aspects of the protocol after appropriate training and documentation.**			
YES ☒ NO ☐	Enrolled in the MedStar Health Occupational Health Program			

LAY SUMMARY: (Objectives and aims, a synopsis of experimental design and methods, and a description of the medical relevance and expected outcome in lay terms- In a high school 12th grade level of understanding)

The purpose of this study is to evaluate the anti-inflammatory activity of various test formulations of nanocrystalline silver (a way to prepare silver metal) and silver-gold combination materials (alloys, or mixtures of metals) in a pig model of dermatitis, or skin inflammation.

Nanocrystalline silver is a chemical formulation of the element silver, which utilizes nanotechnology to release clusters of extremely small and highly reactive silver particles. It has strong anti-inflammatory and antibacterial properties. In the materials that our collaborators are presently developing, silver or silver-gold alloys are sputtered, or sprayed, onto high density polyethylene (HDPE) mesh which is a surface/solid material that can then be applied to a wound like a dressing. The mesh material can also be dissolved in water to form solutions. We hypothesize that the novel materials being prepared in this manner may lead to very effective anti-inflammatory treatments for various skin conditions, and potentially in their solution form, other systemic inflammatory conditions such as those caused by viral infections, etc.

One specific objective is to validate that the novel sputtering conditions, which are being used in these formulations, result in materials with the same or better anti-inflammatory properties seen in previous studies using standard sputtering conditions, and when compared to a commercially produced silver wound dressing. The novel sputtering conditions are a new approach to spraying the metal formulations onto the HDPE at a different velocity/rate than used in previous standard sputtering conditions. Additionally, we will examine the anti-inflammatory properties of silver-gold alloys. The purpose of using silver-gold alloys is to determine if the addition of gold will enhance the anti-inflammatory properties, which we hypothesize may be the case based on previous laboratory data.

In a pig model of dermatitis, inflammation will be induced in the skin by using a chemical compound known to cause skin irritation, dinitrochlorobenzene (DCNB). At experimental day -14, the animals will have DCNB applied to a designated area of the skin on their flanks that is equivalent to about 5-10% of their total body surface. The DCNB will be re-applied on day -7, -3, and Day 0 and the areas photographed and biopsied. Depending on the treatment group the animal will be assigned to, the dermatitis will then be treated on Day 0 with one of several study formulations or control/standard treatments and monitored over a short time course to see if inflammation and other markers of skin irritation are resolved. The study sites will be re-treated on Day 2, photographed and biopsied at Days 0, 2, and 3 and blood samples collected to assess for systemic inflammatory responses. On day 3 the animals will be euthanized.

The long term objective is to develop effective and efficiently produced treatments for inflammation. The experimental groups will include 3 animals each that receive:
1.   Sham- no dermatitis induction, application of vehicle only, treated with saline soaked gauze.
2.   Positive control- DNCB/dermatitis induction, treatments with only saline soaked gauze
3.   Nanocrystalline silver dressing, made with Standard sputtering conditions
4.   Nanocrystalline silver dressing, made with Novel sputtering conditions
5.   Standard of Care (SOC) Silver dressing
6.   65% silver 35% gold Dressing, Standard sputtering conditions
7.   65% silver 35% gold Dressing, Novel sputtering conditions
8.   35% silver 65% gold Dressing, Standard sputtering conditions
9.   35% silver 65% gold Dressing, Novel sputtering conditions

A. If more than one species is requested, specify the different species and provide information for each below.
   (1) Animal Species Requested: __porcine_____

(2) Strain/ Breed: _ Yorkshire (domestic cross, but cross cannot be with Duroc)

   (3) Gender (check all that apply) ☐ **Male** ☐ **Female** ☒ **No Preference**

   Please justify if only one gender is chosen* [NIH].
   (4) Age: _____and/or   **Size:** __15-25kg_____

   (5) Source Requested (if any): ____MHRI approved lab vendor_____

   (6) Total number of animals (each species) requested

Number required to complete the study:	27
Additional animals requested:	3*
Total number of animals requested for entire study (up to 3 years):	30
*1 animal is requested to account for any reason why animal may not complete full time course of experiment (illness, lack of treatable dermatitis, etc.) and 2 animals are requested to confirm the model with reproducible development of dermatitis. The latter two animals may be included as study animals if the Day 0 assessment shows treatable, expected dermatitis.	

Requested housing location: ☒ GHRB Vivarium   ☐ Union Memorial Vivarium
☐ Satellite Location (specify): ☐ Burn Lab ☐Other (Specify; will require IACUC approval)

   B. Humane Use Categories:
   Indicate the total number of animals for the proposed study in each category.

Category B	Category C	Category D	Category E	Total:(B+C+D+E)
		30		30

Section III: Justification of Animal Use

   A. Include background significance, study objectives, study endpoints and success criteria for the study.

Background/Significance
The purpose of this study is to evaluate the anti-inflammatory activity of various test formulations of nanocrystalline silver and silver-gold combination materials (alloys, or mixtures of metals) in a pig model of dermatitis, or skin inflammation.

Nanocrystalline silver utilizes nanotechnology to release clusters of extremely small and highly reactive silver particles. It has strong anti-inflammatory and antibacterial properties, which make it appealing for use in wound dressings and other therapies for tissue injury and diseases that are associated with inflammation. In the materials that our collaborators are presently developing, silver or silver-gold alloys are sputtered, or sprayed, onto high density polyethylene

(HDPE) mesh which is a surface/solid material that can then be applied like a dressing. The mesh material can also be dissolved in water to form solutions. We hypothesize that the novel materials being prepared in this manner may lead to very effective anti-inflammatory treatments for various skin conditions, and potentially in solution form, other systemic inflammatory conditions such as those caused by viral infections, etc.

One specific objective is to validate that the novel sputtering conditions being used in these formulations result in materials with the same or better anti-inflammatory properties seen in previous studies using non-sputtered silver alone, and when compared to a commercially produced silver wound dressing. Additionally, we will examine the anti-inflammatory properties of silver-gold alloys. The purpose of using silver-gold aloys is to determine if the addition of gold will enhance the anti-inflammatory properties, which we hypothesize may be the case based on previous laboratory data.

Developing an anti-inflammatory material that is easy to use and highly effective, beyond currently available treatments, will benefit therapeutic approaches for a variety of diseases. Additionally, through this study we will learn whether the novel sputtering approach that creates novel materials can result in dressings with an anti-inflammatory outcome as good or better than currently commercially available products that contain silver and manufactured through standard processes.

Study Objectives

-Detemine if the sputtering approach used for applying the metals to a mesh material allow for greater bioavailability and therefore greater anti-inflammatory potency compared to standard of care/commercially available silver dressings.

-Determine if adding gold to the nanocrystalline silver products will further increase the potency when used as an alloy.

Study Endpoints

-Molecular and cellular data and photography of treated areas will be collected through the study time course until euthanasia and necropsy which will occur on Study day 4.

Success Criteria:
- Induction of dermatitis with successful time course of treatment applications and sample/data collection.

B. **What is the reason that live vertebrate animals are necessary for this project?**
   (Check all that apply)

X	The complexity of the processes being studied cannot be replicated, duplicated, or modeled in simpler living systems, such as in plants, insects, or other invertebrates.
X	Existing in-vitro or non-living processes cannot produce the required results (e.g., cell culture for monoclonal antibody production, computer modeling of protein synthesis, etc)
	Preclinical studies in living vertebrate animals are necessary prior to human testing
	The animals will be used for teaching/ demonstration purposes
	Other- please describe:

C. Why is the proposed species the most appropriate for this study?

The porcine integumentary system is most similar to human skin and is utilized in this study for the following reasons: porcine skin responds similarly to injury, following similar healing pathways and skin regeneration regimens; surface area of porcine skin is comparable to humans and thus allows for the use of comparably-sized wound or affected area creation; porcine skin is similar to human skin in terms of color, hair follicle composition, sweat gland concentration, and subcutaneous fat content; the porcine model is well characterized and is an accepted model for testing clinical therapies.

The smaller surface areas of the rodent and rabbit models cannot facilitate the larger wounds required in the design of this protocol. The porcine model was chosen as the experimental species because it allows for the testing of multiple sites on the same individual, ruling out other potential confounding variables. Due to the relative similarity between porcine and human integumentary systems, the swine model represents a better model for clinical testing of proposed human assessment tools such as a scoring system for skin inflammation. Rodent models do not closely represent human skin structure.

Previous work has been done using this model for dermatitis induction in pigs (PMIDs 20409150, 20170497, 18550449).

D. What was the method(s) used to determine how many animals are required for this study?

	Numbers were mandated by FDA or other government agency (e.g. GLP work)	Which agency?
	Numbers were based on previous research or experiment by self or others	
	Numbers were calculated using a statistical formula and/or consultation with a statistician	Please reference the name of the formula(S) and/or statistical resource:
	Numbers are based on expected trainee/student enrollment: reflects animal/student ratio required for effective teaching	
	This is a breeding or holding protocol, and numbers represent the estimates of offspring that will be produced and/or animals that will otherwise need to be held while not on study	
X	This is a pilot project which will be used to refine future experiments	
	None of the above methods could be used to determine numbers, and the numbers requested represent the best estimates in the PI's professional judgment.	Please explain why none of the above methods could be used, and how the final numbers were determined:

E. Does the proposed research/training duplicate any previous work?   ☐ Yes ☒ No

If yes, explain why it is necessary to duplicate the experiment or training activity.

F. Describe the statistical methods to be used to analyze your data.

All data will be stored both electronically and in hard copy. Numeric values will be entered into spreadsheets (ex; Excel or SPSS). Values obtained from the assays (performed in triplicate) conducted within this protocol (image analysis, histologic staining, PCR, etc.) will be averaged. Normality will be assessed and will dictate the statistical tests chosen (parametric or non-parametric). When possible, means generated will then be subjected to a Student's T-test or Wilcoxon rank-sum to assess for differences between treated and control animals. In the latter, medians and interquartile ranges will be provided. ANOVAs or Kruskal-Wallis test will be used to assess differences across treatment groups and time points (also when possible).   Image parameters and observations will be tallied and reported using descriptive statistics.   Data may be analyzed as fold change of treated animals at various time points compared to controls at similar time points, or as fold change over time, compared to the day of treatment initiation. A P value of 0.05 will be used.

Section IV: Consideration of Alternatives to Painful Procedures

A. Will any of the proposed procedures cause more than momentary or slight pain or distress to the animals (ie, Categories D or E)?

[☒] Yes, please fill in table below   [☐] No

Databases Searched	Inclusive Dates Searched	Date of the Search	Keywords Used (must include names of painful or distressful procedures)	Number of references retrieved
PubMed	All Available	24OCT2023	Inflammation dermatitis model alternative	128
PubMed	All Available	24OCT2023	Dermatitis porcine model	112
PubMed	All Available	24OCT2023	Dermatitis chemical model alternative	115
Agricola	All Available	31AUG2023	Dermatitis porcine model alternative	0
Google Scholar	All Available	31AUG2023	dermatitis inflammation porcine model alternative	22,000
Google Scholar	All Available	31AUG2023	dermatitis chemical porcine model alternative	21,500

Results of the database search:
   (☐ YES, alternatives were found   <u>or</u>   ☒ NO, alternatives were Not found)

Though references were retrieved using Google scholar, none indicated an alternative to these procedures and the data needed to be generated, and most were not relevant at all to the current study.

However, some papers were found that describe chemical structural models such as QSAR for studying sensitization in allergic dermatitis (not the present model though), and also some novel AI-based approaches for searching for animal alternatives that may be applicable in future studies.

If yes, explain why those alternatives cannot be used in lieu of the proposed procedures that may cause more pain or distress:

Section V: Study Design and Methods

A. **Study Synopsis: Describe your experimental design. Include flow charts, diagrams, or tables as necessary. Ensure that the following information is included:**
   - **Experimental and control groups including numbers in each group**
   - **Study Time course (if applicable) and experimental endpoints**
   - **Biologic samples to be collected (if applicable)**
   - **Analyses to be performed including data analysis**

Experimental and control groups including numbers in each group

The experimental groups will include 3 animals each that receive:
1. Sham- no dermatitis induction, application of vehicle (acetone/olive oil) only, treated with saline soaked gauze.
2. Positive control- DNCB/dermatitis induction, treatments with only saline soaked gauze
3. Nanocrystalline silver dressing, made with Standard sputtering conditions
4. Nanocrystalline silver dressing, made with Novel sputtering conditions
5. SOC Silver dressing
6. 65% silver 35% gold Dressing, Standard sputtering conditions
7. 65% silver 35% gold Dressing, Novel sputtering conditions
8. 35% silver 65% gold Dressing, Standard sputtering conditions
9. 35% silver 65% gold Dressing, Novel sputtering conditions

Study Time course and experimental endpoints

Prior to initiation of dermatitis induction on Day -14, animals will have their bilateral flanks shaved and surgically prepped.

Baseline punch biopsies (n=6, 3-4 mm) will be obtained from a site distant from the targeted study sites and will serve as baseline/uninjured skin for subsequent histology and molecular assays. Half will be flash frozen and half will be preserved in formalin. Baseline blood

---

samples, <12 ml total volume, will be collected and preserved in sodium citrate, SST, and Paxgene tubes.

Study sites will be outlined with a surgical marker, and will be approximately 15cm x 25cm, one on each flank. Therefore with n=3 animals per group, each with 2 study sites, there will be an n=6 study sites per treatment group.

Days -14, -7, -3, 0 = application of DNCB solution (or saline in group 1, shams) to induce dermatitis, photography of treated sites, biopsies of treated sites, blood sample
Day 0, 2 hours +/- 30 minutes after last application of DNCB = treatment application (based on group assigned)/biopsy/photography, blood sample
Day 2 = repeat treatment application, biopsy, photography, blood sample
Day 3 = biopsy, blood sample/photography/euthanasia, necropsy

During the dermatitis induction phase, -14 through 0, after each DNCB (or saline) application, study sites will be dressed with a non-adherent dressing, secured in place with staples or sutures, and then the animal fitted with a custom made neoprene vest to secure. This will protect surrounding skin and environment from contamination. The same dressing regimen will be used after treatment on Day 0 and re-treatment/dressing change on Day 2.

Biologic samples to be collected (if applicable)
Biopsies collected at each time point will be an n=4, 3-4mm from each study site. Blood samples will be <12 ml total volume, will be collected and preserved in sodium citrate, SST, and Paxgene tubes

Analyses to be performed including data analysis
Biopsies will be analyzed histologically using H&E for inflammatory cell infiltration with immunostaining for inflammatory protein markers such as IL6, IL1B and TNF. Skin structure will be assessed using stains for collagen such as Masson's trichrome and Herovici. Frozen biopsies will be processed with nucleic acids isolated and RNA being using downstream in PCR for gene expression analyses of inflammatory and wound healing relevant transcripts. Blood samples will be used for similar inflammation related analyses as well as chemistry.

Photographs will be analyzed using scoring for inflammation. Laser Doppler Images (LDI) may also be obtained at each time point to assess perfusion. These will be analyzed using regions of interest within each image to create replicates, averaged, and compared to baseline.

B. Procedural Details:
If the study requires more than one surgical/ invasive procedure specify if the answers are applicable to all procedures or provide specific answers for each individual procedure clearly indicating which procedure it is for:

Pre-operative procedures
-Fasting, diet modifications, pre-medication, baseline sampling, eye ointment, anesthesia induction
Intra-operative procedures
-Anesthesia maintenance, surgical approach, anatomic locations, closing, etc. Include information on sterility and prep:
Post-operative procedures
-Medications, analgesia, anesthesia recovery, short term (< 24 hrs) and long term (>24 hrs until animal fully recovered)

Receipt of Animals and Animal Housing

Pigs approximately 15-25 kg in weight will be ordered from the vendor and arrive at the George Hyman Research Building's Animal Facility where a controlled environment will be maintained in accordance with the SOP on swine housing. Swine will remain at the MedStar Washington Hospital Center in the GHRB Animal Facility for the duration of the study.

General Animal Welfare

• The animals will be monitored and observed approximately 7 or more days prior to experimental use for acclimation and in accordance with the George Hyman Research Building Animal Facility requirements. Animals will be fasted at least 12 hours prior to surgical procedures.

When animals are to be anesthetized for study procedures, the animals will be sedated by the Animal Research Facility staff with using one of the following regimens. Before or concurrent with *ONE* of the below injections, atropine (0.04-0.07 mg/kg IM) *OR* glycopyrolate (0.005-0.01 mg / kg IM) is administered.

> Ketamine/medetomidine at Ketamine 10 mg/kg and medetomidine 0.2 mg/kg IM. Medetomidine is also an alpha-2-adrenergic agonist like xylazine but is less cardio- and respiratory- depressant. Medetomidine will be reversed with atipamezole (~ 1.0mg/kg IM) if needed (if heart rate drops too low, below approximately 80 bpm).

> OR: Telazol (tiletamine and zolazepam) with ketamine, Telazol 4.4 mg/kg and ketamine 2.2 mg/kg IM.

> OR: Ketamine 15-30 mg/kg and Xylazine 1-4 mg/kg IM

• An ophthalmic ointment will be applied to the animal's eyes.
• In order to prevent bloating and volvuli, a regimen of passing a gastric tube to relieve bloat during procedures (while under anesthesia) may begin at the initial procedure (wound creation). At each procedure, while the animal is on the table and fully anesthetized, a tube may be inserted to relieve any gas formed during anesthesia and should also help when repositioning the animal by providing an axis to help stabilize the stomach in a natural anatomic position. If used, tube will remain in place during recovery until animal begins to show gross purposeful movement and is extubated.
• The animals will be intubated and ventilated with oxygen (2L/min) and Isoflorane 0.5-5.0% (2L/min) administered by inhalation. The level of anesthesia will be monitored by heart rate and the animal's response to stimuli.
• During the procedure measurements will be recorded including percent concentration of isoflurane, heart rate, respiratory rate, end tidal CO_2, oxygen saturation, and temperature. Animal will be monitored with vitals recorded every 15-17 minutes or sooner if changes are noted. A circulating hot water blanket and/or Bair Hugger will be used while the animal is under anesthesia and on the surgical table.
• At the end of the procedure the animals are removed from Isoflurane, ventilated with room air until breathing on its own and then extubated after being returned to pen. The animal will then be monitored until it returns to normal activity.
• All survival surgical procedures will performed using sterile techniques. Any devices or dressings will be provided packaged and sterile. Surgical instruments will packaged and sterilized in a steam autoclave. Surgeons will scrub and wear cap, mask, scrubs, covers and sterile gown and gloves. Additional personnel present will wear scrubs and don a cap, mask, and shoe covers.

Dermatitis Induction:

A peripheral IV will be placed in the ear. Warm IV fluids (Normal saline or lactated ringers will be administered using the 4:2:1 rule). The bilateral flanks and upper portion of the lower extremity area (both sides) of the swine will be shaved, prepped and draped in the typical sterile surgical fashion. Surgical preparation will occur using alternating applications of an acceptable surgical scrub such as povidone iodine or chlorhexidine, and alcohol for a minimum of three (3) times each. The sterile field will be draped out. Six baseline punch biopsies (3-4mm) will be obtained from a site remote to the intended study area in each animal, on each flank. Baseline images (digital photography and laser doppler imaging) of prepped skin will occur.

Prior to application of DNCB, baseline/Day-14 blood samples will be drawn while the animal is anesthetized via an acceptable route for the species such as the femoral, mammary, or saphenous veins. Femoral blood may be obtained under ultrasound guidance. A total of no more than 12 ml of blood (<3% of total blood volume for a 20kg pig) will be obtained. If multiple sticks are required to fill all necessary tubes, or an alternative route/location is needed, attention will be paid to acceptable volumes per route (ie, no more than 5 ml will be drawn from the ear vein, etc.).

Each animal will have one, 15cm x 25cm square study area created on each flank for a total of 2 areas per pig. The total body surface area (TBSA) of this area will be small, approximately 10% TBSA for a 20kg pig. Therefore it is not expected that there will be any systemic pathophysiology (shock, coagulopathy, etc.) requiring intervention.

Study sites will be painted using sterile swabs with the DNCB chemical solution. The solution will be prepared as 10% DNCB v/v in 4:1 acetone:olive oil). These sites will receive a standard non-adherent dressing (Xeroform gauze or similar) stapled in place with the option to suture down the corners of the dressing. The entire procedure site may then be further dressed with Conform® gauze bandage roll and elastic tubular netting for added security. A custom neoprene vest binder, hand-made by research staff using a pattern for a vest previously demonstrated in this laboratory to be a suitable and highly functional protective dressing cover, will then be used to protect dressings (PMID: 23246889).

This DNCB application procedure and re-dressing of the study sites will be repeated on Days -7, -3. At each of these time points, animals will be anesthetized as described, dressings taken down, and digital and LDI images of study sites captured. Then, n=4, 3-4mm punch biopsies will be taken from each study site. Blood samples will be <12 ml total volume, will be collected and preserved in sodium citrate, SST, and Paxgene tubes. Re-application of the DNCB solution will be performed on each study site. Starting at Day -3, a Fentanyl Patch, 25mcg/hour (fentanyl content 2.5-2.66mg) will be positioned and secured on a shaved portion of the forelimb prior to anesthesia recovery as this may be when the dermatitis begins causing pain. Fentanyl patches will be secured. Pigs will be subjected to close monitoring to ensure patches are not ingested. This will occur on day 0 as well, as the patches are only expected to be released over 3 days.

Day 0:
Final application of DNCB;
Waiting period

Imaging, sampling

Day -7:
Second application of DNCB.

Treatments applied

Fentanyl Patch

Imaging, sampling

Day 2:
Treatments re-applied

Imaging, sampling

Day -14:
First application of DNCB.

Imaging, sampling

Day -3:
Third application of DNCB.

Imaging, sampling

Fentanyl Patch

Day 3:
Imaging, sampling

Euthanasia

Necropsy
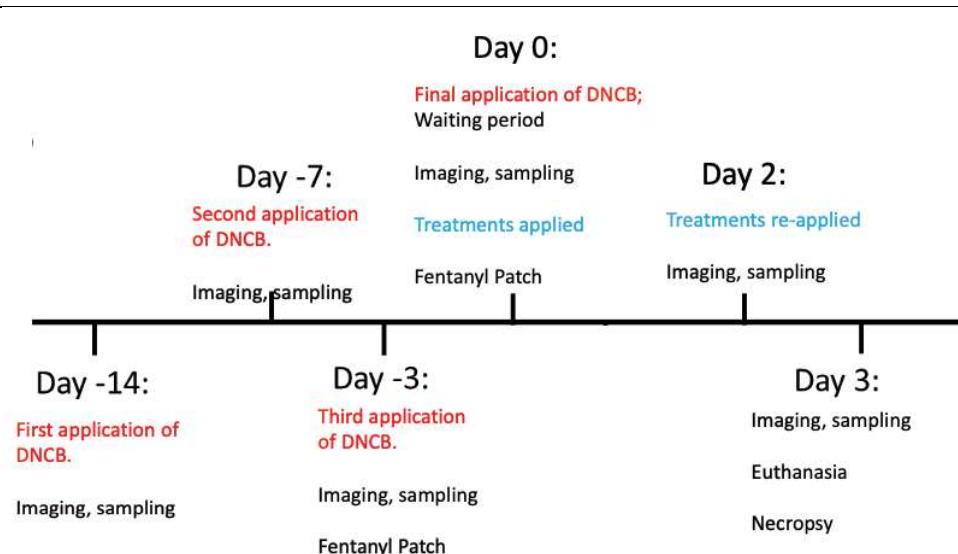
Treatments

On day 0, animal will return to the OR with dressings taken down and will receive a final application of DNCB. After the final application of the DNCB, animals will remain under anesthesia and monitored for 2 hours to allow the compound to dry. Sampling (blood and biopsies) and photography will then occur. After that, the study treatments will be applied, according to the assigned experimental group. Sites will be re-dressed and secured with custom vest as described. Animals will be recovered. On day 2, animal will again return to the OR for study site assessments and will also receive the re-application of experimental treatments, according to their assigned group. Inflammation and skin quality will be assessed by a clinician. Photography and LDI of sites will be performed. Biopsies and blood collection will occur with n=4, 3-4mm punch biopsies will be taken from each study site. Blood samples will be <12 ml total volume, will be collected and preserved in sodium citrate, SST, and Paxgene tubes. Sites will be re-dressed, secured as described and with a vest fitted.

Animals will be recovered after these timepoints as described. At each time point involving punch biopsies, a one-time dose of Buprenex 1 M (0.005-0.10 *mg/kg*) will be given after extubation and during recovery, as soon as gross purposeful movement is observed. Additional analgesics, approved by consultation of the veterinarian, may be administered, if required for the welfare of the animal if there is a concern of pain or distress ongoing from the initial procedures or other possible complications.

Necropsy/Terminal Timepoint:

On day 3, a peripheral IV will be placed in the ear. If the ear cannot be used, a central line can be placed in the jugular vein, carotid artery, or femoral artery/vein and can be placed under ultrasound guidance. Dressings will be removed, study sites will be imaged. Blood samples will be obtained as described. Three or four millimeter full-thickness punch biopsies (up to 9) will be taken from each site and from a surrounding area of normal skin. Biopsies will be fixed in formalin, stored in Allprotect Tissue Reagent(Qiagen, Germantown, MD), or flash frozen for protein isolation. The isoflurane anesthesia will then be increased to 5% for 5 minutes. The animal will then be euthanized using KCL (0.24-0.47mL/kg, 4.2M) or fatal plus (85-150mL/kg). Flat line vitals will be observed prior to proceeding with necropsy.

C. Invasive Procedures

Invasive Procedure(s)   ☒ Yes   ☐ No

Invasive Procedure(s) include: ☐ Acute (non-survival)   ☒ Survival

Invasive Procedure(s) are considered: ☐ Major   ☒ Minor

D. Will the animals undergo MULTIPLE major invasive procedures (defined in the instructions using the 'Guide' definition)? This includes procedures from previous protocols if transferred.

    ☐ Yes   ☒ No

If yes, please provide justification

E. During recovery from anesthesia, what physiological signs will be monitored to assure the animals are stable?

Per relevant recovery protocols in the ARF; including oxygen saturation, respiratory rate, movement.

F. How often will animals be monitored after anesthetic recovery?

During immediate post-operative recovery of the survival procedures, the animal will be continuously monitored by MHRI ARF associates until conscious and physiologically stable. Signs of pain or distress will be documented and reported to the PI who will consult with the veterinarian prior to any treatment. Daily cageside observations of the vests and dressings will be made by study staff and recorded, to monitor for signs of bleeding or a need to be redressed.

G. Indicate who will monitor the animals pre-procedurally and prepare the animals for surgery.

☒ MHRI Animal Facility   ☐ Study Investigators

H. Indicate who will monitor the animals post-procedurally and the frequency of monitoring.

☒ MHRI Animal Facility   ☒ Study Investigators   ☐ Not Applicable as Acute Procedure

Frequency of Monitoring:

Animals will be monitored once daily ~every 24 hours by investigators or twice daily, every ~12-15 hours by investigators if health or study site concerns are noted on weekdays. Wound/dressing/device observations will be recorded. Animals will also be monitored by animal facility staff per relevant routine health monitoring protocols.

I. Potential Complications

Potential Complication due to Procedure	Mitigation
Body weight loss >15%	

	Vessel Dissection	
X	**Infection**	If a study site becomes infected, the dead or infected tissue may be debrided and washed with a wound cleansing agent. Cold atmospheric plasma may also be administered. These measures can be performed to prevent a progression to systemic infection or compromise of other study sites on the animal.
	Inability to ambulate	
	Self-mutilation	
	Stroke	
	Hind limb paralysis	
	Cardiac complications	
	Death	
X	**Other (specify):**	In previous experience with animals in similar studies where animals are repeatedly/frequently turned from side to side while under anesthesia, problems associated with GI bloat and volvuli have occurred. In order to prevent this, a regimen of passing a gastric tube to relieve bloat during procedures (while under anesthesia) may begin at the initial procedure (wound creation). At each procedure, while animal is on the table and fully anesthetized, a tube may be inserted to relieve any gas formed during anesthesia and should also help when repositioning the animal by providing an axis to help stabilize the stomach in a natural anatomic position. Tube will remain in place during recovery until animal begins to show gross purposeful movement and is extubated. Excessive irritation may occur. Excessive, continuous rubbing of the flank areas and lethargy are two signs that may indicate pain or distress from these procedures. These will be monitored and treated with analgesia.

J. **What Clinical signs or other criteria will be used to determine that an animal must be removed from the study ahead of schedule (Humane Endpoints) (check all that apply).** <u>NOTE</u>: Allowing animals to progress to a moribund or near-death state requires scientific justification; you must indicate below why an earlier, more humane endpoint cannot be used.

☐ Body weight loss >20% unresponsive to treatment
☒ Pain unresponsive to treatment
☒ Infection unresponsive to treatment
☐ Vessel dehiscence/dissection
☐ Moribund
☐ Behavioral abnormalities (describe in detail below)
☐ Clinical symptomatology or signs of toxicity (describe in detail below)
☐ Other (specify) _____

Note: A necropsy will be performed in the event of a sudden, unexpected death for any USDA species.

Section VI: Hazardous Agents (biohazards, chemicals)

A. Does the research, testing or instruction require the use of hazardous or biohazardous agents in the animal facility (i.e., human tissue, infectious/biohazardous agents, carcinogens, toxic chemicals, radioisotopes)?

☒YES   ☐ NO

If "yes", specify the hazardous agent(s) to be used and attach an SDS.
Dinitrochlorobenzene (DNCB) (10% in olive oil-acetone); SDS is attached.

B. Describe or attach a copy the containment/handling protocol to be followed in protecting other animals and personnel from the hazardous agents.

DNCB should be handled with gloves and sleeves to prevent skin exposure. It is an irritant. Exposure after treatment will be minimized as the treated areas of animals are covered with protective vests and dressings. DNCB will be present on dressings and vests that have been removed and on the underlying treated pig skin. DNCB could therefore be on the cage surfaces on which animals have been rubbing. PPE that covers exposed staff skin (gloves, long sleeves) should be worn by staff handling the animals and removing or recovering dressings that were in contact with DNCB. Materials used to make and apply DNCB will be packaged in containers and marked with the hazardous material label. These will be disposed of per facility hazardous waste procedures. Staff preparing and handling the DNCB are appropriately trained in chemical safety and will wear eye protection, gloves, sleeves, and prepare the diluted treatment formulation under a hood with external exhaust (such as room 108, 315 in the GHRB).

Section VII: Husbandry/Housing and Disposition of Animals

A. Do you expect to follow MHRI quarantine and conditioning procedures?

☒YES   ☐NO

If "yes", proceed to Question B. If "no", describe the quarantine and conditioning procedures to be performed prior to the start of the project.

B. Are you requesting an exemption from the MHRI Animal Social Housing and Environmental Enrichment which includes group housing of compatible animals?
☐NO

☒YES
☒Exemption from social housing
☐Exemption from Enrichment

If yes, what is the justification for this/these exemption request(s)?

We request that animals be single housed in their own pen after study site/dermatitis creation because of the risk of animals pulling off dressings.

C. Describe any non-standard diet, housing or environmental modifications, and how they will be accomplished.

n/a

D.

Will individual(s) other then the MHRI Animal Facility staff be responsible, for meeting MHRI standards of animal husbandry and housing?
☐ Yes   ☒ No

If yes, identify location and describe at what point in the study ARF staff versus Investigators, will be responsible for husbandry and welfare of the animals.

E. List locations other than the MHRI Animal Facilities where you will house, perform surgery or perform experimental procedures on your animals. If the facility is off-site, is it AAALAC accredited and/or USDA Certified?

n/a

F. Euthanasia (per 'Report of the AVMA Panel on Euthanasia (2013)')
☐ **CO2 (rodents only)**
☒ **KCl under deep anesthesia**
☒ **Pentobarbital-based solution (e.g. Fatal Plus, Beuthanasia-D etc.)**
☐ **Exsanguination under anesthesia (rodents only)**

Euthanasia agent:	Dose/Route:
potassium chloride	IV under general anesthesia (0.24 – 0.47 ml per kg body weight, using a 4.2M, 1-2mmol/kg concentration)
Fatal Plus	IV under general anesthesia at a concentration of 85-150 mg/kg

G. Secondary method for ensuring death
☐ **Bilateral thoracotomy**
☒ **Flatline vitals**
☐ **Cervical dislocation**
☐ **Exsanguination**
☐ **Other (Specify)**

Section VIII: Principal Investigator Assurances (PI)

Please indicate by check marks that you agree to all the following statements:

[☒] The information provided herein is accurate to the best of my knowledge.

[☒] Procedures involving animals related to this protocol will be performed only by trained or experienced personnel, or under the direct supervision of trained or experienced persons.

[☒] Any change in the care and use of animals involved in this protocol which would affect the welfare of the animals, will be promptly forwarded to the MHRI IACUC for review; such changes **will not** be implemented until the committee's approval is obtained.

[☒] The number of animals proposed is the minimum necessary to conduct valid experimentation.

[☒] I have considered alternative methods to using animals, including a literature search (where appropriate) to ensure that I am not unnecessarily duplicating previous experiments.

Signature:

_____   __10/30/2023__
Principal Investigator   **Date**

> (Submit completed electronic applications to: MHRI Office of Research Integrity at ORI.helpdesk@medstar.net. For further information, contact the IACUC Coordinator at 301-560-2912.)

MEDSTAR HEALTH RESEARCH INSTITUTE
INSTITUTIONAL ANIMAL CARE AND USE COMMITTEE (IACUC) PROTOCOL

☒ Initial ☐ Amendment

If this is a Renewal (new application after end of 3rd year) please list old protocol number(s):
(*Approval for protocols is granted for 3 years. And all protocols will undergo an annual review. After 3 years, the protocol must to be resubmitted on a new form)

MHRI IACUC Protocol #	**2023-019**	
Protocol Title:	Treatment of Abdominal Surgical Adhesions in Pigs with Nanocrystalline Silver Gels.	

Principal Investigator (PI):		**Jeffrey W. Shupp, M.D.**
Inst./Dept./Sect.:	MWHC/Surgery/Trauma/Burns	
Address:	110 Irving St NW, Suite 3B55, Washington, DC 20010	
Office phone:	202-877-7347	Email:	jeffrey.w.shupp@medstar.net

Co- investigator (Co-I): (If applicable)	**Lauren T. Moffatt, Ph.D.**	
Address:	108 Irving St NW, Rm 304, Washington, DC 20010	
Office phone:	202-877-2064	E mail:	lauren.t.moffatt@medstar.net

Emergency Contact Information:

Name	Office number	After hours/emergency number
Lauren Moffatt, Ph.D.	202-877-2064	202-674-8497
Jeffrey W. Shupp, M.D.	202-877-7347	202-801-7774 (pager)

Study Type (Check all that apply): ☒ **Drug** ☐ **Device** ☐ **Training** ☐ **Breeding**

☒ **Procedure** ☒ **Pilot** ☐ **Other: Specify**

Hazard Use (x-rays, radioisotopes, biohazards, etc.)
☐ **Biological Hazard** (Bio-safety Approval required)   ☒ **Other hazardous material(s) (specify):**
　　☐ ABSL1 ☐ ABSL2　　　　　　　　　　　　　　　10% Neutral Buffered Formalin
☐ **Radiation Hazard** (Radiation Safety Approval required)   ☐ None

---

Signature and Date - Principal Investigator (PI):	**Signature and Date Co-Investigator (Co-I):**
Name (typed/printed): Jeffrey W. Shupp, MD Date:	Name (typed/printed): Lauren Moffatt, PhD Date:

For IACUC USE ONLY
CURRENT VERSION OF PROTOCOL:

Date Received:	Radiation Safety approval date:
Approval Date:	Bio-Safety Approval date:
Expiration Date (3 Year):	Species:
Amendment date(s):	Guide exceptions: Y N
1st Continuation approval date:	2nd Continuation approval date:

PI ☒ Co-I ☐	**NAME:** JEFFREY W. SHUPP, MD	**EMAIL:**	jeffrey.w.shupp@medstar.net
Yes ☒ No ☐	Relevant AALAS training modules completed		
Briefly describe training plan or qualifications:	**Attending surgeon with experience in all relevant procedures and 10+ years of experience working with this species.**		
Role on Protocol	**Overall responsibility for the study. Ensure compliance and completion of the study surgical procedures and data collection. Will complete surgical procedures and train less senior personnel.**		
YES ☒ NO ☐	Enrolled in the MedStar Health Occupational Health Program		

PI ☐ Co-I ☒	**NAME:** LAUREN T. MOFFATT, PHD	**EMAIL:**	lauren.t.moffatt@medstar.net
Yes ☒ No ☐	Relevant AALAS training modules completed		
Briefly describe training plan or qualifications:	**Senior researcher with about 10 years of experience working with this species.**		
Role on Protocol	**Project Manager. Procedure coordination, setup and assistance, documentation and record keeping. Anesthesia monitoring during surgical procedure.**		
YES ☒ NO ☐	Enrolled in the MedStar Health Occupational Health Program		

PI ☐ Co-I ☐	**NAME:** JIANQUI WU, MD	**EMAIL:**	**JIANQIU.X.WU@MEDSTAR.NET**
Yes ☒ No ☐	Relevant AALAS training modules completed		
Briefly describe training plan or qualifications:	**Previous experience in surgical procedures, in particular swine, and monitoring and recovery in this species. International medical training and certification.**		
Role on Protocol	**Study Support who can assist with study procedures under the direction of the surgeon, data collection, sample processing. Anesthesia monitoring during surgical procedure.**		
YES ☒ NO ☐	Enrolled in the MedStar Health Occupational Health Program		

PI ☐ Co-I ☐	NAME: Bonnie Carney, PhD	EMAIL:	Bonnie.c.carney@medstar.net
Yes ☒ No ☐	Relevant AALAS training modules completed		
Briefly describe training plan or qualifications:	Several years of experience in working with porcine models, specifically in wound creation and healing, as well as models for shock. Will be trained by Dr. Shupp on any aspects of surgical procedures that are specific to this model. Dr. Carney is a Certified Surgical First Assistant (CSFA).		
Role on Protocol	Prepare for and conduct all procedures commensurate with training, data and sample collection and processing, and anesthesia monitoring. Teach less senior staff.		
YES ☒ NO ☐	Enrolled in the MedStar Health Occupational Health Program		

PI ☐ Co-I ☐	NAME: Eriks Ziedins, BS	EMAIL:	ERIKS.E.ZIEDINS@MEDSTAR.NET
Yes ☒ No ☐	Relevant AALAS training modules completed		
Briefly describe training plan or qualifications:	~6 months of experience on pig OR procedures in other IACUC protocols.		
Role on Protocol	Assist with procedures under the direction of the surgeon, conduct monitoring, sample collection, sample processing, and sample analysis commensurate with training.		
YES ☒ NO ☐	Enrolled in the MedStar Health Occupational Health Program		

PI ☐ Co-I ☐	NAME: Cameron D'Orio, BS	EMAIL:	CAMERON.S.D'ORIO@MEDSTAR.NET
Yes ☒ No ☐	Relevant AALAS training modules completed		

Briefly describe training plan or qualifications:	Previous experience (~3 months) on pig protocols in the OR. Training completed on monitoring, sample and data collection.
Role on Protocol	Assist with procedures under the direction of the surgeon, conduct monitoring, sample collection, sample processing, and sample analysis commensurate with training.
YES ☒ NO ☐	Enrolled in the MedStar Health Occupational Health Program

PI ☐ Co-I ☐	NAME: Edward Kelly, MD	EMAIL: Edward.j.kelly@MEDSTAR.NET
Yes ☒ No ☐	Relevant AALAS training modules completed	

Briefly describe training plan or qualifications:	**Surgical fellow. ~2.5 years experience working with pigs and similar duration of proficiency in the listed procedures. ~4 years of clinical experience working with human patients in an OR and clinic setting. Will be trained by Dr. Shupp on surgical procedures specific to this model.**
Role on Protocol	Perform all study related procedures commensurate with training, and assessments, teach less senior colleagues.
YES ☒ NO ☐	Enrolled in the MedStar Health Occupational Health Program

PI ☐ Co-I ☐	NAME: Taryn Travis MD	EMAIL: Taryn.e.travis@MEDSTAR.NET
Yes ☒ No ☐	Relevant AALAS training modules completed	

Briefly describe training plan or qualifications:	**Attending burn surgeon and general surgeon. ~7 years of experience working with pigs and the same duration of experience in similar models. ~10 years working in an OR and clinic setting with burn and trauma patients.**
Role on Protocol	Perform all study related procedures and assessments, teach less senior staff.
YES ☒ NO ☐	Enrolled in the MedStar Health Occupational Health Program

PI ☐ Co-I ☐	NAME: Shawn Tejiram MD	EMAIL: Shawn.tejiram@MEDSTAR.NET
Yes ☒ No ☐	Relevant AALAS training modules completed	

Briefly describe training plan or qualifications:	**Attending general surgeon and burn surgeon. About 5 years of experience conducting experiments with this species and ~8 years human clinical experience in OR and clinic settings with the same procedures.**
Role on Protocol	Perform all study related procedures and assessments, teach less senior staff.
YES ☒ NO ☐	Enrolled in the MedStar Health Occupational Health Program

PI ☐ Co-I ☐	NAME: Arjun Kaushik, MS	EMAIL: Arjun.kaushik@MEDSTAR.NET
Yes ☒ No ☐	Relevant AALAS training modules completed	

Briefly describe training plan or qualifications:	**Very minimal experience conducting experiments with this species, but familiar with small animal modeling and expert in laboratory bench work. Has completed training on large animal monitoring, sample processing, and equipment.**
Role on Protocol	Assist with procedures under the direction of the surgeon, conduct monitoring, sample collection, sample processing, and sample analysis commensurate with training.
YES ☒ NO ☐	Enrolled in the MedStar Health Occupational Health Program

PI ☐ Co-I ☐	NAME: Shane Mathew MD	EMAIL: Shane.mathew@MEDSTAR.NET
Yes ☒ No ☐	Relevant AALAS training modules completed	

Briefly describe training plan or qualifications:	**Surgical resident. Very minimal experience conducting experiments with this species but ~4 years human clinical experience in OR and clinic settings. Will be trained by Dr. Shupp on this model and relevant procedures. Has completed training on large animal monitoring, equipment, and some porcine surgical procedures to date.**
Role on Protocol	Perform all study related procedures and assessments commensurate with training.
YES ☒ NO ☐	Enrolled in the MedStar Health Occupational Health Program

PI ☐	Co-I ☐	NAME:	Desiree Pinto MD	EMAIL:	Desiree.pinto@MEDSTAR.NET

Yes ☒ No ☐	Relevant AALAS training modules completed
Briefly describe training plan or qualifications:	**Surgical resident. No prior experience conducting experiments with this species but ~4 years human clinical experience in OR and clinic settings. Will be trained by Dr. Shupp on this model and relevant procedures. Has completed training on large animal monitoring, equipment, and some porcine surgical procedures to date.**
Role on Protocol	Perform all study related procedures and assessments commensurate with training.
YES ☒ NO ☐	Enrolled in the MedStar Health Occupational Health Program

LAY SUMMARY: (Objectives and aims, a synopsis of experimental design and methods, and a description of the medical relevance and expected outcome in lay terms- In a high school 12th grade level of understanding)

Adhesions are a common complication of surgical procedures and radiation treatments and cause painful symptoms, and can potentially require additional surgeries. They occur when tissue damage leads to an inflammatory response which can form tissue connections (the adhesions) between surfaces in the abdomen. Past research by other groups suggests that viscous solutions or gels are a promising method for preventing adhesions by preventing tissue contact and promoting healing by releasing therapeutic agents. Hyaluronic acid and carboxymethylcellulose are biodegradable and non-toxic materials that have previously been used to make gels and other treatments to prevent adhesions.

Nanocrystalline silver utilizes nanotechnology to release clusters of extremely small and highly reactive silver particles. It has strong anti-inflammatory and antibacterial properties. Incorporating nanocrystalline silver into viscous polymer solutions to apply to the wound site may reduce the inflammatory reaction, and so prevent adhesions from forming. Additionally it has been previously shown that nanocrystalline silver dressings have an anti-inflammatory effect even when applied nearby or adjacent to, but not directly on, the wound site. Therefore the silver dressings will be applied externally with the hypothesis that inflammation will still be decreased in the abdominal cavity due to penetration of the product.

Longer term, this study may provide the foundation for a preventive treatment of adhesions that could be used in many kinds of patients to prevent complications including additional surgeries.

In this experiment, we will do a surgery to induce the formation of adhesions on Day 0. Animals will then be treated based on their experimental or control group assignment listed below, and recovered. On Days 2 and 4, we will change their dressings and check their incision sites. On Day 7, animals will come back to the OR for sample and data collection and euthanasia.

Groups (each will have 5 animals in the group):
1. Sham surgery, no adhesions to be formed [Shams, normal group]
2. Adhesion induction protocol, but no treatment [no treatment controls]
3. Treatment with Seprafilm [comparator/similar product group]
4. Treatment with gel, no silver [vehicle only controls]
5. Treatment with silver gel [treatment group 1]
6. No internal treatment, but silver dressing placed over the abdomen after closure [treatment group 2]

We will compare the extent of adhesion formation between groups to determine the effectiveness of the nanocrystalline gel for this purpose.

In addition to the 30 animals in the 6 experimental groups, we will use up to 3 animals to optimize the method for adhesion induction, to be sure the adhesions are present and will be able to demonstrate a change based on intervention. Two (2) additional animals may be used if

any experimental animals do not complete the time course or do not form adhesions as expected.

A. If more than one species is requested, specify the different species and provide information for each below.

(1) **Animal Species Requested: <u>Porcine (<u>Sus</u> scrofa)</u>**

(2) **Strain/ Breed: <u>Yorkshire (domestic cross, but cross cannot be with Duroc)</u>**

(3) **Gender** (check all that apply) ☐ **Male** ☐ **Female** ☒ **No Preference**

Please justify if only one gender is chosen* [NIH].

(4) **Age: <u>N/A (commensurate with weight)</u> and/or Size: 35-45 kg** (kg/lbs)

(5) **Source Requested** (if any): **<u>MHRI-approved vendor</u>**

(6) **Total number of animals (each species) requested**

Number required to complete the study:	**30**
Additional animals requested:	**2 + 3 = 5**
Total number of animals requested for entire study (up to 3 years):	**35**

Requested housing location: ☒ GHRB Vivarium ☐ Union Memorial Vivarium
☐ Satellite Location (specify): ☐ Burn Lab ☐Other (Specify; will require IACUC approval)

B. **Humane Use Categories:**
Indicate the total number of animals for the proposed study in each category.

Category B	Category C	Category D	Category E	Total:(B+C+D+E)
		35		**35**

Section III: Justification of Animal Use

A. **Include background significance, study objectives, study endpoints and success criteria for the study.**

Background

Adhesions are a common complication of surgical procedures and radiation treatments and cause painful symptoms, and can potentially require additional surgeries. They occur when tissue damage leads to an inflammatory response which can form tissue connections (the adhesions) between surfaces in the abdomen. Past research by other groups suggests that viscous solutions or gels are a promising method for preventing adhesions by preventing tissue contact and promoting healing by releasing therapeutic agents (PMID 37531241, 37344187). Hyaluronic acid and carboxymethylcellulose are biodegradable and non-toxic polymers that have previously been used to make gels and other treatments to prevent adhesions (PMID 37531241, 37344187, 37250473).

Nanocrystalline silver has strong anti-inflammatory and antibacterial properties (PMID 36646192, 26290672). Incorporating nanocrystalline silver into viscous polymer solutions to apply to the wound site may reduce the inflammatory reaction, and so prevent adhesions from forming. Additionally it has been previously shown that nanocrystalline silver dressings have an anti-inflammatory effect even when applied at a distance (not directly on) the wound site (PMID

20409150). Therefore the silver dressings will be applied externally with the hypothesis that inflammation will still be decreased in the abdominal cavity.

Longer term, this study may provide the foundation for a preventive treatment of adhesions that could be used in many kinds of patients to prevent complications including additional surgeries.

Purpose / Objective:

Study Objectives
- The primary objective is to compare the extent of adhesion formation (grossly and histologically) between treatment and control groups to determine the effectiveness of the nanocrystalline gel for preventing adhesions.
- Secondary assessments will include systemic measure of inflammatory response using blood samples and other histologic measures including inflammatory markers in local and distant tissue samples.

Study Endpoint
- Evaluation of the extent of adhesions at 7 days after treatments/surgeries.
- Animals will be euthanized at Day 7 data and sample collection completion while under anesthesia.

Thirty (30) animals will be needed to complete the experimental design. Two (2) animals are needed for the study to cover any unexpected occurrences that would result in an animal being excluded or not completing the full study. Three (3) animals are being requested for confirmation of adequacy of the surgical procedures to induce adhesions for the model. A total of 35 animals are being requested for the study.

B. **What is the reason that live vertebrate animals are necessary for this project?**
   (Check all that apply)

X	The complexity of the processes being studied cannot be replicated, duplicated, or modeled in simpler living systems, such as in plants, insects, or other invertebrates.
X	Existing in-vitro or non-living processes cannot produce the required results (e.g., cell culture for monoclonal antibody production, computer modeling of protein synthesis, etc)
X	Preclinical studies in living vertebrate animals are necessary prior to human testing
	The animals will be used for teaching/ demonstration purposes
	Other- please describe:

C. **Why is the proposed species the most appropriate for this study?**

Most porcine organ systems are most similar to humans and are utilized in this study for the following reasons: porcine organ tissue responds similarly to injury, following similar healing pathways and regeneration regimens; the porcine model, especially for tissue injury and inflammatory response to injury, is well characterized and is an accepted model for testing clinical therapies. Examples of studies that demonstrate abdominal surgical adhesions as an outcome of importance in pigs include: PMIDs 33455390, 33400026, 24590429, 22261595, 22906336, 23895276, 28594257. Further, previous studies have utilized the currently

D. **What was the method(s) used to determine how many animals are required for this study?**

	Numbers were mandated by FDA or other government agency (e.g. GLP work)	Which agency?
	Numbers were based on previous research or experiment by self or others	Please reference the publication or protocol number:
	Numbers were calculated using a statistical formula and/or consultation with a statistician	Please reference the name of the formula(S) and/or statistical resource:
	Numbers are based on expected trainee/student enrollment: reflects animal/student ratio required for effective teaching	
	This is a breeding or holding protocol, and numbers represent the estimates of offspring that will be produced and/or animals that will otherwise need to be held while not on study	
X	This is a pilot project which will be used to refine future experiments	**This number of animals, in this pilot study, is in keeping with gaining meaningful inference as to the feasibility of the direction of this research based on the PI's past research.**
	None of the above methods could be used to determine numbers, and the numbers requested represent the best estimates in the PI's professional judgment.	Please explain why none of the above methods could be used, and how the final numbers were determined:

E. **Does the proposed research/training duplicate any previous work?** ☐ Yes ☒ No

If yes, explain why it is necessary to duplicate the experiment or training activity.

F. **Describe the statistical methods to be used to analyze your data.**

Means and standard deviations of values from multiple experimental sites will be provided and compared using a Student's T-test or ANOVA (when appropriate). A paired student's T-test or repeated measures ANOVA (mixed model) may be used for certain variables as well. Categorical variables will be described by frequencies and percentages and Chi-square and Fisher exact tests as appropriate will be used to compare proportions of categorical variables. If the data are not normally distributed, non-parametric tests will be applied (ie, Kruskal Wallis). Statistical significance is defined as $P < 0.05$.

Section IV: Consideration of Alternatives to Painful Procedures

A. Will any of the proposed procedures cause more than momentary or slight pain or distress to the animals (ie, Categories D or E)?

[⊠] Yes, please fill in table below   [ ] No

Databases Searched	Inclusive Dates Searched	Date of the Search	Keywords Used (must include names of painful or distressful procedures)	Number of references retrieved
Agricola	All Available	01AUG2023	(1)Nanocrystalline silver adhesions, (2)surgical adhesion model alternative	(1) 2 results; (2) 7 results
PubMed	All available	01AUG2023	(1)Nanocrystalline silver adhesions, (2)surgical adhesion model alternative	(1) 10 results; (2) Although 187 papers resulted, no references were found for alternatives to this model.
Ovid	from 1946 thru present available	01AUG2023	(1)Nanocrystalline silver adhesions, (2)surgical adhesion model alternative	(1) Although 5,697 references resulted, no references were found for alternatives to this model. (2) Although 4,295 references resulted, no references were found for alternatives to this model.

Results of the database search:
([ ] YES, alternatives were found   or   [⊠] NO, alternatives were Not found)

If yes, explain why those alternatives cannot be used in lieu of the proposed procedures that may cause more pain or distress:

Section V: Study Design and Methods.

A. Study Synopsis: Describe your experimental design. Include flow charts, diagrams, or tables as necessary. Ensure that the following information is included:
- **Experimental and control groups including numbers in each group**
- **Study Time course (if applicable) and experimental endpoints**
- **Biologic samples to be collected (if applicable)**
- **Analyses to be performed including data analysis**

At least 30 animals will be required to achieve study objectives. Animals will have visual, olfactory, and auditory contact in the vivarium. The animals will be acclimated to the test facility housing for 5-7 days prior to surgery.

Surgical Procedures – On Day 0, blood samples will be collected prior to surgery. Then, animals will have adhesions induced surgically (except those in Group 1) by abrasion of the cecum and abdominal wall with dry sterile gauze. Group 1 animals will undergo anesthesia, abdominal incision and access to tissues, but no abrasion. After this procedure, animals will be treated as follows:

Groups (each will have 5 animals in the group):
1. Sham surgery, no adhesions to be formed [Shams, normal group]
2. Adhesion induction protocol, but no treatment [no treatment controls]
3. Treatment with Seprafilm [comparator/similar product group]
4. Treatment with gel, no silver [vehicle only controls]
5. Treatment with silver gel [treatment group 1]
6. No internal treatment, but silver dressing placed over the abdomen after closure [treatment group 2]

Adhesion induction will occur initially in up to 3 animals with no further treatments to confirm the adequacy of the adhesions for study. If these adhesions are found to be adequate and consistent, these 3 animals may be included in group 2 above.

Animals will be recovered and monitored after surgery, and will have dressings changed and incision sites checked on Days 2 and 4. These time points are clinically translatable to when a patient that underwent a laparotomy for abdominal surgery would need to have their dressings changed and incision sites examined. Previous studies in our porcine models have involved similar time points after an initial surgical procedure or injury in order to do dressing take downs and sample acquisitions, with no adverse impact to the animals.

Animals will continue on study until Day 7 postop where they will be anesthetized, samples and data collected, and then euthanized. Target tissues will be collected for histopathological analyses. Blood samples will also be collected for systemic response analyses.

B. Procedural Details:
If the study requires more than one surgical/ invasive procedure specify if the answers are applicable to all procedures or provide specific answers for each individual procedure clearly indicating which procedure it is for:

Pre-operative procedures
-Fasting, diet modifications, pre-medication, baseline sampling, eye ointment, anesthesia induction
Intra-operative procedures
-Anesthesia maintenance, surgical approach, anatomic locations, closing, etc. Include information on sterility and prep:
Post-operative procedures
-Medications, analgesia, anesthesia recovery, short term (< 24 hrs) and long term (>24 hrs until animal fully recovered)

The animals will be acclimated to the facility, monitored, and observed by MHRI animal facility staff approximately five or more days prior to the initial surgical procedure. The MHRI animal facility staff will evaluate the animal twice daily on the weekdays and once per day on the weekends and holidays. A pre-experimental inspection will be performed for the animal by the attending licensed veterinarian or veterinarian technician, during the acclimation period to assess the animal prior to use on the study.

Prior to study treatment, final selection of the animal for the study will be based on the cageside and clinical observations, and pre-experimental inspection. If the animal is noted to have health

problems, it may be excluded from the study. If the animal has entered the study and contracts a condition or disease that might interfere with the purpose of the study, the Principal Investigator will discuss the case with the veterinarian and the Sponsor representative to determine the steps to take.

PRE-OPERATIVE THERAPY
The animal will be fasted a minimum of 12 hours prior to any scheduled surgical procedure and the time of fasting will be documented in the individual animal record. The animal will have access to water *ad libitum.*

ANESTHESIA PROCEDURE
For all surgical procedures the animal will be anesthetized with a combination of ketamine (15 - 40mg/kg IM), xylazine (1 - 5mg/kg IM), and glycopyrrolate (0.004-0.01 mg/kg, IM, SC, or IV). The glycopyrrolate can be administered as part of the cocktail mixture or separately as directed by the veterinarian. Alternatively, the animal will be anesthetized with a cocktail mixture of ketamine, 15-40mg/kg, xylazine, 1-5mg/kg, and atropine, 0.05-0.5mg/kg, administered intramuscularly. An antibiotic, Ceftiofur, 3-5mg/kg, IM, SID, will be administered at the time of surgical preparation.

An ophthalmic ointment will be applied to each of the animal's eyes. The animals will be intubated and ventilated with oxygen and isoflurane, to effect, administered by inhalation, as necessary. Lidocaine ointment may be applied to the intubation tube as needed to facilitate placement. The hair from the abdominal region will be clipped and a cannula will be inserted into an ear vein for the administration of intravenous fluids during the surgical procedure. The animal will then be moved to the surgical suite, placed on a circulating warm air blanket on the surgical table to help maintain body temperature during the procedure, and connected to the anesthesia machine for maintenance of anesthesia with oxygen (2L/min), and isoflurane 0.5-5.0% (2L/min). The animal will be on a mechanical respirator during the entire procedure.

The animal will be in Stage 3 Plane 2 level of anesthesia before surgery is undertaken. This stage is characterized by the loss of the palpebral (blink) reflex, the pupils become fixed in one position (usually central) and respiration is still regular with good use of the chest muscles and diaphragm.

To monitor the depth of anesthesia the following reflexes will be monitored:
1. Palpebral reflex – touching the eyelids causes blinking. The animal is lightly anesthetized if blinking is present.
2. Toe pinch reflex - pinching the toe or foot web will cause a pain response. If the animal withdraws the toe, anesthesia is not deep enough.
3. Corneal reflex- touching the cornea of the eye with a tuft of cotton results in a blink. Anesthesia is too deep if the corneal reflex is absent.

Once the surgical procedure has begun and the animal is draped, vital signs monitoring will be used to monitor the depth of anesthesia.

To stabilize the animal's physiologic homeostasis while under anesthesia, the animal will be maintained on 0.9% Sodium Chloride, USP, intravenous drip at the rate of 10 – 20ml/kg/hr, and on the circulating warm air blanket.

The survival surgical procedures will be performed using aseptic techniques. Surgical instruments will be packaged and sterilized in a steam autoclave. Surgeons will scrub and wear bonnet or cap, mask, scrubs, shoe covers and sterile gown and gloves. Additional personnel present will wear mask,

scrubs and don shoe covers. The skin at the incision area will be cleansed 3 times alternating with alcohol and/or chlorhexidine and the animal will be draped.

ANESTHESIA MONITORING

During each procedure, vital signs will be monitored and will include (per SOP): % concentration of isoflurane, heart rate, blood pressure, respiratory rate, O_2 saturation, CO_2 level, and body temperature. In some instances, some parameters may not be able to be recorded and in such situations a notation will be made on the anesthesia monitoring form. The animal will be monitored a minimum of every 17 minutes or sooner, if changes are noted.

ADHESION INDUCTION AND TREATMENTS (DAY 0)

Day 0 blood samples will be drawn while the animal is anesthetized via an acceptable route for the species such as the femoral, mammary, or saphenous veins. A total of no more than 20 ml of blood (<3% of total blood volume for a 30kg pig) will be obtained. If multiple sticks are required to fill all necessary tubes, or an alternative route/location is needed, attention will be paid to acceptable volumes per route (ie, no more than 5 ml will be drawn from the ear vein, etc.).

A standard midline incision will be made into the abdominal cavity using a scalpel or bovie electrocautery at the discretion of the PI and board certified surgeon, Jeffrey Shupp MD. The skin subcutaneous tissue, and fascia will be meticulously divided taking care to ensure adequate hemostasis. Once the peritoneum is identified it will be bluntly entered with the surgeons finger as to not disrupt the abdominal viscera. After sweeping the abdominal contents and ensure there are no adhesions the peritoneum will be incised caudally and cranially with the surgeons hand protecting the abdominal contents from injury. After examination of the abdominal cavity, the experimental procedures will begin. In the right lower quadrant the terminal ileum and cecum will be mobilized. To create adhesions between the parietal and parenchymal peritoneum abrasion will be performed using a laparotomy pad or dry sterile gauze pad, except the "sham" procedure group (Group 1).

After the abrasion procedure (meant to induce adhesions), treatment is applied for Groups 3, 4, and 5 internally directly to the surfaces abraded. Group 2 and Group 6 will receive no internal treatment.

The abdominal cavity will then be closed by approximating the fascia using 0 Vicryl sutures in an interrupted figure of 8 fashion. Subcutaneous tissue will be approximated using 3-0 Vicryl interrupted sutures. The skin will be approximated with surgical clips.

Animals in Group 6 will have the incision and surrounding area covered by a nanocrystalline wound dressing. The remaining animals will have their incisions dressed with sterile island dressings. All dressings will be secured in place with sutures or staples. All dressings and treatment materials (Seprafilm and nanocrystalline silver) are provided from the manufacturer in a sterile package.

Animals will be recovered after the application of a Fentanyl Patch (25mcg/hour) placed and secured on a shaved portion of the skin. Subsequently, a custom made neoprene vest may be secured around the animal to prevent dressings from coming off.

Animals will undergo a check of the sites, external dressing changes, and photography of the incisions 2 and 4 days post surgery while under anesthesia.

Animals will continue on study Day 7 postop where they will be euthanized and target tissues will be collected for histopathological analyses.

SURGERY COMPLETION
The animals will be disconnected from isoflurane and ventilated with room air via a battery-operated mechanical ventilator. The animal will be returned to their pen while connected to the ventilator and will remain connected to the ventilator until breathing on their own. Once breathing on their own, they will be disconnected from the ventilator, and extubated. The animal will be monitored until it achieves a sternal position. Animal monitoring will be performed and documented and specifically, heart rate, respiration rate, O$_2$ saturation, and body temperature will be recorded, as obtainable, a minimum of every 17 minutes.

POST-OPERATIVE CARE
During immediate post-operative recovery, the animal will be monitored by MHRI animal facility staff until conscious and physiologically stable. Signs of pain or distress will be documented and reported to the project manager or PI who will consult with the veterinarian prior to any treatment. The animal will be observed closely during the immediate post-operative period for excessive bleeding from the incision site which we will be able to see through dressings, cardiovascular or respiratory depression, hypothermia or other complications. During time points when dressings are down, if any observations of hematoma, extensive bruising/swelling occurs at incision sites post-procedure, the principal investigator, project manager and veterinarian will consultant regarding appropriate therapy.

A one-time dose of Buprenex, 0.3mg, IM, and a Fentanyl Patch, 25mcg/hour (fentanyl content 2.5mg) positioned and secured on a shaved portion of the forelimb, will be given immediately post-operative on Day 0. The Fentanyl patch is designed to release the Fentanyl over a 3-day period. Additional analgesics, approved by consultation of the veterinarian, may be administered, if required for the welfare of the animal. A one-time dose of Buprenex, 0.3mg, IM, may be given post-operative on all other procedure days, without the additional of a fentanyl patch, unless there is a concern of pain or distress ongoing from the initial procedures or other possible complications.

IN-LIFE STUDY ASSESSMENTS
During the in-life period, animals will undergo checks of the incision sites with dressing changes on postop Days 2 and 4.

Table: Drugs/dosages for independent phases of the study

Drug Name	Drug Type	Reason	Dose & Route	Duration and/or Frequency
Pre-Operative Medications and Anesthesia				
Ketamine	Sedative	Sedation and pain	15 to 20mg/kg, IM	At induction to effect
Xylazine	Sedative	Sedation, anesthesia, muscle relaxation & analgesia	1 to 5 mg/kg, IM	At induction to effect
Atropine	Anticholinergic	Decrease secretions	0.05-0.5mg/kg, IM	Single dose

Glycopyrrolate	Anticholinergic	Decrease secretions	0.004-0.01 mg/kg, IM, SC, or IV	Single dose
Isoflurane	Secondary Anesthetic	Anesthesia	To effect in O_2	If needed at induction to effect and to maintain anesthesia
Lidocaine	Anesthetic	Anesthesia Induction	2%, 20mg/mL, oral	If needed at induction for placement of intubation tube
Ceftiofur	Antibiotic	Reduce infection	3-5mg/kg, IM, SID	Single dose for Day 0 procedure only
Intra-Operative Medications				
Isoflurane in 100% O_2	Halogenated Volatile Anesthetic	1° General anesthetic	0.5 to 5% or to effect, Inhalation	Throughout procedure
Post-Operative Medications				
Buprenorphine	Opioid Analgesic	Pain Management	0.3 mg, IM	Once post-surgery
Fentanyl Patch	Analgesic	Analgesia	25 mcg/hr, Transdermal	Once post-surgery
Meloxicam	Nonsteroidal Anti-Inflammatory Drug (NSAID)	Pain management	0.4 mg/kg SQ once a day or oral dose 0.2-0.4 mg/kg SID (24hrs)	Single dose as needed upon consultation with veterinarian
Terminal Procedures				
Fatal-Plus® C IIN	Short Acting Barbiturate	Euthanasia	85 - 150mg/kg, IV	Single dose for termination
KCL (4.2M Solution)	Circulatory Collapse	Euthanasia	2.4 - 4.7mL/10kg, IV	Single dose for termination

VETERINARY INTERVENTION AND CARE

In accordance with accepted veterinary practices, the animal may be administered concurrent therapy (such as additional analgesics, antibiotics or fluid therapy) as required to maintain general good health. Concurrent therapy will be administered according to the instructions of the Attending Veterinarian in concurrence with the Principal Investigator and/or Co-investigator. The identity, dose, route and frequency of administration will be documented in the study files. During the course of the study, unscheduled blood, body fluid, or tissues specimens may be collected for diagnostic purposes, at the request of the veterinarian.

MORIBUNDITY

The Principal Investigator and/or Co-investigator will be notified immediately (same day) of any animal found moribund. Observations with respect to the animal's condition upon discovery along with the time and date of discovery will be documented and communicated to the Project Manager. Euthanasia of moribund animals will be authorized by the Principal Investigator and/or Co-investigator, with the concurrence of the attending veterinarian. If possible, a terminal blood and tissue specimens will be collected before the animal is euthanized. The animal will be anesthetized with a one-time intramuscular injection of a mixture of ketamine, 15-25 mg/kg, xylazine, 3-5 mg/kg, and glycopyrrolate (0.004-0.01 mg/kg, IM, SC, or IV). The glycopyrrolate can be administered as part of the cocktail mixture or separately as directed by the veterinarian (see Table 5). Once anesthetized the animal will be euthanized with Fatal Plus (390 mg/ml pentobarbital sodium; 1% propylene glycol; 29% ethyl alcohol, 2% benzyl alcohol) given intravenously at a concentration of 85 -150mg/kg. The animal will be subjected to a gross necropsy and removal of the treated skin areas.

EARLY DEATH

The Principal Investigator and/or Co-investigator will be notified immediately (same day) upon the discovery of an animal's death and the following procedures will be completed as soon as possible after the discovery. An estimate of the time of death and a description of any abnormal physical findings will be made.

1. Any early death animal will undergo a comprehensive necropsy.
2. If any gross anatomic abnormalities are observed, a specimen will be taken, with attempt to harvest the lesion with normal margins and immersion fixed in 10% neutral buffered formalin for histological processing.

TERMINAL ENDPOINT/FOLLOW-UP

On the day of the scheduled endpoint, at 7 days postop, animal will be anesthetized. A blood sample will be obtained prior to euthanasia and as described for the baseline sample collection of no more than 30 ml total, divided between sodium citrate, K2 EDTA, SST and PAXgene tubes. Animal will be euthanized. Samples of the abdominal wall, cecum, and abrasion if visible will be collected. Each will be used for paraffin-embedding and sectioning for histological analysis (e.g., H&E). Tissues will be stained to determine cellularity, vascularization, and tissue morphology. Wright Giemsa will be used to stain inflammatory cells. Neutrophil, and macrophage phenotypes will be assessed by immunohistochemistry. Additionally, immunohistochemistry may be performed to assess cytokines IL-1β, tumor necrosis factor (TNF). Since healing involves the cooperation between several different cell types and the involvement of various growth factors, cytokines, and the extracellular matrix (ECM), we will interrogate the harvested tissue sections and compare the inflammatory cellular microenvironment.

Necropsy Procedure

A comprehensive necropsy, defined as an examination of the external surface of the body, orifices, and thoracic and abdominal cavities and contents, a gross visual assessment of the treatment region, heart, and other organs, excluding the nervous system, will be performed. Any abnormalities will be described completely and recorded. The disposition of the carcass will be per facility SOP.

C. Invasive Procedures

Invasive Procedure(s)   ☒ Yes   ☐ No

Invasive Procedure(s) include: ☐ Acute (non-survival)   ☒ Survival

Invasive Procedure(s) are considered: ☒ Major   ☐ Minor

D. Will the animals undergo MULTIPLE major invasive procedures (defined in the instructions using the 'Guide' definition). This includes procedures from previous protocols if transferred.

☐ Yes   ☒ No

If yes, please provide justification

E. During recovery from anesthesia, what physiological signs will be monitored to assure the animals are stable?

Upon completion of the surgical procedures the animal will be disconnected from isoflurane and ventilated with room air via a battery-operated mechanical ventilator. The animal will be returned to their pen while connected to the ventilator and will remain connected to the ventilator until breathing on their own. Once breathing on their own, they will be disconnected from the ventilator, and extubated. The animal will be monitored until they achieve a sternal position. Animal monitoring will be performed and documented and specifically, heart rate, respiration rate, O_2 saturation, and body temperature will be recorded, as obtainable, a minimum of every 17 minutes.

F. How often will animals be monitored after anesthetic recovery?

During immediate post-operative recovery, the animal will be monitored until conscious and physiologically stable. Signs of pain or distress will be documented and reported to the project manager who will consult with the veterinarian prior to any treatment. The animal will be observed closely during the immediate post-operative period for excessive bleeding from the surgical sites, any cardiovascular or respiratory depression, hypothermia or other complications. Daily observations of the sites will be made and recorded, to monitor for signs of bleeding and infection that may be seen through dressings. Attempts to monitor the animal's temperature, heart rate, and respiration rate may be made, but no animal will be physically restrained or sedated to obtain these values.

G. Indicate who will monitor the animals pre-procedurally and prepare the animals for surgery.

☒ MHRI Animal Facility   ☐ Study Investigators

H. Indicate who will monitor the animals post-procedurally and the frequency of monitoring.

☒ MHRI Animal Facility   ☒ Study Investigators   ☐ Not Applicable as Acute Procedure

Frequency of Monitoring:

The MHRI Animal Facility staff will evaluate the animal per routine husbandry activities. Study investigators will observe the animal post-procedure twice daily on weekdays and once daily on weekends or holidays. All observations will be recorded in the individual animal care records. Additional cageside observations can be recorded at any time to help manage the animals.

I. Potential Complications

Potential Complication due to Procedure		Mitigation
X	**Body weight loss >15%**	Nutritional supplementation with consultation from the veterinarian.

	Vessel Dissection	
X	**Infection**	Infections will be treated per the guidance of the attending veterinarian. Impact on the study and/or failure to control may result in euthanization of the animal prior to the scheduled study follow-up/endpoint.
	Inability to ambulate	
	Self-mutilation	
	Stroke	
	Hind limb paralysis	
X	**Cardiac complications**	Intra-operative complications, such as anesthesia-related events during intubation and intra-operative anesthesia maintenance may result in cardiac complications; failure to control may result in euthanization of the animal.
	Death	
X	**Other (specify):**	Wound/incision site dehiscence will be treated by attempted re-closure or dressing application depending on extent. This may involve an unscheduled procedure under anesthesia to re-close and/or apply dressings. Herniations may occur. Severe circumstances where complex or lengthy surgical intervention would be required to correct dehiscence or herniations or uncontrolled infections could warrant early euthanasia. Such situations will be reviewed with the attending veterinarian.

J. **What Clinical signs or other criteria will be used to determine that an animal must be removed from the study ahead of schedule (Humane Endpoints) (check all that apply).**
*NOTE: Allowing animals to progress to a moribund or near-death state requires scientific justification; you must indicate below why an earlier, more humane endpoint cannot be used.

- ☐ Body weight loss >20% unresponsive to treatment
- ☒ Pain unresponsive to treatment
- ☒ Infection unresponsive to treatment
- ☐ Vessel dehiscence/dissection
- ☒ Moribund
- ☐ Behavioral abnormalities (describe in detail below)
- ☐ Clinical symptmatology or signs of toxicity (describe in detail below)
- ☒ Other (specify) __see additional information__

Complications can be divided into two groups: immediate and delayed. Immediate complications include any complication occurring within 24 hours of the procedure directly attributable to the procedure itself. Delayed complications include any procedure-related clinical symptom occurring after the immediate 24-hour postoperative period.

As any adverse event can present in unique ways it is important that if any such observations are noted they are promptly reported to the Study Director/PI or appointed study personnel (i.e. co-investigators). The responsible study personnel may make initial recommendations about treatment of the animal(s) and/or alteration of study procedures. All such actions will be properly documented in the study records and, when appropriate, by protocol amendment. If

immediate communication with the Study Director/PI is not possible, treatment of the animal(s) for minor injuries or ailments may be approved by the responsible veterinarian without notification of the Study Director/PI when such treatment does not impact fulfillment of the study objectives. If the condition of the animal(s) warrants significant therapeutic intervention or alteration in study procedures, the Study Director/PI will be contacted when possible to discuss appropriate action. If the condition of the animal(s) is such that emergency measures must be taken, a responsible veterinarian will attempt to consult with the Study Director/PI prior to responding to the medical crisis, but the veterinarian has authority to act immediately at his/her discretion to alleviate suffering. The Study Director/PI will be fully informed of any such events and will subsequently inform the Study Coordinator.

If an animal needs to be euthanized, they will be euthanized with potassium chloride (0.24 – 0.47ml per kg body weight, using a 4.2M, 1-2mmol/kg concentration) will be administered IV while the animal is under general anesthesia. Potassium chloride is a euthanasia method recommended in the 'Report of the AVMA Panel on Euthanasia (2020)' if administered by IV while the animal is under general anesthesia. Alternatively, Fatal Plus (390mg/ml pentobarbital sodium; 1% propylene glycol; 29% ethyl alcohol, 2% benzyl alcohol) administered IV at a concentration of 100-150mg/kg while the animal is under general anesthesia. To confirm that the animal has died, the following parameters will be monitored: no visible respirations (apnea), the absence of pupillary reflex (fixed, dilated pupils), readings of zero for the heart rate and pO_2.

Note: A necropsy will be performed in the event of a sudden, unexpected death for any USDA species.

Section VI: Hazardous Agents (biohazards, chemicals)

A. Does the research, testing or instruction require the use of hazardous or biohazardous agents in the animal facility (i.e., human tissue, infectious/biohazardous agents, carcinogens, toxic chemicals, radioisotopes)?
☒YES ☐ NO

If "yes", specify the hazardous agent(s) to be used and attach an SDS.

- 10% Neutral buffered formalin (NBF) will be used to perfusion-fix the tissue biopsies.

B. Describe or attach a copy the containment/handling protocol to be followed in protecting other animals and personnel from the hazardous agents.

A Safety Data Sheet (SDS) for 10% NBF is on file in the Pre-Clinical surgical suite lab. Personnel involved in handling and dosing have previous experience and are appropriately trained in using 10% NBF. Fixation with 10% NBF will be done in the surgical suite thus no other animals will be exposed. The use of PPE (mask with eye shield, gloves, and laboratory gown) will be enough to minimize exposure.

Section VII: Husbandry/Housing and Disposition of Animals

A. Do you expect to follow MHRI quarantine and conditioning procedures?
☒YES ☐NO

If "yes", proceed to Question B. If "no", describe the quarantine and conditioning procedures to be performed prior to the start of the project.

<div style="border:1px solid black; height:2em;"></div>

    B. Are you requesting an exemption from the MHRI Animal Social Housing and Environmental Enrichment which includes group housing of compatible animals?

        ☐**NO**

        ☒**YES**

            ☒**Exemption from social housing**

            ☐**Exemption from Enrichment**

If yes, what is the justification for this/these exemption request(s)?

> We are requesting an exemption from the MHRI Animal Social Housing Policy by single housing the animals for the entire study.
> - The swine will undergo surgical procedures for which a surgical sites will be created and closed. To prevent other animals from interfering with the sites and dressings, the animals need to be singly housed.
>
> It is for these reasons that we are requesting animals to be singly housed for the duration of the study (exemption from social housing).

    C. Describe any non-standard diet, housing or environmental modifications, and how they will be accomplished.

> None required.

    D. Will individual(s) other than the MHRI Animal Facility staff be responsible, for meeting MHRI standards of animal husbandry and housing?

        ☐ **Yes**   ☒ **No**

If yes, identify location and describe at what point in the study ARF staff versus Investigators, will be responsible for husbandry and welfare of the animals.

<div style="border:1px solid black; height:2em;"></div>

    E. List locations other than the MHRI Animal Facilities where you will house, perform surgery or perform experimental procedures on your animals. If the facility is off-site, is it AAALAC accredited and/or USDA Certified?

> The animals will all be housed, and surgery and experimental procedures will be done at the MHRI Animal Facilities and no off-site facility will be used.

    F. Euthanasia (per 'Report of the AVMA Panel on Euthanasia (2013)')

        ☐ **CO2 (rodents only)**

        ☒ **KCl under deep anesthesia**

        ☒ **Pentobarbital-based solution (e.g. Fatal Plus, Beuthanasia-D etc.)**

        ☐ **Exsanguination under anesthesia (rodents only)**

Euthanasia agent	Dose/Route
Potassium chloride (4.2M KCl concentration)	2.4 – 4.7ml per 10kg / IV
Fatal Plus (390mg/ml pentobarbital sodium)	85 - 150mg/kg / IV

    G. Secondary method for ensuring death

- ☐ **Bilateral thoracotomy**
- ☒ **Flatline vitals**
- ☐ **Cervical dislocation**
- ☐ **Exsanguination**
- ☐ **Other (Specify)**

Section VIII: Principal Investigator Assurances (PI)

Please indicate by check marks that you agree to all the following statements:

[☒] The information provided herein is accurate to the best of my knowledge.

[☒] Procedures involving animals related to this protocol will be performed only by trained or experienced personnel, or under the direct supervision of trained or experienced persons.

[☒] Any change in the care and use of animals involved in this protocol which would affect the welfare of the animals, will be promptly forwarded to the MHRI IACUC for review; such changes **will not** be implemented until the committee's approval is obtained.

[☒] The number of animals proposed is the minimum necessary to conduct valid experimentation.

[☒] I have considered alternative methods to using animals, including a literature search (where appropriate) to ensure that I am not unnecessarily duplicating previous experiments.

Signature: _____   _____
                   Principal Investigator   **Date**

(Submit completed electronic applications to: MHRI Office of Research Integrity at ORI.helpdesk@medstar.net. For further information, contact the IACUC Coordinator at 301-560-2912.)